UNIVERSITÉ DE TOURS

DOCTORAL SCHOOL SSBCV

INRA UMR 85 Physiology of Reproduction and Behavior

Integrative Ovarian Biology Team

THESIS presented by:

Priscila Silvana BERTEVELLO

presentation: **4th July 2019**

to obtain the title of : **PhD at University of Tours**

Discipline / Specialty: Life Science

LIPIDS IN BOVINE OVARIAN FOLLICLE: MASS SPECTROMETRY ANALYSIS AND REGULATION

THESIS lead by:

Mme UZBEKOVA Svetlana	Researcher, HDR, INRA, Tours

RAPPORTEURS :

Mme MEYNARDIER Annabelle	Assistant Professor, HDR, Ecole Nationale Vétérinaire de Toulouse
Mr SANDRA Olivier	Research Director, INRA, HDR, Jouy-en-Josas

---

JURY :

Mr GUERIF Fabrice	University Professor - Hospital Practitioner, CHU Bretonneau, Tours
Mme MEYNARDIER Annabelle	Assistant Professor, Ecole Nationale Vétérinaire de Toulouse
Mme LABBE Catherine	Research Director, INRA, Rennes
Mme METAYER-COUSTARD	Researcher, UMR BOA INRA/University of Tours
Mr SANDRA Olivier	Research Director, INRA, Jouy-en-Josas
Mme UZBEKOVA Svetlana	Researcher, HDR, INRA, Tours

UNIVERSITÉ DE TOURS

ÉCOLE DOCTORALE SSBCV

INRA UMR 85 Physiologie de la Reproduction et des Comportements

Equipe Biologie Intégrative de l'Ovaire

THÈSE présentée par :

Priscila Silvana BERTEVELLO

soutenue le : **04 juillet 2019**

pour obtenir le grade de : **Docteur de l'université de Tours**

Discipline/ Spécialité : Science de la Vie

LIPIDES DU FOLLICULE OVARIEN: ANALYSE PAR SPECTROMETRIE DE MASSE ET REGULATION

THÈSE dirigée par :

Mme UZBEKOVA Svetlana	Chargée de Recherche, HDR, INRA, Tours

RAPPORTEURS :

Mme MEYNARDIER Annabelle	Maître de conférences, HDR, Ecole Nationale Vétérinaire de Toulouse
Mr SANDRA Olivier	Directeur de recherche, HDR, INRA, Jouy-en-Josas

---

JURY :

M GUERIF Fabrice	Professeur des Universités - Praticien Hospitalier, Université de Tours
Mme LABBE Catherine	Directrice de recherche, INRA, Rennes
Mme MEYNARDIER Annabelle	Maître de conférences, Ecole Nationale Vétérinaire de Toulouse
Mme METAYER-COUSTARD	Chargée de Recherche, UMR BOA INRA, Université deTours
M SANDRA Olivier	Directeur de recherche, INRA, Jouy-en-Josas
Mme UZBEKOVA Svetlana	Chargée de Recherche, HDR, INRA, Tours

DEDICATION

To Luiz Cordeiro, my husband, friend, and partner, you are awesome; your support, advice, and care throughout my Ph.D. are highly appreciated and always propelled me beyond my imaginations and in ways untold. To my close family, Luiz and Fernanda, your support and understanding, encouragement and love gave me the energy to face every day with renewed vigor, a fire that kept burning throughout my Ph.D. studies – thank you. To my far away family, my mother Silvana, my father Gilberto, brothers, sisters, aunts, uncles, cousins, cousins, and nieces, I offer my thanks to you for letting me be away from home, your encouragement and prayers can never be overstated.

ACKNOWLEDGMENTS

My sincere thanks go to Dr. Svetlana Uzbekova, as my Ph.D. research director and advisor, very inspirational and a central figure throughout the entire period of my studies. She not only offered me precise guidance throughout my studies, but most importantly, spend a lot of time advising me on the tricks and tactics on how to be a successful scientist. For my Ph.D. and for my life thereafter, I will forever remain very grateful to Dr. Uzbekova.

To the reviewers and thesis jury members, for the time you took to review my thesis, I truly appreciate your help.

I would like to acknowledge our collaborative team at PAIB (*Pôle d'Analyse et d'Imagerie des Biomolécules*), Platform CIRE (*Chirurgie et Imagerie*); Valerie Labas, Ana Paula Teixeira Gomes, and Charles Banliat were very supportive in the acquisition of mass spectrometry data for the project. I would also like to acknowledge the help of Pascal Papillier, Marie Claire Blanche for their contributions towards the development of the thesis. I would also like to thank Dr. Alexandre Seyer for collaboration in HPLC analysis and Dr. Anaïs Vitorino Carvalho for microarray analysis. Thanks to the BINGO Research group members for all the ideas and support that we shared. Guidance on the choices of suitable for the studies in this dissertation from Dr. Virginie Maillard, Dr. Sebastien Elis, and Dr. Veronique Duranthon are highly acknowledged. And also to Philippe Monge, Danielle Monniaux, Rozenn Dalbies-Tran, Sandrine Freret, Pascal Papillier, Peggy Jarrier-Gaillard, Maud Peyny, Alice Desmarchais, Olfa Ghazouani, Sawouda Manrouf, Mouhamad Oseikria, Anna Grandchamp, Aurelien Binet, Maria Pellicer-Rubio, and Ophelie Teteau for the welcome and friendship.

I also wish to thank the Department of Medicine at The University of State of Rio Grande do Norte at Mossoro /Brazil for supporting me financially throughout my Ph.D. studies.

And also my thanks go to all personal of the Unit of Reproductive Physiology and Behavior (PRC) of INRA, Nouzilly for the welcome, kindness, listening, and support. In this way, my thanks begins to the Director, Florian Guillou and the Adjunct Director, Thierry Magallon; and also to the Director of the School of Doctoral Science Health Biology and Chemistry of the Living (SSBCV), Tierry Moreau and the University of Tours.

I would like to thank the members of the ICF team, Emilie Corbin, Cécile Douet, Guillaume Tsikis, Yann Locatelli, Ghilaine Goudet, Florance Guignot, Marie Saint-Dizier, Karine Reynaud, Nadine Gerard, and especially Pascal Mermillod who kindly presented me to my thesis supervisor.

In continuity, I would like to thank the administrative, logistics and IT team, Marie Françoise Pinault, Ghislaine Ploux, Marie Jaros, Sophie Mary, Manon Binoit, Thérèse Hiribarren, Chantal Flon, Patrick Trezy, Barbara Corbière, Gaël Ramé, Pascal Bernard, Thierry Delpuech, Albert Arnould, Robert Vincent, Jean-Yves Durbize, Oliver Gallant and Julien Gagneux.

The experience of the thesis is also the moment where trainees, doctoral, post-doctoral students of all horizons meet and become friends. To this I thank sincerament my office mates, Erika Caldas, Agostinho Soares de Alcantara Neto, Leticia Fiori, Juliana Martins, Glaucia Bragança, Namya Mellouk, Alix Barbe, Alice Bongrani, Laura Helou, Shifa Tahir, Francesco De Pascalli, Manon Charles, Patrycja Kurowska, Tsige Hailay, Pai Sutisa and other friends from “churrascos”, “petit gourmandizes” and beer. Thank you for all these unforgettable moments together.

A considerable number of other people have helped make my days and my work more enjoyable and simple, if only by a smile or a kind word. Even though all the names cannot be quoted here, all of you are assured of my recognition.

SUMMARY

Ovarian follicle provides a favorable environment for enclosed oocytes, which acquire their competence to support embryo development in tight communications with somatic follicular cells and follicular fluid (FF). Among the numerous antral follicles only few become dominant and designated to ovulate. Follicular growth requires a lot of energy provided from different substrates, including fatty acids (FA). FA metabolism in cumulus cells (CC) is known to be crucial for oocyte maturation and is fundamental for steroidogenic properties of theca (TH) and granulosa cells (GC). In order to enlighten lipid metabolism regulation within the ovarian follicles, the objectives of this study were ***a)*** to analyze lipid composition in follicular cells, oocyte and FF; and ***b***) to decipher transcriptional regulation of follicular lipid metabolism by analysis of gene expression in TH, GC, CC and enclosed oocyte with respect to final follicular growth.

First, using liquid chromatography and mass spectrometry (MS), 438 and 439 lipids representing different classes of glycerophospholipids, glycerorolipids, sphingolipids, sterols and fatty acyls were identified in FF and follicular cells, respectively. *Second,* MALDI-TOF MS imaging allowed the mapping of 281 lipid features through ovarian sections, 52 of them we identified. Nile Red staining of ovarian sections demonstrated follicular size-dependent differential distribution of neutral lipids in GC and TH cell layers. *Third,* we compared lipid fingerprints obtained by MALDI-TOF MS on isolated follicular cells (TH, GC, CC and the oocytes) and FF from the follicles 3-8 mm, and determined differentially abundant lipids between these follicular compartments. Comparison of lipid fingerprints between the small follicles (SF, mean size 5 mm) and large dominant follicles (LF, mean size 13 mm) revealed drastic changes in FF lipidome. More than 55% of detected features varied more than two-fold between LF and SF ($p<0.05$). Lipids in TH, GC and CC were also affected by follicular size (about 5%, 15% and 10% of lipids varied, respectively), in contrast to the oocytes that showed less than 2 % of differential lipids between SF and LF. From all these molecular species detected by MALDI MS, 197 lipids were identified revealing the major changes in membrane and signaling lipids in both somatic follicular cells and FF.

Forth, gene expression analysis using global transcriptomic data revealed that lipid metabolism-related genes expressed either constitutively or more specifically in TH, GC, CC and the oocytes, highlighted their specific functions including lipid uptake, lipolytic degradation, FA transport and oxidation, *de novo* FA synthesis and elongation, lipoprotein production, membrane building, lipid storage and others. Analysis of 18 candidate genes in TH and GC of SF and LF revealed significant increase of FA beta-oxidation and oxidative stress in TH and GC of dominant LF, respectively. All these data indicate the putative protective role of follicular cells concerning the enclosed oocyte.

Lipid composition of FF, mural cells and enclosed oocyte-CC complex coupled to particular gene expression patterns presumes intensive lipid exchanges between these compartments and particular involvement of the oocyte in FA elongation, synthesis of glycerophospholipids, glycerolipids and lipid droplet formation. We have also demonstrated that lipid fingerprints of the oocytes and CC significantly changed during oocyte maturation or after exposition of oocyte-CC to omega-3 polyunsaturated FA *in vitro* and *in vivo*.

In conclusion, our data suggest that the ovarian follicle is capable to transform the FA from nutrition uptake and use them to supplement follicular cells and enclosed oocyte with membrane lipids, energy, and signaling mediators. Lipid metabolism is therefore likely involved in maintenance of follicular homeostasis and regulating of follicular atresia or dominance thus assuring the development of competent oocyte for subsequent embryonic development.

Keywords: ovarian follicle; lipids; mass spectrometry imaging; MALDI MS profiling; gene expression; oocyte; granulosa; theca; follicular fluid; bovine; follicle size.

RESUME

Le follicule ovarien constitue un environnement adapté à l'ovocyte, qui acquière sa compétence à soutenir le développement embryonnaire au cours de la folliculogenese, en communication permanente avec les cellules et le liquide folliculaire (LF). Parmi les nombreux follicules antraux, seuls quelques-uns deviennent dominants et pourront ovuler. La croissance folliculaire nécessite beaucoup d'énergie provenant de différents substrats, y compris les acides gras (AG). Il est établi que le métabolisme des AG dans les cellules du cumulus (CC) est crucial pour la maturation de l'ovocyte et pour les propriétés stéroïdogèniques des cellules de la thèque (TH) et des granulosa (CG). Dans le cadre de ce travail nous avons tenté de mieux comprendre les rôles de lipides ovariens en ayant pour objectifs: a) d'analyser la composition lipidique des cellules (TH, CG, CC, ovocyte) et du liquide folliculaire et leur distribution au sein de l'ovaire, par spectrométrie de masse (SM); b) de comparer l'expression des gènes des enzymes impliquées dans le métabolisme des AG dans les cellules de la TH, CG, CC et les ovocytes dans les follicules bovins de différentes tailles.

Premièrement, en utilisant la chromatographie liquide et la spectrométrie de masse, 438 et 439 lipides représentants différentes classes de glycérophospholipides, glycérorolipides, sphingolipides, stérols et acyles gras ont été identifiés dans les cellules et le LF, respectivement. Deuxièmement, l'imagerie par SM MALDI-TOF a permis de cartographier 281 espèces lipidiques sur des coupes d'ovaires, dont 52 ont été identifiées. La coloration par le rouge du Nil sur des coupes d'ovaires a montré une distribution différentielle des lipides neutres dans les CG et TH de follicules de différentes tailles. Troisièmement, nous avons comparé les empreintes lipidiques obtenues par SM MALDI-TOF sur des cellules folliculaires isolées (TH, CG, CC et les ovocytes) et LF de follicules de 3 à 8 mm, et les lipides avec une abondance différentielle entre ces compartiments ont été caractérisés. La comparaison des empreintes lipidiques entre les petits follicules (PF, taille moyenne 5 mm) et les gros follicules dominants (GF, taille moyenne 13 mm) a révélé des modifications drastiques du lipidome du liquide folliculaire, plus de 55% des espèces détectées montent une abondance différentielle au-dessus de 100% entre les PF et GF ($p<0,05$). Les lipides des cellules de TH, CG et CC étaient également affectées par la taille folliculaire (environ 5%, 15% et 10% des lipides variaient, respectivement), contrairement aux ovocytes qui présentaient moins de 2% de lipides différentiels entre PF et GF. Parmi toutes ces espèces moléculaires détectées par MALDI MS, 197 lipides ont été identifiés, révélant les principaux changements des lipides membranaires et de signalisation dans ces cellules folliculaires somatiques et les LF.

Enfin, une analyse des données transcriptomiques in silico a révélé que les gènes liés au métabolisme des lipides sont exprimés de manière constitutive ou plus spécifiquement dans les cellules TH, CG, CC et les ovocytes. Ces patrons d'expression ont mis en évidence les fonctions spécifiques de chaque type

cellulaire, notamment l'absorption des lipides, la dégradation lipolytique, le transport et l'oxydation des AF, la synthèse *de novo* et l'élongation des AG, la production de lipoprotéines, la construction de membranes, le stockage de lipides et autres. L'analyse par qPCR de gènes candidats dans les cellules de la TH et les CG de PF et de GF a révélé une augmentation significative de la bêta-oxydation des AG et du stress oxydatif dans les TH et CG de gros follicules dominants, respectivement. Toutes ces données indiquent le rôle protecteur des cellules folliculaires vis-à-vis de l'ovocyte qu'ils enferment.

La composition lipidique du LF, des cellules somatiques et de leur complexes ovocyte-CC inclus, associés aux patrons d'expression génique particuliers, supposent des échanges lipidiques intenses entre ces compartiments et une implication particulière de l'ovocyte dans l'élongation des AG, la synthèse de glycérophospholipides et glycérolipides, et la formation de gouttelettes lipidiques. Nous avons également démontré que les empreintes lipidiques des ovocytes et des CC changeaient de manière significative pendant la maturation de l'ovocyte ou après l'exposition de complexes ovocyte-CC à l'AG polyinsaturé oméga-3 *in vitro* et *in vivo*.

En conclusion, nos données suggèrent que le follicule ovarien est capable de transformer les AG de l'apport nutritif et de les utiliser pour fournir aux cellules folliculaires et l'ovocyte des lipides membranaires, de l'énergie et des médiateurs de signalisation. Le métabolisme des lipides est donc probablement impliqué dans le maintien de l'homéostasie folliculaire et la régulation de l'atrésie ou dans la dominance folliculaire, assurant ainsi le développement de l'ovocyte compétent pour le développement embryonnaire ultérieur.

Mots-clés: follicule ovarien; lipides; imagerie par spectrométrie de masse; profilage par MALDI MS; expression du gène; ovocyte; granulosa; thèque; fluide folliculaire; bovine; taille du follicule.

TABLE OF CONTENT

ACKNOWLEDGMENTS 4
SUMMARY 6
RESUME 8
TABLE OF CONTENT 10
ABBREVIATION LIST 13
LIST OF TABLES 21
LIST OF FIGURES 21
INTRODUCTION 23
1 Lipids in mammalian cells 23
1.1 Classification, structure and properties 23
1.1.1 Structure and nomenclature 24
1.2 Lipidomics 28
1.2.1 Tools and applications 28
1.3 Methods and techniques of lipid analysis 31
1.3.1 General workflow of lipid analysis in biological samples 31
1.3.2 Experimental approaches to analyze lipids 31
1.4 Regulation of lipid metabolism 36
1.4.1 Lipids transport in body fluids 36
1.4.1 FA transporters 43
1.5 Lipid synthesis 47
1.5.1 Membrane synthesis 47
1.5.2 Glycerophospholipid synthesis 47
1.5.3 Sphingolipid synthesis 48
1.5.4 Cholesterol synthesis 48
1.6 Lipid storage 49
1.7 Steroidogenesis 51
2 Physiology of the ovarian follicle and gamete production 53
2.1 Ovary: morphologic structure, function and energy metabolism 53
2.2 Folliculogenese and ovogenesis 53
2.2.1 The key steps of folliculogenesis and oogenesis 55
2.2.2 Functional changes in somatic cells and oocyte during folliculogenesis 57
2.2.3 Oocyte competence 62
3 Lipids metabolism in the ovarian follicle 64

3.1 Effect of lipid metabolism on reproductive performance in cow 64
3.2 Energy metabolism during folliculogenesis 65
3.3 Lipid uptake by ovarian cells 66
3.3.1 Lipids in follicular fluid and impact on somatic cells 67
3.3.2 Lipids in the oocyte-cumulus complexes (COC) 69
OBJECTIVES 73
1 General objective 74
2 Specific objectives 74
MATERIALS AND METHODS 75
1 Ethics 75
2 Chemicals 75
3 Biological material 75
3.1 Biological material collection *in vivo* 76
3.2 Collection of ovaries for in situ lipidomic analysis 76
4 Lipidomic analysis 76
4.1 Nile Red staining 76
4.2 Lipid identification 77
4.3 MALDI-TOF MS analysis of lipids of individual oocytes, follicular cells and fluid 77
4.4 Mass Spectrometry Imaging (MSI) by MALDI-TOF MS 80
5 Gene expression analysis 81
RESULTS 82
1 Identification of lipids in bovine ovarian follicle and gene expression analysis of controlling enzymes 83
1.1 Article 1 83
2 Lipid species in follicular cells and fluid in bovine follicles of different sizes 84
2.1 Article 2 84
3 Lipid profiling modulations in bovine oocytes 85
3.1 MALDI-TOF mass spectrometry analysis of lipids in single bovine oocytes during IVM 85
3.1.1 Abstract 85
3.1.2 Introduction 86
3.1.3 Materials and methods 86
3.1.4 Results and discussion 89
3.1.5 Conclusion 91
3.2 Effect of n-3 PUFA on lipid profiles on bovine oocytes as detected by MALDI-TOF mass spectrometry 92
3.2.1 Article 3 92

4 Lipid profiling modulations in somatic cells 95
4.1 Comparison of lipid profiles and gene expression in granulosa and cumulus cells in bovine. 95
4.2 Analysis of lipids in granulosa cells of postpartum Holstein dairy cows fed with diets with differing energy levels. 97
DISCUSSION 99
1 Lipid metabolism in follicular wall cells. 99
2 Lipids in follicular fluid. 106
3 Lipid content and regulation in Cumulus-Oocyte Complex (COC) 110
CONCLUSIONS 115
BIBLIOGRAPHY 117
PUBLICATION LIST 137

ABBREVIATION LIST

17β-HSD	17-beta-hydroxysteroid dehydrogenase
3β-HSD	3-hydroxy-delta-5-steroid dehydrogenase, beta family
A	
ABCA1	ATP-binding cassette A1 lipid
ACAC	acetyl-coenzyme-A carboxylase
ACADS/ACADSB	acyl-CoA dehydrogenase short-chain
ACADVL	acyl-CoA dehydrogenase very long-chain
ACC	acetyl-CoA carboxylase
ACL	ATP-citrate lyase
ACOX	flavoprotein acyl-CoA oxidase
ACSL	acyl-CoA synthetase long-chain
AGPAT	acylglycerol-3-P acyl transferase
AMH	anti-Mullerian hormone
APCI	chemical ionization at atmospheric pressure
Apo	apolipoprotein
ATGL	adipose triglyceride lipase
ATP	adenosine triphosphate
B	
BMP	bone morphogenetic protein
C	
C	carbon
CACT	carnitine acylcarnitine translocase
cAMP	cyclic adenosine monophosphate
CC	cumulus cells
CD36	CD36 Molecule (thrombospondin receptor)
CDP	cytidine diphosphate;
CDP-DAG	diacylglycerol synthase
CE	cholesteryl ester
Cer	ceramides
CERS	dihydroceramide synthase

cGMP	cyclic guanosine monophosphate
-CH 3	methyl group
CHCA	α-Cyano-4-hydroxycinnamic acid
CID	collision-induced dissociation
CK	choline kinase
CL	corpus luteum
CL	cardiolipins
CMP	cytidine monophosphate
CoA	coenzymes A
-COOH	carboxylic acid
CPET	CDPEtn-1,2-diacylglycerol ethanolaminephosphotransferase
CPT1A	carnitine palmitoyltransferase 1A
CPT2	carnitine palmitoyltransferase 2
CPTc	CDP-choline:1,2-diacylglycerol cholinephosphotransferase
CPT-Cho	CDP-choline:1,2-diacylglycerol phosphatidylcholine
CPT-Etn	CDP-choline:1,2-diacylglycerol phosphatidylethanolamine
CV	coefficient of variation
CYP11A1	cytochrome P450 family 11 subfamily A member 1
CYP17A1	cytochrome P450 Family 17 subfamily A member 1
CYP19A1	cytochrome P450 family 19 subfamily A member 1

D

Da	dalton
DG	diglycerides or diacylglycerols
DGAT2	diacylglycerol acyl transferase 2
DHA	docosahexaenoic acid
DHAP	2,5-dihydroxyacetophenone
DHCR7	7-dehydrocholesterol reductase
DHEA	dehydroepiandrosterona
DNL	*de novo* lipogenesis

E

E2	estradiol
EGF	epidermal growth factor

ELOVL	elongation of very long chain fatty acid
ER	endoplasmic reticulum
ESI	electrospray ionization

F

FA	fatty acyls or fatty acid
FABP	fatty acid binding proteins
FAC	fatty acyl carnitines
FAD	fatty acid desaturase
FADH2	flavin adenine dinucleotide + 2 hydrogens
FAS	fatty acid synthesis
FAT	fatty acid translocase
FATP	fatty acid transport protein
FC	free cholesterol
FF	folicular fluid
FFA	free fatty acids
FSH	follicle stimulating hormone
FSHR	follicle stimulating hormone receptor
FT-ICR	fourier transform / cyclone ion resonance

G

G3P	glycerol-3-phosphate
GalCer	galactosylceramide
GC	granulosa cells
GDF9	growth differentiation factor 9
GL	glycerolipids
GlcCer	glucosylceramide
GM	ganglioside
GNRH	gonadotropin releasing hormone
GO	gene onthology
GP	glycerophosphates
GP	glycerophospholipids
GPAT	glycerol-3-P acyl transferase
GPL	glycerophospholipids

H

HACD	3-hydroxyacyl-CoA dehydratase
HADHA	hydroxyacyl-CoA dehydrogenase trifunctional multienzyme complex subunit alpha
HCD	higher energy collision dissociation
Hcer or HexCer	hexosylceramides
HCer	hexosylceramide
HDL	high-density lipoprotein
Hex2Cer	dihexosylceramides
HMG-CoA	3-hydroxy-3-methylglutaryl-CoA
HMGCR	3-hydroxy-3-methylglutaryl-CoA reductase
HMGCS	3-hydroxy-3-methylglutaryl-CoA synthase
HPLC	high performance liquid chromatography
HSD3B2	gene 3-beta-hydroxy-delta (5)-steroid dehydrogenase
HSL	hormone-sensitive lipase

I

ICM-MS	intact cell MALDI-TOF mass spectrometry
IDL	intermediate-density lipoprotein
IGF	insulin growth factor
IPP	isopentenyl pyrophosphate
IVF	*in vitro* fertilization
IVM	*in vitro* maturation

K

KAR	3-ketoacyl-CoA reductase

L

LacCer	lactosylceramide
LC/MS	liquid chromatography/mass spectrometry
LCFA	long-chain fatty acid
LC-HRMS	liquid chromatography- high resolution mass spectrometry
LD	lipid droplet
LDL	low-density lipoprotein

LDLR	low-density-lipoprotein receptor
LF	large follicle
LGP	lyso-glycerophosphates
LH	luteinizing hormone
LHCGR	luteinizing hormone/choriogonadotropin receptor
LIPE	lipase E- hormone sensitive type E
LPA	lyso-glycerophatidic acid or lysophosphatidic acid
LPC	lyso-glycerophosphatidylcholines
LPE	lyso-glycerophosphatidylethanolamines
LPI	lyso-glycerophosphatidylinositols
LPL	lipoprotein lipase
LPL	lysophospholipids
LTQ	linear trap quadropole

M

m/z	ion mass to ion charge number ratio
MALDI	matrix assisted laser desorption / ionization
MG	monoglycerides
MGL	monoacylglycerol lipase
miRNA	microRNA
mRNA	messenger RNA
MS	mass spectrometry
MS/MS	tandem mass spectrometry
MSI	mass spectrometry imaging
MUFA	monounsaturated

N

NAD	nicotinamide adenine dinucleotide
NADH	nicotinamide adenine dinucleotide + hydrogen
NADPH	nicotinamide adenine dinucleotide phosphate
Nd:YAG	neodymium-doped yttrium aluminum garnet
NEB	negative energy balance
NEFA	non-esterified fatty acids
NPH	normalized peak height

NR	Nile Red
NRF	Nile Red fluorescence

O

–OH	hydroxyl group
OO	oocyte
OOC or COC	oocyte-cumulus complex

P

P450scc	cytochrome P450 side-chain cleavage enzyme
PA	phosphatidic acids
PC	phosphatidylcholines or glycerophosphatidylcholines
PCA	principal component analysis
PCR	polymerase chain reaction
PDE3A	cAMP-phosphodiesterase
PE	phosphatidylethanolamines / glycerophosphatidylethanolamines
PG	phosphatidylgylcerols / glycerophosphatidylglycerols
PGP	phosphatidylgylcerolphosphate
PGPS	PG-P synthase
Pi	inorganic phosphate
PI	phosphatidylinositols / glycerophosphoinositols
PIS	phosphatidylinositols synthase
PK	polyketides
PKA	protein kinase A
PLIN	perilipin
PNPLA2	patatin like phospholipase domain containing 2
PPARG	peroxisome proliferator-activated receptor-gamma
PR	prenol lipids
PRG	progesterone
PS	phosphatidylserines or glycerophosphatidylserines
PSD1/2	phosphatidylserine decarboxylase isoforms
PSS	phosphatidylserine synthase isoforms
PUFA	polyunsaturated fatty acid

Q

qRT-PCR	quantitative real time polymerase chain reaction
RNA	ribonucleic acid
RNase	ribonuclease

R

ROI	region of interest
RT-PCR	reverse transcriptase polymerase chain reaction

S

SCD	stearoyl-coA desaturases
SE	steryl esters
SF	small follicle
SHBG	sex hormone binding globuline
SL	sphingolipids
SM	sphingomyelins
SMase	sphingomylenase
SMPD1/4	sphingomyelin phosphodiesterase
SMS	sphingomylelin synthase
SP	sphingolipids
SPT	serine palmitoyl transferase
SRB1 or SR-BI	scavenger receptor class b member 1
ST	sterol lipids / sterols
StAR	steroidogenic acute regulatory
STAR	steroidogenic acute regulatory protein
SuSM	sulfoglycosphingolipids

T

TCA	tricarboxylic acid cycle
TER	2,3-trans-enoyl-CoA reductase
TG or TAG	triglycerides / triacylglycerols
TGFB	transforming growth factor-beta superfamily
TH	theca cells
TIC	total ion count

TNF	tumor necrosis factor
TOF	time-of-flight
TT	testosterone.
TZP	transzonal projection

U

UV	ultra violet

V

VLCFA	very-long-chain FA
VLDL	very-low-density lipoprotein

Z

ZP	zona pellucida / pellucid zone

LIST OF TABLES

Table 1. Lipid classification……..……..24

Table 2. Methods and techniques frequently used to determine lipid and fatty acid composition……..……...32

Table 3. Annotations of oocyte lipid species differently abundant during *in vitro* maturation..……..…….....91

LIST OF FIGURES

Figure 1. Nomenclature features of fatty acids…….……..……25

Figure 2. Lipid families and scheme of main lipid transformations……26

Figure 3. Lipidomic analysis of biological samples workflow……30

Figure 4. Schematic representation of MALDI-TOF mass spectromter…….……..……34

Figure 5. Scheme of the main steps of FA metabolism……38

Figure 6. FA elongation cycle……..……..……40

Figure 7 Scheme of FA elongation and desaturation……...……40

Figure 8. Scheme of long-chain FAs oxidation in peroxisomes and mitochondria……..……44

Figure 9. Lipid transporters. FA and cholesterol uptake by membrane transporters……44

Figure 10. Schema of biosynthesis pathways for the phospholipid and sphingolipid classes biosynthesized in mammalian cells……..……..…….46

Figure 11. Simplified scheme of cholesterol synthesis……49

Figure 12. Major pathways of steroidogenesis……50

Figure 13. Morphology of the ovary……..……52

Figure 14 Follicular dynamics in three wave cycle……..……...……54

Figure 15. Folliculogenesis and atresia……...……56

Figure 16. Main functional changes in follicular cells and oocyte during folliculogenesis…….....58

Figure 17. Steriods hormones synthesis in ovarian cells……...…….60

Figure 18. Schematic mechanisms of mobilization and catabolism of free FAs in the cumulus–oocyte complex……...……70

Figure 19. Principle of MALDI-TOF mass spectrometry analysis of lipids……..……..78

Figure 20. Principle of differential analysis of lipid abundance……..……79

Figure 21. Mass spectrometry imaging of lipids on ovarian sections……..……80

Figure 22. Lipid fingerprints of single bovine oocyte in the range 200-1000 m/z……89

Figure 23. Heat map representation of differently abundant lipids in the oocytes during IVM……...89

Figure 24. PCA of differently abundant lipids in immature and mature (22h IVM) bovine oocytes…….…….……..90

Figure 25. Relative abundance and identification of differential lipids detected in single immature and mature oocytes by ICM-MS lipid profiling…….…90

Figure 26. Analysis of lipid composition using MALDI-TOF mass spectrometry profiling in bovine oocytes and cumulus cells after 24h IVM with or without DHA 1 µM treatment……....93

Figure 27. Scheme of lipid content and metabolic lipid pathways in theca cells of bovine ovarian follicles……101

Figure 28. Scheme of lipid content and metabolic lipid pathways in granulosa cells of bovine ovarian follicles…….……103

Figure 29. Hypothetical scheme of lipid content in follicular fluid and interactions between the compartments in bovine ovarian follicles……..……107

Figure 30. Hypothetical scheme of lipid metabolism related in oocyte-cumulus complex, and interactions between the compartments in bovine ovarian follicle…….……...112

INTRODUCTION

INTRODUCTION

1 Lipids in mammalian cells

Lipids, defined in the "Principles of biochemistry" as " *water-insoluble organic substances, oily or greasy, which are extractable from cells and tissues by nonpolar solvents"*, are present in all the living cells in different forms and represent the hydrophobic fraction of small biomolecules (<1500 Da), known as metabolites. In different species, lipids evolves differently than genes and their products: less than 2% of lipids accumulate proportionally to the phylogenetic distances comparing to 84% of genes and 25% of protein-coding transcripts, wherein, the lipidomes of rodents, primates and bats were clearly tissue-specific (Khrameeva *et al.*, 2018). Lipids are essential components of plasma cell membranes and play indispensable roles in the processes that are associated with cell cycle progression, cell proliferation, differentiation and organ morphogenesis. Cell membrane and organelles play a fundamental transition in the lipid landscape dividing the secretory pathway by membrane territories, allowing an adaptation from biogenic barrier functions. The lipid composition of cellular membrane is tailored to suit their specialized tasks: structure, signaling and controlling membrane-bound lipid transporters (Van Meer, Voelker and Feigenson, 2008). Apart from serving as signaling molecules to regulate developmental processes and defensive mechanisms, lipids have primarily functions as energy storage and to provide essential components for membrane assembly (Lizardo *et al.*, 2018).

1.1 Classification, structure and properties

There are three primary groups of lipids. The first group is simple lipids of fat and waxes, which are generally esters of fatty acids (FA) containing various glycerols and alcohols, respectively. The second group is the complex lipids, which are simple lipids containing additional functional groups, like a phosphoric acid residue or carries a carbohydrate group. The third group is the derived lipids. This group includes steroids, hydrocarbons, hormones, soluble vitamins and others (Liebisch *et al.*, 2013).

The mostly used lipid classification system contains eight categories (**Table 1**) as described in the LIPID MAPS website (http://www.lipidmaps.org). This classification was presented by the International Lipid Nomenclature and Classification Committee in 2005 (Fahy *et al.*, 2005) and updated in 2009 (Fahy *et al.*, 2009). Each of the eight category is divided into classes, subclasses and, in the case of some subclasses of prenol lipids, 4th-level classes.

1.1.1 Structure and nomenclature

The main lipid classes are presented in Table 1.

Table 1. Lipid classification.

LIPID MAPS [Category]/Class - Common Name	**Class abbreviation**
1.Fatty acyls [**FA**]	
Fatty acids	**FA**
2.Glycerolipids [GL]	
Monoglycerides	**MG**
Diglycerides	**DG**
Triglycerides	**TG**
3.Glycerophospholipids [**GP**]	
Cardiolipins	**CL**
Phosphatidic acids	**PA**
Phosphatidylcholines	**PC**
Phosphatidylethanolamines	**PE**
Phosphatidylgylcerols	**PG**
Phosphatidylgylcerolphosphate	**PGP**
Phosphatidylinositols	**PI**
Phosphatidylserines	**PS**
Lysophospholipids	Prefix **L**
4.Sphingolipids [**SP**]	
Ceramides	**Cer**
Sphingomyelins	**SM**
Hexosylceramides	**HexCer**
Glucosylceramide	**GlcCer**
Galactosylceramide	**GalCer**
Dihexosylceramides	**Hex2Cer**
Lactosylceramide	**LacCer**
5.Sterol lipids [**ST**]	
Sterols	**ST**
Steryl esters	**SE**
Free cholesterol	**FC**
Cholesteryl ester	**CE**
6.Prenol lipids [PR]	PR
7.Saccharolipids [SL]	SL
8.Polyketides [PK]	PK

(Adapted from (Fahy *et al.*, 2005; Liebisch *et al.*, 2013)).

FATTY ACIDS

Fatty acids (FAs) are the major blocks of the complex lipids and thus the fundamental category of all biological lipids. FA consist of a carboxylic group (-COOH) and an aliphatic linear tail comprising a number of carbon atoms greater than four and generally even at one end of the methyl group (-CH 3)

(Ratnayake and Galli, 2009). Soluble in organic solvents, the hydrophobicity of the FAs correlates with the length of their carbon chain.

According to (Moran *et al.*, 2012), FA classification depends on the number of carbon atoms: FAs having 4 to 10 carbon atoms are known as short chain, 12 to 14 carbon atoms are medium chain FAs, and FA with 16 or more carbon atoms are referred as long chain FAs.

1. Number of carbon-carbon double bonds also differs from the FA without double bonds are referred to as saturated, while the hydrocarbon tail having at least one unsaturated double bond is called monounsaturated (MUFA) and those having multiple double bonds are called polyunsaturated fatty acids (PUFA).
2. Position of the double bonds in the chain, also called position isomerism: these are double bonds located at different positions in the carbon chain. The position of the double bonds is indicated by the symbol " = ". A nomenclature determined by International Union of Pure Applied Chemistry (IUPAC), where "*n*" indicates the position of the first carbon atom unsaturation number in the carboxylic group (−COOH).
3. Configuration of the double bonds: in unsaturated FAs, the configuration can be Cis or Trans. Cis-configuration is characterized by the position of the two hydrogen atoms on the same side of the bond plane. Trans-configuration is characterized by the two hydrogen atoms in the other bond plane. The carboxylic carbon is labeled C−1 and the following are numbered sequentially. In the common nomenclature, Greek letters are used to identify carbon atoms. The carbon adjacent to the carboxylic carbon (C−2) is designated by α and the other carbons are by β, γ, δ, ε, etc. The Greek letter ω is specific to the carbon atom furthest from the carboxylic group, whatever the length of the tail of the hydrocarbons **(Figure 1).**

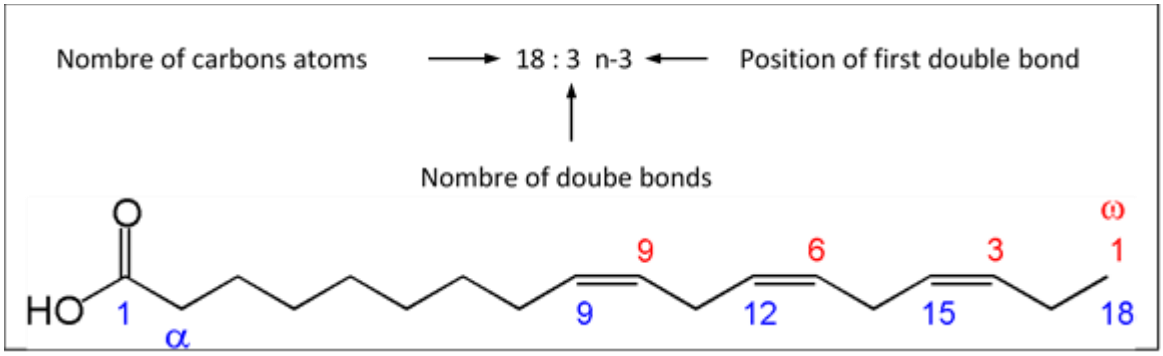


Figure 1. Nomenclature features of fatty acids (ex: α-linolenic acid).

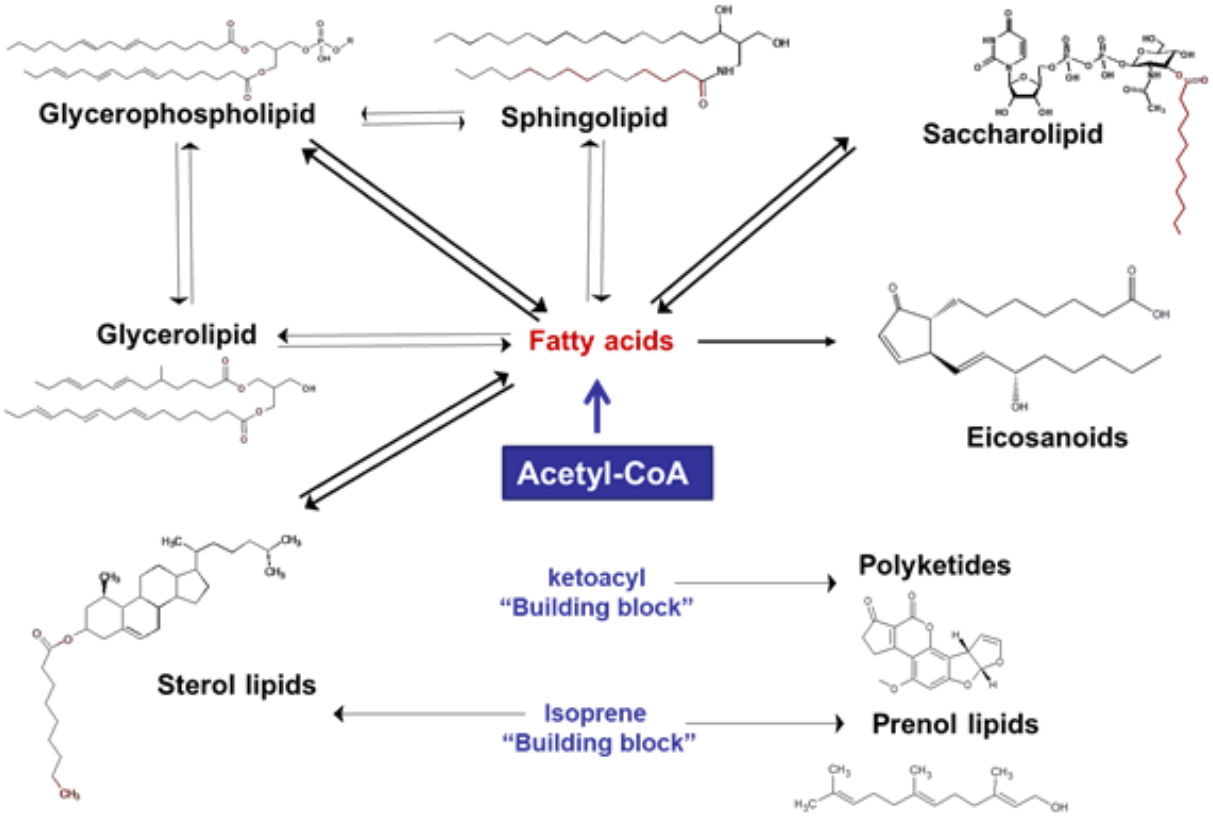


Figure 2. Lipid families and scheme of main lipid transformations (from A. Seyer, 2014)

Schematic representation of the main lipid categories and their transformation is shown in **Figure 2**.

GLYCEROLIPIDS

The **glycerolipids** (GL) are essentially bond to all glycerol-containing lipids. The category/class is nominated by the mono-, di- and tri-glycerols, the most well-known being the fatty acid esters of glycerol (acylglycerols) (Fahy *et al.*, 2005). Triglycerides (TGs) are mainly stocked in lipid droplets. In nutrition, triglycerides are the majority of fats in the oils of seeds and storage of fat in animal tissues (Ratnayake and Galli, 2009).

GLYCEROPHOSPHOLIPIDS

Glycerophospholipids (GP) are components of cell membranes asymmetrically distributed across the membrane bilayer. GP consist of a glycerol bound with two FAs and a phosphate group linked to an alcohol molecule. The amphipathic characteristic of this molecules determines the bilayer cell membrane structure and fluidity; GP also act as precursors for the synthesis of a series of biologically active compounds (Montigny *et al.*, 2016). The major group of phospholipids have phosphatidic acid (PA) as a common backbone, which consists of a glycerol molecule esterified to two FAs and esterified phosphate group. The phosphate group is esterified to the "bases" like choline, ethanolamine, serine and inositol to form the major GPs as phosphatidylcholines (**PC**), phosphatidylethanolamines (**PE**), phosphatidylserines (**PS**) and phosphatidylinositols (**PI**) (Vance, 2014), which are highly abundant in mammalian cells. In normal cell, **PCs** are in higher abundance in the outer-side of the bilayer of cell outer membrane, while others phospholipids such as **PEs** (second most abundant mammalian membrane phospholipid) and **PSs**, as well as **PIs**, are found in highest concentration on the inner-side (Vance and Steenbergen, 2005; Fadeel and Xue, 2009; Zemski Berry *et al.*, 2011).

SPHINGOLIPIDS

Sphingolipids (SP) are a complex family of compounds that share a common structural feature: they have a sphingoid base, which is converted into ceramides, phosphosphingolipides, glycosphingolipids and others. **Ceramides (Cers)** are an important subclass of derivatives of sphingoid base linked with an amino alcohol and a FA (Ratnayake and Galli, 2009). The ceramides are involved in the regulation of signal transduction processes including cell differentiation (Okazaki *et al.*, 1990), apoptosis (Hannun and Obeid, 1995) and inflammatory responses (Masini *et al.*, 2008). Another class of polar lipids is the sphingolipids (Christie, 2003) dominated by **sphingomyelins (SM). SM** contain choline, a quaternary amino group, as a result of phosphocholine transfer from PC to ceramide, which is catalyzed by sphingomyelin synthase (Milhas, Clarke and Hannun, 2011). SM function as a structural components of plasma membranes (Vance and Steenbergen, 2005). The products of SM metabolism, such as ceramide, sphingosine, sphingosine-1-phosphate, and diacylglycerol (DG) molecule, are also involved in cell signaling (Merrill, 2002).

STEROLS

Sterols (**ST**) are lipids that contain a common steroid core, a fusion structure of four rings with a side chain hydrocarbon and an alcohol group. The most important is **cholesterol**, a precursor of many compounds of steroid hormones (Trigatti, Rigotti and Krieger, 2000; Tajima *et al.*, 2007), particularly important for ovarian function. STs are also important constituents of cell membranes (Fahy *et al.*, 2005).

PRENOLS

The **prenol lipids (PR)** are formed from the precursors of 5 carbons. The carotenoids, vitamins E and K and ubiquinone are the examples of prenol lipid class (Ratnayake and Galli, 2009).

SACCHAROLIPIDS

The term "**saccharolipid**" **(SL)** is used to describe the compounds, where the FAs are directly linked to a carbohydrate, thereby forming structures that are compatible with the dual layer membrane (Fahy *et al.*, 2005).

POLYKETIDES

The **polyketides (PK)** are synthesized by the polymerization of acetyl and propionyl subunits. They include a large number of secondary metabolites and natural products of animal and vegetable origin, bacterial, fungal and marine, and characterized by high structural diversity (Fahy *et al.*, 2005).

1.2 Lipidomics

1.2.1 Tools and applications

In the last decades, the emergence of new techniques of very high precision analyzes, "omics" sciences, have contributed to the development and understanding of biological systems, whose main objective remains the search for predictive biomarkers of a physiological or pathological state. The complete characterization of biological systems can be done according to the four levels of genomics, transcriptomics, proteomics and metabolomics (Roux *et al.*, 2011). Into metabolomics, the lipidomic has emerged as an independent discipline (Lam and Shui, 2013; Han, 2016) the technological developments, particularly in mass spectrometry, have considerably increased the number of studies associated with lipidic analyzes (Roux *et al.*, 2011; Lam and Shui, 2013; Han, 2016).

Mass spectrometry (MS) ionization methods such as electron impact, laser desorption and rapid atomic bombardment were recognized in the application for lipid detection. Only a few "soft ionization" methods now play an important role in lipid analysis. Chemical Ionization at Atmospheric Pressure (APCI), electrospray ionization (ESI) and desorption / ionization mass spectrometry (MALDI) are considered widely used methods in "lipidomic" studies, since they allow the detection of intact lipid molecules and give only a small extent of fragmentation (reviewed by (Fuchs and Schiller, 2008)).

Lipidomics is a discipline that studies cellular lipids on a large scale based on analytical chemistry principles and technological tools, particularly mass spectrometry. Analytical technique rapidly advanced and novel applications of lipidomics, especially using MS, have emerged also in the biomedical research (Griffiths *et al.*, 2001; Yang, Kui; Han, 2017).

In fact, MSs allows detection and structural identification of charged or molecular elemental species (ions) according to their mass-load ratio (m/z). Analysis can be operated in both positive and negative ion modes (collision induced by dissociation), thus potentially expanding coverage. The systems, although widely varied, contain four main compartments, consisting of a system to introduce the molecules, followed by a source that makes it possible to transform them into gaseous ions and one or more analyzers separating their ions according to their a m/z interface, a detector for counting them, and finally an information processing system for recording mass spectra. Evolution of new sources of ions and mass analyzers (soft), the direct analysis of many compounds made it possible to measure a wide range of molecular compounds much faster, more accurate and more sensitive. This greatly reduced scanning times, improving resolution and specificity (Griffiths *et al.*, 2001; Pflege, Fowler and Koffa, 2010).

The identification of lipids is a challenge, because many molecular ion species are desorbed during the MALDI MS process. In general information from the profiling or imaging experiment, defines the molecular weight of the lipid based on the assumption that the ion is a $[M+H]^+$, $[M+Na]^+$, $[M+K]^+$ or $[M-H]^-$. Even, a fragmented ion of a larger lipid, for example by loss of H2O, or losing the polar head group to form a dehydrated or non-dehydrated fragment ion. Therefore, to verify the assumptions about the nature of the ion being considered is primordial for identification of the lipid species (Zemski Berry *et al.*, 2011).

Modern mass spectrometers, such as quadrupole mass analyzers, readily reach the mass measurement accuracy level of 0.1 Da. Thus, it provides information on the elemental composition of the desorbed ion of the tissue, i.e. ion species molecules. However, high-resolution instruments are capable of much better accuracy and mass resolution, such as orbitrap, Fourier transform / cyclone ion resonance (FT-ICR), and advanced flight analyzer (TOF) time. The resolution mass spectrometers allow the mass accuracies, high resolution between 20 ppm to 1 ppm (TOF, orbitrap and FT-ICR), that allow the exact mass of ions to be determined within errors at the fourth or fifth decimal place; and low resolution in 30 ppm to more (Zemski Berry *et al.*, 2011).

Lipidomic analysis allow the mapping of metabolic pathways of lipid classes, subclasses and individual species to help understand molecular mechanisms of lipid metabolism in biological systems.

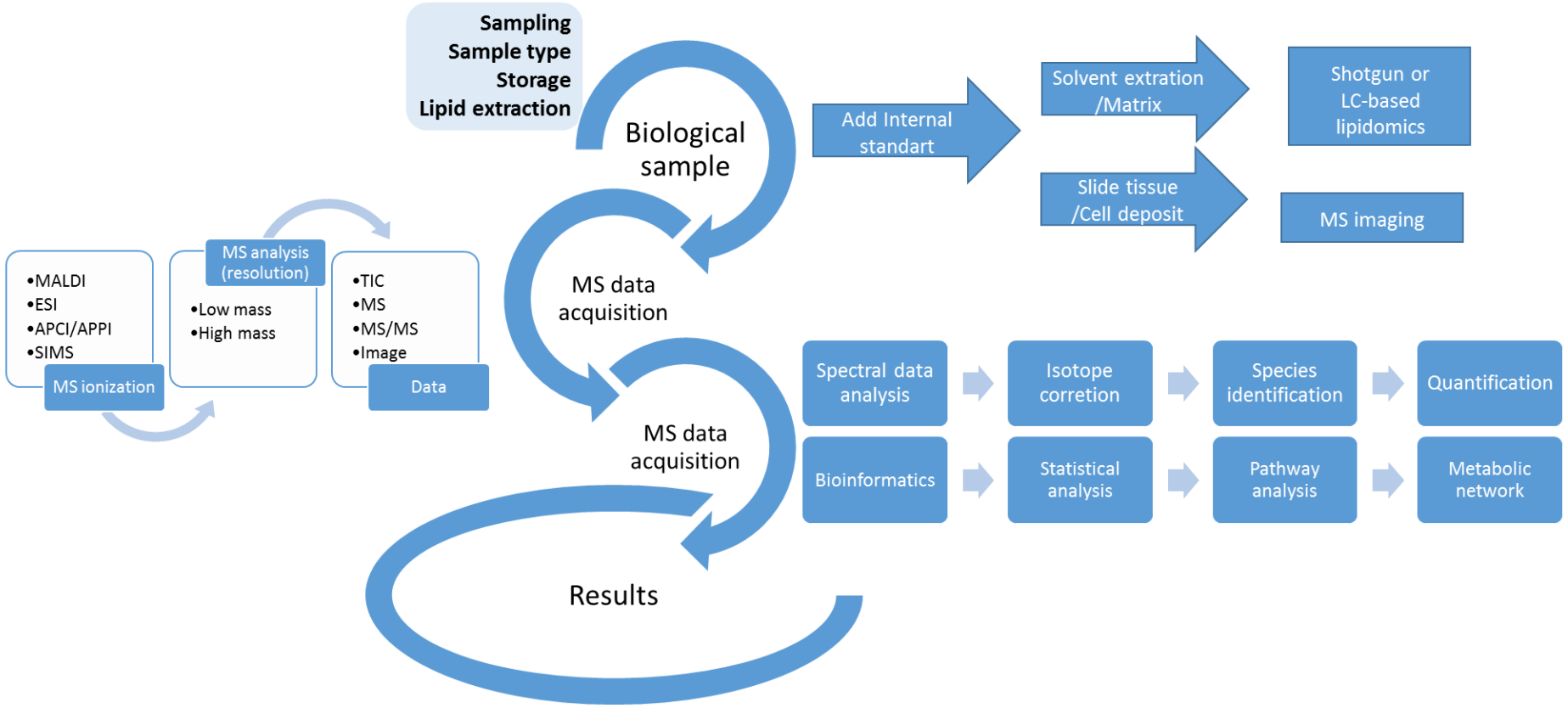


Figure 3. Lipidomic analysis of biological samples workflow. Sample preparation, mass spectrometry-based analysis (i.e., MS data acquisition), and data processing. (Adapt from (Yang Xianlin, 2017)). **Abbreviation:** MS: mass spectrometry; MS/MS: tandem mass spectrometry; LC: liquid chromatography; I.S.: internal standard; ESI: electrospray ionization; MALDI: Matrix assisted laser desorption/ionization; APCI: Atmospheric pressure chemical ionization; APPI: Atmospheric pressure photoionization; SIMS: Secondary ion mass spectrometry; TIC: total ion chromatogram.

1.3 Methods and techniques of lipid analysis

1.3.1 General workflow of lipid analysis in biological samples

General workflow of lipid analysis is shown **in Figure 3**. To perform lipid analysis, the collection and storage of the sample requires adequate conditions to avoid lipid degradation and/or oxidation. As far as profiling analysis of lipid species is concerned, most techniques use biological extracts, and lipid solutions are analyzed either by shotgun lipidomics or by chromatography-based lipidomics, particularly LC-based lipidomics. Alternatively, the tissue slice or cell samples are directly submitted to MS imaging. The addition of appropriate internal standards for qualitative and quantitative lipidic analysis is mandatory. Some commonly used methods as an internal standard are normalization to total protein, wet/dry tissue weight or volume of fluid for lipid quantification. Another critical factor is achieving sufficient efficiency and unbiased recovery of individual lipid species (lipid extraction performance) from biological materials (reviewed by (Yang Xianlin, 2017)).

1.3.2 Experimental approaches to analyze lipids

Lipid analysis is based on chromatographic methods, particularly liquid chromatography (LC) and thin-layer chromatography (TLC) (Christie, 2003). Applications of individual MS methods in lipid analysis have particularly been used after the invention of the so-called "soft-ionization" techniques, allowing the analysis of intact lipid molecules with only a small extent of fragmentation. These techniques are electrospray ionization (ESI), atmospheric-pressure chemical-ionization (APCI) and matrix-assisted laser desorption and ionization (MALDI) usually coupled to a time of flight (TOF) mass analyzer. Note that even if the detection of the intact lipid molecules is possible by the soft-ionization methods, MS/MS techniques are employed to recording mass spectra of intact lipids. Another technique for the analysis of phospholipids, but not lipids in general, is ^{31}P high resolution nuclear magnetic resonance (NMR) spectroscopy (Schiller and Arnold, 2002). Moreover, this technique has the disadvantage of being less sensitive than established methods and requires expensive equipment (Schiller *et al.*, 2006).

The most commonly used methods and techniques in lipidomics are listed in **Table 2.**

Table 2. Methods and techniques frequently used to determine lipid and fatty acid composition.

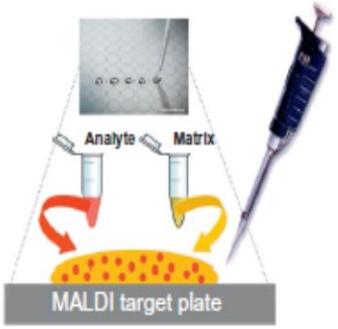
Technique	Applicable to	Advantages	Disadvantages
Mass spectrometry			
MALDI	All lipid classes, including complex lipids with highly polar residues	Simple, fast and sensitive technique. Sample impurities (e.g., salts, detergents) are tolerated to a high extent; may be combined easily with TLC	Individual lipid classes are detected with different sensitivities. Signal suppression of minor, less sensitively detectable PLs may occur when crude mixtures are analyzed
ESI	Principally all lipid classes; more useful for polar compounds	Can be coupled easily to HPLC, therefore, very suitable for the screening of complex mixtures; currently used most frequently in lipid analysis	Individual lipid classes are detected with different sensitivities. Signal suppression may occur when crude mixtures are analyzed. Very sensitive to contaminants (buffers, salts and detergents)
DESI	All lipid classes, including complex lipids	Can be performed under ambient conditions with minimal sample preparation, making it suitable for direct tissue analysis; Sensitive technique for 2D and 3D imaging of lipids from unmodified complex biological samples; definition of histology and tumor margins	The phenomenon of mutual conversion and ion suppression among different lipids may lead to a systemic error when detecting complex lipid extracts by direct analysis of ESI-MS; limited sensitivity
APCI	Principally all lipid classes; more useful for polar compounds	Separation of isomers and isobars; reduction of sample matrix effects; reduction of ion suppression; highly sensitive targeted analysis; offline or online 2D LC-MS for comprehensive profiling analysis; less susceptible to the effect of ionization suppression and salt buffer effects	Low throughput; pre-knowledge required for targeted analysis (e.g., for estabilishment of selected reaction monitoring (SRM) transitions); retention time drift; effects of mobile phase (e.g., composition, salts, or additives); complex data processing; limited identification of phosphoinositides, saccharolipids, as well as cardiolipins
APPI	Analysis of compounds that ionize poorly by ESI and APCI; detecting steroids, sphingolipids, some amino acids, nucleosides and purines	Separation of isomers and isobars; reduction of sample matrix effects; reduction of ion suppression; highly sensitive targeted analysis; offline or online 2D LC-MS for comprehensive profiling analysis; less susceptible to the effect of ionization suppression and salt buffer effects	Low throughput; pre-knowledge required for targeted analysis (e.g., for estabilishment of selected reaction monitoring (SRM) transitions); retention time drift; effects of mobile phase (e.g., composition, salts, or additives); complex data processing; limited identification of phosphoinositides, saccharolipids, as well as cardiolipins
SIMS	No prior sample treatment; determination of the molecular	Straightforward analysis without prior sample preparation; providing the closest possible to	Difficult to detect intact lipids due to severe source fragmentation

	composition and individual compound localization on tissue section with high spatial resolution; single cell detection	physiological conditions; high spatial resolution (submicrometer grade)	
Technique	**Applicable to**	**Advantages**	**Disadvantages**
NMR spectroscopy			
^{31}P NMR	Phospholipids	Nondestructive; direct, quantitative analysis of virtually all PLs	Expensive equipment. Relatively low sensitivity. High concentrations of detergent needed
^{1}H NMR	All lipids	Nondestructive; enables compositional analysis in addition to structural studies (of purified compounds); more sensitive than ^{31}P NMR	Crowded spectra in the case of lipid mixtures. Bulk lipids (cholesterol) detected primarily. Expensive equipment. Highly purified solvents required (for diluted samples)
^{13}C NMR	All lipids	Nondestructive; enables structural studies (of purified compounds); provides very good spectral resolution	Mixtures of lipids give crowded spectra. Bulk lipids (cholesterol) detected primarily. Expensive equipment. Very low sensitivity
Chromatography			
TLC	All lipid classes (solvent system depends on the mixture and the stationary phase)	Highly established method; simple, fast and inexpensive; can be established in all laboratories; using a suitable dye (e.g., primuline), densitometric analysis of spot intensities is possible	Provides only limited resolution. Differentiation of individual FAs is very difficult
HPLC	Nearly all known lipid and PL classes (after establishment of a suitable solvent system)	Differentiation of individual lipid classes (normal phase) and fatty acid composition (reversed phase) highly established; quantitative method	UV detection systems are not suitable for the detection of saturated FAs. UV absorptions depend strongly on fatty acid composition. Therefore, UV detectors are replaced increasingly by refractive index or mass detectors (more expensive detection systems)
GC	Works only with apolar compounds; hydrolysis and derivatization of PL is required prior to fatty acid analysis	Highly established for fatty acid compositional analysis of lipids; since GC is generally coupled with MS, detection of unusual FAs is possible (fragmentation patterns)	Requires volatile compounds and/or derivatization. Generally, complex mixtures must first be fractionated into the individual components

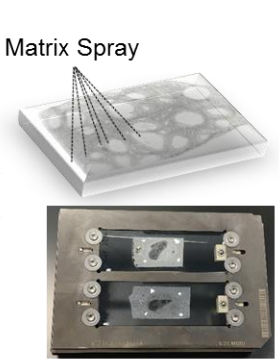
Abbreviations: ESI: Electrospray ionization; DESI: Desorption ESI; APCI: Atmospheric pressure chemical ionization; APPI: Atmospheric pressure photoionization; SIMS: Secondary ion mass spectrometry; GC: Gas chromatography; HPLC: High-performance liquid chromatography; MALDI: Matrix-assisted laser desorption and ionization; MS: Mass spectrometry; NMR: Nuclear magnetic resonance; PL: Phospholipid; TLC: Thin-layer chromatography; UV: Ultraviolet (Schiller *et al.*, 2006; Eberlin *et al.*, 2011; Yang, Kui; Han, 2017).



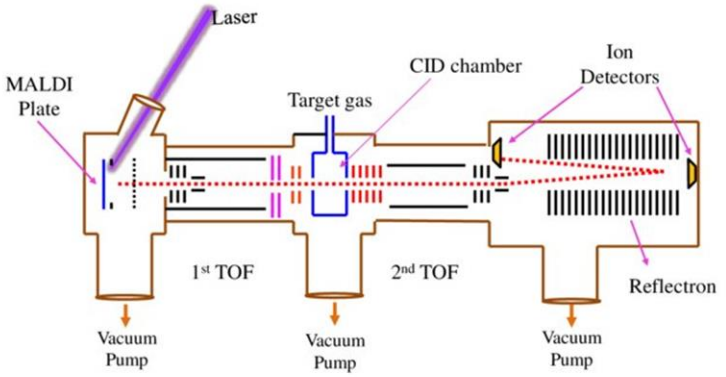
A. Ultraflex MALDI TOF/TOF mass spectrometry (Bruker®)



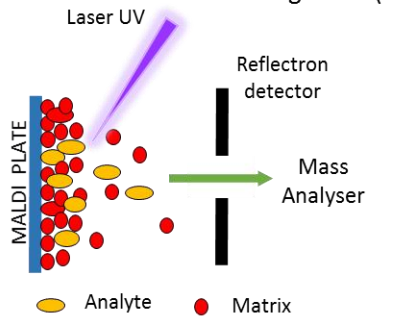
B. Sample preparation to cells, fluid and single cell (ICM)



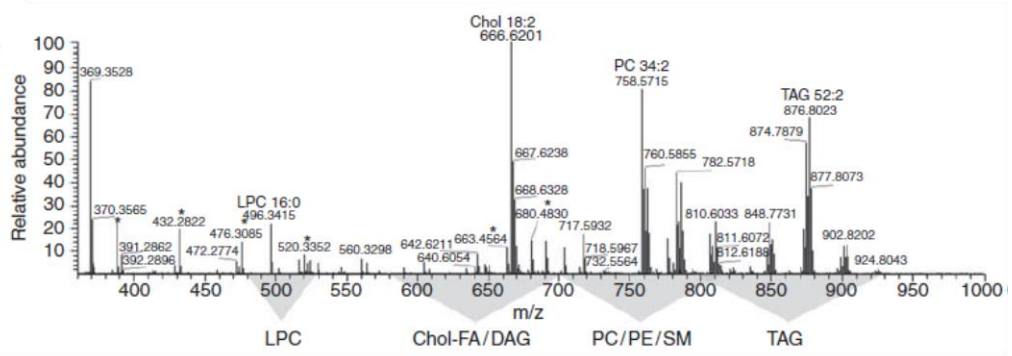
C. Sample preparation to tissue slides (IMS)



D. Schematic diagram of MALDI TOF Mass Spectrometer (Courtesy of Dr Dickson Wambua)



E. MALDI laser desorption process



F. MALDI spectrum

Figure 4. Schematic representation of MALDI-TOF mass spectrometry: A. Ultraflex MALDI TOF/TOF MS (Bruker®); **B.** and **C.** Sample cocrystalyzation with organic matrix; **D.** Laser desorption ionization to generate analytes ions, and detection in TOF MS; **E.** Detail of MALDI laser desorption process; **F.** A typical MALDI mass spectrum for species lipid. (Adapted from Cho et al. 2015 and Schwudke et al; 2011). **Abbreviation:** MALDI-matrix assisted laser desorption / ionization; TOF-time-of-flight; MS-mass spectrometry; ICM-intact cell MALDI-TOF; IMS-imaging mass spectrometry.

1.3.2.1 Mass spectrometry imaging

MALDI-MS is also largely used for mass spectrometry imaging (MSI) (Stoeckli *et al.*, 2001) that allows localization of individual molecular species directly on tissue sections (Jackson, Wang and Woods, 2005; Murphy, Hankin and Barkley, 2009; Chaurand *et al.*, 2011). MALDI MSI have merged specificity of lipid identification with two-dimensional molecular mapping to enable biochemical studies of lipids across regions of a biological tissue and/or single cells. MALDI MSI was adapted for analysis of biomolecules less than 1000 Da, thus including lipids. In addition, this low molecular weight facilitates the diffusion of lipids into a matrix crystal driven by the high concentration of the lipid within the microstructure of the tissue. It is also possible to obtain information regarding the lipid concentration at the tissue level, because the technique allows a resolution of 10-100 μm (reviewed by(Zemski Berry *et al.*, 2011)). MSI requires an appropriate matrix choice, allowing high quality and sensitivity to visualize lipid profiles of cells (including individual cells), tissues and even whole bodies. Peak ions corresponding to PC species prominent in the positive ion mode are detected preferentially, eliminating the effective analysis of other classes of positively charged lipids (reviewed by(Yang, Kui; Han, 2017)).

MALDI-TOF MS approaches used in this study are presented in **Figure 4**.

1.3.2.2 High Performance Liquid Chromatography (HPLC)

The high-performance LC (HPLC) is versatile and many lipids including GP, GL, SL, ST and FAs can be separated without any derivatization steps (Christie, 2003; Wenk, 2005). Mixtures of lipids and phospholipids can be separated according to their reaction to certain polymer compounds (termed "stationary phases"). The most established stationary phases for the separation of PL by HPLCA are based on silica gel and aluminum oxide. In this context, the term "normal silica gel" ("normal phase") or chemically modified silica gel ("reverse phase") is used respectively for separation. As a general rule, 'normal' columns are used for separating PL blends into individual PL subclasses, whereas 'inverted' columns are most commonly used for PL sorting according to differences in their fatty acid composition [reviewed by(Malviya *et al.*, 2010)].

1.3.2.3 LC/MS (by LTQ Orbitrap Velos)

Lipidomics relies on tandem MS/MS experiments that are either performed on-line with liquid chromatography or by infusion of total lipid extracts directly into a spectrometer (“shotgun” lipidomics). Generally assumed that collision-induced dissociation of lipid precursors produces fragment ions that are either characteristic for the entire lipid class or distinguish specific structural moieties in individual species. With the use of hybrid tandem mass spectrometers and a robotic nanoflow ion source, it has become possible to acquire full tandem mass spectra from hundreds of plausible lipid precursors. The

use of shotgun profiling by data-dependent acquisition was first developed for – and applied with – time-of-flight mass spectrometers (reviewed by(Schuhmann *et al.*, 2011)).

The LTQ Orbitrap Velos instruments equipped with a dual pressure linear ion trap supports high-resolution isolation of precursor ions (Olsen 2009). Hybrid linear ion trap Orbitrap tandem mass spectrometers (Makarov *et al.*, 2006) have advanced in rapid acquisition of MS/MS spectra, higher mass resolution, and optional MS fragmentation (Schwudke *et al.*, 2011). Higher energy collision dissociation (HCD), together with the high mass resolution and mass accuracy of the Orbitrap analyzer (LTQ Orbitrap), have performance in a quantification in total lipid extracts, accounting for biologically interesting lipid species comprising polyunsaturated and odd numbered FA moieties (Schuhmann *et al.*, 2011).

1.4 Regulation of lipid metabolism

The main aspects of lipid absorption, transport, storage and synthesis, including the lipid synthesis from different substrates, lipid transport via lipoproteins and lipid storage were first described in hepatic and adipose tissues, however these processes take place also in other tissues including ovary.

1.4.1 Lipids transport in body fluids

Biological mechanisms of absorption and transport of lipids in ruminants were described by (Bauchart, 1993). In bovine, short-chain FAs produced by fermentation in rumen are absorbed from the intestines into the intestinal lymph. During digestion, most TG are converted into MG and FAs. Then, while passing through the intestinal epithelial cells, the MG and FAs are resynthesized into new TG molecules that enter the lymph, dispersed droplets called *chylomicrons* that remain in lymph fluid. Also, most of the cholesterol and phospholipids absorbed from the gastrointestinal tract enter in the chylomicrons. The chylomicrons are then transported through the thoracic duct and emptied into the circulating venous blood at the juncture of jugular and subclavian veins. Chylomicron enriched in TG are hydrolyzed by lipoprotein lipase (LPL), and releasing FAs and glycerol can be stored in various tissues, mainly in adipose, skeletal muscle, heart, liver and ovary. The lipases also causes hydrolysis of phospholipids, which also releases FAs s to be stored in the cells in the same way (Bauchart, 1993; Ramasamy, 2014). Once inside the cell, the FA can be used for energy or synthesis of a new TG with new glycerol supplied from cell storage. The fat stored in adipose tissue will be transported to the other tissue mainly in form of free fatty acids (FFA) or non-esterified fatty acids (NEFA). These FAs are strongly ionized in the plasma and the ionic portion combines immediately with plasma albumin molecules. The transport is achieved by hydrolysis of the TG back into FAs and glycerol (Ramasamy, 2014).

Lipoproteins synthesis occur in liver to transport TG, cholesterol and PL. There are four major types of lipoproteins classified by their densities, as measured by ultracentrifugation column graduation: (1) ultra-low-density lipoproteins (chylomicrons), which contain mainly TG (more than 85%), 6-12% of phospholipids and 1-3% of cholesterol and only 1-2% of protein.

(2) very-low-density lipoproteins (VLDL), which contain high concentrations of TG and moderate concentrations of both cholesterol and phospholipids;

(3) intermediate-density lipoproteins (IDL), which are VLDL from which a part of TG has been removed, so the concentrations of cholesterol and phospholipids are increased;

(4) low-density lipoproteins (LDL), which are derived from IDL by the removal of almost all the TG, leading to high concentration of cholesterol and a moderately high concentration of phospholipids;

(5) high-density lipoproteins (HDLs), which contain a high protein concentration (about 50%) but much smaller concentrations of cholesterol and phospholipids (Brown and Goldstein, 1986; Ramasamy, 2014).

Each type of lipoprotein has a specific set of apolipoproteins (apo−). Apolipoprotein A−I (apoA1) associated with lecithin-cholesterol acyltransferase – membrane adhesion – is a component of HDL and chylomicrons. Apoplipoprotein B plays a particularly important role in lipoprotein transport, and a structure of chylomicrons, VLDL, LDL and IDL. Apolipoprotein C-II is an activator of lipoprotein lipase in chylomicrons, VLDL, IDL and HDL (Ramasamy, 2014). Chylomicrons, VLDL and HDL contain apolipoprotein A-IV (apoA4) which acts primarily in reverse cholesterol transport (Steinmetz *et al.*, 1990) and intestinal lipid absorption via chylomicron assembly and secretion (Ramasamy, 2014). Apolipoprotein E (apoE) plays an important role in the transportation and uptake of cholesterol by high affinity interaction with lipoprotein receptors, including LDL receptor (Chang *et al.*, 2017). The receptor bounding LDL is internalized by endocytosis. In mammals, the cholesterol content of the cell membranes is controlled by a family of membrane-bound transcription factors designated as sterol-regulated transcription proteins (SREBPs) (Goldstein and Brown, 2009; Rudenko *et al.*, 2011).

Other member of the LDL receptor family is scavenger receptor class B type I (SR-BI) that transports cholesterol esters selectively to steroidogenic cells (Rigotti, Miettinen and Krieger, 2003). The ATP-binding cassette A1 lipid (ABCA1) transporter is a key regulator of cholesterol (involved in reverse cholesterol transport from cells) and phospholipid transport to lipid free apolipoproteins (Favari *et al.*, 2009; Fujimoto *et al.*, 2009). Both have been associated with mammalian fertility (Attie, 2006; Fujimoto *et al.*, 2009).

The primary function of the lipoproteins is the transport of lipid components throughout the blood to

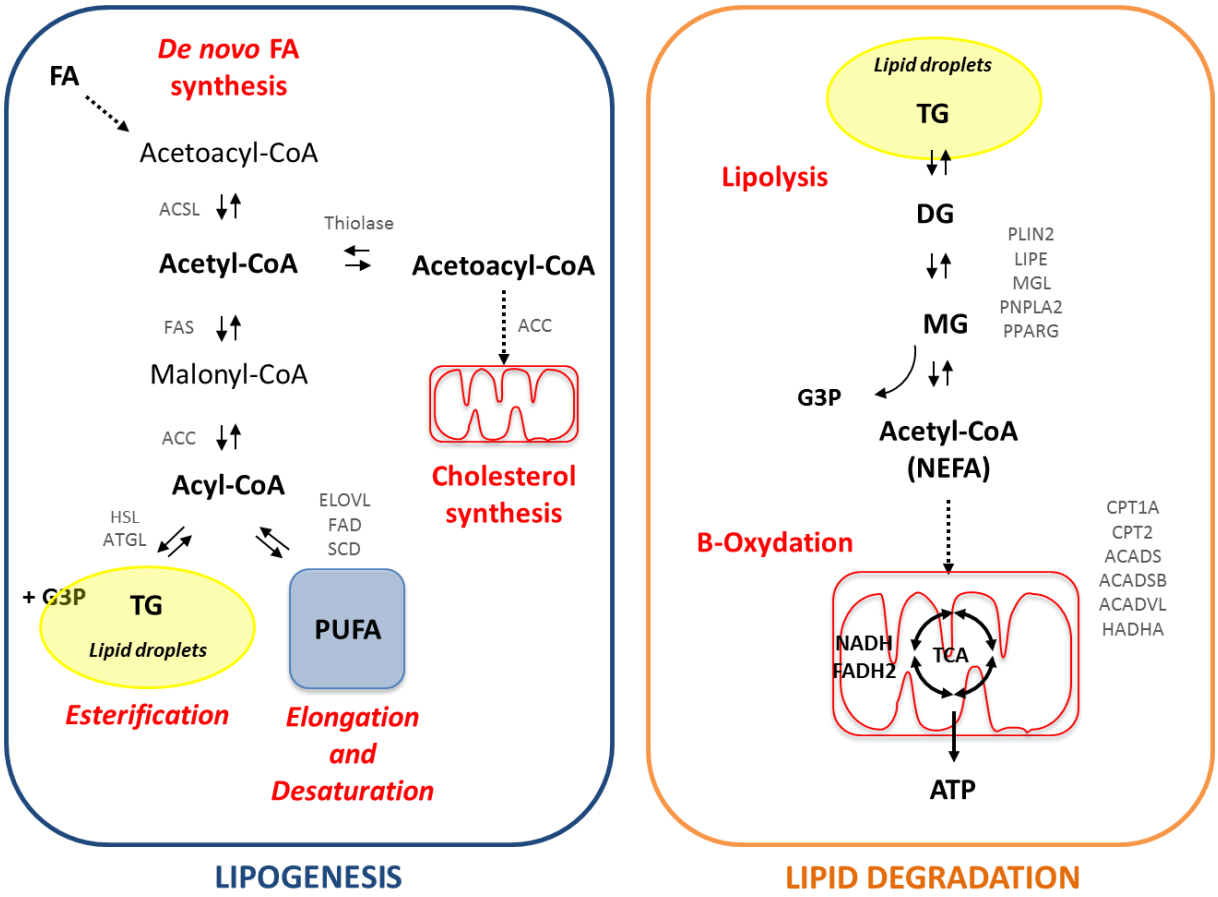


Figure 5. Scheme of the main steps of FA metabolism. Abbreviations: fatty acids (FA), acyl-CoA synthetase long-chain (ACSL), multi-enzymatic complex fatty acid synthase (FAS), ACC, acetyl-CoA carboxylase, hormone-sensitive lipase (HSL), adipose triglyceride lipase (ATGL), elongation of very long chain fatty acids (ELOVL), fatty acid desaturase (FAD), stearoyl-CoA desaturase (SCD), glycerol-3-phosphate (G3P), triacylglycerol (TG), diacylglycerol (DG), monoacylglycerol (MG), polyunsaturated fatty acid (PUFA), non-esterified fatty acids (NEFA), perilipin 2 (PLIN2), lipase E (LIPE, Hormone Sensitive Type E), monoacylglycerol lipase (MGL), patatin like phospholipase domain containing 2 (PNPLA2), peroxisome proliferator-activated receptor-gamma (PPARG), carnitine palmitoyltransferase 1A (CPT1A), carnitine palmitoyltransferase 2 (CPT2), acyl-CoA dehydrogenase short-chain (ACADS/ACADSB), acyl- Fatty acid metabolism CoA dehydrogenase very long-chain (ACADVL), hydroxyacyl-CoA dehydrogenase trifunctional multienzyme complex subunit alpha (HADHA), tricarboxylic acid cycle (TCA), nicotinamide adenine dinucleotide + hydrogen (NADH), Flavin adenine dinucleotide + 2 hydrogens (FADH2), adenosine triphosphate (ATP).

peripheral tissues and to other lipoproteins. When back to the liver, after lipid delivering, the lipoproteins are reconstructed. In reproduction system, lipoproteins contribute to intra-follicular cholesterol homeostasis that appears to be important for successful oocyte and embryo development (Fujimoto *et al.*, 2009; Santander *et al.*, 2018).

The schematic representation of several main steps of FA metabolism and its enzymatic regulation is presented in **Figure 5**.

1.4.1.1 Lipogenesis

Lipogenesis includes both FA synthesis and TG synthesis, where FAs are esterified to glycerol, during this process Acetyl-CoA is finally converted to TG. Synthesized FA can be further modified to GP, whose phosphate moiety can bear a number of different head groups, including serine, ethanolamine, inositol, choline, and glycerol (Van Meer, Voelker and Feigenson, 2008). All cells have a machinery to perform the synthesis of FAs in greater or lesser efficiency (Nakamura and Nara, 2003). The most common way for new generation of FAs occurs in the cytosol starting with Acetyl-CoA molecules and the enzyme acetyl-CoA carboxylase (ACC) (Grevengoed, Klett and Coleman, 2014). The biosynthesis of lipids and FAs is a complex interaction of multiple pathways beginning with the generation of palmitate (palmitic acid, C16:0). In the following steps, palmitate undergoes elongation and/or unsaturation steps to yield different FAs. Most of them are used for TG synthesis and stored within lipid droplets (Yamashita *et al.*, 2014; Saponaro *et al.*, 2015).

When the carbohydrates, main nutrition substrates for ruminants, enter into the body, they can be used immediately for energy or can be stored in as glycogen, the excess is rapidly converted into TG in the liver, then transported mainly as lipoproteins and stored in the adipose tissue (Blasiole, Davis and Attie, 2007; Saponaro et al., 2015). One of the factors, which plays a key role in the control of adipogenesis and lipogenesis in adipose tissue in ruminants, is peroxisome proliferator-activated receptor PPAR-γ (Bionaz et al., 2013). This transcription factor is also expressed in ovarian tissue and involved in controlling the female reproduction and fertility (Vitti et al., 2016).

1.4.1.2 *De novo* FA synthesis

***De novo* lipogenesis (DNL),** also referred as *de novo* fatty acids synthesis, is the synthesis of FA chains from acetyl-CoA subunits produced during glycolysis in the liver (Smith and Tsai, 2008). It occurs in cell cytoplasm where citric acid is converted to acetyl-CoA by ATP-citrate lyase (ACL) and subsequently to malonyl-CoA by acetyl-CoA carboxylase (ACC). DNL occurs mainly in the liver, but in adipose tissue as well, in low rates though. This process requires the two enzymes ATP-citrate lyase (ACL), acetyl-CoA carboxylase (ACC) and the multi-enzymatic complex fatty acid synthase (FAS).

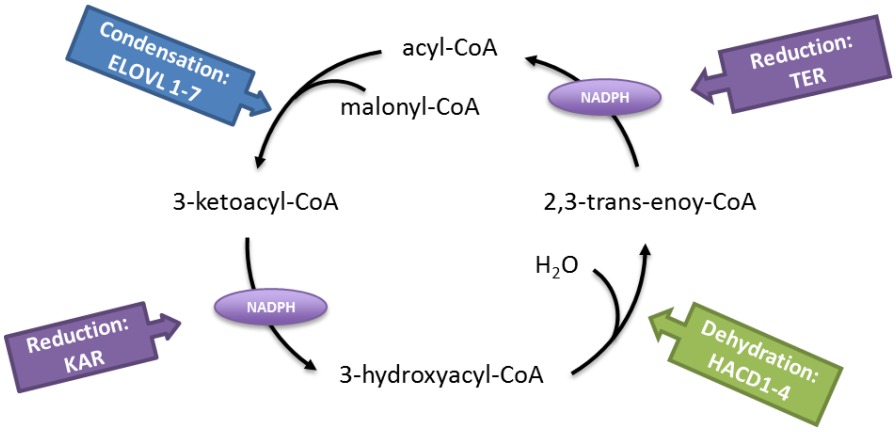


Figure 6. **FA elongation cycle**. The FA elongation cycle and the mammalian enzymes involved in each step are illustrated. Acyl-CoA is elongated to have two more carbon units in each elongation cycle, which consists of four steps (condensation, reduction, dehydration and reduction). (Adapted from (Kihara, 2012) . Abbreviations: 3-ketoacyl-CoA reductase (KAR), nicotinamide adenine dinucleotide phosphate (NADPH), FA elongases 1 to 7 (ELOVL1-7), 3-hydroxyacyl-CoA dehydratase 1 to 4 (HACD1-4), 2,3-trans-enoyl-CoA reductase (TER).

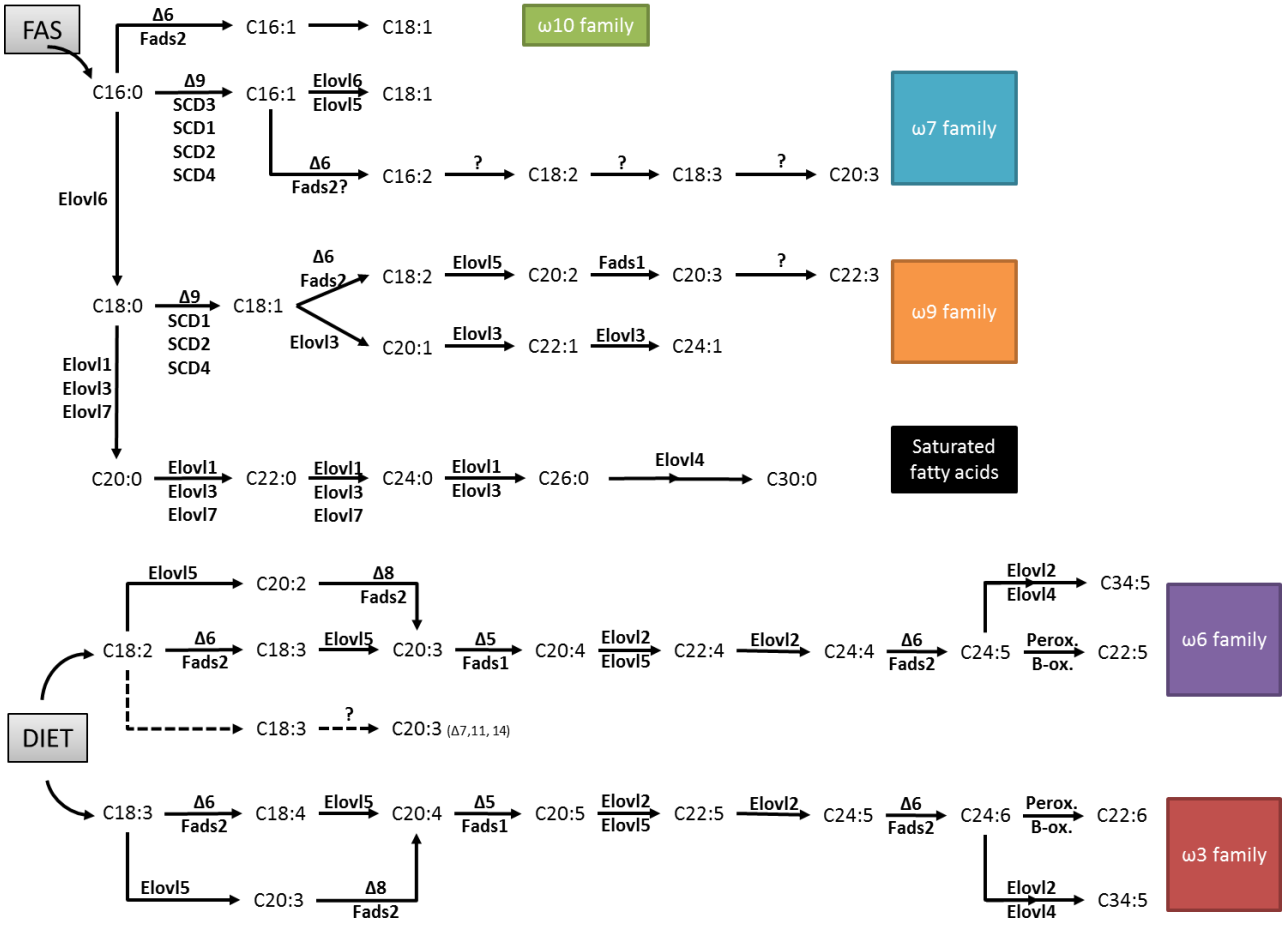


Figure 7. Scheme of FA elongation and desaturation (Adapted from (Guillou *et al.*, 2010). Abbreviation: **FAS** - fatty acid synthesis; **Elovl** - elongation of very-long-chain fatty acids; **SCD** - stearoyl-coA desaturases; **Fads** - fatty acid desaturases.

Glyceraldehyde 3-phosphate (G3P) can be synthesized directly from non-carbohydrate substrates such as pyruvate, lactate or amino acids.

1.4.1.3 Fatty acids elongation and desaturation

In many mammalian tissues, there are three elongation systems located in the cytosol, mitochondria and endoplasmic reticulum (ER). In the cytosol, FA elongation is part of *de novo* lipogenesis with a saturated FA (16:0-palmitate, 18:0-stearate, and lesser extent 14:0-myristate). The mitochondrial FA elongation occurs by the addition of 2C units from acetyl-CoA, via enoly-CoA reductase, but not malonyl-CoA (Raphael and Sordillo, 2013). FA elongation in ER's membranes is the major pathway for determining the chain length of saturated, monounsaturated, and polyunsaturated FAs. In mouse, rat and human, FA elongation utilizes malonyl-CoA, NADPH, and fatty acyl CoA as substrates under the action of seven FA elongases (ELOVL1-7) (Gurr, Harwood and Frayn, 2002; Donald B. Jump, 2009). Elongation is the pathway that use endogenous FAs from lipogenesis and exogenous FAs from diet and seldom produce non-esterified FA. Very long chain FA are most commonly found in sphingolipids, although they are also important constituents of glycerophospholipids, triacylglycerols and sterol- and wax-esters (Jakobsson, Westerberg and Jacobsson, 2006; Donald B. Jump, 2009; Guillou *et al.*, 2010).

Four separate enzymatic reactions of elongation pathway are shown in **Figure 6**: (1) condensation between the fatty acyl-CoA and malonyl-CoA to yield 3-ketoacyl-CoA;(2) reduction of 3-ketoacyl-CoA to generate 3-hydroxyacyl-CoA; (3) dehydration of 3-hydroxyacyl-CoA to produce trans-2-enoyl-CoA; and (4) reduction of trans-2-enoyl-CoA to form the elongated acyl-CoA (Osei *et al.*, 1989; Cinti *et al.*, 1992).

In mammals, the enzymes elongases (ELOVL, elongation of very-long-chain fatty acids) work as the initial enzymes and elongation-control enzymes in condensation reaction. Among the seven known ELOVLs, ELOVL 1, ELOVL 3, ELOVL 6, and ELOVL 7 catalyze saturated FAs and mono-unsaturated FAs (MUFAs). For polyunsaturated FAs (PUFA), the elongases ELOVL 2, ELOVL 4 and ELOVL 5 are selective (Donald B. Jump, 2009; Kihara, 2012). In mice, the *Elovl*, *Elovl1*, *Elovl5* and *Elovl6* genes are expressed ubiquitously, whereas *Elovl2*, *Elovl3*, *Elovl4* and *Elovl7* show more tissue-specific expression levels, indicating that this is related to the tissue needs for the Very-Long-Chain FA (VLCFA) synthesized by the different elongases (Guillou *et al.*, 2010).

Desaturases are selected for a substrate-specific to interact with the elongases (**Figure 7**). The acyl-coenzymes A (CoA) desaturases introduce a double bond to the long chain FA acyl chain at a specific position, characterizing the biological properties of these complex FAs. In desaturases, Δ-number indicate the molecule position in which the double bond will be introduced. Δ9, Δ6 and Δ5-desaturases

are expressed in mammals. Also, desaturases are separated into two distinct families, stearoyl-coA desaturases (SCD) (Paton and Ntambi, 2009) and fatty acid desaturases (FADS) (Nakamura and Nara, 2004). SCDs introduce a single double bond at position D9 counting from the carboxylic acid moiety of saturated fatty acids such as palmitic and stearic acid. Furthermore, SCD-1 (Δ9-desaturase) is co-localized with diacylglycerol acyl transferase 2 (DGAT2) in the ER (Man *et al.*, 2006), which may explain why MUFAs produced endogenously are incorporated more efficiently into non-polar lipids than dietary MUFAs. The Δ6- and Δ5-desaturases genes were designated as FADS. These enzymes can introduce a double bond at position D6 on the acyl chain of linoleic (C18:2n - 6) and a-linolenic (C18:3n - 3) acids (essential fatty acids of the n - 6 and n - 3 series, respectively) (Guillou *et al.*, 2010). De Antueno and coworkers (De Antueno *et al.*, 2001) showed that, like Δ6-desaturase, Δ5-desaturase utilizes members from both the n - 6 (C20:3) and n - 3 (C20:4) series as substrates.

1.4.1.4 Lipolysis

Lipolysis is the intracellular catabolism of TGs, where they are successively hydrolyzed in DG (diacylglycerides) and MG (monoacylglycerides) to finally release three molecules of FA and one molecule of glycerol per one TG molecule. Hydrolysis of TG to DG is controlled by ATGL (adipose triglyceride lipase) and hydrolysis of DG to MG by HSL (hormone sensitive lipase encoded by gene *LIPE*). MGs are hydrolyzed by a different enzyme, MAGL (monoacylglycerol lipase, encoded by), which releases glycerol and the latter FA and has no known regulatory role. TG hydrolysis is generally complete, although some DGs and MGs may accumulate. Since glycolytic activity is low in adipose tissues, the final glycerol is released into the bloodstream for use by other tissues.

1.4.1.1 Degradation of Fatty Acids to Acetyl Coenzyme A by Beta-Oxidation

1.4.1.1.1 Mitochondrial

Degradation and oxidation of short, medium, and long chain FAs occur in the mitochondria through aerobic process of breaking down a FA into acetyl-CoA units, a cyclical series of reactions (Christian and Spremulli, 2012). The transport of FAs into the mitochondria are made by carnitine palmitoyltransferase (CPT) system. Once inside the mitochondria, FAs split away from carnitine and are degraded and oxidized by progressive release of two-carbon segments in the form of acetyl-CoA from acyl-CoA at the carboxyl terminal. Each cycle generate NADH, FADH2 and acetyl coenzyme A (CoA), until the last when two acetyl-CoA molecules are produced from the catabolism of a four-carbon FA (Qu et al. 2016). The bond is broken between the second carbon/beta carbon and the third carbon/gamma

carbon, hence the name beta oxidation (Kumari, 2018). FAs move in this pathway as CoA derivatives utilizing NAD and FAD hydrogens. Hydrogens are transported by NADH+ and FADH2+ to the respiratory chain leading to synthesis of ATPs molecules (Niemann and Rohrbach, 2016; Kumari, 2018).

1.4.1.1.2 Peroxisomal

Fatty acid beta-oxidation of very long chain FAs (C22:0, C24:0, C26:0) is performed in peroxisomes (Baarine *et al.*, 2012), as well as in others metabolic process such as FA alpha-oxidation, glyoxylate detoxification, and biosynthesis of ether phospholipids (plasmalogens). Peroxisomes are likely derived from the ER (Schrader and Fahimi, 2008). In general, peroxisomal beta oxidation exhibits widely identical structures compared to mitochondria but differs regarding the first metabolic step, which is processed by isoforms of the flavoprotein acyl-CoA oxidase (ACOX1 and 2). Scheme of both ways of FA oxidation is shown in **Figure8**.

1.4.1 FA transporters

Cell uptake and transport of long chain FAs involve both passive diffusion and protein-mediated transport. Proteins associated with membrane transport include FA transport proteins (FATPs), FA translocase (FATs) /CD36-SRB2, FA binding proteins (FABPs), and mitochondrial enzymes complex carnitine palmitoyltransferases (**Figure 9**).

The fatty acid transport protein (FATP) complexes transport non-esterified long-chain FAs (LCFAs) through both a passive flip-flop as well as across the plasma membrane. First, FAs are accumulated on the plasma membrane by binding to protein CD36, also known as fatty acid translocase (FAT) or scavender receptor class B member, which subsequently deliver the FAs to FATPs. CD36 is a main protein involved in FA transport across the plasma membrane (Bonen *et al.*, 2004). Translocation of CD36 from an intracellular depot to the cell surface is insulin-induced and also appears to be involved in mitochondrial FA oxidation, as this protein is located on the mitochondrial membrane and seems to be required to participate in moving FA across the mitochondrial membrane in muscle tissues (Koonen *et al.*, 2005; Glatz and Luiken, 2017).

Regulation of FA uptake as well as intra- and extracellular transport of a single ligand as long chain FA, cholesterol or retinoid to the peroxisome, mitochondria or endoplasmic reticulum are realized by Fatty Acid Binding Proteins (FABP). There are nine FABPs identified so far, and they show tissue-specific expression (L=FABP1 (liver), I=FABP2 (intestinal), H=FABP3 (muscle and heart), A=FABP4 (adipocyte), E=FABP5 (epidermal), Il=FABP6 (ileal), B=FABP7 (brain), M=FABP8 (myelin) and T=FABP9 (testis). (Chmurzyńska, 2006).

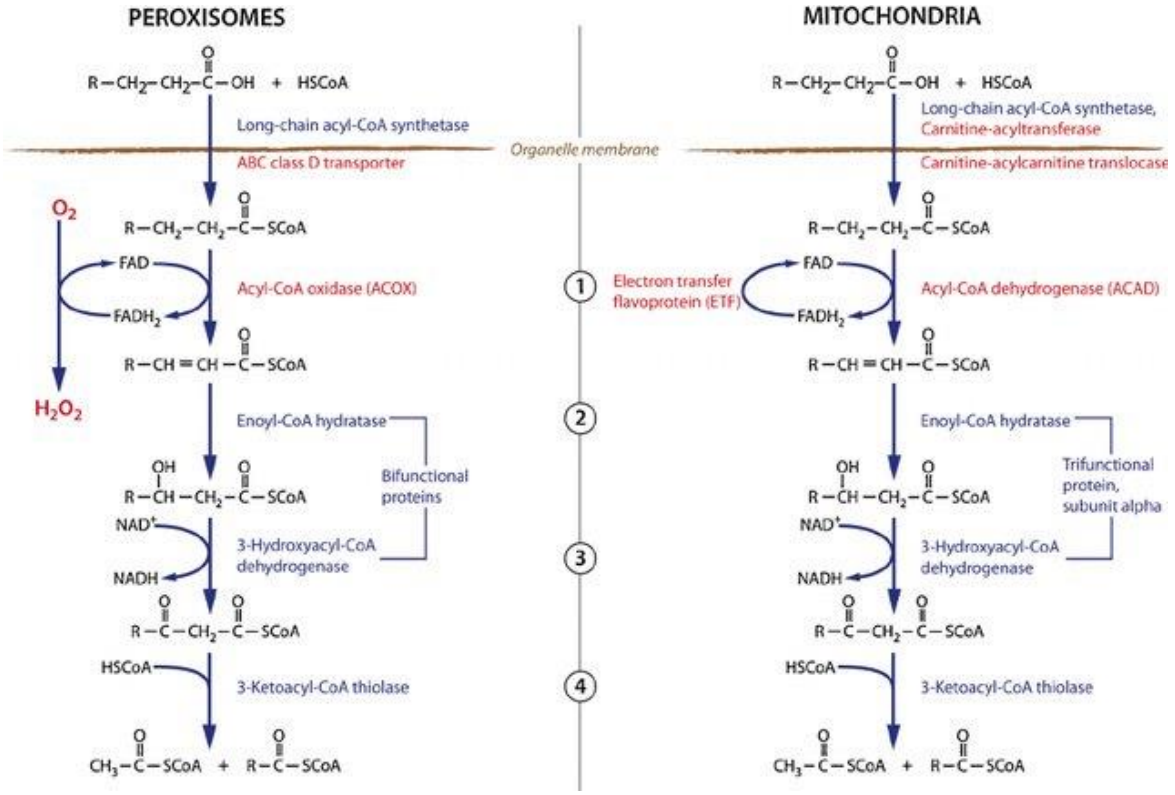


Figure 8. Scheme of long-chain FAs oxidation in peroxisomes and mitochondria (from (Schrader *et al.*, 2015).

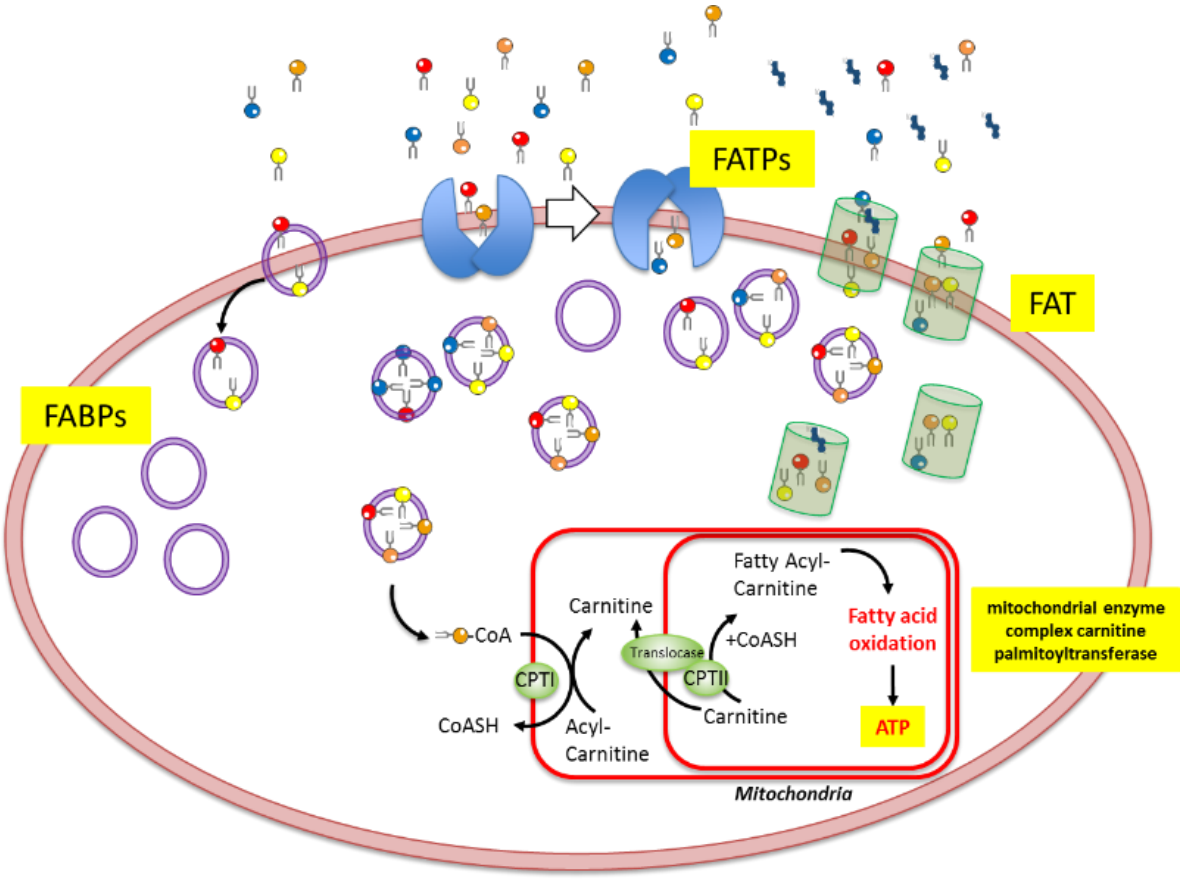


Figure 9. Lipid transporters. FA and cholesterol uptake by membrane transporters. FATP: fatty acid transport proteins; FABP: fatty acid binding proteins; FAT: fatty acid translocase (CD36); CPT: carnitine palmitoyl-transferases.

Carnitine palmitoyltransferase (CPT) transport system allows long-chain FAs to penetrate the mitochondrial inner membrane from cytoplasm. The components involved in this transport system are CPTI, the carnitine acylcarnitine translocase (CACT) and CPTII. CPTI manages the FA entry on the mitochondrial outer membrane (LEIJ *et al.*, 1999; Qu *et al.*, 2016). It catalyzes the rate-limiting step of FA oxidation by converting acyl-CoAs into acylcarnitines. CACT is an inner membrane protein that exchange acylcarnitine and carnitine between outer and inner mitochondrial membranes. CPTII is located in the matrix side of the mitochondrial inner membrane (Rufer, Thoma and Hennig, 2009) and it is responsible for converting acylcarnitine back into acyl-CoAs for oxidation.

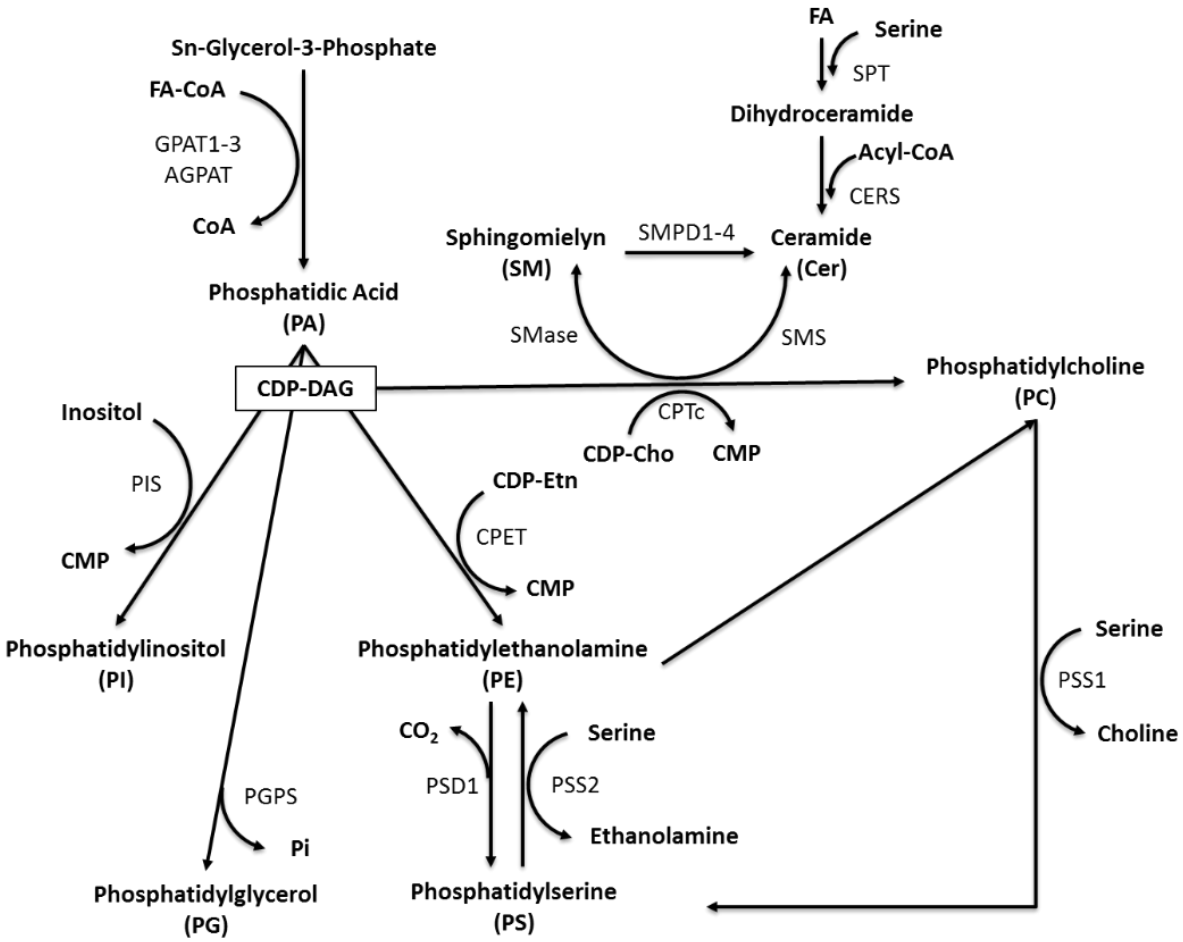


Figure 10. Schema of biosynthesis pathways for the phospholipid and sphingolipid classes biosynthesized in mammalian cells. Abbreviation: **CMP**-cytidine monophosphate; **CDP**-cytidine diphosphate; **GPAT1/3**-glycerol-3-P acyl transferase; **AGPAT**-acylglycerol-3-P acyl transferase; **CDP-DAG**-diacylglycerol synthase; **CPT-Cho**-CDP-choline:1,2-diacylglycerol phosphatidylcholine; **CPTc**-CDP-choline:1,2-diacylglycerol cholinephosphotransferase; **PIS**-PI synthase; **CPT-Etn**-CDP-choline:1,2-diacylglycerol phosphatidylethanolamine; **CPET**-CDPEtn:1,2-diacylglycerol ethanolaminephosphotransferase; **PSD1/2**-phosphatidylserine decarboxylase isoforms; **PGPS**-PG-P synthase; **Pi**-inorganic phosphate; **PSS**-Phosphatidylserine synthase isoforms; **SMS**-sphingomylelin synthase; **SMase**-sphingomylenase; **SMPD1/4**-Sphingomyelin phosphodiesterase; **CERS**-dihydroceramide synthase; and **SPT**-serine palmitoyl transferase (Adapted from (Zemski Berry *et al.*, 2011).

1.5 Lipid synthesis

1.5.1 Membrane synthesis

Phospholipids play a central role in the biochemistry of cells membrane. These molecules constitute not only the lipid bilayer defining the outer confines of a cell, but also serve as the structural entities which confine subcellular components (Pulfer and Murphy, 2003). The mechanisms involved in the formation of these hydrophobic molecules help the understanding of the levels of dynamic organization both across the lipid bilayer (lipid asymmetry) and in the lateral dimension (lipid domains) of membranes (Van Meer, Voelker and Feigenson, 2008). Principle metabolic pathways were summarized in **Figure 10**.

1.5.2 Glycerophospholipid synthesis

Glycerophospholipids PC and PE are the most abundant species of phospholipids in eukaryotic membranes. The PS and PI lipids are less abundant, thus play important roles in the structure and function of the membranes. The base for the production of phospholipids are FAs both from dietary source and internal synthesis. The synthesis of PC and PE occurs in endoplasmatic reticulum (ER) membrane, in association with mitochondrial reactions, by CDP-choline pathway, known as a part of Kennedy pathway (Gibellini and Smith, 2010; Yang, Lee and Fairn, 2018). The other half is the CDP-ethanolamine pathway which is responsible for the biosynthesis of PE species (Gibellini and Smith, 2010). The CDP-choline pathway begins with an uptake of choline accomplished by different choline transporters (Michel, Yuan and Ramsubir, 2006). Inside the cell, the choline undergoes enzymatic reaction of phosphorylation catalyzed by choline kinase (CK) resulting in PC. The CK isoforms are also able to phosphorylate ethanolamine (Kent, 1995). PE synthesis use CDP-ethanolamine pathway, which uses a series of similar reactions such as for PC, instead of choline use ethanolamine to form PE.

The process of synthesis of phosphatidylinositol (PI) begins with the consumption of phosphatidate (PA) on the cytosolic leaflet of the ER produce cytidine diphosphate diacylglycerol (CDP-DAG), called CDP-DAG pathway. The CDP-DAG is then used as a substrate by the phosphatidylinositol synthase enzyme (PIS) to catalyze the production of phosphatidylinositol (PI) from CDP-DAG. CDP-DAG is also used in the mitochondria by the phosphatidylglycerophosphate synthase (PGPS) to produce phosphatidylglycerol (PG)-phosphate, which is, in turn, dephosphorylated to produce PG (Yang, Lee and Fairn, 2018).

The PS synthesis occurs through utilizing different substrates involving distinct enzymes (PS synthase I and II). The reaction involves exchange of L-serine with phosphatidylcholine, catalysed by PS synthase

I, or with phosphatidylethanolamine, catalysed by PS synthase II. It is strictly dependent on calcium ions and requires no further source of energy (Gibellini and Smith, 2010; Holthuis and Menon, 2014).

The PC are more abundant in the external leaflet of the bilayer of the regular external cell membrane, whereas the aminophospholipids, like PS and PE, as well as the PI, are found in greater concentration in the inner leaflet (Fadeel and Xue, 2009), thus defining the electric potential difference of the cell (Zemski Berry *et al.*, 2011). There are phospholipid (PL) translocations in lipid bilayers that allow interchanges between internal and external PLs for adequate membrane integrity and functionality. The spontaneous flip-flop of PLs between leaflets of a bilayer is associated with energy expenditure. Scramblases proteins can mediate the bidirectional transfer of PLs between leaflets in an energy-independent manner thereby crumbling the symmetry of the membrane. Conversely, flippases (inward movement) and floppases (outward movement) are energy-dependent proteins that couple the consumption of ATP with the movement of lipids across the bilayer (Holthuis and Menon, 2014; Yang, Lee and Fairn, 2018).

1.5.3 Sphingolipid synthesis

The biosynthesis of sphingolipids is quite complex but a simplified version is described by Merril (2002). The palmytoyl-CoA combining with serine to make 3-ketosphinganine by serine palmitoyltransferase that is converted to sphinganine by 3-ketosphinganine redutase. Sphinganine can then transform to dihydroceramide, by dihydroceramine synthase. This dihydroceramide can be desaturated to form ceramide by dihydroceramine desaturase, containing the long-chain base sphingosine (Merrill, 2002; Zemski Berry *et al.*, 2011). Ceramides are biosynthetic intermediates of sphingolipids and therefore the central core of sphingolipid metabolism. The enzyme-mediated reaction by sphingomyelin phosphodiesterase (SMPD) converts sphingomyelin to ceramide (Schuchman *et al.*, 1991; Acuña *et al.*, 2016). Ceramides may also arise from *de novo* biosynthesis or turnover of glycosphingolipids (Yang, Lee and Fairn, 2018).

1.5.4 Cholesterol synthesis

Cholesterol is *de novo* synthesized by cells, even with an abundant source of dietary origin (70-80%). Cholesterol is transported by the circulation in lipoprotein particles, as well as cholesterol esters (CE). The cholesterol biosynthesis pathway involves enzymes that are in the cytoplasm, mitochondria, ER, and peroxisomes. Synthesis of cholesterol, is dependent on two-carbon acetate group of acetyl-CoA. The first step is mevalonate synthesis, by a series of reactions that begins with the formation of 3-hydroxy-3-methylglutaryl-CoA (HMG-CoA), which itself culminates with the synthesis of the isopentenyl pyrophosphate (IPP). All the reduction reactions of cholesterol biosynthesis use NADPH as

a cofactor. Acetoacetyl-CoA and a third mole of acetyl-CoA are converted to HMG-CoA by the action of the cytosolic version of HMG-CoA synthase (HMGCS). HMG-CoA is then converted to mevalonate by HMG-CoA reductase (HMGCR) – limiting step of cholesterol biosynthesis (**Figure 11**). This enzyme is bound in the endoplasmic reticulum and needs a phosphorylation to become active. Mevalonate is converted to the IPP, by mevalonate kinase. After that, the squalene synthase catalyzes the two-step head-to-head condensation of two molecules of IPP, yielding squalene. Squalene then undergoes a two step cyclization to yield lanosterol, first by squalene epoxidase (also called squalene monooxygenase) and in the second step through the action of the enzyme lanosterol synthase (2,3-oxidosqualene-lanosterol cyclase). The terminal reaction in cholesterol biosynthesis is catalyzed by the enzyme 7-dehydrocholesterol reductase (DHCR7) and squalene is converted to cholesterol (Nes, 2011; Holthuis and Menon, 2014).

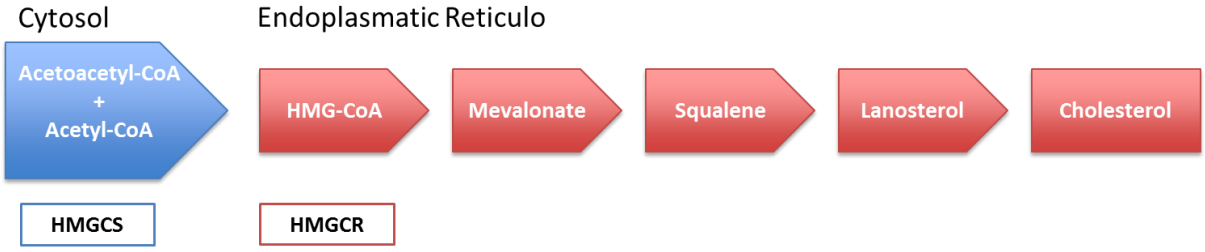


Figure 11. **Simplified scheme of cholesterol synthesis.** Abbreviations: 3-hydroxy-3-methylglutaryl-CoA (HMG-CoA); HMG-CoA synthase (HMGCS); HMG-CoA reductase (HMGCR).

Membranes, constituted by different lipids (phospholipids, glycolipids, and cholesterol) and various proteins, acting as receptors and channel pores, regulate the entry and exit of FA and other molecules and ions as part of the cellular metabolism.

1.6 Lipid storage

TG are the main neutral derivatives of glycerol and the most important fat reserve in animals. TG are stored in lipid droplets (LDs), highly dynamic organelles that play a very important role in the regulation of intracellular lipid storage and lipid metabolism in different tissues (Hashemi and Goodman, 2015). LDs are functionally linked to many physiological and pathological conditions, including obesity and related metabolic diseases. LDs are consist of neutral lipid core, a surface phospholipid monolayer and proteins, which are either embedded in or bound to phospholipid layer. In somatic cells, captured FAs are esterified into TG and cholesterol esters (CE) and thus could be stored as neutral lipids in LDs.

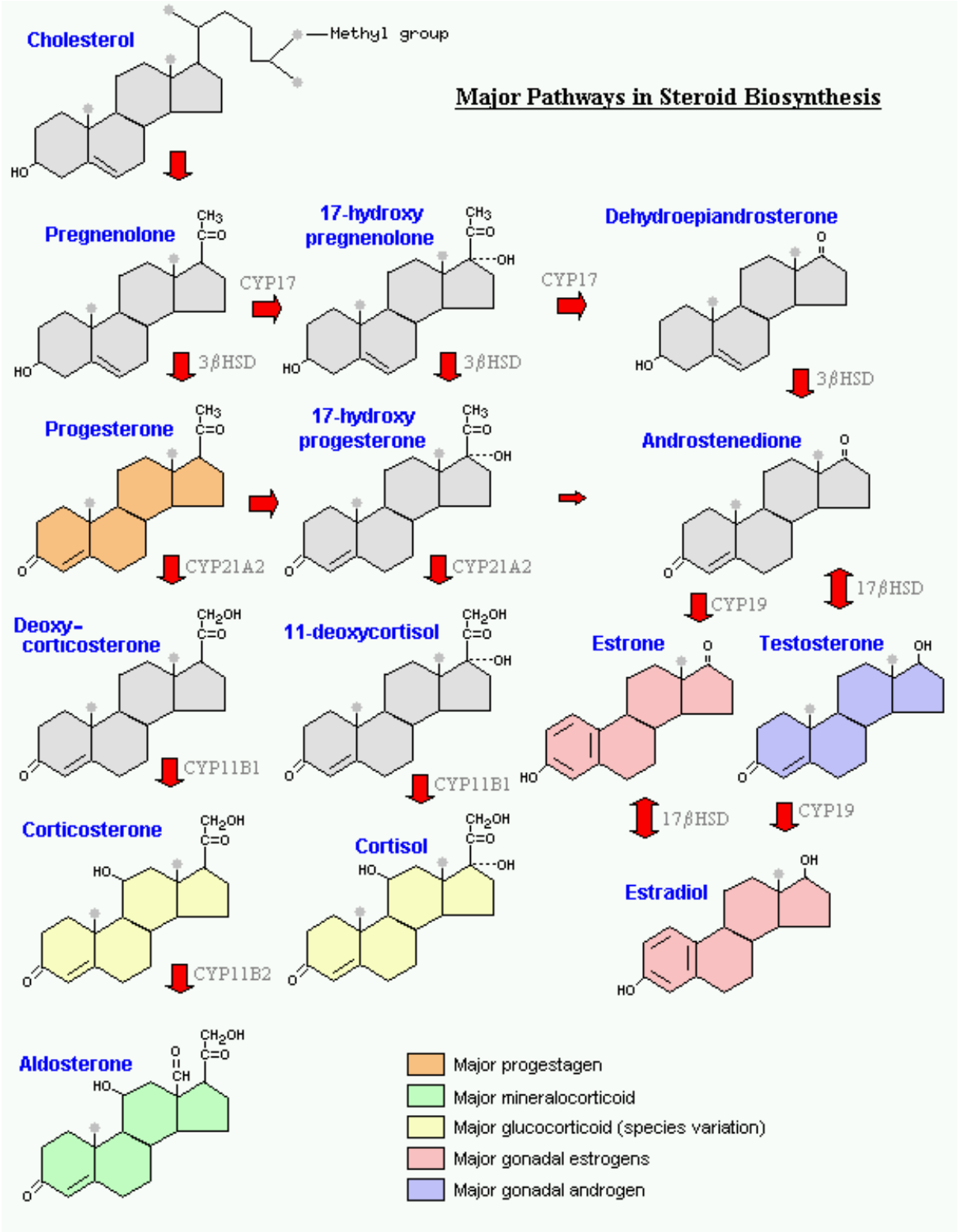


Figure 12. Major pathways of steroidogenesis (from (Gunter, 2016); https://drjengunter.wordpress.com/2016/01/11/). Steroid hormons are derivates of cholesterol and are produced in the adrenal glands in the ovaries. The main ovarian steroids are shown in rose (estrogens). **Abbreviation:** CYP- Cytochrome P450 Family, 3βHSD- 3-Hydroxy-Delta-5-Steroid Dehydrogenase, beta family.

LDs are especially abundant in adipose tissue and regulate fat storage and hydrolysis. LDs in steroidogenic cells, such as ovarian granulosa and adrenocortical cells, as well as testicular Leydig cells, primarily accumulate CE (Sato *et al.*, 2006). Steroids are also highly concentrated energy stores. However, they are not typically sources of energy; in mammals, and they are normally metabolized and excreted.

All LDs contain the proteins, essentially perilipins (PLIN). One of them is PLIN2, alias adipose differentiation-related protein (ADRP), which may control the stabilization of lipid droplets and lipolysis for utilization (Gu *et al.*, 2015). PLIN2 is predominant in granulosa cells (Khor *et al.*, 2014). Higher levels of PLIN2 have been suggested to be protective against lipotoxicity and insulin resistance in skeletal muscle (Jagerstrom *et al.*, 2009), and also in cumulus cells (Aardema *et al.*, 2013).

1.7 Steroidogenesis

Steroidogenesis is generation of steroids from cholesterol. Together with the phospholipids, steroids are components of cell membranes and regulate membrane fluidity. Steroids hormones function as signaling molecules. Biosynthesis of steroid hormones is regulated by pituitary trophic hormones and other steroidogenic stimuli. The steroidogenic acute regulatory (StAR) protein is an indispensable component in the regulation to translocate cholesterol from the outer to the inner mitochondrial membrane in steroidogenic cells, the rate-limiting step in steroid hormone formation. In all steroidogenic tissues, regardless of the hormones synthesized, the initial step in steroidogenesis is the conversion of cholesterol to the first steroid, pregnenolone. This conversion occurs via the action of the cytochrome P450 side-chain cleavage enzyme (P450scc), which is present in the inner mitochondrial membrane in all steroidogenic cells. Pregnenolone then exits from the mitochondria and is converted to progesterone by 3-βhydroxysteroid dehydrogenase (3-βHSD) in the ER. Steroidogenic cells do not store significant levels of steroidogenic hormones, stimulation being necessary to synthesize new steroids, requiring a constant supply of cholesterol as a precursor for conversion to steroid hormones. In brief, cholesterol used for steroidogenesis can be derived from a mix of sources: (1) *de novo* cellular cholesterol synthesis in the ER, (2) the mobilization of CEs stored in LDs, and (3) lipoprotein-derived CEs obtained by either LDL receptor-mediated endocytic uptake or “selective” cellular uptake via the scavenger receptor, class B type I (SR-BI) (Shen, Azhar and Kraemer, 2016).

Schematic representation of main steps of steroidogenesis is presented in **Figure 12**.

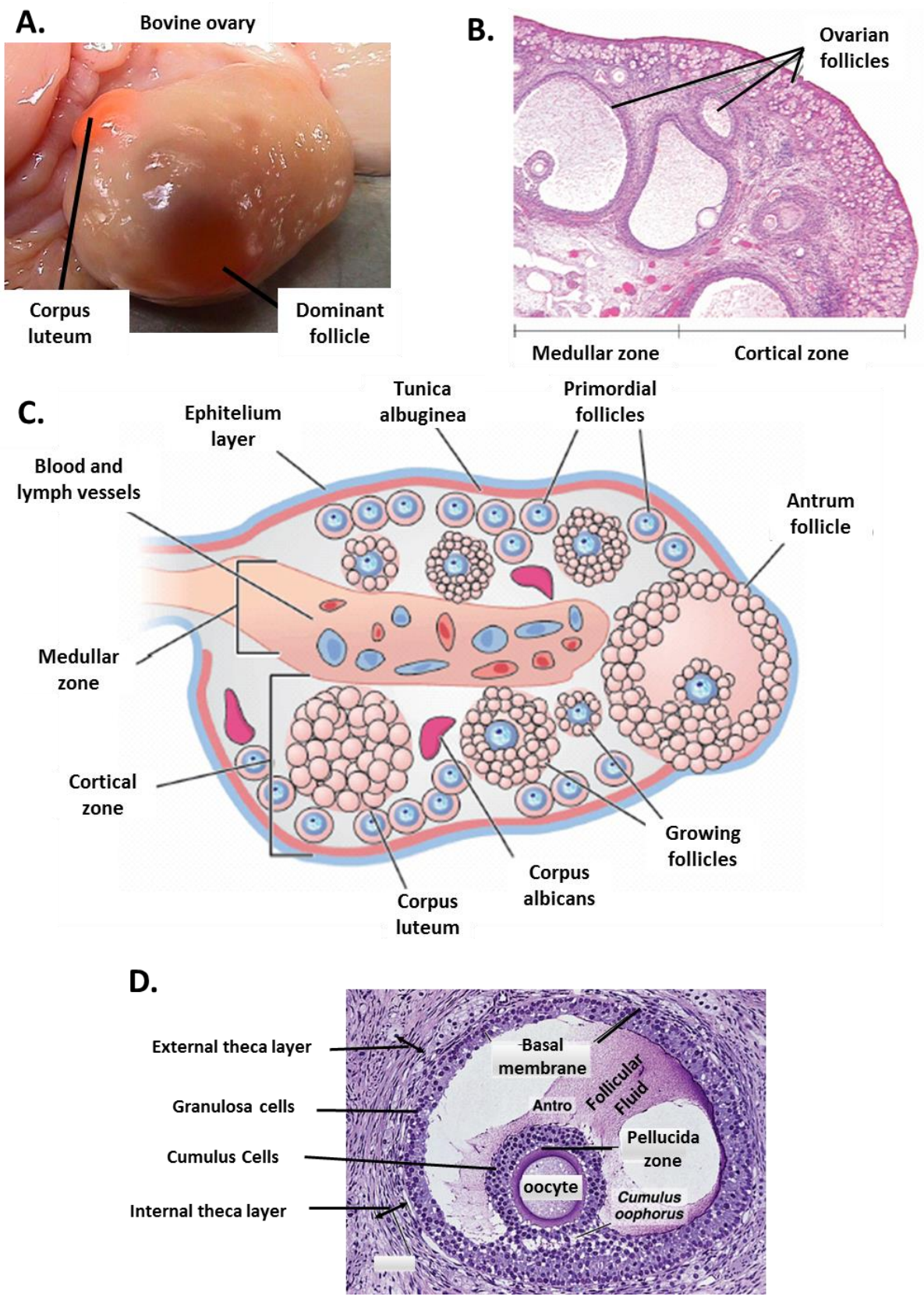


Figure 13. Morphology of the ovary. **A.** Bovine ovary recovered post-mortem, showing pre-ovulatory antral follicle. **B.** Histological section of ovary showing follicles in different stages of development. **C.** Scheme of ovarian structures, medullary and cortical zones, showing different phases of folliculogenesis. **D.** Compartments of ovarian antral follicle. **A.** Photo courtesy of Dr. Cordeiro; **B, C, D** from (Junqueira and Carneiro, 2010).

2 Physiology of the ovarian follicle and gamete production

2.1 Ovary: morphologic structure, function and energy metabolism

The main function of the ovary is to produce a fertilizable oocyte at each ovulation and to create endocrine environment for initiation of a pregnancy, by production of sexual steroid hormones. Reproductive processes are regulated by combined activities of central nervous system, secretory tissues, target tissues and various hormones. Two closely related processes, oogenesis and folliculogenesis, take place within the ovary. These processes start during the fetal life and continue through female life under the strict control of different endocrine and environmental factors at each step.

Each ovary is attached to the uterus by the ligaments, transpierced by arteries, veins and ovarian lymphomas, besides nerves. The ovary consists of an outer cortex and a central medulla, which is rich in connective tissue and enclosing the nerves, lymph vessels, and blood vessels. The cortex is the outer layer, lined with germinal epithelium, which contains follicles, each one encloses an oocyte. The vessels pass towards the cortical zone, where the follicles and this arrangement allow a follicle communication and development. The ovary is bordered by a dense subepithelial conjunctive layer, the albuginea.

The ovarian follicles themselves are composed of different cell types: an oocyte, which is surrounded by granulosa cells (GC) and later by *cumulus oophorus* (specialized GC attached to oocyte). GC layer side internal and external theca layers (**Figure 13**).

2.2 Folliculogenese and ovogenesis

Folliculogenesis is the process of ovarian follicular growth and differentiation, which is interconnected with the oogenesis – growth and maturation of enclosed oocyte. Two phases of folliculogenesis are distinguished as basal and terminal (also called antral). In basal folliculogenesis is a slow and continuous stage regulated by autocrine and paracrine ovarian factors. The terminal is strictly controlled by gonadotrophins, LH (luteinizing hormone) and FSH (follicle stimulating hormone) both hormones from the pituitary origin. Folliculogenesis starts usually during fetal and perinatal period and continues until ovulation, with formation of *corpus luteum* from remaining follicular cells. At each stage, the majority of ovarian follicles stop their growth and are eliminated by atresia (Hall and Guyton, 2016; Moore, Persaud and Torchia, 2016). Ovulation, the last stage of folliculogenesis, may take place only when the proper endogenous factors (developmental, endocrine and metabolic) and environmental (nutritional, seasonal and social interaction) factors are favorable for it.

In cow, estrous cycle averages 21 days. Two or three FSH stimulated waves of follicular growth usually occur during the bovine estrous cycle. During growth of a cohort of antral follicles in a wave, they undergo recruitment, selection, dominance, and loss of dominance or ovulation. During recruitment, a cohort of primordial follicles begins to grow and all "recruited" follicles thereafter become dependent on FSH for their continued growth to ovulatory size (Assidi, Dieleman and Sirard, 2010). Dominance enables a single follicle to prevent growth of other follicles or grow in a hormonal milieu unfit for growth of other follicles. Loss of dominance results in atresia of the dominant follicle, thus initiating growth of a new follicular wave (Ireland *et al.*, 2000). Each follicular wave culminates in development of a single nonovulatory or ovulatory dominant follicle (**Figure 14**). A dominant follicle develops to ovulatory size and usually undergoes atresia unless it ovulates.

This phenomenon occurs until the exhaustion of the non-renewable reserve, and involves several steps.

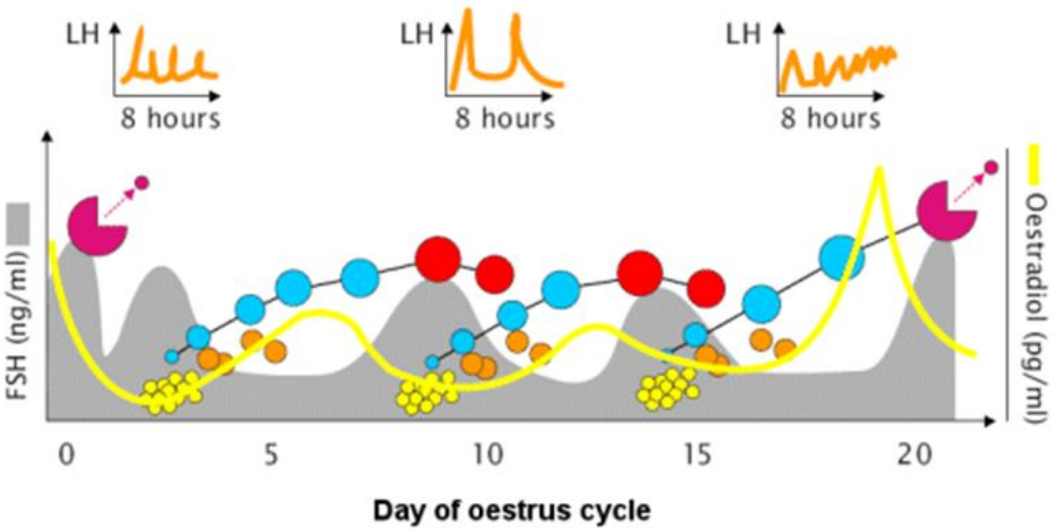


Figure 14. Follicular dynamics in three-wave cycle. Schematic illustration of the pattern of secretion of follicle-stimulating hormone (FSH), luteinizing hormone (LH), and estradiol (E2); and the pattern of growth of ovarian follicles during the estrous cycle in cattle (Adapt from Forde et al. 2011; image from Merck & Co., Inc., Kenilworth, NJ, USA (www.msdprivacy.com/us/en/index.html)).

2.2.1 The key steps of folliculogenesis and oogenesis

The main steps of follicular development accompanied by massive atresia are shown in **Figure 15**.

Primordial follicles consist of an oocyte surrounded by a single layer of flattened somatic cells. As the follicle grows it becomes a **primary follicle**, containing a growing oocyte surrounded by cuboid granulosa cells. At this stage, the zona pellucida begins to form around the oocyte (**Figure 15A**).

Secondary follicles are characterized by extensive proliferation of granulosa cells (GC). The oocyte becomes large and theca cells are identifiable. GC proliferation increase number of cell layers and estrogen production increases. Theca cells produce the androgens and provide a structural scaffold, together they form cell network that support the vascular system.

The **tertiary (antral) follicles** are distinguished by the formation of a cavity: *the antrum* containing the FF, exuding blood plasma and follicular cells.

In antrum follicles, GC differentiate (morphologically and metabolically) and aggregate around the oocyte, forming specialized *cumulus oophorus*, tightly connected with enclosed oocyte, which has nutritive and protective role (Tanghe *et al.*, 2002). On the other hand, the theca (TH) cells are organized, vascularized and separated from the granulosa cells by basal lamina. TH cells undergo a morphological (inner layer/outer layer) and functional differentiation. The cells of the internal theca express LH receptors (LHR) and those of granulosa FSH receptors (FSHR). All these stages are common to all mammals (Tajima *et al.*, 2007; Monniaux *et al.*, 2014).

Throughout the folliculogenesis, follicles undergo basal or antral atresia. In preantral follicles, oocyte dies first; later the GC are the first cells to become atretic and are characterized by pyknosis and chromatolysis of the nuclei and shrinkage of the cytoplasm leading to belatedly cell dissolution (**Figure 15B)**

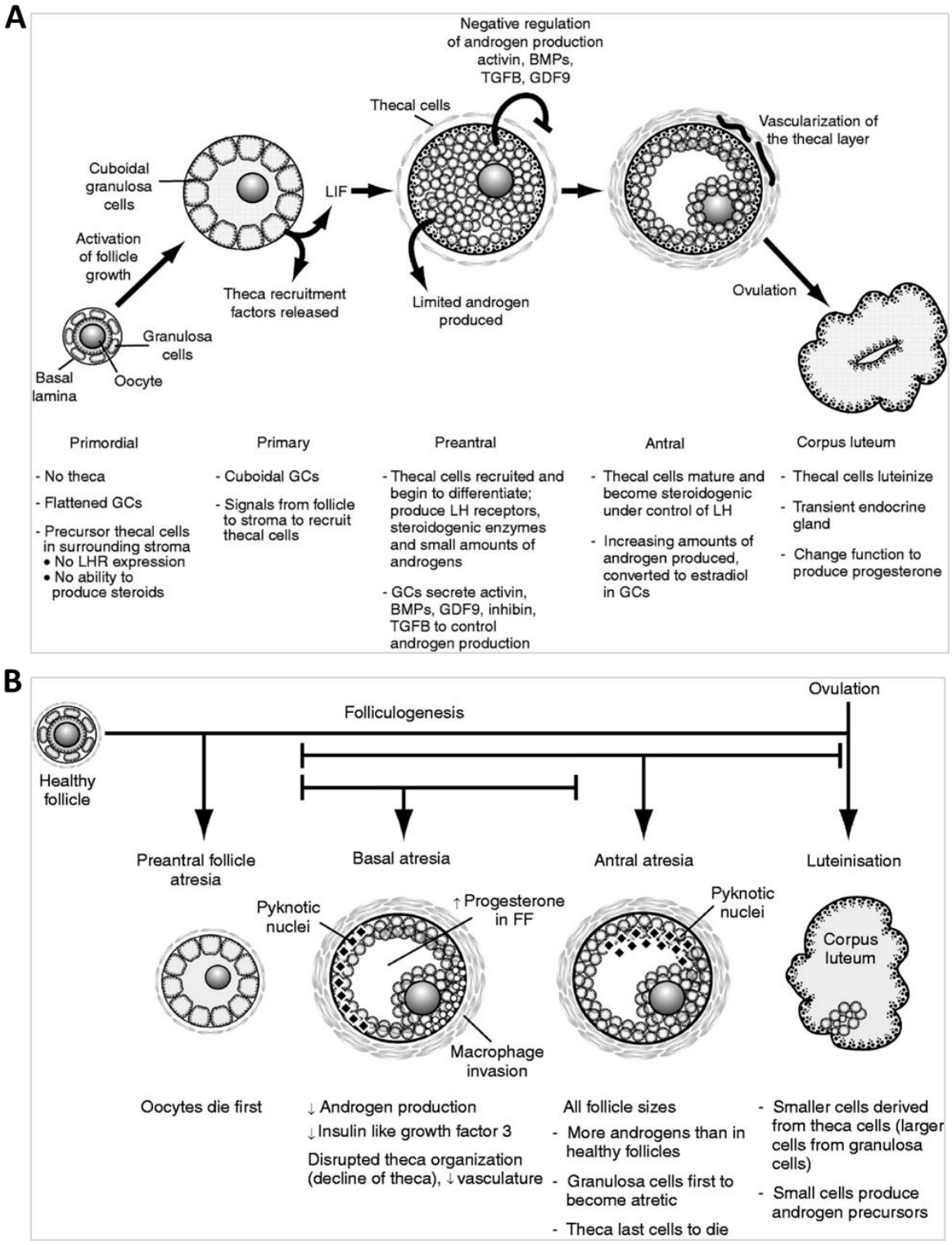


Figure 15. Folliculogenesis and atresia (*from Young and McNeilly, 2010*). **A.** Scheme of follicular development and main growth factors, hormones and signal molecules, regulating it. **B.** Scheme of atresia events; **Abbreviation:** BMP-Bone morphogenetic protein, TGFB-transforming growth factor-beta superfamily, GDF9 -Growth Differentiation Factor 9.

2.2.2 Functional changes in somatic cells and oocyte during folliculogenesis

2.2.2.1 Basal folliculogenesis.

The development to the primary and secondary stage can take place in the absence of hormones, but FSH receptors (FSHR) are present in GC and LH receptors in theca cells (TH) of these early follicles. The transition of primary to secondary follicle is promoted by local intra-ovarian paracrine factors produced by oocytes, GC and TH. Basal folliculogenesis is characterized by a high mitotic activity of GC, which synthesizes gap-junction components, cytokines (kit-ligand receptor, KITLG), growth factors (EGF, FGF) and Anti-müllerian hormone (AMH). Gap junction channels are composed of connexins, and the most representative connexins are the 43 and 37, expressing in GC and oocyte, respectively (Fair, 2003; Hatzirodos, Hummitzsch, Irving-rodgers, *et al.*, 2014). The TH participate in the regulation of basal folliculogenesis through the expression of the key factors for progestogen (CYP11A1, STAR, HSD3B2) and androgen (CYP17A1) synthesis and growth factors (BMP4, BMP7, NGF, FGF7, EGF, TGF…), which enhance proliferation of GC. Conversely, GC control the gene expression and secretory activity of TH through the secretion of growth factors and cytokines as KITLG (reviewed by (Hutt, McLaughlin and Holland, 2006), as well as the development of its vascularization through the secretion of angiogenic factors (VEGF, reviewed by (Fraser, 2006).

In developing follicles, gap junctions couple the growing oocyte and its surrounding follicle cells into a functional syncytium. The oocyte initiates the synthesis of growth factors, particularly GDF9 and BMP15 (both belonging to the Bone Morphogenetic Protein family) as well as components of its zona pellucida (ZP1, -2, -3 and -4) and of gap-junctions (connexins 37 and 42) involved in the connections with its surrounding granulosa/cumulus cells. The growth of the preantral follicle is driven by permanent bi-directional molecular dialog between oocyte and granulosa cell. Oocyte–secreted factors GDF9 and BMP15 activate the SMAD2/3 signaling pathway in GC and support their proliferation and survival, whereas KITLG produced by GC activates the PI3K/AKT pathway essential for the growth and survival of the oocyte (reviewed by (Monniaux, 2016).

Along the basal folliculogenesis, the growing oocyte is blocked in the prophase of the first meiosis and initiates a high transcriptional activity. A part of RNA is used for protein synthesis for current metabolism and untranslated mRNA is accumulated in ribonucleic particles. Among these “maternal” transcripts many are oocyte-specific; their roles are not well understood but globally they are necessary for early embryo development (Zheng and Dean, 2007).

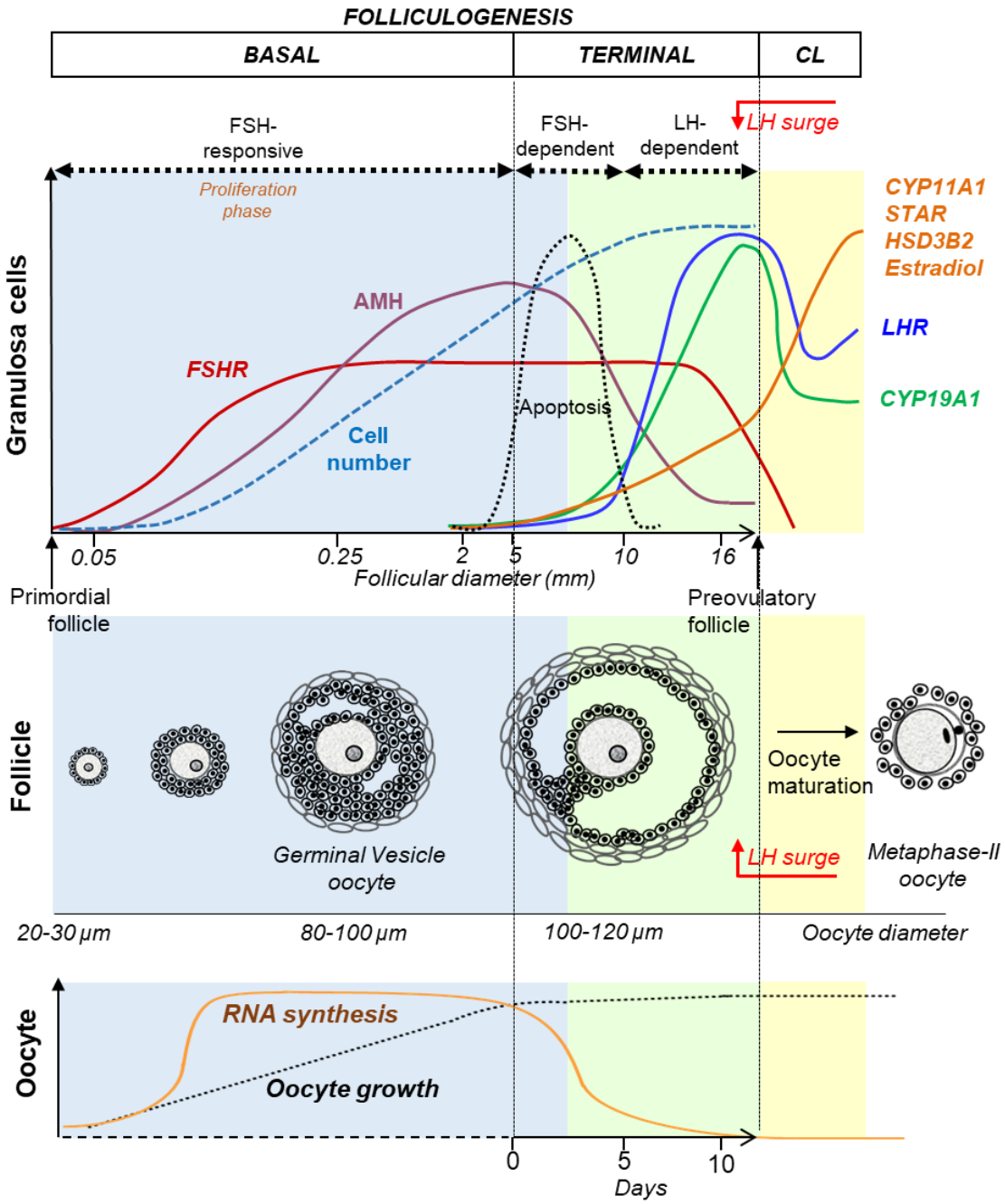


Figure 16. Main functional changes in follicular cells and oocyte during folliculogenesis.

During basal folliculogenesis, the growing FSH-responsive follicles are characterized by GC proliferation, oocyte growth, and the formation and development of TH and antrum. Terminal folliculogenesis is strictly dependent on supply of FSH, then LH. Along with antrum growth, GC differentiate into steroidogenic cells, while the oocyte reaches its full size and ceases its transcriptional activity gradually. FSH-dependent follicles enter atresia when FSH levels fall below a threshold. Final maturation of the LH-dependent dominant follicle is characterized by meiotic resumption in the oocyte and ovulation, both are triggered by the LH ovulatory surge. Corpus luteum (CL) is formed from ovulated follicles. **Abbreviations**: AMH: anti-Mullerian hormone, CYP11A1: cytochrome P450 family 11 subfamily A member 1, CYP19A1: cytochrome P450 family 19 subfamily A member 1, FSHR; follicle stimulating hormone receptor, HSD3B2: hydroxy-delta-5-steroid dehydrogenase, 3 beta- and steroid delta-isomerase 2, LHCGR: luteinizing hormone/choriogonadotropin receptor, STAR: steroidogenic acute regulatory protein. Adapted from(Monniaux *et al.*, 2018).

2.2.2.2 Terminal folliculogenesis.

During terminal stage of folliculogenesis, antrum rapidly increases and accumulates follicular fluid (FF), which is formed by serum transudation and the accumulation of metabolism and secretion products from follicular cells. The ability of GC to proliferate and to produce AMH progressively decreases during this period. Also, GC become responsive to FSH, synthesize increasing amounts of inhibin and differentiate into steroidogenic cells. Activins and inhibins are produced by GC and act regulating the LH-induced androgen synthesis produced by TH (Campbell and Baird, 2001; Hsueh *et al.*, 2015), and therefore, they ensure the estradiol supply. LH acts through specific receptors, constitutively present on TH, for stimulating androgen production. These receptors mediate the short-term effects of LH by activating the STAR protein, which translocates cholesterol from the outer to the inner mitochondrial membrane. There, the first step in steroid synthesis is performed by the CYP11A1 enzyme, resulting in the production of pregnenolone (Kallen *et al.*, 1998). **Figure 16** represents the main functional changes in the follicular cells (notably GC) and the oocyte through different stage of folliculogenesis.

The pulse frequency of LH dictates the amounts of steroid hormones; each pulse of LH is followed by an increase in secreted androgen and estradiol. Moreover, LH exerts long-term trophic effects on TH by enhancing the expression of enzymes involved in progesterone (STAR, CYP11A1, and HSD3B2) and androgen (CYP17A1) production. GC express CYP11A1, STAR, HSD3B2 and notably CYP19A1, the aromatase enzyme catalyzing the synthesis of estradiol from the androgens produced by TH. FSH stimulates the production of estradiol and progesterone via PKA, which activates the expression of CYP11A1 and CYP19A1, and those in turn stimulate the STAR expression. The presence of LH-pulsatile and IGF1 facilitates the mitochondrial internalization of cholesterol, thus increasing the bioavailability of the p450-scc substrate. AMH is inhibitory by counteracting FSH but limited by aromatase production in large antral follicles (reviewed by (Dewailly *et al.*, 2016)). Besides, testosterone diffusing into the mural GC layer represents the substrate for FSH-induced CYP19A1 for follicular estradiol synthesis.

The ovarian theca cells synthesize and secrete androgens (progesterone/testosterone) and ovarian granulosa cells convert androgens to estradiol, by aromatase and 17β-HSD (17-Beta-Hydroxysteroid Dehydrogenase) (Stocco, 2001; Miller, 2017). Steroidogenesis by follicular cells therefore requires the involvement of different enzymes regulating processes from lipid uptake, FA metabolism and steroid synthesis (**Figure 17**).

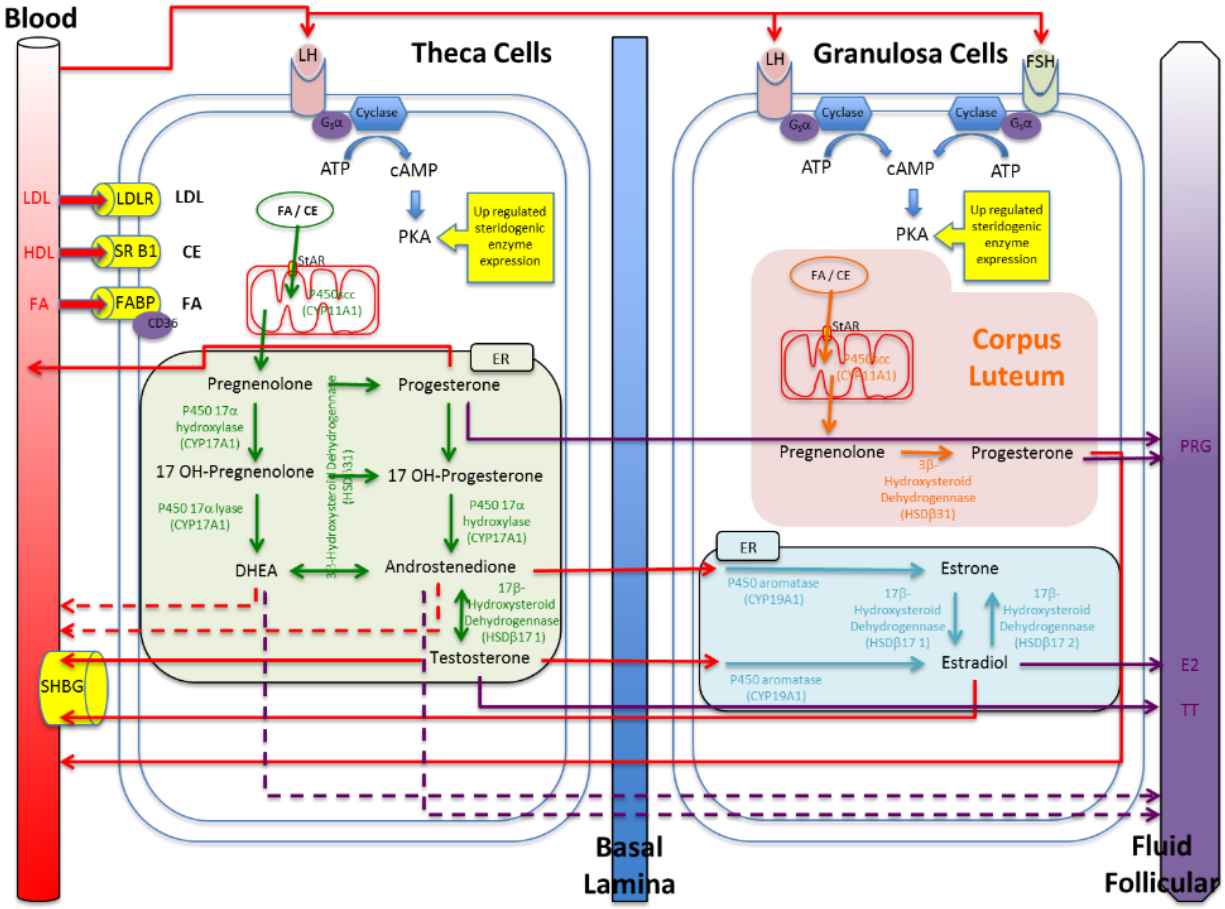


Figure 17. Steriods hormones synthesis in ovarian cells. Abbreviation: **LH** - Luteinizing Hormone; FSH - Follicle Stimulating Hormone; **PKA** - Protein Kinase A; **LDL** - Low-Density-Lipoprotein; **LDLR** - Low-Density-Lipoprotein Receptor; **HDL** - High-Density-Lipoprotein; **SRB1** - Scavenger Receptor Class B Member 1; **CE** - Cholesterol; **FA** - Fatty Acid; **FABP** - Fatty Acid Binding Protein; **CD36** - CD36 Molecule (Fatty acid translocase); **StAR** - Steriodogenic Acute Regulatory Protein; **ER** - Endoplasmatic Reticulo;**DHEA** - Dehydroepiandrosterona; **SHBG** - Sex Hormone Binding Globuline; **PRG** - Progesterone; **E2** - Estradiol; **TT** - Testosterone.

When the follicle starts terminal folliculogenesis, its enclosed oocyte has reached more than 80% of its maximal size. During terminal folliculogenesis, the transcriptional activity of the oocyte decreases steadily and becomes undetectable in the preovulatory follicle. However, before LH surge triggering oocyte maturation, oocyte are still arrested in prophase of the first meiotic division. The mechanisms of meiotic arrest involve elevated levels of cyclic adenosine monophosphate (cAMP), produced by adenylyl cyclase by the oocyte itself (Sánchez and Smitz, 2012), or/and passed through gap junctions from the CC to the oocyte (Russell *et al.*, 2016). Also via gap junction communication, the CC may mediate an inflow of cyclic guanosine monophosphate (cGMP) to the oocyte (also via gap junction communication), and prevents the activation of oocyte cAMP-phosphodiesterase (PDE3A), the enzyme that is responsible for the degradation of cAMP and by doing so, circumvents meiotic resumption (Uyar, Torrealday and Seli, 2013).

During terminal folliculogenesis, the concentrations of androgens, AMH and IGF binding proteins decrease in the FF while those of estradiol and inhibin increase dramatically. In dominant follicle, GC become endowed with LH receptors and therefore the follicle is able to ovulate in response to an LH surge. All follicles except the dominant one(s) become atretic (characterized by apoptosis of the GC) when FSH levels fall below the threshold needed to sustain their development. Only the dominant, most mature follicle will continue its development even in the unfavorable FSH environment, owing to an increased sensitivity to FSH and a highly developed vascularization. In addition, its GC become LH responsive before those of all other follicles in the cohort, so that the dominant follicle can benefit from LH supply until the preovulatory stage. The large estradiol amounts secreted by the preovulatory follicle affect the secretion of GNRH1 from the hypothalamus and ultimately trigger the pituitary LH surge that brings about ovulation (Monniaux *et al.*, 2018).

2.2.2.3 Ovulation

Prior to ovulation, in response to LH peak, preovulatory follicles increase the synthesis of different inflammatory cytokines (interleukines, tumor necrosis factor TNF), prostaglandins, anti-inflammatory glucocorticoids like cortisol and activity of proteolytic enzymes (especially metalloproteases as collagenases (MMPs), and serine proteases, SERPINs). Local production of plasminogens activator and matrix metal protease inhibitors (TIMPs) also considerably increased. Steroids and prostaglandins regulate the expression of these factors. Through the activity of different proteolytic enzymes, concurrent expression of protease and anti-proteases within the preovulatory follicle, extracellular matrix is

deteriorated, follicular wall degrades and finally ruptures, and oocyte is expulsed into the oviduct (Curry and Smith, 2006).

The mechanism of action of the described factors during ovulation is similar to inflammatory reactions. They also modulate steroidogenesis and may be involved in oocyte maturation by affecting cumulus-oocyte complex (COC). The pre-ovulatory LH surge is initiated the oocyte meiotic maturation, a cascade of processes leading to the progression of the oocyte (by that time suspended in prophase I of the first meiotic division) to the metaphase-II stage and ending with the extrusion of the first polar body. An event essential for the oocyte to resume meiosis is the expansion of cumulus cells (CC). Cumulus expansion is dependent on the stimulation of LH-induced epidermal growth factor (EGF)-like peptides, via the activation of protein kinase A (PKA) and in response to high levels of cAMP produced by GC and CC (Uyar, Torrealday and Seli, 2013). CC expansion or mucification occurs due to an increase of the intercellular spaces and secretion of the matrix composed essentially of hyaluronic acid; this matrix allows CC to remain attached. From a mechanical point of view, cumulus expansion facilitates the expulsion of COC at the time of ovulation and could facilitate, by its synthesis of hyaluronic acid, the acrosomal reaction of spermatozoa (Y.-Q. Su *et al.*, 2007; Richards and Pangas, 2010). In mature oocyte, molecular factors associated with oocyte meiotic arrest are degraded or have drastically decreased levels; globally massive degradation of oocyte transcripts occurs. On the other hand, transcripts involved in signaling pathways essential for meiosis resumption and the maintenance of meiotic arrest are retained (Cui *et al.*, 2007; Y. Su *et al.*, 2007). In cow, ovulated oocyte is already mature, because it performed its meiotic maturation and ready to be fertilized. Successful embryo development after fertilization depends on oocyte developmental competence that it acquired during folliculogenesis, and especially during the final maturation stage.

2.2.3 Oocyte competence

Oocyte developmental competence or quality is the ability of an oocyte to undergo successful maturation, fertilization and embryo development capable of continuing its development to term and producing a live birth. Quality is dependent on cytoplasmic and nuclear maturation, that results in the accumulation of organelles, metabolites and maternal RNAs during the growth and maturation of the oocyte (Mermillod *et al.*, 2008). Various models of good and poor oocyte quality were used to understand the essential factors leading to success development; these models are related to follicular

size, maternal age, oocyte metabolic status, follicular environment, oocyte maturation conditions *in vivo* vs *in vitro* (reviewed in (Reader, Stanton and Juengel, 2017).

During post-natal life, oocytes undergo growth and maturation, stockpiling mRNAs, proteins, metabolic substrates and organelles. Follicles produce energy from different substrates including carbohydrates, amino acids and lipids. Oocytes preferentially metabolize pyruvate, while the somatic cells of the ovarian follicles are more glycolytic. Intricate metabolic relationship between the oocyte and its somatic environment is critical for oocyte growth and developmental competence. The CC provide the oocyte with energy transforming glucose to pyruvate and supply it to oocyte via gap-junctions (Sutton-McDowall, Gilchrist and Thompson, 2010). Competence to embryo development and quality depends on oocyte metabolism that includes both amino acid, carbohydrate and non-glucose-dependent, metabolic pathways such as FA synthesis and catabolism (beta-oxidation) and glutamine catabolism. These metabolic pathways not only involved in energy supply but also on redox potential and anabolism, which may impact oocyte competence (review by (Collado-Fernandez, Picton and Dumollard, 2012).

In bovine, the oocytes from the follicles less that 2mm in size are meiotically incompetent, i.e. not able to resume meiosis under *in vitro* maturation (IVM) conditions. Follicles of larger size contain the oocytes competent to resume meiosis and reach metaphase-II stage after IVM. Nuclear, or meiotic maturation is dependent on the formation and maintenance of the meiotic spindle (Bennabi, Terret and Verlhac, 2016), however, embryo developmental competence of mature oocyte is more related to cytoplasmic maturation. Cytoplasmic maturation is the process characterized by the migration of cortical granules (Golgi origin) to the cortical area close to the plasma membrane of the oocyte in association with the cytoskeleton. A perivitelline space is placed between the oocyte and the zona pellucida immediately before the time of ovulation. There is release of the content of the cortical granules in this space during fertilization, causing significant changes in the zona pellucida, which prevents the penetration of supernumerary spermatozoa. In addition, migration and fusion of mitochondria are observed in association with lipid droplets (Dadarwal *et al.*, 2015). The studies examining differences in mitochondria in relation to developmental competence provide evidence that a critical number, distribution pattern and morphology of mitochondria are required for successful oocyte and embryo development (Reader, Stanton and Juengel, 2017).

Cytoplasmic maturation involves not only the reorganization and distribution of the organelles, especially mitochondria, cortical granules and vesicles, but also the final storage of RNA, proteins, lipids (lipid droplets) and transcription factors required during fertilization and early embryo development (Sirard *et al.*, 2006; Ferreira *et al.*, 2009; Mao *et al.*, 2014). In bovine, oocyte maturation led to change

in lipid content especially in TG quantity, as shown by mass spectrometry analysis (González-Serrano et al., 2013).

Also, oocyte and follicular size (Fair, 2003; Mermillod *et al.*, 2008), secretory and steroidogenic activity of cumulus cells (Wigglesworth *et al.*, 2015) are fundamental for efficient cytoplasmic oocyte maturation. Interruption of CC-oocyte communication prior to oocyte maturation or fertilization affects oocyte developmental competence (Zhang *et al.*, 1995). Also, bovine oocytes stripped of their cumulus cells before maturation have reduced fertilization rates and affected embryonic development (Binelli and Murphy, 2010; Buratini and Price, 2011). In these oocytes denuded from CC before IVM, reduction in total lipids and significant changes in lipid composition were observed as compared to cumulus enclosed oocytes, which are more competent in terms of embryo quality after *in vitro* development (Auclair *et al.*, 2013; Alessandra A. Vireque *et al.*, 2017).

3 Lipids metabolism in the ovarian follicle

3.1 Effect of lipid metabolism on reproductive performance in cow

Reproductive performance in cows is influenced by nutritional and metabolic status, as previously reviewed (Leroy, Opsomer, *et al.*, 2008; Friggens *et al.*, 2009). In postpartum and early lactation, dairy cows undergo a negative energy balance that is associated with drastic elevations in lipid concentrations in blood and in FF, and this reflects as a significant negative influence on fertility (Leroy *et al.*, 2004; Beever, 2006; Leroy, *et al.*, 2008; Ospina *et al.*, 2010a, 2010b; Leroy *et al.*, 2014; Valckx *et al.*, 2014; Roelen *et al.*, 2015). FF from heifers and lactating cows showed higher levels of at least 24 different FAs in the FF, particularly palmitic acid and stearic acid, and lower levels of docosahexaenoic acid (Bender et al., 2010). Circulating TG levels decrease at delivery, while NEFA levels increase dramatically, relative changes that are also reflected in FF in dairy cows (Leroy *et al.*, 2004). In experiments to increased or altered fat in the diet, cows that were fasted for 4 days also exhibited increased NEFA in both plasma and FF (Jorritsma *et al.*, 2003; Aardema *et al.*, 2013).

Dietary fat supplementation particularly during lactation, is known to influence reproductive performance in ruminants, and it is well accepted that this effect is mostly direct rather than by modifying energy status of cows (Staples, Burke and Thatcher, 1998; Mattos, Staples and Thatcher, 2000); fat supplementation possibly affects FF and lipid levels in the follicle and oocyte (Dunning, Russell and Robker, 2014). Palmitic and stearic acid had a dose-dependent inhibitory effect on the amount of fat stored in lipid droplets and a concomitant detrimental effect on oocyte developmental competence. Oleic

acid, in contrast, had the opposite effect, causing increased lipid storage in lipid droplets and an improvement in oocyte developmental competence (Aardema *et al.*, 2011, 2013). Specifically polyunsaturated fatty acids, PUFA, were considered important for reproductive processes, as example, steroid hormone production via cholesterol and prostaglandin precursors using arachidonic acid pathway, respectively (Urlep and Rozman, 2013; Tessaro, Ayala and Martins, 2015).

Among the PUFA, previous research has focused on the effect of omega-6 (n-6) and especially omega-3 (n-3) FA. Some studies had reported that dietary supplement of PUFAs in cattle could enhance reproductive performance and oocyte developmental potential (Wathes, Abayasekara and Aitken, 2007). Developmental competence of oocytes and quality of blastocyst were enhanced by dietary PUFAs in cows (Fouladi-nashta *et al.*, 2007). Thus, beef heifers given dietary fish oil supplementation for 46 days exhibited dose-dependent alterations in specific n-3 and n-6 FAs in FF (Childs *et al.*, 2008). There were no differences detected in oocyte lipid content, but oocytes from animals that were fed with fish oil had better morphology and improved membrane integrity in response to freezing (Zeron *et al.*, 2002). Heifers with moderate body condition score had less FA in aspirated COCs than heifers with low body condition score; and a lipid supplement in the diet increased the total FA content of whole COCs in both groups (Adamiak *et al.*, 2006).

The feeding of diets supplemented with n-3 PUFA (enriched alpha−linolenic acid, ALA, C18:3, precursor of PUFA) led to an increase in the size of the pre-ovulatory follicles (Ambrose *et al.*, 2006) and in number of small follicles (Zachut *et al.*, 2010) and also had a tendency toward increasing conception rates (Ambrose *et al.*, 2006; Dirandeh *et al.*, 2013). *In vitro*, addition of ALA, FA that cannot be synthesized by mammalian cells, in maturation medium for bovine oocytes increased blastocyst rate and quality (Marei, Wathes and Fouladi-Nashta, 2009).

One of the recent studies demonstrated that supplementation with n-3 diets had a tendency to increase the number of large follicles and decrease in infertility or early embryo mortality rate at 21 days after artificial insemination in post-partum dairy cows (Elis *et al.*, 2016). Moreover, n-3 PUFA diet also directly affected the cleavage rate and tended to increase the blastocyst rate after *in vitro* maturation (IVM) and *in vitro* fertilization (IVF) in cows (Zachut *et al.*, 2010; Moallem *et al.*, 2013).

3.2 Energy metabolism during folliculogenesis

Energy metabolism of ovarian cells and oocytes of primordial follicles is mainly anaerobic and glycolytic, because these cells have abundant glycogen and occasional lipid droplets, which could provide a source of energy for migrating follicles (Collado-Fernandez, Picton and Dumollard, 2012).

The growing primary follicles are situated on the well vascularized corticomedullary border, but their energy demand consists of oxidized pyruvate from glycogen reserves (Harris, Leese and Gosden, 2009). Follicular glucose consumption and lactate production rates increase *in vitro* from the primary/ secondary stages to the antral and ovulatory stages of follicular development (Boland *et al.*, 1994; Harris *et al.*, 2007).

With the growing follicle, its FF acts as a reservoir of oxygen and nutrients limited by the thickening and nutritional requirements of the GC layer and insufficient supply of theca capillaries (Redding, Bronlund and Hart, 2007). In cattle, Clark and Stokes reported a marked increase in intra-follicular oxygenation with antrum formation, with peak at the end of the initial antral stage, before decreasing through the antrum to pre-ovulatory phases and finally increasing around time of ovulation (Clark and Stokes, 2011). In general, lipid metabolism in somatic GC and TH cells revolves around the production of cholesterol and steroidal hormones biosynthesis. The GC secrete progesterone and estradiol and the cells of the internal TH produce progesterone, androgens and estrogens, whereas outer TH layers have limited secretory function (Young and McNeilly, 2010). Lipoprotein lipase, an extracellular lipase tethered to capillary walls by heparin sulfate proteoglycans and activated by apolipoprotein (Apo) on the surface of circulating lipoproteins, hydrolyses lipoprotein triacylglycerol-releasing free FAs, which can then be taken up by cells. Lipolysis of intracellular TG within lipid droplets is catalyzed by intracellular lipases including LIPE (or hormone-sensitive lipase (HSL)) and adipocyte triglyceride lipase (ATGL) (Young and McNeilly, 2010; Dunning, Russell and Robker, 2014). Intracellular TG stored within lipid droplets is surrounded by a phospholipid monolayer and lipid droplet coat proteins of the perilipin family, which regulate droplet size and promote lipogenesis or lipolytic activity under the appropriate metabolic or hormonal conditions (Dunning, Russell and Robker, 2014). *In vitro*, gonadotrophins cause a dramatic increase in follicular glucose uptake and lactate production (Roberts *et al.*, 2004; Sutton-mcdowall, Gilchrist and Thompson, 2004), as well as being influenced by insulin and by ovarian growth factors that also interfere with glucose metabolism (Roy and Terada, 1999). However, the proportion of glucose metabolized by glycolysis showed a decrease along follicle growth and oocyte-cumulus maturation (Sutton *et al.*, 2003; Sutton-mcdowall, Gilchrist and Thompson, 2004).

3.3 Lipid uptake by ovarian cells

The majority of circulating FAs and TG are carried throughout the blood in lipoprotein particles, i.e. HDLs, LDLs and VLDLs for transport through the circulation to tissues. Also free FAs attached to serum albumin are transported through the blood. The FAs and cholesterol arrive in ovary, metabolized or

stored as TG in lipids droplet or reserved in FF and these substrates are utilized by ovarian somatic cells and oocytes for energy production in numerous species (reviewed by (Grummer and Carroll, 1988).

HDL of FF is favorably related to serum HDL cholesterol (Gautier *et al.*, 2010; Valckx *et al.*, 2012), indicating that serum HDL particles can be passively balanced; however, there is no similar correlation for VLDL in FF and serum (Gautier *et al.*, 2010). Thus, due to the porosity of the basal membrane of the follicle that is permeable to serum proteins up to 300 kDa (Fujimoto *et al.*, 2009) in mammals HDL would be the only lipoproteins present in the FF, thus excluding LDL and VLDL. However, LDL and/or VLDL are sometimes detected in the FF of women (Wald *et al.*, 2010). They may be synthesized by GC, which in humans express the ApoB-100 lipoprotein marker and thus produce and secrete native VLDL in similar to a serum way, except for a slightly higher TG content and less cholesterol (Gautier *et al.*, 2010). Thus, the LDL and VLDL particles detected in follicular fluid may, in fact, be generated by ovarian cells. These HDL lipoproteins have important functions in steroidogenesis by GC and TH layers, serving as the predominant source of cholesterol (Azhar, Tsai and Reaven, 1990; Azhar *et al.*, 2006). Abnormal lipoprotein metabolism is related to female infertility both in mice and human (Miettinen, Rayburn and Krieger, 2001; Yesilaltay *et al.*, 2006).

Receptor expression patterns may imply different regulation of cholesterol supply at different stages of follicular development. Accumulation of LDL and VLDL particles in the FF of large antral follicles may enhance cholesterol availability for the intense steroidogenic activity that is essential at these stages. HDL receptor scavenger receptor class B, member 1 (SRBI) and Apolipoprotein B (ApoB) are associated with better quality of oocytes and embryos (Gautier *et al.*, 2010). However, it is not clear either lipoproteins found in FF influence oocyte quality via their ability to deliver lipid substrates such as TG or other components of these surrounding apolipoproteins, which are known to have scavenging properties, protect cells from oxidative stress (Dunning, Russell and Robker, 2014).

3.3.1 Lipids in follicular fluid and impact on somatic cells

Follicular fluid protects the oocyte against proteolysis, as well as collaborates in the extrusion process during ovulation, and acts as a buffer against adverse blood influences. FF provides an appropriate microenvironment for the oocyte that leads to it capacity to proper embryo development, FF thus influences the quality of the embryo (reviewed by (Matoba *et al.*, 2014)). Changes in FF metabolome may indicate the increased oxidative stress related to lower fertility (Guerreiro *et al.*, 2018). Extracellular vesicles are present in different body fluids including FF and carry biomolecules such as proteins,

mRNAs, miRNAs, metabolites and lipids. These vesicles can be internalized by follicular cells suggesting their importance in intra-follicular communication and metabolic substrate exchange (Collado *et al.*, 2018).

The correlations of FA composition between serum and FF were reported in several studies. Dairy cows have lower levels of TG in FF even though levels of free FAs have been significantly elevated in serum (Leroy, *et al.*, 2004). Linoleic, palmitic and oleic acids predominate in the total FA fraction of bovine FF (Sata *et al.*, 1999). Oleic, palmitic and stearic acids were the most prevalent free FA in the FF of lactating cows, and were approximately 40% of serum levels (Jo L.M.R. Leroy *et al.*, 2005). Free FA level in FF may be related to follicular maturation (Renaville *et al.*, 2010), since the follicles with higher estrogen to progesterone ratio (E2/P4) have more palmitic and oleic acids and less stearic and linoleic acids in FF. In human, most serum metabolites, including TG and free FAs are reflected in FF, but at lower levels (Valckx *et al.*, 2012). In postpartum cows, potential variations in serum concentrations of metabolites due to nutritional changes also affect FF, and this may lead to changes in GC and oocyte quality (Jo L.M.R. Leroy *et al.*, 2005). A comparative study between the follicular environment of heifers and cows showed that heifer has lower glucose and FA levels. This condition determined a reduced quality of the oocytes (smaller diameter and number of lipid droplets) and limited maturation potential that probably related to nutrient reserves in FF (Warzych *et al.*, 2017).

Van Montfoort and collegues (2014) suggest a link between lipid metabolism and reproduction/fertility. In humans the follicular fluid contains all relevant lipoprotein subclasses that reach the follicular fluid either by diffusion, like high-density lipoproteins (HDL), or by local production within the granulosa cells, as very low-density lipoproteins (VLDL) (van Montfoort *et al.*, 2014). Decreased fertility are often associated with high concentrations of free FAs in blood and FF (Metwally *et al.*, 2007; Jungheim *et al.*, 2011; Robker, Wu and Yang, 2011; Valckx *et al.*, 2012; Yang *et al.*, 2012). High levels of saturated FAs induce lipotoxicity in follicular cells (Aardema *et al.*, 2011, 2013; Lolicato *et al.*, 2015). High levels of oleic acid present in FF in combination with the accumulation and storage of lipids by cumulus cells serves to prevent the harmful exposure of saturated FAs to oocytes and embryos (Aardema, Vos and Gadella, 2018).

Changes in serum concentrations of non-esterified FAs (NEFA) induced by fasting reflect on the composition of FF in cattle (Comin *et al.*, 2002), as well as negative energy balance (NEB) of postpartum dairy cows (Leroy et al., 2004). NEB can also affect follicular growth and development by increasing NEFA concentrations acting on ovarian cells. *In vitro* studies have shown that especially palmitic (C16: 0) and stearic (C18: 0) have a negative effect on cell viability of human granulosa (Mu *et al.*, 2001), as

well as on the proliferation of GC in cattle (Vanholder *et al.*, 2005). In both studies, induction of apoptosis and late necrosis were observed, may be related by the dose / response of saturated FAs and also of oleic acid (C18: 1) combined with albumin.

It has been demonstrated in rat Leydig cells that NEFAs are able to inhibit LH-induced testosterone production by reducing the amount of free cholesterol available for steroidogenesis (Meikle *et al.*, 2001). There appears to be a similar effect in TH cells, that limited androgen production and hence the availability of substrates for the steroidogenesis of GC. The effect of NEFA *in vivo* would then inhibit steroidogenesis and proliferation in both TH and GC (Vanholder *et al.*, 2005).

3.3.2 Lipids in the oocyte-cumulus complexes (COC)

The energetic requirements of the oocyte for the resumption of meiosis seem to be met by an increase in oxidative metabolism around the time of GVBD; pyruvate being used as the main substrate, and supplemented by glutamine and glycine that can feed the TCA cycle. Metabolites such as glucose and FAs are also considered to play a key role in the maturation of bovine and swine oocytes (in review by (Collado-Fernandez, Picton and Dumollard, 2012).

In a comparative analysis of bovine, ovine and porcine oocytes it was revealed that pig oocytes have about times more TG (74 ng) than in ruminants (McEvoy *et al.*, 2000). Palmitic, stearic and oleic acids were found the most abundant, but porcine oocyte had more palmitic acid, while the cattle and sheep presented relatively more oleic acid in their oocytes (Genicot *et al.*, 2005). The variations in oocyte lipid content are perhaps indicative of distinct physiological requirements during early embryo development across species. Certainly, the long-chain FAs prevalent in mammalian oocytes are energy rich and differing levels of unsaturated FAs, such as oleic acid, could influence cellular membrane fluidity. Illustrated by changing membrane integrity, where lipid content influences oocyte viability following cryopreservation (reviewed in (Zhang *et al.*, 2012)). Lipid analysis by MALDI MS performed on individual oocytes of human, ovine and bovine showed significant difference in their lipid composition (Ferreira *et al.*, 2010).

Immature and mature oocytes have different lipid profiles in mice (Ami *et al.*, 2011) and bovine (González-Serrano *et al.*, 2013). Also, total lipid content and number of lipid droplets changed during oocyte maturation (Aardema *et al.*, 2011; Auclair *et al.*, 2013). It was hypothesized that selective uptake and/or synthesis of FAs *de novo* by the oocytes as well as specific needs for energy storage and metabolism are related to the type of FAs present in oocyte and its environment (Dunning, Russell and Robker, 2014). Bovine oocytes during *in vitro* maturation (IVM) with 10% of fetal serum have more TG

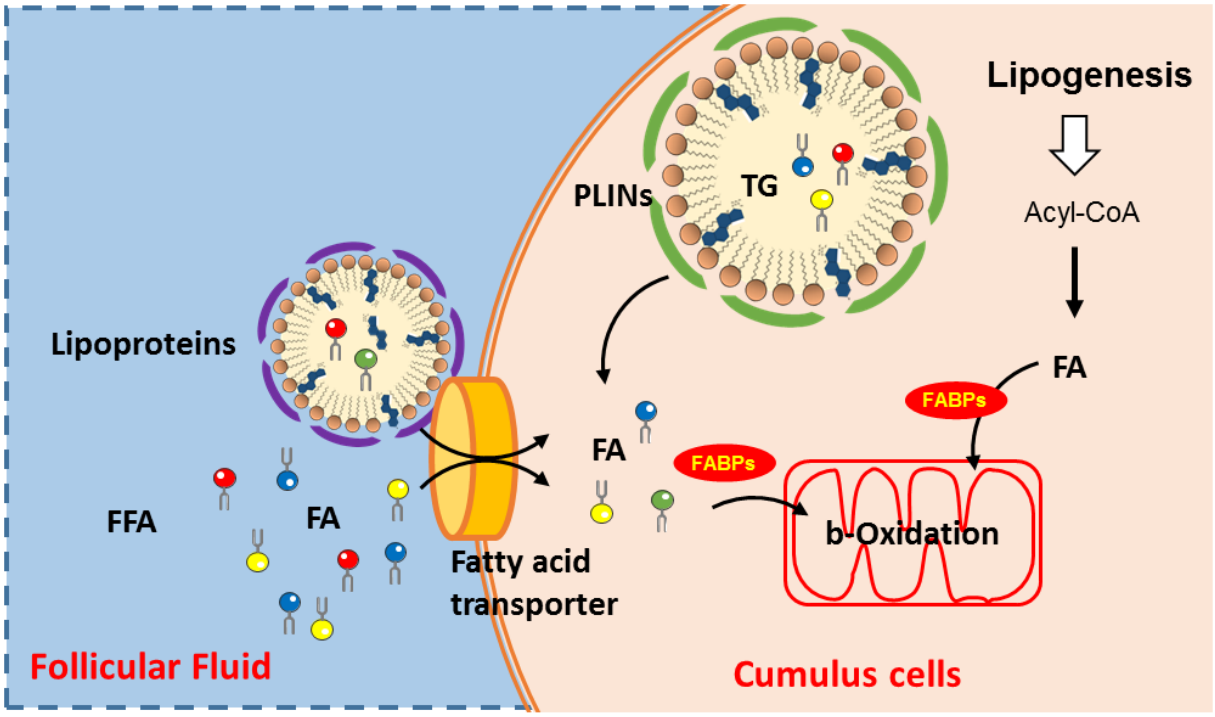


Figure 18. Schematic mechanisms of mobilization and catabolism of free FAs in the cumulus–oocyte complex.

Free FAs (FFAs) in follicular fluid are bound to albumin and likely enter cells via FA transporters and transporters by FABPs family. The mobilization of TG and cholesterol from lipoproteins in follicular fluid may occur via extracellular lipoprotein lipase available for cellular uptake, liberating FAs. Intracellular triacylglycerol is stored in cumulus within lipid droplets (LD) surrounded by proteins, (Perilipin family). After activation, lipid droplet proteins facilitate lipase-mediated hydrolysis of triacylglycerol and release of FAs. The lipogenic process generates FAs, which can be mobilized and oxidized directly by mitochondria to general ATP. Intracellular FAs generated via either transport or lipolysis or lipogenese are then available for metabolism via b-oxidation in mitochondria. FA are transported via FABPs, and are then available for metabolism via b-oxidation in mitochondria. The ATP and small molecules generated in this process can be transported to oocytes via Gap junctions and transzonal projections (TZPs) for use in competence and developing oocytes (adapted from Dunning et al. 2014 and Sanchez-Lazo et al.; 2014).

and cholesterol than those matured under serum-free conditions (Kim *et al.*, 2001). Growth factors, cytokines and metabolites present in culture medium also increase intracellular lipid level in the oocytes via induction of carrier-mediated uptake of FAs and/or TG biosynthesis. Fatty acid synthase abundance in the oocyte increased during IVM (Auclair *et al.*, 2013).

During IVM, lipase activity was higher in the oocyte compared to CC; moreover, it remained constant in the oocyte while decreased in CC (Cetica *et al.*, 2002). Hormone-sensitive lipase activity are detected in COCs and likely to be regulated during of oocyte maturation (Auclair *et al.*, 2013). It was hypothesized that extracellular lipases may mediate FA transfer from FF lipoproteins to CC, and that oocyte lipases help to release FAs from the oocyte lipid stock (Yang *et al.*, 2010; Aardema *et al.*, 2011). The metabolic cooperation between cumulus and oocyte is coordinated by bidirectional communication via gap junctions and exosome communications that allow free passage of small molecules (<1kDa), including ions, amino acids, pyruvate, glucose, FAs, nucleotides and other signaling molecules (Kidder and Mhawi, 2002; Goodenough and Paul, 2009; Zhou *et al.*, 2016). Paracrine signaling from the oocyte to CC regulates much of the flow of ions and molecules to the oocyte and orchestrates the associated local signaling events, which is the key in acquiring of oocyte competence (reviewed in (Russell *et al.*, 2016), and CC regulate oocyte energy metabolism of enclosed oocyte including glucose (Sutton-McDowall, Gilchrist and Thompson, 2010) and lipid metabolism (Auclair *et al.*, 2013; Sanchez-Lazo *et al.*, 2014).

Moreover, in situation of excessive level of saturated FAs, CC act as a barrier, protecting oocytes from *in vitro* induced lipotoxic effects (Aardema *et al.*, 2013; Lolicato *et al.*, 2015) through SCD-specific conversion of saturated FAs under non inhibiting conditions(Aardema *et al.*, 2017). Evidences apparent of this traffic were showed by transport of Fatty Acid Binding Protein 3 (FABP3) protein from cumulus cells to the oocyte via TZPs, that demonstrated the increase involved in carrying lipids to the oocyte (Del Collado *et al.*, 2017). **Figure 18** represents the general mechanisms of lipid and FA metabolism between follicular fluid and cumulus-oocyte complex. FA catabolism to produce ATP occurs preferentially in the mitochondrial matrix via b-oxidation, which increases dramatically during COC maturation *in vitro* (Dunning *et al.*, 2010). Lipid droplets accumulate during oocyte growth, and oxidation of FAs can generate a high number of ATP molecules, making these molecules good candidates for energy supply during oocyte maturation and early embryo development, especially in animals (Sturmey *et al.*, 2009). Several studies have reported the association of mitochondria with lipid inclusions, vesicles and endoplasmic reticulum during oocyte maturation (Hyttel, P., Fair, T., Callesen, 1997; Comin *et al.*, 2002). The use of FAs by beta-oxidation may result in increased availability of carbohydrates, such as

glucose, for use in other non-ATP pathways, including synthesis of nucleic acids and hyaluronic acid, cell signaling and redox regulation (Sutton-mcdowall *et al.*, 2012).

Mitochondrial FA oxidation (FAO) is reduced in murine oocytes and CC matured *in vitro* as compared with COCs matured *in vivo*, demonstrating that this metabolic pathway is regulated by follicular factors at the time of ovulation (Dunning *et al.*, 2014). The expression of Cpt1b (responsible for the entry of long chain FAs into the mitochondria) in mouse oocytes at the MII stage has been reported (Gentile *et al.*, 2004; Dunning *et al.*, 2010). Other transcripts of genes involved in b-oxidation, including acyl-CoA synthetases, acyl-CoA dehydrogenases and enoyl-CoA hydratase, were detected in also in human oocytes and CC (Montjean, Entezami and Lichtblau, 2012). Inhibition of FAO during oocyte IVM significantly impaired the oocyte maturation and developmental competence in mouse, bovine and porcine species (Dunning *et al.*, 2010; Paczkowski *et al.*, 2013; Sanchez-Lazo *et al.*, 2014)**.**

In bovine oocyte and surrounding CC, the proteins FA synthase (FAS), acetyl-coenzyme-A carboxylase (ACAC), carnitine palmitoyltransferase (CPT), perilipine 2 (PLIN2) and FA binding protein 3 (FABP3) were detected and their abundance varied during IVM. Key genes related to lipogenesis, lipolysis and FAO were mainly up-regulated during maturation, and MALDI MS lipid profiles of CC before and after IVM also significantly differed suggesting intense lipogenic and lipolytic activity in CC, which may be involved in regulation of oocyte maturation (Sanchez-Lazo *et al.*, 2014).

The correlation between lipid metabolism, follicular development, and oocyte competence represents an emerging topic of high relevance in dairy cattle fertility and reproduction. This review highlights the initial aspects of this process. Recent data suggest a link between lipid metabolism and reproduction/fertility, not only at the systemic level but also locally at the ovarian level that maintains its own metabolism, probably in a self-regulated manner. The activities managed by the antral follicles and the quality of the oocytes are far from being fully understood, although recent knowledge about the various endocrine, paracrine, genetic and metabolic factors involved has led to a better understanding of this immensely complex puzzle. In this context, the thesis work is to propose to discover a specific lipid profile from different follicular compartments and oocyte and correlate them to the lipid metabolism of the growing antral follicle.

OBJECTIVES

OBJECTIFS

La caractérisation des lipides et la compréhension des mécanismes de leur métabolisme au sein des différents compartiments d'un follicule ovarien peuvent contribuer dans les technologies de reproduction à améliorer la fertilité des bovins. Les thématiques de recherche de mon équipe d'accueil visent à comprendre les mécanismes moléculaires des problèmes de fertilité femelle, en particulier ceux qui impliquent la qualité de l'ovocyte. L'équipe étudie notamment les mécanismes du métabolisme des acides gras impliqués dans la régulation de la folliculogenèse et du développement des ovocytes, avec pour objectif final d'améliorer la fertilité des animaux d'intérêt agronomique. Différents modèles expérimentaux *in vivo* et *in vitro*, ainsi que différentes technologies d'analyse des lipides et de leurs régulateurs au niveau des ARN et des protéines sont utilisés. La famille des lipides est complexe, présentant une très grande diversité de molécules et de régulations ; le défi consiste donc à pouvoir analyser toute cette diversité dans différents tissus.

Notre objectif était d'approfondir les connaissances sur le rôle des lipides dans les processus de la reproduction, au niveau de l'ovaire, dans la perspective de générer des gamètes viables et en bonne santé. Le rôle du métabolisme des acides gras dans la folliculogenèse et la maturation de l'ovocyte est de plus en plus étudié, car il est prouvé que la capacité de métaboliser des lipides est cruciale pour la qualité de l'ovocyte, et en conséquence, pour l'efficacité de la reproduction.

Ainsi, l'objectif général de ma thèse est d'élucider la relation entre les profils lipidiques intra-folliculaires et ceux de l'ovocyte, ainsi que les mécanismes du métabolisme des acides gras au sein du follicule ovarien en phase du folliculogenèse terminale. La connaissance des espèces lipidiques dans différents compartiments folliculaires peut être utile pour comprendre les performances reproductives et la fertilité potentielle chez les mammifères. Nous avons cherché à analyser la composition et la distribution spatiale d'espèces lipidiques et de gènes du métabolisme des acides gras dans les follicules ovariens bovins, au cours de la croissance terminale des follicules à antrum.

Les objectifs spécifiques sont présentés ci-dessous:

- caractériser les espèces lipidiques dans les différents compartiments du follicule antral (fluide folliculaire, cellules de la thèque, granulosa et cumulus) et des ovocytes bovins par spectrométrie de masse MALDI-TOF, comparer les profils lipidiques respectifs et identifier les lipides ovariens ;
- analyser la distribution spatiale d'espèces lipidiques dans le follicule ovarien par imagerie moléculaire par spectrométrie de masse;
- étudier l'expression de gènes liés au métabolisme des lipides dans les cellules folliculaires somatiques et les ovocytes des follicules antraux ;
- évaluer la composition lipidique et l'expression des gènes liés au métabolisme des lipides dans les follicules de différentes tailles ;
- comparer la composition lipidique des ovocytes dans différentes conditions physiologiques

OBJECTIVES

The overall project of my host team is to understand the molecular mechanisms of female fertility problems, particularly targeted at oocyte quality. The role of lipid metabolism is studied at different levels from animal to ovarian cells and oocyte, during reproductive cycle, with the final objective to improve fertility of the animals of agronomic interest, like ruminants and especially dairy cows, which have particular lipid metabolism post-partum. Energy metabolism deregulations are associated, in most of cases, with decreasing reproductive capacities. Fatty acids (FA) and lipids in general regulate reproductive processes especially those that are evolutionarily conserved, such as the meiotic maturation of the oocyte, which is essential for embryo developmental competence. Although research on FA metabolism in female reproduction is in progress in many scientific teams, lipid content, location and site/modes of action of FA in the ovary and, more specifically, in an ovarian follicle, remain little known. Research team BINGO ("Biologie Intégrative de l'Ovaire"),where my work was realized, investigates the mechanisms of FA metabolism that are involved in regulation of folliculogenesis and oocyte development and uses different experimental *in vivo* and *in vitro* models as well as different technologies to analyze lipids and their regulators at RNA and protein level.

The lipids present in the ovaries has been studied since the 1950s, but many aspects of their functioning, metabolism and location have been limited by the existing technology. Mostly, specific lipids were studied in association with enzymes and proteins related to their activity, such as in the production of steroids, or enzyme-mediated lipid transformations. However, a more accurate characterization and location of these molecules began better explored with the advances in mass spectrometry (MS). Lipidomics is used to study the identity, abundance and modifications of lipids that are present in a cell, tissue or organism. Their applications are prominent in clinical research because it has been used successfully for the discovery of candidate biomarkers in cancer research (Gustafsson *et al.*, 2011) and cancer therapy (Meriaux *et al.*, 2010; Manzanares-Meza, Gutiérrez-Román and Medina-Contreras, 2017). Consequently, analysis of lipids at ovarian level became possible with the emergence of these new technologies as MS Imaging (Goto-Inoue *et al.*, 2011; Lagarrigue *et al.*, 2011).

Lipid family is complex and presents a very large diversity of molecules, so analyzing and quantifying all this diversity is a challenge. We aimed to enlighten the role of lipids in the processes involved in the female reproduction, in ovary, where the challenge is to generate viable and healthy gametes. Role of lipid metabolisms in folliculogenesis and oocyte maturation are more and more studied now because there is the evidence that capacity to metabolize fat is crucial for oocyte quality and thus reproduction efficiency.

Crucial point for this study is the development of lipidomic approaches, especially lipid identification in faint quantity of biological material, as follicular cells or oocytes. Lipidomics seems to be an area where progress is incremental, closely related to the improvements that are made to mass spectrometers, and its specialized development plays an important role, allowing using in this study of ICM-MS (Intact Cell MALDI-TOF Mass Spectrometry) and MSI to perform the analyses of bovine ovaries and their particular compartments (cells and fluid).

1 General objective

Lipids are part of all the cells and FA are essential for their metabolism. Oocyte development and quality assured by its follicular environment during folliculogenesis. General hypothesis that the lipids composition in the various compartments of the antral follicle can metabolically compromise oocyte competence to embryo development. Lipid characterization and the understanding of mechanisms in the follicular capacity to metabolize lipids in the different compartments may serve to improve fertility in bovines. Thus, we assumed the general objective of elucidating the relationship between intrafollicular lipid profiles and enclosed oocyte, as well as the mechanisms of FA metabolism within the antral bovine ovarian follicle. The knowledge of lipid species in several follicles compartments is fundamental to understand reproductive performance and potential fertility in mammals. We aimed to analyze composition and spatial distribution of lipid species, and genes of FAs metabolism in bovine ovarian follicles.

2 Specific objectives

The corresponding specific aims are presented below:

- to characterize lipid species in different compartments of antral follicle (follicular fluid, theca, granulosa and cumulus cells) and oocyte by MALDI-TOF MS, compare lipid fingerprints and identify ovarian lipids
- to analyze the spatial distribution of molecular lipid species in ovarian follicle from bovine ovary sections
- to investigate expression of lipid metabolism related genes in somatic follicular cells and oocytes from antral follicles
- to evaluate lipid composition and expression of lipid metabolism related genes in small and large follicles, enclosing the oocytes with different competence
- to compare lipid composition between the oocytes in different physiological conditions

MATERIALS AND METHODS

MATERIALS AND METHODS

The present study had required the adaptation of lipidomic approaches to analysis of ovarian tissues and follicular fluid. A summary of the experimental procedures used in our studies are listed below. Detailed description is mainly given in Article 1 and 2. Most of the experimental procedures were performed in the laboratory (material collection, MALDI-TOF lipid profiling, MS Imaging, Nile Red imaging, lipid identification in situ, real time PRC, lipid annotation, etc). The identification of lipids was performed by specialized lipidomic platform (Profilomic, CEA). Microarray hybridization was performed by transcriptomic platform (INRA, BDR, Joue-en-Josas).

1 Ethics

It was not necessary to request approval for ethics committee when the biological materials used came from local commercial slaughterhouse. For *in vivo* animals the approved experimental protocols by the local ethics committee were required (CEEA VdL, reference number of the protocol 2012-10-4 and 01607.02-Prolific project; and the protocol 2015-100115278976-v5-Bovomega3 Project), according to the directives of the French Council for animals protection.

2 Chemicals

All chemicals were purchased from Sigma-Aldrich (Saint-Quentin Fallavier, France). LC–MS grade water (H2O) and methanol (MeOH) were from VWR International (Plainview, NY). Internal standard mix for lipid identification was purchased from Avanti Polar Lipids, Inc (Alabaster, AL). Exceptions were indicated in the description of materials and methods.

3 Biological material

The collection of ovarian cells and fluids was performed either postmortem (ovaries from slaughterhouse) or *in vivo*, by ovum-pick up under ultrasound control.

Follicles were aspirated and treated either individually, after dissection and measurement (to isolate the cells separately from the each follicle), or aspirated liquids were pooled to recover cumulus-oocyte-

complexes and granulosa cells. The internal layer of each follicle were scraping off gently to recovered granulosa cells (GC), and isolating theca cell layers (TH). Oocytes were separated individually from their CC by repetitive aspirating-ejecting movements using a P100 Gilson pipette in 100-µl drops under observation with a stereomicroscope, then CC centrifuged 10 min 5000 g. CC pellet and individual oocytes were rinsed twice in (260 mM sucrose 20 mM Tris-HCl pH 6.8; Tris-sucrose). The samples were snap-frozen in liquid nitrogen and kept at -80°C (within 1 week)

3.1 Biological material collection *in vivo*

Before ovarian cycle follicular dynamic in cows were monitored weekly with a transrectal ultrasonographic examination using a linear probe (LV 513 6.0/8.0-MHz transducer; Mylab30; Esaote) allowing detection and measurement of antral follicles, immature 4-10 mm follicles were aspirated by ovum pick up to individually separated oocyte, cumulus and granulosa cells. The oocytes were separated individually from their cumulus cells (CC), and then rinsed twice in Tris-sucrose. Cells were washed in sterile PBS and centrifuged (for 10 min 5000g at 4°C), and then the pellets were rinzed with Tris-sucrose twice. All samples were snap-frozen in liquid nitrogen and kept at -80°C up to analysis.

3.2 Collection of ovaries for in situ lipidomic analysis

The whole ovaries, transported from the local slaughterhouse on ice, were frozen in nitrogen steam and cut with cryostat within 4 days for immediate analysis by Mass spectrometry Imaging (MSI) or .

4 Lipidomic analysis

4.1 Nile Red staining

Nile Red fluorescence (NRF) was used for the quantification and localization of neutral lipids in a general panorama of ovarian tissue sections. Originally developed to use in culture cell or single-cells, based in original protocol from Fowler & Greenspan (Fowler and Greenspan, 1985), but also in COC to Nile correlate the morphological appearance bovine oocytes with its lipid content (Jlmr L M R Leroy *et al.*, 2005). The NRF lipid analysis technique was adapted to use in bovine ovaries sections and at the first time scanned using AxioScan.Z1 scanner (Carl Zeiss SAS, German) wherein the protocols were here developed. (**Article 1 and 2**)

4.2 Lipid identification

Total lipids were extracted from a pool of ovarian follicular cells (GC and TH) and follicular fluid (FF), and also *in situ* lipid extraction experiments were performed manually at multiple user-defined points across the tissue targeting follicles from cryo-sections of freshly frozen bovine ovaries to performance a lipid identification using Liquid chromatography coupled to high-resolution mass spectrometry (LC-HRMS and Tandem high-resolution mass spectrometry (HRMS/MS) (widely described in **Article 1**).

4.3 MALDI-TOF MS analysis of lipids of individual oocytes, follicular cells and fluid

Exploring lipid species content was the main motivation to understand the dynamics of lipid metabolism within the different ovarian compartments. Therefore, MALDI-TOF mass spectrometry was adapted to analyse bovine follicular cells, fluid and single oocytes. Workflow is presented in **Figure 19**. (**Article 1 and 2**).

Briefly, frozen oocytes were thawed in ice and placed on the MTP Ground Steel 384 MALDI plate (Bruker Daltonics, Germany) to dry. TH, GC, CC samples were defrosted in an ice bath and 5 µl of cell suspension or FF were dried by SpeedVac System (SPD 1010-230, Thermo Savant Eletronic Corporation, France) for 10 minutes at 45°C. Pellets were re-suspended in DHAP (2,5-dihydroxyacetophenone) matrix at 20 mg/mL solubilized in 90% methanol, 2% trifluoroacetic acid in water (4 µl for cells and 8 µL for FF samples). The matrix/sample mixtures were sonicated for 4 min using an ultrasonic bath sonicator (FisherBrand 15,052, Fisher Scientific) to solubilize lipids. One microlitrer of the matrix/sample mix was overlayed with 1,5 µL of the same solution of matrix. Each sample was spotted onto MALDI plate in 3 replicates (at the exception of single oocyte), then dried at room temperature for 30 min. 3000 spectra per spot (as a sum of 1000 consecutive laser shots in 3 shot steps) were acquired, using Bruker UltrafleXtreme MALDI-TOF instrument (Bruker Daltonics, Germany). Spectra were acquired in positive and negative ion modes using reflecton, in the m/z 100 – 1200 range. External calibration was performed using a mixture of small molecules and peptides (1 µL of calibrant solution containing Cafein, MRFA peptide, Leu-Enkephalin, Bradykinine 2-9, Glu1-fibrinopeptide B; reserpine; Bradykinine; Angiotensine I) and mix in 1 µL of DHAP matrix. To increase mass accuracy (mass error < 0.05%), internal calibration was subsequently applied to all spectra. Lock mass correction was performed with highest intensity peak, corresponding to the glycerophosphocholine (PC 32:1, m/z 732.556) in positive mode, and glycerophosphatidylinositol (PI 38:4; m/z 885.5499) in negative mode, using FlexAnalysis 4.1 software (Bruker). Each spectrum was converted to a .txt file using FlexAnalysis 3.4 software and processed using MALDI Progenesis software version 1.2

(Nonlinear Dynamics, Newcastle upon Tyne, UK). Peaks were manually detected. The peaks with a ratio signal to background < 5 and the isotopes were not considered for analysis. Coefficient of variation (CV %) of intensity values (normalized peak height, NPH) was calculated for all the peaks in three technical replicates per sample. NPH values were used for comparative analysis of lipid profiling between the compartments (**Figure 20**).

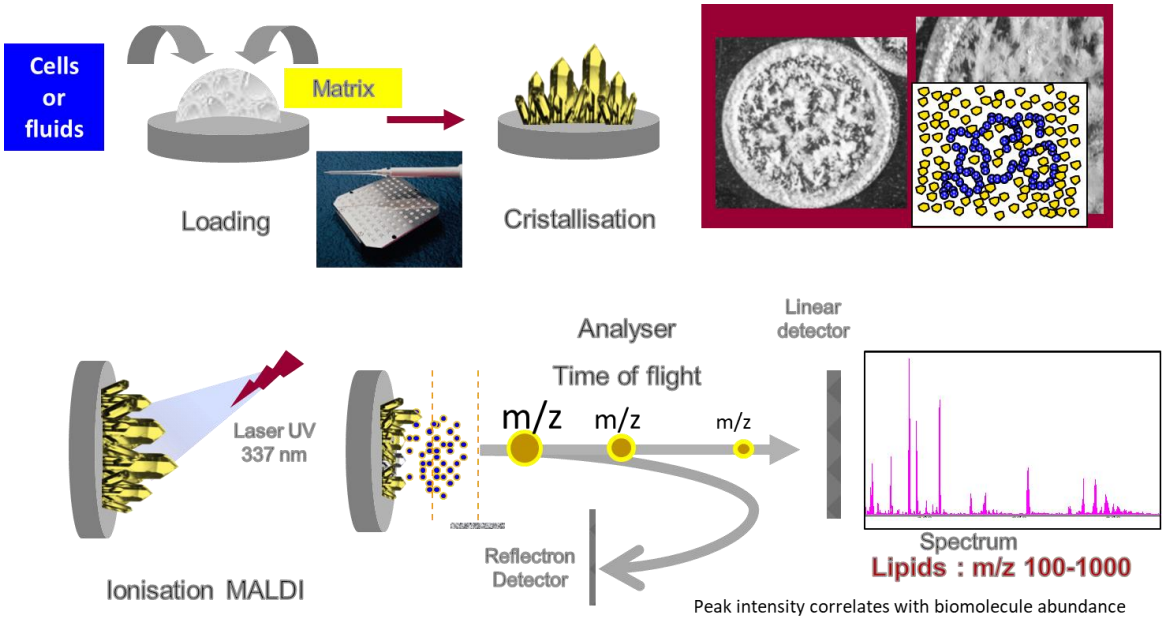


Figure 19. Principle of MALDI-TOF mass spectrometry analysis of lipids.

Briefly, frozen oocytes were thawed in ice and placed on the MTP Ground Steel 384 MALDI plate (Bruker Daltonics, Germany) to dry. TH, GC, CC samples were defrosted in an ice bath and 5 µl of cell suspension or FF were dried by SpeedVac System (SPD 1010-230, Thermo Savant Eletronic Corporation, France) for 10 minutes at 45°C. Pellets were re-suspended in DHAP (2,5-dihydroxyacetophenone) matrix at 20 mg/mL solubilized in 90% methanol, 2% trifluoroacetic acid in water (4 µl for cells and 8 µL for FF samples). The matrix/sample mixtures were sonicated for 4 min using an ultrasonic bath sonicator (FisherBrand 15,052, Fisher Scientific) to solubilize lipids. One microlitrer of the matrix/sample mix was overlayed with 1,5 µL of the same solution of matrix. Each sample was spotted onto MALDI plate in 3 replicates (at the exception of single oocyte), then dried at room temperature for 30 min. 3000 spectra per spot (as a sum of 1000 consecutive laser shots in 3 shot steps) were acquired, using Bruker UltrafleXtreme MALDI-TOF instrument (Bruker Daltonics, Germany). Spectra were acquired in positive and negative ion modes using reflecton, in the m/z 100 – 1200 range. External calibration was performed using a mixture of small molecules and peptides (1 µL

of calibrant solution containing Cafein, MRFA peptide, Leu-Enkephalin, Bradykinine 2-9, Glu1-fibrinopeptide B; reserpine; Bradykinine; Angiotensine I) and mix in 1 µL of DHAP matrix. To increase mass accuracy (mass error < 0.05%), internal calibration was subsequently applied to all spectra. Lock mass correction was performed with highest intensity peak, corresponding to the glycerophosphocholine (PC 32:1, m/z 732.556) in positive mode, and glycerophosphatidylinositol (PI 38:4; m/z 885.5499) in negative mode, using FlexAnalysis 4.1 software (Bruker). Each spectrum was converted to a .txt file using FlexAnalysis 3.4 software and processed using MALDI Progenesis software version 1.2 (Nonlinear Dynamics, Newcastle upon Tyne, UK). Peaks were manually detected. The peaks with a ratio signal to background < 5 and the isotopes were not considered for analysis. Coefficient of variation (CV %) of intensity values (normalized peak height, NPH) was calculated for all the peaks in three technical replicates per sample. NPH values were used for comparative analysis of lipid profiling between the compartments (**Figure 20**).

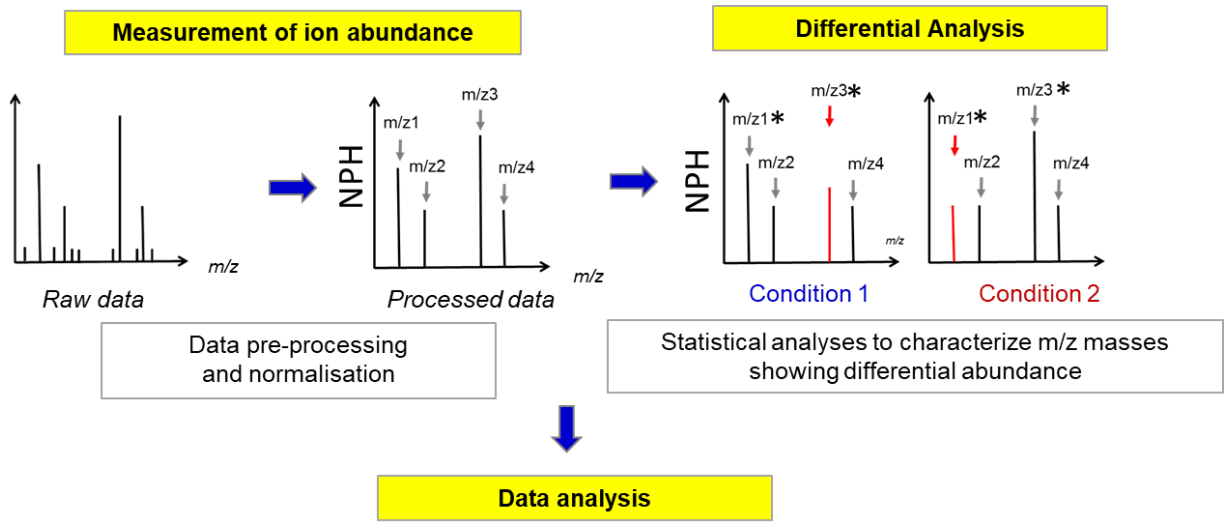


Figure 20. Principle of differential analysis of lipid abundance. Raw spectra are processed (smoothing, background subtraction, alignment, normalization) and the peaks are automatically detected. The normalized peak height values (NPH) are used for differential analysis.

4.4 Mass Spectrometry Imaging (MSI) by MALDI-TOF MS

MSI of lipids was adapted from that described for porcine ovary (Uzbekova *et al.*, 2015), and workflow of MSI is shown in **Figure 21**. Sections of freshly frozen whole ovaries were mounted onto conductive microscope slides. A mixture of small molecules and peptides (1 µL of calibrant solution containing Cafein, MRFA peptide, Leu-Enkephalin, Bradykinine 2-9, Glu1-fibrinopeptide B; reserpine; Bradykinine; Angiotensine I), i.e. the external mass calibration (1 µL) was placed near the tissue section and mixed (1:1 v/v) with the CHCA (α-Cyano-4-hydroxycinnamic acid) matrix. Ovary sections were scanned using a histology slide scanner (OpticLab H850 scanner, Plustek, Ahrensburg, Germany). These images were used to overlay histological and molecular images.

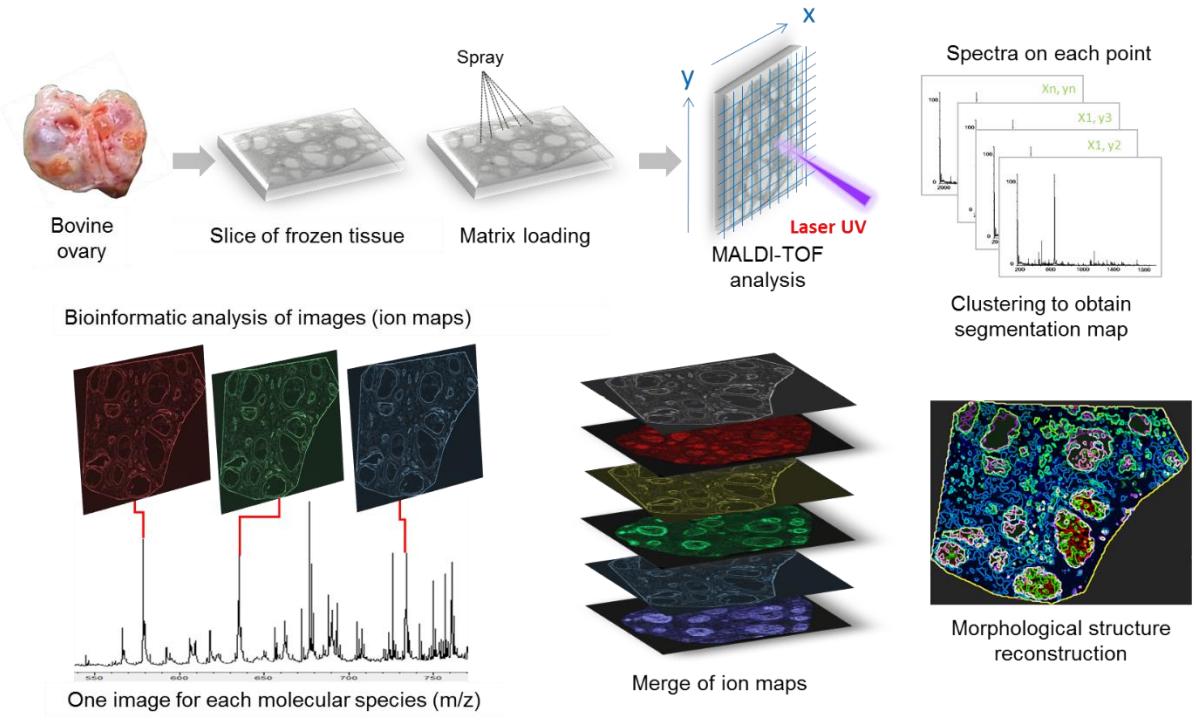


Figure 21. Mass spectrometry imaging of lipids on ovarian sections. (Adapted from Uzbekova et al, 2015).

Slides were coated with CHCA matrix sprayed at 7 mg/mL in 60/40 acetonitrile/H2O, 0.2% trifluoroacetic acid using an Image Prep device (Bruker Daltonik GmbH, Bremen, Germany), and then vacuum-dried. MSI sequence was performed from one ovarian section targeting several regions of interest (ROIs) corresponding to whole ovary image, and posteriorly ROIs of individual antral follicles.

Spectra were acquired using an UltrafleXtreme MALDI-TOF instrument (Bruker Daltonik GmbH, Bremen, Germany) equipped with a Smartbeam laser (Nd:YAG, 355 nm) monitored by the FlexControl

3.4 software (Bruker Daltonics, Bremen, Germany) in positive mode, at 2.0 kHz laser repetition rate, in the 100–1200 m/z range, using a spatial resolution set at 25 µm, to individual follicles (article 1), and 100µm, to whole ovary image (article 2) in medium focus setting, and collecting 500 spectra per pixel as a sum of 50 consecutive laser shots in 10 random walk shot steps. For a better mass accuracy across a tissue section image, raw spectra from all datasets were first aligned to a lock mass set at m/z 760.5780 corresponding to $[M+H]^+$ of PC 34:1. The unprocessed MSI sequence was then imported into the SCiLS Lab software (version 2016b, SCiLS, GmbH, Bremen, Germany). MSI sequence was loaded and pre-processed, according the used instrument type (TOF). Data were baseline reduced using a convolution algorithm with the setting of 20 for peak width and normalized to the total ion count (TIC). For each region of interest (ROI, individual follicle), 2D ion density maps using medium denoising were created from the average projection spectrum and, after data partitioning (bisecting k-Means), a segmentation map, that reconstructs morphological structures, was generated.

5 Gene expression analysis

Total RNA was extracted either from the pools of isolated TH, GC, CC and oocytes (n=50) or from somatic cells of individual follicles using TriZol reagent (Invitrogen, Cergy Pontoise, France). After isopropanol precipitation, the RNA concentration was determined using a NanoDrop ND-1000 spectrophotometer (Nyxor Biotech, Paris, France), for microarray hybridization, RNA integrity was checked on a Bioanalyzer 2100 (Agilent Technologies, Santa Clara, CA, USA). Total RNA was treated by RQ1 DNAse (Promega, Charbonnières, France) following the manufacturer's instructions before converting to cDNA.

In this work, gene expression analysis was performed: first, in silico, by analysis of transcriptomic data obtained by microarray hybridization from TH, GC, CC and oocyte RNA (microarray hybridization was performed by A. Carvalho, BDR, Jouy-en-Josas (**Article 1**); and second, by real time PCR (see detailed description in **Articles 1 and 2**).

RESULTS

RÉSULTATS

Dans ce travail, nous avons caractérisé les lipidomes des cellules et du liquide des follicules ovariens chez la vache, pour la première fois. Différentes approches d'analyse des lipides ont été développées, y compris des méthodes originales de spectrométrie de masse telles que l'imagerie de lipides par SM et le phénotypage moléculaire sur des cellules intactes et des fluides en utilisant la spectrométrie de masse MALDI-TOF. Les empreintes lipidiques ont été comparées entre les différents compartiments folliculaires et entre ces mêmes compartiments dans différentes conditions physiologiques. En outre, la transcriptomique a été utilisée pour analyser le contrôle transcriptionnel du métabolisme des lipides dans les cellules folliculaires ovariennes et les ovocytes.

1. Identification des lipides et analyse d'expression des enzymes régulant leur métabolisme dans le follicule ovarien bovin

1.1 Article 1

Bertevello PS, Teixeira-Gomes AP, Seyer A, Vitorino Carvalho A, Labas V, Blache MC, Banliat C, Cordeiro LAV, Duranthon V, Papillier P, Maillard V, Elis S and Uzbekova S (2018) Lipid Identification and Transcriptional Analysis of Controlling Enzymes in Bovine Ovarian Follicle. Int J Mol Sci 19. doi: 10.3390/ijms19103261

Le follicule ovarien renferme l'ovocyte en croissance, qui acquière sa compétence pour soutenir le développement de l'embryon, grâce à des échanges moléculaires permanents entre les cellules folliculaires somatiques et le liquide folliculaire. La stéroïdogenèse dans les cellules de thèque (TH) et de granulosa (CG) a largement été étudiée et les études portant sur les mécanismes moléculaires du métabolisme des acides gras (AG) dans les cellules du cumulus (CC) et les ovocytes émergent. Néanmoins, peu de données sont actuellement disponibles concernant la régulation du métabolisme des lipides dans les follicules ovariens. Dans cette étude, nous avons étudié la composition lipidique et la régulation transcriptionnelle du métabolisme des AG dans les follicules ovariens de 3–8 mm chez le bovin. En utilisant la chromatographie liquide et la spectrométrie de masse, 438 et 439 lipides ont été identifiés dans les cellules folliculaires et le liquide folliculaire, respectivement. À partir des empreintes lipidiques MALDI-TOF obtenues dans le liquide folliculaire, les cellules TH, CG, CC et ovocytes, et de l'imagerie des lipides par spectrométrie de masse sur les coupes ovariennes, nous avons identifié 197 lipides et déterminé les espèces les plus abondantes dans chaque compartiment. La transcriptomique a révélé des gènes liés au métabolisme des lipides, qui sont exprimés de manière constitutive ou plus spécifiquement dans les TH, CG, CC ou les ovocytes. Couplées à une composition lipidique différentielle, ces données suggèrent que le follicule ovarien contient la machinerie métabolique potentiellement capable de métaboliser les AG issus des nutriments, les transformer et produire des lipoprotéines, effectuer la lipogénèse *de novo* et accumuler des réserves lipidiques, assurant ainsi l'apport énergétique à l'ovocyte, la synthèse des membranes cellulaires et la signalisation pour maintenir l'homéostasie folliculaire.

RESULTS

In the present work, for the first time we characterized the lipidomes of ovarian cells and fluid in cows. For these studies, different approaches of lipid analysis including original mass spectrometry methods as MS imaging and molecular profiling on intact cells and fluid using MALDI-TOF MS were developed. Lipid composition was compared between the different follicular compartments, and between the same compartments in different physiological conditions. In addition, transcriptomics was used to analyze transcriptional control of lipid metabolism in ovarian follicular cells and enclosed oocyte.

1 Identification of lipids in bovine ovarian follicle and gene expression analysis of controlling enzymes

1.1 Article 1

Bertevello PS, Teixeira-Gomes AP, Seyer A, Vitorino Carvalho A, Labas V, Blache MC, Banliat C, Cordeiro LAV, Duranthon V, Papillier P, Maillard V, Elis S and Uzbekova S (2018) Lipid Identification and Transcriptional Analysis of Controlling Enzymes in Bovine Ovarian Follicle. Int J Mol Sci 19. doi: 10.3390/ijms19103261

Abstract

Ovarian follicle provides a favorable environment for enclosed oocytes, which acquire their ompetence in supporting embryo development in tight communications with somatic follicular cells and follicular fluid (FF). Although steroidogenesis in theca (TH) and granulosa cells (GC) is largely studied, and the molecular mechanisms of fatty acid (FA) metabolism in cumulus cells (CC) and oocytes are emerging, little data is available regarding lipid metabolism regulation within ovarian follicles. In this study, we investigated lipid composition and the transcriptional regulation of FA metabolism in 3–8 mm ovarian follicles in bovine. Using liquid chromatography and mass spectrometry (MS), 438 and 439 lipids were identified in FF and follicular cells, respectively. From the MALDI-TOF MS lipid fingerprints of FF, TH, GC, CC, and oocytes, and the MS imaging of ovarian sections, we identified 197 peaks and determined more abundant lipids in each compartment. Transcriptomics revealed lipid metabolism-related genes, which were expressed constitutively or more specifically in TH, GC, CC, or oocytes. Coupled with differential lipid composition, these data suggest that the ovarian follicle contains the metabolic machinery that is potentially capable of metabolizing FA from nutrient uptake, degrading and producing lipoproteins, performing *de novo* lipogenesis, and accumulating lipid reserves, thus assuring oocyte energy supply, membrane synthesis, and lipid-mediated signaling to maintain follicular homeostasis.

International Journal of
Molecular Sciences

MDPI

Article

Lipid Identification and Transcriptional Analysis of Controlling Enzymes in Bovine Ovarian Follicle

Priscila Silvana Bertevello [1], Ana-Paula Teixeira-Gomes [2,4], Alexandre Seyer [5], Anaïs Vitorino Carvalho [1,3], Valérie Labas [1,4], Marie-Claire Blache [1], Charles Banliat [1], Luiz Augusto Vieira Cordeiro [1], Veronique Duranthon [3], Pascal Papillier [1], Virginie Maillard [1], Sebastien Elis [1] and Svetlana Uzbekova [1,4,*]

1 UMR PRC, INRA 85, CNRS 7247, Université de Tours, IFCE, 37380 Nouzilly, France; priscila.bertevello@inra.fr (P.S.B.); anais.carvalho@hotmail.fr (A.V.C.); valerie.labas@inra.fr (V.L.); marie-claire.blache@inra.fr (M.-C.B.); Charles.Banliat@inra.fr (C.B.); Luiz-Augusto.Viera-Cordeiro@inra.fr (L.A.V.C.); pascal.papillier@inra.fr (P.P.); virginie.maillard@inra.fr (V.M.); sebastien.elis@inra.fr (S.E.)
2 UMR ISP, INRA 1282, Université de Tours, 37380 Nouzilly, France; ana-paula.teixeira@inra.fr
3 UMR BDR, ENVA, INRA, Université Paris-Saclay, 78350 Jouy-en-Josas, France; veronique.duranthon@inra.fr
4 PAIB (Pôle d'Analyse et d'Imagerie des Biomolécules), Plate-forme CIRE (Chirurgie et Imagerie pour la Recherche et l'Enseignement, INRA, Université de Tours, CHRU de Tours, 37380 Nouzilly, France
5 Profilomic SA, F-92100 Boulogne-Billancourt, France; alexandre.seyer@medday-pharma.com
* Correspondence: svetlana.uzbekova@inra.fr; Tel.: +33-247-427-951

Received: 30 September 2018; Accepted: 18 October 2018; Published: 20 October 2018



Abstract: Ovarian follicle provides a favorable environment for enclosed oocytes, which acquire their competence in supporting embryo development in tight communications with somatic follicular cells and follicular fluid (FF). Although steroidogenesis in theca (TH) and granulosa cells (GC) is largely studied, and the molecular mechanisms of fatty acid (FA) metabolism in cumulus cells (CC) and oocytes are emerging, little data is available regarding lipid metabolism regulation within ovarian follicles. In this study, we investigated lipid composition and the transcriptional regulation of FA metabolism in 3–8 mm ovarian follicles in bovine. Using liquid chromatography and mass spectrometry (MS), 438 and 439 lipids were identified in FF and follicular cells, respectively. From the MALDI-TOF MS lipid fingerprints of FF, TH, GC, CC, and oocytes, and the MS imaging of ovarian sections, we identified 197 peaks and determined more abundant lipids in each compartment. Transcriptomics revealed lipid metabolism-related genes, which were expressed constitutively or more specifically in TH, GC, CC, or oocytes. Coupled with differential lipid composition, these data suggest that the ovarian follicle contains the metabolic machinery that is potentially capable of metabolizing FA from nutrient uptake, degrading and producing lipoproteins, performing de novo lipogenesis, and accumulating lipid reserves, thus assuring oocyte energy supply, membrane synthesis, and lipid-mediated signaling to maintain follicular homeostasis.

Keywords: ovarian follicle; lipids; mass spectrometry imaging; MALDI MS profiling; gene expression; oocyte; granulosa; theca; follicular fluid; bovine

1. Introduction

In dairy cows, lipid metabolism is crucial to maintain proper reproductive function, which is affected by negative energy balance (NEB) occurring during the early postpartum period, due to the elevated mobilization of fat reserves to liberate the energy that is required for milk production [1,2]. Oocyte competence or capacity to support embryo development after fertilization is one of the key factors affected by misbalanced fatty acid (FA) metabolism during the NEB period [3]. Indeed, high

concentrations of free FAs in plasma and follicular fluid (FF) during NEB lead to lipotoxicity within the ovarian follicle and impair oocyte quality, thus reducing cow fertility [4]. The impaired lipid composition of FF, which is particularly rich in saturated free FA (C18:0 stearic and C16:0 palmitic acids) in lactating cows, may explain their lower fertility as compared to heifers [5], as well as the seasonal variations of oocyte developmental competence in dairy cows [6].

Oocytes develop and acquire their developmental competence in the ovarian follicle through tight bidirectional communication with follicular somatic cells, with each compartment secreting specific regulation factors [7–10]. Ovarian morphological and functional organization supports follicular development and oogenesis, protecting the growing oocyte. Inside the pre-antral follicle, epithelial-like granulosa cells (GC) and mesenchymal-like theca cells (TH) face each other across a basement membrane; these mural cells enclose the oocyte, which grows through folliculogenesis. TH cell layers are transpierced by blood microvessels, and since antrum appearance, the follicle is filled with a fluid that is rich in proteins, steroids, and lipids, coming from the blood and secretory activity of follicular somatic cells—TH, GC, and cumulus cells (CC), too [11,12]. CC are the differentiated GC, which are tightly connected and metabolically coupled with an oocyte via gap junctions [13] and form the oocyte cumulus complex (OCC). The interaction between TH and GC is essential for the maintenance of the original architecture and functions of ovarian cells, especially for the synthesis of steroids, which regulates reproductive function, in response to the follicle stimulation hormone (FSH) and luteinizing hormone (LH). The closest follicular environment of the oocyte, including FF, GC, and especially CC, has a crucial impact on the acquisition of oocyte developmental competence [12,14–16] and possesses molecular factors that are predictive of oocyte developmental potential [17–19].

Energy metabolism significantly varies between the different types of ovarian follicular cells, especially in oocytes and CC, notably relying on different energy sources, including amino acids, pyruvates over glucose, and fatty acids [20,21]. To produce energy, oocytes use lipid reserves, besides the glucose derivate supplied by CC [22].

Free FAs are the major blocks for the synthesis of glycerolipids, such as triacylglycerids (TG), which are mainly used for intracellular energy storage, forming together with cholesterol esters (CE) intracellular lipid droplets (LDs) as reservoirs of caloric reserves. LDs are also caches of FAs and sterol components that are needed for the biogenesis of the membranes [23]. The cholesterol that is used by ovarian cells is derived from either the cellular uptake of plasma lipoproteins, which contain cholesterol, or de novo synthesis [24]. Free FAs and cholesterol form the structural basis for the synthesis of paracrine hormones such as prostaglandins and steroids, which play crucial roles in female reproduction, with particular involvement in the ovulation process [25] and the pre-ovulatory maturation of OCC in bovine [26]. Three lipid families are crucial components of the biological membrane structure: glycerophospholipids containing diacylglycerols (DG) in their hydrophobic part; sphingolipids (SL) with a ceramide as the hydrophobic part, and sterols (ST)—the major non-polar lipids [27]. Hydrolysis of the glycerolipids and SL produces messenger lipids such as DGs, ceramides, unsaturated FAs, and lysophosphatidic acid (LPA), and other membrane lipids may have signaling functions [28].

In the ovary, circulating free FAs are transported from blood as complexes with albumin inside the ovarian follicle, and should be metabolized to form de novo membranes or used as energy sources for the oocyte [21,29]. It is known that in somatic cells, captured FAs are esterified into TG and cholesterol esters (CE), and thus could be stored as neutral lipids in lipid droplets (LDs) for further use [23]. Ovarian follicular somatic cells, in particular TH and GC, receive and metabolize nutritive molecules, including lipids in lipoprotein form from FF [20], and transform them either for storage in LDs, or the building of a membrane bilayer, ATP production, or signaling molecules.

Although lipids are an integral part of all of the biological membranes and universal energy reserves, the distribution of lipids in mammalian ovaries is not homogenous, as was detected by mass spectrometry imaging (MSI). In porcine ovary, the MSI of lipids was performed using

matrix-assisted laser desorption/ionization time-of-flight mass spectrometry (MALDI-TOF MS), which clearly discriminated stroma and ovarian follicles through ovarian sections with a particularly specific distribution of glycerophospholipids, sphingolipids, and cholesterol derivatives between somatic cells (GC/TH) and FF inside the follicles [30]. In mice ovary, the localization and intensity of several lipids, including phosphatidylinositol (PI 38:4) and arachidonic acid (C20:4), varied between preovulated and post-ovulated stages [31].

MALDI-TOF MS profiling is a technique that allows the direct detection of the endogenous molecules in a relatively wide mass range beginning from 100 Da to 25,000 Da (ions of lipids, or peptides and proteins), in scarce biological samples. In bovine, this technique was used to analyze lipid fingerprints in oocytes [32–34], CC [35,36], and FF [37].

The enzymatic pathways involved in lipid transformations were studied preferentially in lipogenic organs such as adipose tissue [38], liver [39], and also in cancer cells [40]. The proteins that are involved in FA metabolism may have tissue specific distribution, as shown for FA binding proteins encoded by numerous *FABP* genes, with each one preferentially expressed in different tissue [41]. The importance of triacylglycerol and FA metabolism in the oocyte–cumulus complexes and the crucial role of FA oxidation for oocyte quality in mouse was underlined in the review by Dunning et al. [42]. In bovine, until now, the studies reporting on the expression of lipid metabolism-related genes in ovarian cells were focused on only a few key enzymes in oocytes, CC, and GC [35,43–47]. Expression of the main FA transforming enzymes involved in lipogenesis, lipolysis, FA oxidation, and FA transport has revealed active lipid metabolism in the oocyte and surrounding CC and GC. Besides, both lipid synthesis and FA oxidation are involved in the regulation of GC proliferation and steroidogenesis [46]. FA oxidation in CC was crucial for oocyte maturation in bovine [35,44]. However, the mechanisms through which somatic ovarian follicular cells metabolize lipids for oocyte energy supply to promote oocyte quality, and genes regulating lipid metabolism in ovarian follicles, are still poorly elucidated.

The objective of this study was to investigate the lipid composition and transcriptional regulation of FA metabolism in bovine ovarian follicles. We focused our analysis on follicles between 3–8 mm in diameter, which are routinely used for recovering the oocytes for in vitro embryo production technologies in bovine [48]. Lipid identification and their distribution in ovarian follicular compartments (FF, oocyte, CC, GC, and TH), coupled with the gene expression analysis of lipid metabolism-related genes in follicular cells, may enlighten these mechanisms.

2. Results

2.1. Analysis of Lipids in Bovine Ovarian Follicular Cells and Fluid

2.1.1. Analysis of Lipids by Nile Red on Ovarian Sections

Nile red fluorescence (NRF) was analyzed on ovarian sections in the equal surface of FF, TH, and GC layers. NRF was more intensive in the cellular compartments of ovarian follicles than in FF (intensity of red fluorescence correlates with a quantity of neutral lipids) (Figure 1A). Normalized NRF intensity was compared between TH, GC, and FF compartments in 15 follicles (5.49 $\pm$ 0.28 mm in diameter) from seven ovaries (Figure 1B). Average NRF intensity was significantly lower in FF (0.53 $\pm$ 0.05 arbitrary units, au) as compared with GC and TH layers (7.65 au $\pm$ 0.75; 4.81 au $\pm$ 0.37, respectively). NR staining in the GC layer was significantly higher than in TH layer ($p < 0.05$).

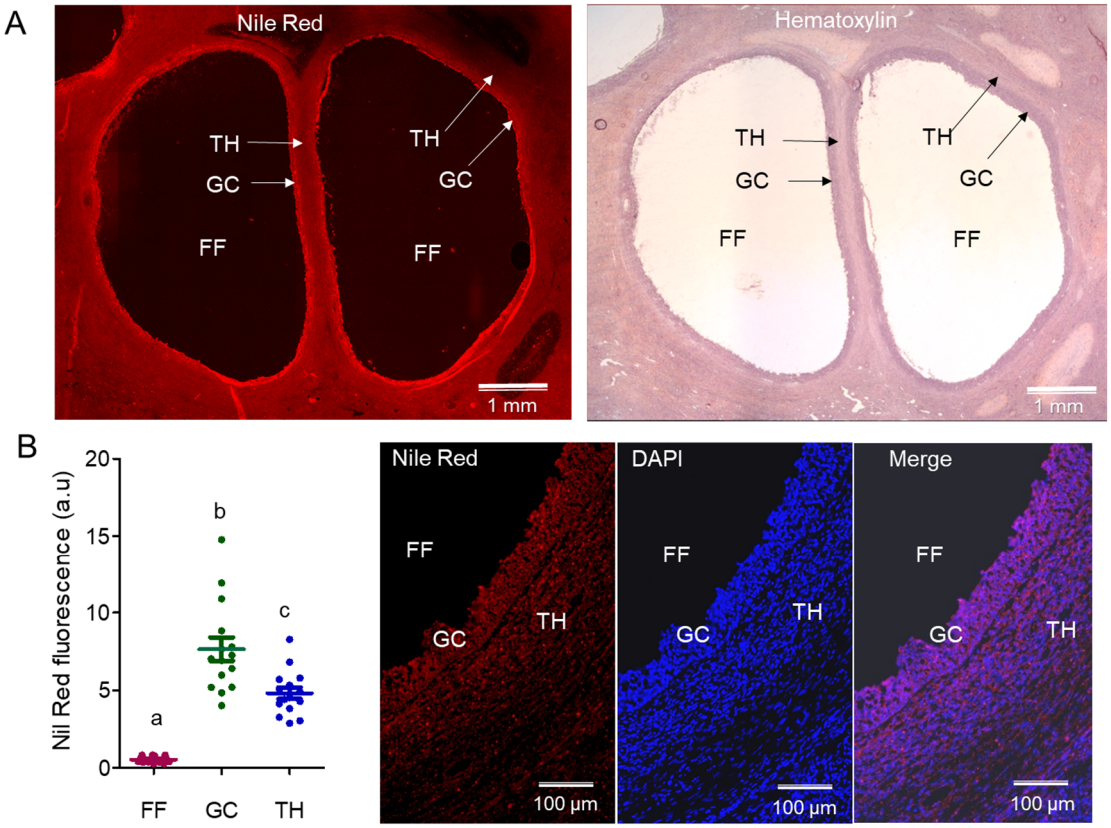


Figure 1. Quantification of lipids in bovine follicular compartments by Nile red fluorescence (NRF). (**A**) Nile red staining (left picture) and hematoxylin coloration of ovarian section (right picture). (**B**) Scatter plot represents Nile red fluorescence quantification in follicular fluid (FF), granulosa cells (GC), and theca cells (TH) in 15 follicles with an average size of 5.5 mm. Different letters mean significant difference at $p < 0.05$, (Kruskal–Wallis test and Dunn's multiple comparison test). Representative region of the follicle stained with Nile Red (lipids) and DAPI (DNA) is shown.

2.1.2. Lipid Composition of Follicular Cells and Fluid

Using liquid chromatography coupled with high-resolution MS (LC/HRMS), 438 different lipids were formerly identified in FF and 439 were formerly identified in the follicular cells of the same ovarian follicles (Supplementary data, Table S1). All of the detected lipids belonged to five families and 21 classes (Table 1).

Table 1. Classification and distribution of lipids detected in bovine ovarian follicle.

Lipid Family/% from total lipids	**Lipid Classes/**% from total lipids
Fatty acyls (FA)/1.48%	Free fatty acid (**FFA**)/0.91%; Fatty acyl carnitine (**FAC**)/0.57%.
Glycerolipids (GL)/28.7%	Diacylglycerol (**DG**)/1.48%; Triacylglycerol (**TG**)/27.2%.
Glycerophospholipids (GPL)/52.56%	Lyso-phosphatidylcholine (**LPC**)/3.64%, phosphatidylcholine (**PC**)/30.33%; Lyso-phosphatidylethanolamine (**LPE**)/0.22%; phosphatidylethanolamine (**PE**)/12.88%; Lyso-phosphatidylinositol (**LPI**)/0.11%, phosphatidylinositol (**PI**)/1.71%; phosphoserine (**PS**)/2.85%; Glycerophosphates (here phosphatidic acids, **PA**)/0.23%; Phosphatidylglycerols (**PG**)/0.46%.
Sphingolipids (SL)/9.46%	Ceramides (**Cer**)/1.25%; Sphingomyelin (**SM**)/6.50%; Hexosylceramide (**HexCer**)/0.29%, Ganglioside (**GM**)/0.45%; Sulfoglycosphingolipid (**SuSM**)/1.02%.
Sterol Lipids (ST)/7.75%	Cholesteryl ester (**CE**)/7.41%; Sterols (**ST**)/0.34%

Among the five lipid families, detected in FF and follicular cells, similar proportions of sterols (ST, 8.9% and 6.6%, respectively), sphingolipids (SL; 10.7% and 8.2%, respectively) and glycerophospholipids (GPL; 52.5% and 52.6%, respectively) were observed in both compartments (Figure 2A). A significant difference was reported in fatty acyls (FA family), which represented about 3% of the lipids in FF, but was not detected in follicular cells, and in the glycerolipid family (GL), which represented 24.8% of the lipids in FF and 32.6% of the lipids in follicular cells ($p < 0.05$).

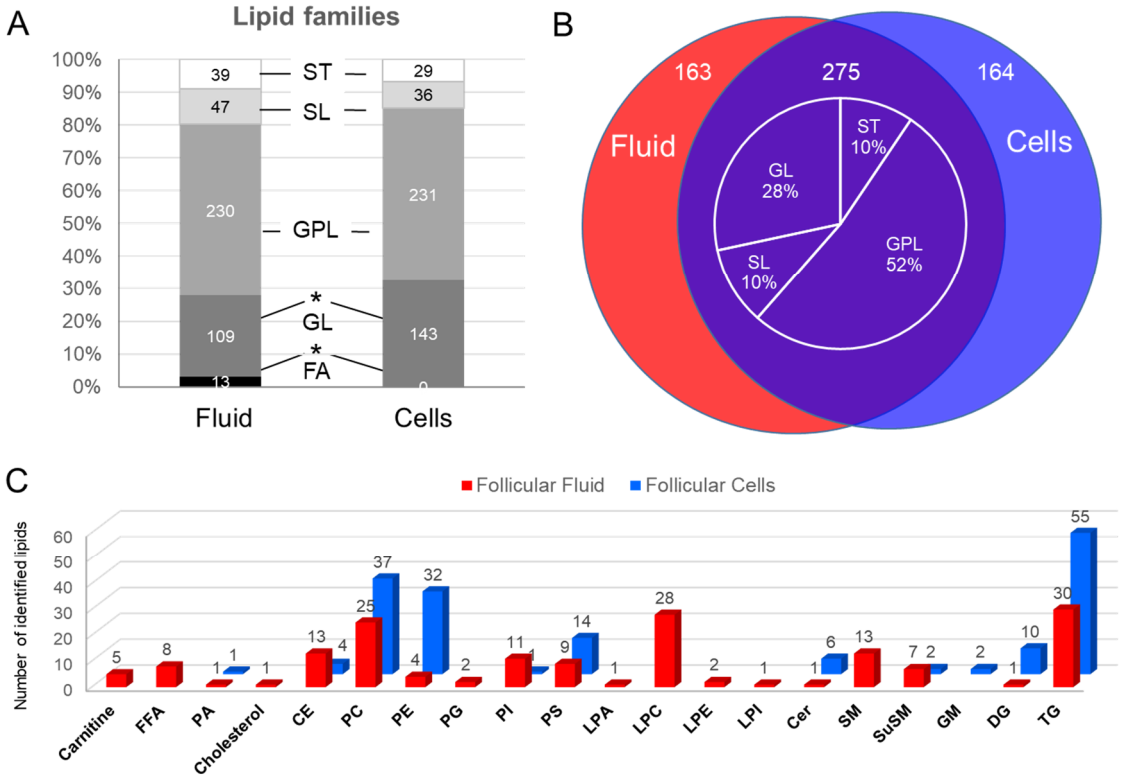


Figure 2. Identification of lipids in bovine 3–8 mm follicles by liquid chromatography coupled with high-resolution MS (LC/HRMS). (**A**) Family distribution of all of the lipids detected in follicular cells and fluid. * indicates significant difference ($p < 0.05$, Chi-squared test). (**B**) Venn diagram presents all of the lipids identified in follicular fluid (FF, red circle) and follicular cells (blue circle). Distribution by families of 275 common lipid species is shown. (**C**) Distribution by classes of the lipids, detected either in follicular cells only (164 species, blue bars) or in FF (163 species, red bars). Number of identified lipids are indicated above the bars. ST—Sterols; SL—Sphingolipids; GPL—Glycerophospholipids; GL—Glycerolipids; FA—Fatty acyls; FFA—Free fatty acid; PA—Phosphatidic acid; CE—Cholesteryl esters; PC—phosphatidylcholines; PE—phosphatidylethanolamines; PG—phosphatidylglycerols; PI—phosphatidylinositols; PS—phosphatidylserine; LPA—Lyso-Phosphatidic acid; LPC—Lyso-phosphatidylcholins; LPE—Lyso-phosphatidylethanolamine; LPI—Lyso- phosphatidylinositols; Cer—Ceramides; SM—Sphingomyelins; SuSM—Sulfoglycosphingolipids; GM—Gangliosides; DG—Diacylglycerols; TG—Triacylglycerols.

From all of the identified lipids, 275 lipid features were common between follicular cells and FF; 164 and 163 features were only detected in either follicular cells or FF, respectively (Figure 2B). Among the common lipids, 52% were GPLs represented mainly by phosphatidylcholine (PC) and phosphatidylethanolamine (PE) (37.1% and 13.8% of total lipids) and two lyso-phosphatidylcholine (LPC). GLs, representing 28% of common lipids, were mainly TG (77 species). These lipids mostly have long carbon chains. Free cholesterol, 25 CE and 23 sphingomyelin (SM), were also identified in both compartments. Lipid species, which were detected either only in FF (163 lipids) or in follicular cells (164 lipids), showed different class distribution (Figure 2C). Five carnitine isoforms,

eight free FA, hydroxycholesterol, two phosphatidylglycerols (PG), 32 lyso-glycerophospholipids (28 lyso-phosphatidylcholine (LPC), LPA, two phosphatidylethanolamine (LPE) and lyso-phosphoinositol (LPI)) and 13 SM were identified in FF only. In the cells, neither free FA nor was a specific lyso-GPL identified. Also, CE and PI lipid classes were more represented in FF, whereas more DG, TG, PE, PC, and PS were detected in follicular cells compared to FF.

2.1.3. Mass Spectrometry Imaging of Lipids in Ovarian Follicle

MALDI-TOF mass spectrometry imaging (MSI) performed at 25-µm resolution on a bovine ovarian section allowed the direct mapping of lipids inside the antral follicles. In total, an average spectrum showed 248 molecular species (m/z 104–827, supplementary data, Table S2) with different intensities throughout the follicle surface (Figure 3A). Both protonated species ($[M + H]^+$) and salt adducts species (sodium $[M + Na]^+$ and potassium $[M + K]^+$) were detected. The identification of lipids by mass spectrometry from liquid extraction surface analysis LESA and classical lipid extracts from FF and cells allowed the characterization of 44 features, which belong mostly to PC, SM, and LPC classes (Table S2). Using MSI, the distribution of identified lipids, which were presented as density maps, is shown in Figure 3B; details of their identification are shown in Table A1 (Appendix A). Several lipid ions were mostly located on the internal part of the follicles, representing FF, as different LPC (m/z 496.43 LPC 16:0; m/z 522.43 LPC 18:1; m/z 524.46 LPC 18:0), SM (m/z 725.59-SM (d18:1/C16:0); m/z 741.59-SM (d18:0/C17:0), or PC (m/z 760.62-PC 34:1). Others lipids were more abundant in the external part, representing follicular cell layers –TH and GC. This is the case for several PC (m/z 780.58 PC 35:1; m/z 796.56-PC 35:2, 808.61-PC 39:5). Many lipids were located on both the fluid and cellular parts of the follicle, for example PC 34:0 (m/z 748.63) and PC 32:0 (m/z 772.56).

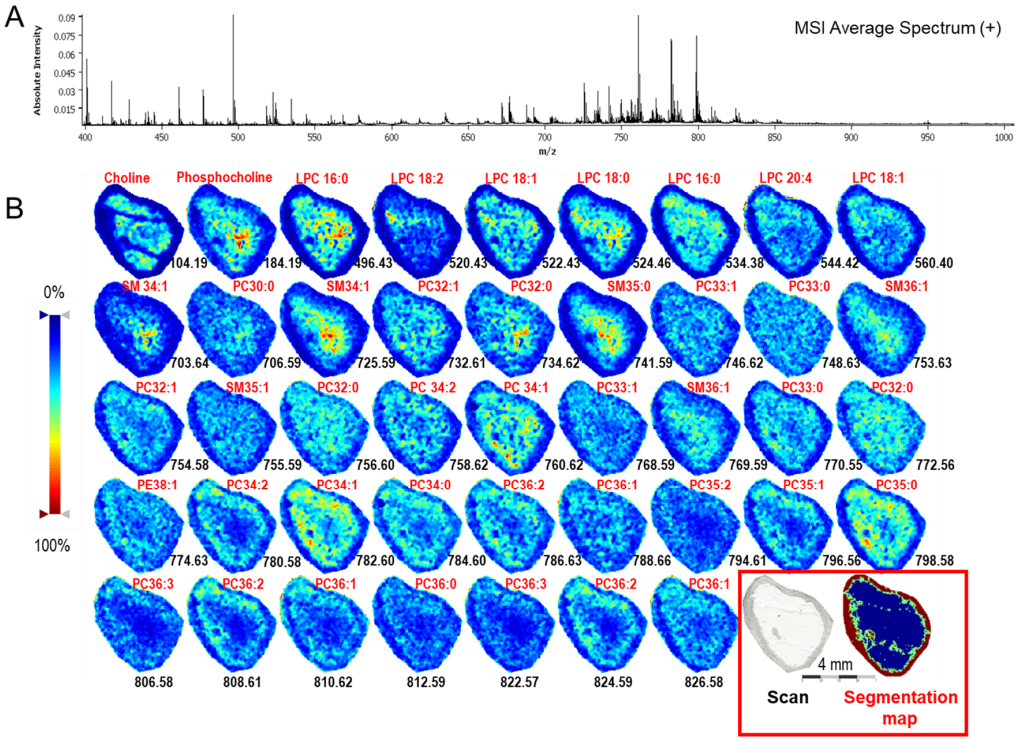


Figure 3. High-resolution mass spectrometry imaging (MSI) of individual bovine follicles. (**A**) Average spectrum of molecular species in the 100–1000 m/z range. (**B**) Ion density maps of detected lipids in individual follicles. Spatial segmentation map was obtained by hierarchical clustering using the bisecting *k*-means algorithm. Lipid identification was performed by LC–HRMS and/or by direct infusion and MS/MS. LPC—Lyso-phosphatidylcholine; PC—Phosphatidylcholine; SM—Sphingomyelin.

From the MSI sequences, unsupervised hierarchical clustering was performed, in which similar spectra were grouped using multivariate statistical analysis. The created segmentation map using the major clusters was taken for molecular reconstructions of the ovarian follicle for comparison with a histological image. An MSI segmentation map (Figure 3B) demonstrated that the lipid profiles were different between FF and the wall of the follicle; moreover, the mural cellular part of the follicle showed the segmentation into the two layers.

2.1.4. MALDI-TOF Profiling and Lipid Identifications in Follicular Compartments

Lipid profiles generated by MALDI-TOF MS on the cellular and fluid compartments of individual follicles were compared between the oocyte, CC, GC, TH, and FF samples (n = 12 per condition). The size range of the analyzed individual follicles was 4.2–7.6 mm in diameter. The total lipid profile from each sample included the spectra acquired in both the positive and negative ion modes. Examples of such spectra and a number of peaks detected in the 100–1000 m/z range in the positive and negative ion modes for each compartment are shown in Figure 4. In the positive mode, more peaks in the 600–800 m/z range were detected, compared to the negative ion mode, where more peaks in the m/z 300–400 range were detected in all of the compartments. Visibly, spectra from OO, CC, GC, TH, and FF looked different one from another, in both peak number and relative intensity.

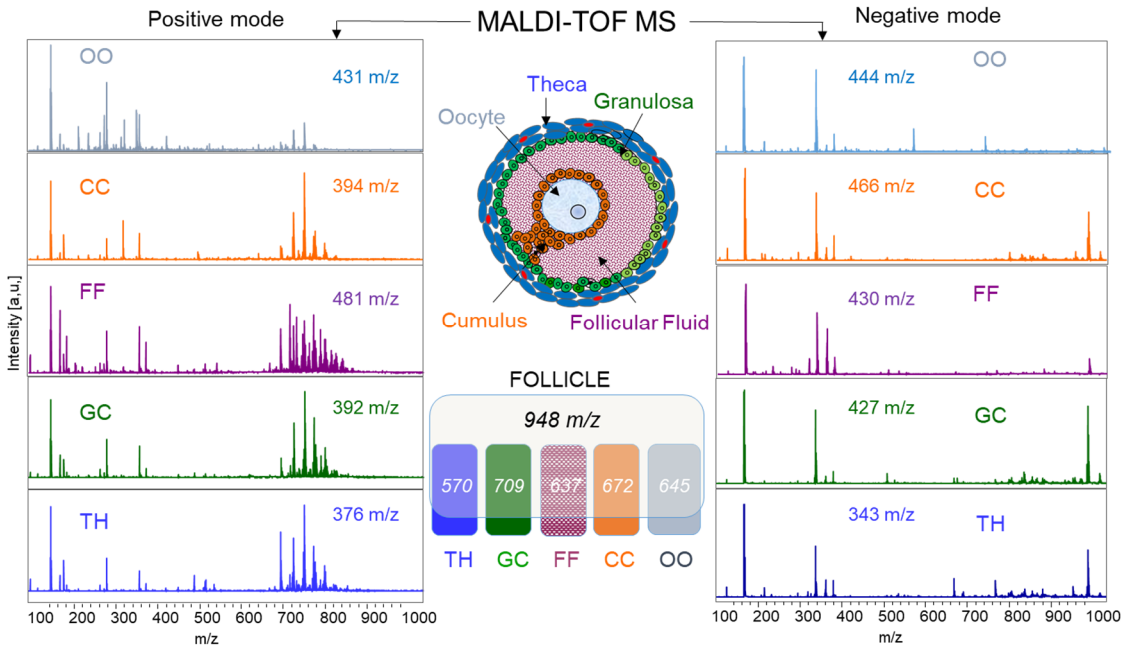


Figure 4. MALDI-TOF profiling performed on isolated follicular compartments. Examples of spectra and number of peaks obtained from individual oocyte (OO), cumulus cells (CC), follicular fluid (FF), granulosa cells (GC) and theca cells (TH) are shown for both positive (left) and negative (right) ion modes. After alignment of spectra from all of the compartments, 948 m/z were detected from the average spectrum. The number of common peaks between the compartments and the whole follicle are indicated in white italics.

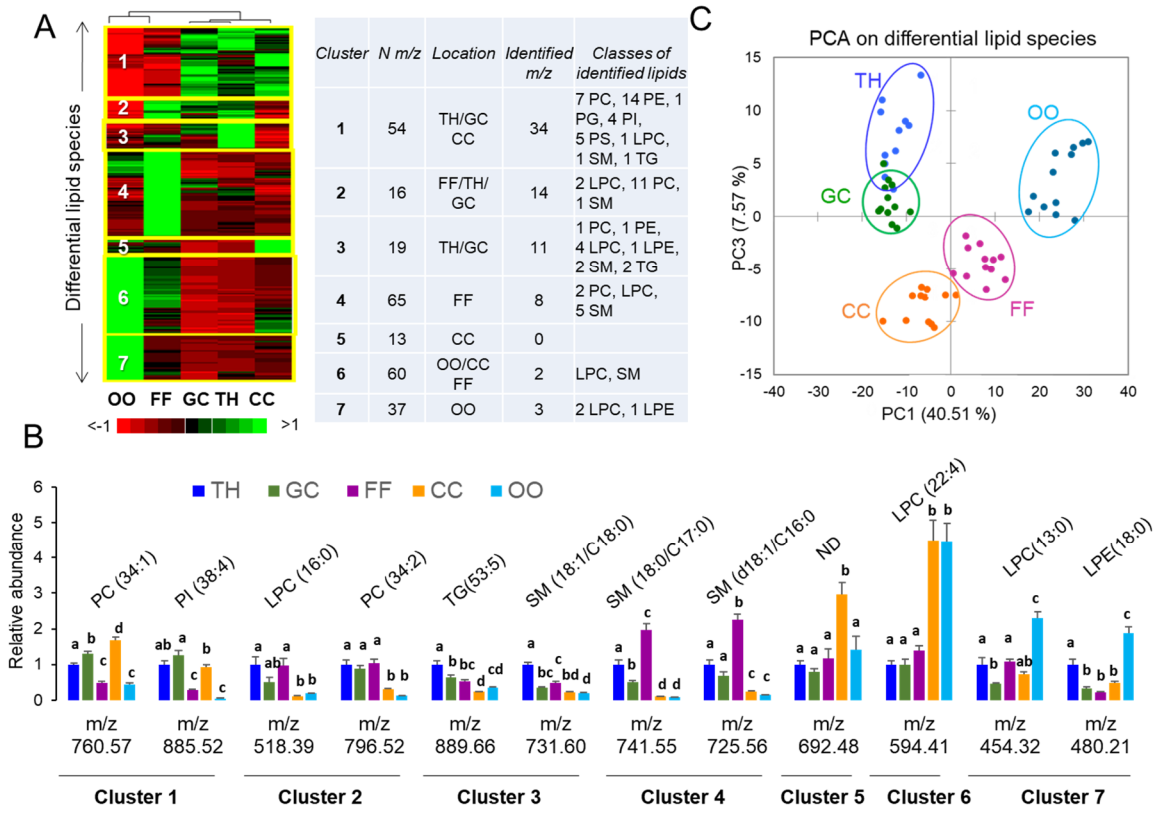
In order to compare the lipid profiles between the follicular compartments, all of the spectra were aligned, and the peaks were detected from the average spectra in both ion modes, bearing in total 948 peaks (462 m/z and 486 m/z in the positive and negative ion mode, respectively).

In order to identify the peaks observed by MALDI-TOF MS profiling, different lipid extracts from the follicular cells and fluid were analyzed by high-resolution mass spectrometry using two strategies as LC-MS and direct infusion for MS/MS structural analyses. All of the identified lipids are presented in Supplementary Tables S3 and S4. For the positive and negative modes, 120 and

62 m/z were identified, respectively. In the positive mode, most of the identified ions were PC (52.3%), LPC (20.3%), and SM (18.8%). FAC, DG, and TG represented 2.3%, 1.6%, and 4.7% of the identified peaks, respectively. From the negative ions, 54.8% of the identified m/z were annotated PE, whereas the PI and PS classes each represented 14.5% of the molecular species. FFA and sulfoglycosphingolipid (SuSM) represented 9.7% and 4.8% of identified peaks, respectively.

Normalized peak height values (NPH) of each molecular species were measured for all of the samples. The coefficients of variation of MALDI MS profiling were calculated from all of the peaks and ranged from 15.8% to 32.9% in different tissues (Table A2, Appendix A); mean CV% values were 22.6% and 20.4% for the positive and negative ion modes, respectively.

The differential analysis of lipid composition was performed by comparison of the mean NPH values between TH, GC, FF, CC, and the oocytes (n = 12 per each follicular compartment). By ANOVA, 338 and 196 differentially abundant m/z species were detected in the positive and negative mode, respectively ($p < 0.05$; maximum fold change >three). All of the NPH values and statistics are shown in Supplementary Data Table S5. The NPH log-values (relative abundance) of 264 of the most abundant differential peaks was presented here as a heat map (Figure 5A).



Cluster	N m/z	Location	Identified m/z	Classes of identified lipids
1	54	TH/GC CC	34	7 PC, 14 PE, 1 PG, 4 PI, 5 PS, 1 LPC, 1 SM, 1 TG
2	16	FF/TH/ GC	14	2 LPC, 11 PC, 1 SM
3	19	TH/GC	11	1 PC, 1 PE, 4 LPC, 1 LPE, 2 SM, 2 TG
4	65	FF	8	2 PC, LPC, 5 SM
5	13	CC	0	
6	60	OO/CC FF	2	LPC, SM
7	37	OO	3	2 LPC, 1 LPE

Figure 5. Differential analysis of lipids in bovine TH (theca), GC (granulosa cells), FF (follicular fluid), CC (cumulus cells), and oocytes (OO) by MALDI-TOF MS lipid profiling. (**A**) Heat map representation of differentially abundant lipids (ANOVA, $p < 0.05$). Enclosed table showed the number of peaks per cluster, their specific localization to the ovarian compartment, and the main lipid classes of the identified differential lipids. (**B**) Examples of identified differentially abundant lipids between ovarian compartments (n = 12 per compartment). Different letters indicate significant differences ($p < 0.05$, Tukey test for multiple pairs comparison). (**C**) Discrimination of ovarian follicular compartments by their lipid profiles, by principal component analysis. LPE—Lyso-phosphatidylethanolamine, LPC—Lysophosphatidylcholine, PC—Phosphatidylcholine, PE—Pphosphatidylethanolamine, PI—phosphatidylinositol, SM—Sphingomyelin, TG—Triacylglycerol.

Lipid features were distributed in seven clusters according to their relative abundances; each cluster represented specific follicular compartment abundance of lipid species. Globally, clusters 1, 2, and 3 (54 m/z, 16 m/z and 19 m/z, respectively) contained the lipids, which were more abundant in somatic follicular cells. Cluster 4 included the lipids that were more abundant in FF. Peaks from clusters 6 and 7 (60 m/z and 37 m/z, respectively) were mostly represented in the oocyte. Thirteen features from cluster 5 were preferentially detected in CC. Lipid identification allowed the annotation of 66.3% of differential lipid species from clusters 1–3, which were mainly represented in somatic cells, and 7.2% of the lipids from clusters 4–7, representing FF and OCC (Supplementary Data, Table S6). Among the 120 lipids that were more abundant in the OCC, only several features were identified: three LPC (LPC 13:0, LPC 14:1, and LPC 22:4), SM 32:1, and LPE 18:0. The lipids that were abundant in FF (clusters 2 and 4) belonged to the PC, LPC, and SM lipid classes. TH-specific cluster 3 included the LPC, PC, SM, PE, CE, and TG classes of lipids. The GC lipid profiles were more similar to other somatic cells, and the mostly abundant lipids in follicular somatic cells (clusters 1 and 2) were mainly PC, but also PE, PS, PI, and several lipids belonging to the SM and TG classes. Several peaks may have two or more identifications (Supplementary Data, Table S6); here, we presented the identification with the lowest delta to the exact m/z value. Examples of differentially abundant identified lipids in each cluster are shown (Figure 5B).

Principal component analysis was performed using NPH values of the most differential lipids, and it clearly discriminated TH, GC, CC, oocyte, and FF compartments (Figure 5C).

2.2. Analysis of Gene Expression in Bovine Ovarian Follicular Cells

Among more than 22,000 genes analyzed using bovine microarray, 11,761 genes showed significant difference of expression between follicular cells (TH, GC, CC) and the oocyte ($p < 0.05$, Benjamini–Hochberg (BH) correction). Gene set enrichment analysis (Supplementary Table S7) revealed that differentially expressed genes (DEGs) were significantly enriched in gene ontology (GO) terms as metabolic pathways ($p = 0.0004$) and in GO terms related to the ribosome, cell cycle, peroxisome, spliceosome, and focal adhesion ($p < 0.001$). Among numerous other terms, FA metabolism, FA degradation, proteasome, progesterone-mediated oocyte maturation, pentose phosphate pathway, and pyruvate metabolism were also significantly enriched in the list of DEGs ($p < 0.05$). DEGs were involved in several significantly enriched pathways, such as the mTOR, p53, TGF-beta, PI3K-AKT, FoxO, ErbB, and MAPK signaling pathways ($p < 0.05$).

The results on gene expression obtained by microarray hybridization were validated by real-time PCR analysis on several genes that were involved in lipid and FA metabolism. Overall, the same expression patterns were observed using these two approaches for most of the analyzed genes (Figure 6). As shown, *FASN* (fatty acid synthase), *CPTA1* (involved in FA oxidation), and lipase *PNPLA2* are expressed similarly in all of the compartments. In contrast, the other genes that are involved in GL synthesis (*AGPAT9* and *DGAT2*), lipid storage (*PLIN2*), and FA transporter FABP3 were more expressed in oocytes. Transcriptional factor *PPARG* was strongly expressed in oocytes and more abundant in GC and CC compared to TH.

In order to decipher the involvement of different follicular cells in the regulation of lipid metabolism inside the follicle, we analyzed the mRNA expression of the genes, which controls the main steps of the lipid and steroid turnovers. The normalized expression values of 468 genes that were selected by their involvement in energy metabolism, steroidogenesis, were compared between TH, GC, CC, and the oocytes from follicles of 3–8 mm. Among them, 432 genes were found to be differentially expressed. Gene description, expression values, and statistics are reported in the Supplementary Data, Table S8. Principal component analysis (PCA) was performed using the expression values of these genes, and clearly discriminated follicular cells (Figure 7A). Hierarchical clustering regrouped the most discriminant DEGs; a heat map representation of this analysis is shown in Figure 7B. From the heat map, seven clusters were defined according to gene expression patterns; Table 2 presents cluster composition. The representative genes for each cluster are shown in Figure 7C.

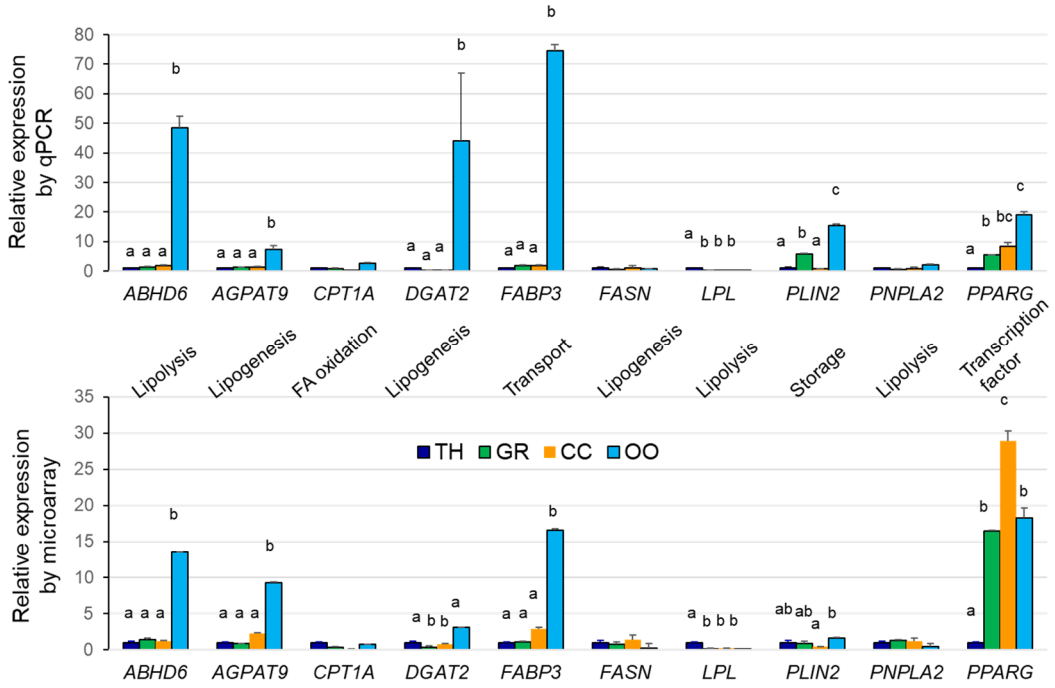


Figure 6. RT-qPCR validation of microarray gene expression analysis. Graphs are presented as the mean+/SEM of normalized expression values of several independent RNA samples per tissue (n = 4 for microarray, and n = 6 for RT-qPCR analysis). Different letters indicate difference at $p < 0.05$ (ANOVA, Tukey post-hoc test). *ABHD6*—Abhydrolase Domain Containing 6, *AGPAT9*—1-Acyl-Sn-Glycerol-3-Phosphate O-Acyltransferase 9, *CPT1A*—Carnitine Palmitoyltransferase 1A, *DGAT2*—Diacylglycerol O-Acyltransferase 2, *FABP3*—Fatty Acid Binding Protein 3, *FASN*—Fatty Acid Synthase, *LPL*—Lipoprotein Lipase, *PLIN2*—Perilipin 2, *PNPLA2*—Patatin Like Phospholipase Domain Containing 2, *PPARG*—Peroxisome Proliferator Activated Receptor Gamma.

Table 2. Cluster composition of differentially expressed genes.

Clusters	***Differentially Expressed Genes***
Cluster 1 **(TH, GC)**	*ABHD12, ABHD13, ACADM, ACSBG1, ACSS1, AKR1E2, BDH2, CLN1, CYP2C87, CYP4V2, CYP7A1, ESR2, GJA1, GPAM, GPD1, GPX1, GPX3, GPX7, GPX8, HMGCL, HSDL1, HSDL2, LIPA, MCCC1, MLYCD, OSBPL7, PLA2G16, PLA2G1B, PLBD2, PLSCR2, SPTSSA, SULT2A1, UGCG*
Cluster 2 **(TH, GC, CC)**	*ABHD14B, ABHD3, ABHD7, ACAD10, APOA2, APOC3, APOE, APOL3, APOM, CD36, ACSS3, CYP4F2, DAGLB, HSD17B11, HSD17B7, LCAT, MCCC2, OSBPL1A, PIK3C2G, PLCG1, PLSCR1, PNPLA5, PNPLA7, PPARGC1A, SCARB2, SCP2, SCD5*
Enriched GO terms (clusters 1–2): Ketone body, phospholipid scrambling, cholesterol binding, sterol transporter activity, phospholipase activity, acyl-CoA, glycerophospholipid biosynthetic processes, FA oxidation, unsaturated FA metabolism, cellular response to oxidative stress. Pathways: arachidonic acid metabolism, PPAR and AMPK signaling, glutathione and glycerophospholipid metabolism.	
Cluster 3 **(CC)**	*ABHD15, ABHD16A, ACADL, ACADS, ACADVL, ACAT1, ACOX2, AGPAT5, AKR7A2, CDS2, CHPT1, CHST14, COMTD1, CYP19A1, CYP20A1, CYP51A1, DECR1, DGKA, FADS2, G6PC3, GPAA1, HSD11B1L, HSD3B, HSD3B7, LDLR, PI4KA, PIP5K1A, PKM2, PLCB4, PLD3, PPAP2A, SDHA, SLC27A3, SLC2A1, SLC2A3, SMPD1, SRD5A1, STARD7, STARD3NL, SUCLG1*
Cluster 5 **(CC)**	*CHST11, CHST8, CYP2U1, DGKE, HSD17B1, LSS, OSBPL2, PFKFB3, PLA2G7, PNPLA6, PPARG, SCD, UGGT2*

Table 2. *Cont.*

Clusters	*Differentially Expressed Genes*
Enriched GO terms (clusters 3, 5): FA beta-oxidation using acyl-CoA dehydrogenase, steroid, organic cyclic compound, glycerophospholipid biosynthetic processes; FA beta-oxidation, FA catabolic process, estrogen biosynthesis, bile acid metabolic process, regulation of cholesterol metabolic process. Pathways: glycerophospholipid and FA metabolism, phosphatidylinositol and phospholipase D signaling; PPAR, choline metabolism, FA degradation, steroidogenesis, AMPK signaling	
Cluster 4 **(TH)**	*ACSF2*, *AGMO*, *AGPAT4*, *APOA1*, *CH25H*, *CHST1*, *CHST7*, *CYP27A1*, *CYP7B1*, *LPL*, *OXCT1*, *PDK4*, *PFKM*, *PIK3CG*, *PIK3R2*, *PLCD3*, *PLCXD3*, *PLD4*, *PLIN5*, *PLSCR4*, *PLTP*, *PPAP2A*, *PTPLA*, *SCARB1*, *SDHD*, *SMPD3*, *SMPDL3B*, *STARD5*, *SULT1A1*, *TM7SF2*
Enriched GO terms (cluster 4): Sterol import, regulation of cholesterol storage, regulation of sequestering of triglyceride and triglyceride synthesis; monocarboxylic acid bile acid biosynthetic process; sterol metabolic process. Pathways: PPAR signaling, primary bile acid biosynthesis, glycerolipid metabolism; Phospholipase D signaling pathway, Phosphatidylinositol signaling system, HDL-mediated transport	
Cluster 6 **(CC, OO)**	*ABHD11*, *ACADSB*, *ACSL6*, *AKR1A1*, *C2CD2L*, *CHST10*, *OGFOD2*, *OSBP2*, *PDK1*, *PPRC1*, *PPT2*, *SLC2A8*, *SMPD4*, *SOAT1*, *THEM4*, *UGT*, *MCC*
Cluster 7 **(OO)**	*ABHD10*, *ABHD17C*, *ABHD4*, *ABHD5*, *ABHD6*, *ACAA1*, *ACACA*, *ACAD11*, *ACAT2*, *ACER3*, *ACO1*, *ACOT7*, *ACOT9*, *ACP6*, *ACSL3*, *ACSL4*, *ACYP1*, *AGPAT9*, *AKR1B1*, *APOO*, *C2CD4A*, *C2CD5*, *CDS1*, *CEPT1*, *CERKL*, *CERS2*, *CHERP*, *CHKA*, *CHST12*, *CPT1C*, *CRLS1*, *CS*, *CYP26A1*, *CYP27B1*, *DECR2*, *DGAT2*, *DGKI*, *EBPL*, *ELOVL3*, *ELOVL4*, *ELOVL5*, *ELOVL7*, *EPT1*, *FABP3*, *FABP5*, *FADS3*, *FAR1*, *GK*, *GPAT2*, *GPD1L*, *GPLD1*, *HADHB*, *HMGCS1*, *HSD11B2*, *HSD17B12*, *LPCAT2*, *MBOAT2*, *NFKBIE*, *OGFOD1*, *OSBPL10*, *OSBPL11*, *OSBPL3*, *OSBPL8*, *OSBPL9*, *OXSM*, *PDK2*, *PDK3*, *PFKFB1*, *PFKFB2*, *PI4K2B*, *PI4KB*, *PIK3C2A*, *PIK3CA*, *PIK3C3*, *PIK3CB*, *PIK3R1*, *PIP4K2A*, *PIP4K2B*, *PIP4K2C*, *PIP5K1B*, *PIP5K1C*, *PITPNA*, *PITPNM1*, *PLA2G12A*, *PLA2G15*, *PLAA*, *PLCG2*, *PLCH1*, *PLD6*, *PLIN2*, *PNPLA4*, *PPAP2C*, *PPARGC1B*, *PTPLAD2*, *SOD1*, *SOD2*, *SPTLC1*, *SPTLC2*, *SRBD1*, *STARD4*, *SUCLA2*, *SUCLG2*, *THEM2*, *TM7SF3*, *UGDH*, *UGP2*, *UGT8*
Enriched GO terms (clusters 6–7): Glycerophospholipid and phosphatidylinositol biosynthetic processes; long-chain fatty-acyl-CoA biosynthesis and acyl-CoA metabolic process; FA elongation (saturated and unsaturated) FA; lipid phosphorylation; sphingolipid metabolic process; membrane lipid biosynthetic process. Pathways: Phosphatidylinositol and inositol lipid-mediated signaling; PPAR signaling; FA elongation, FA degradation; GL and GPL metabolism; peroxisome, choline metabolism; sphingolipid metabolism	

Clusters 1 and 2 represent the genes that were overexpressed in somatic cells (GC/CC and TH/GC/CC, respectively). Among them, there were a number of genes regulating steroidogenesis and the synthesis of cholesterol (cytochromes P450 and others), genes involved in the synthesis of Acyl-CoA (*ACFS2*) and different membrane lipids and TG (*SCD5*), genes involved in lipid degradation as cholesterol esterases *(LIPA*, *LCAT)*, phospholipases A and C *(PLA2G1B*, *PLCG1)*, and di- and monoacylglycerol lipases (as *DAGLB*, *ABDH3*, etc.). In addition, these two clusters enclosed the genes involved in FA oxidation (*ACAD10*, *ACSS3*) and lipid transporters *(CD36*, *OSBPL7*, *CSP2*, *SCARB2)*. Genes coding for apolipoproteins (*APOA2*, *APOC3*, *APOL3*, *APOM*), gap-junction proteins (*GJA1*) and *GPX* peroxidases showed the same expression pattern. These clusters were significantly enriched in the following biological process GO terms: phospholipid scrambling, cholesterol binding, ketone body, and bile-acid biosynthetic processes, acyl-CoA, glycerophospholipid biosynthetic processes, sterol transport, FA oxidation, unsaturated FA metabolism, and cellular response to oxidative stress. Enriched pathways included arachidonic acid metabolism, PPAR signaling, and glycerophospholipid metabolism. Genes with more abundant expression in CC constituted clusters 3 and 5. Globally, the genes of these clusters are also involved in cholesterol and steroid transport and metabolism (*LDLR*, *STARD7)*, regulator of lipid synthesis (as *FADS2*, *SCD*), lipolysis (as *ABHD16A*), and in FA oxidation (*ACADVL*). Enriched GO terms included FA beta-oxidation using acyl-CoA dehydrogenase, steroid, lipid, glycerophospholipid, and monocarboxylic acid biosynthetic processes; FA oxidation, FA

catabolic process, the regulation of cholesterol metabolic process. Enriched pathways were related to glycerophospholipid and FA metabolism, PPAR, phosphatidylinositol and phospholipase D signaling, choline metabolism, and FA degradation.

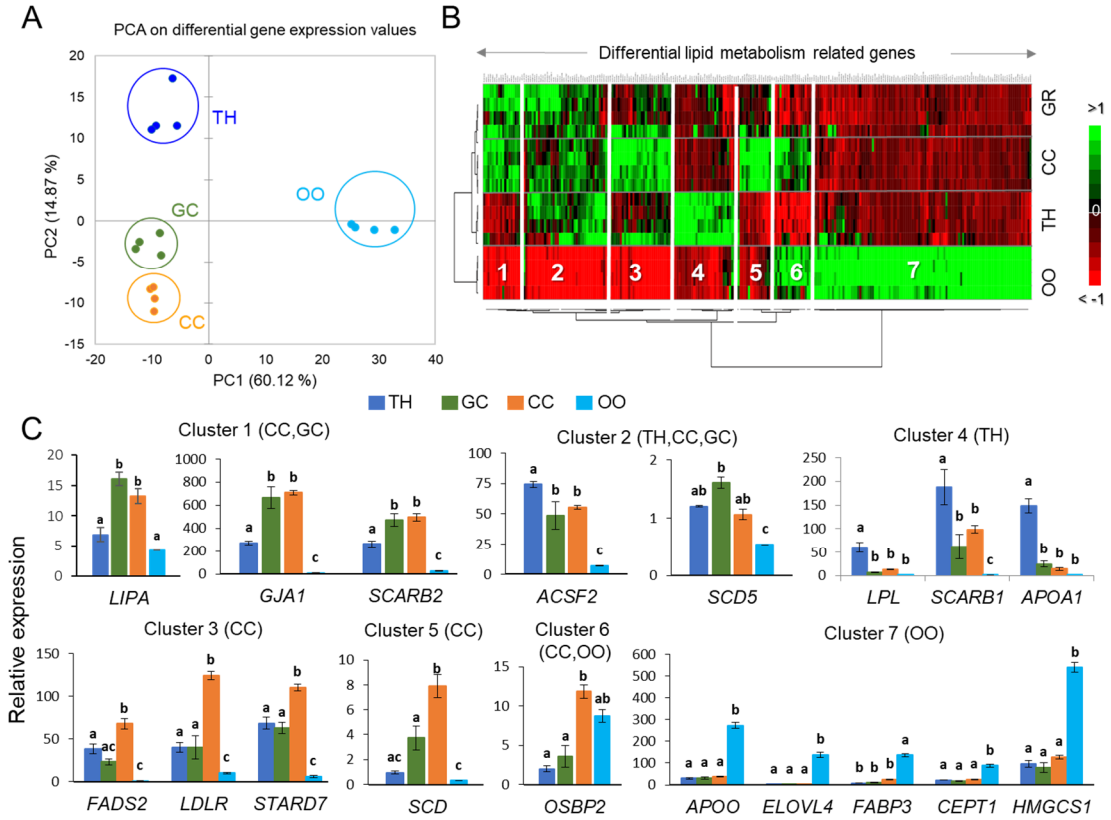


Figure 7. Differential analysis of gene expression in bovine theca (TH), granulosa cells (GC), cumulus cells (CC), and oocytes (OO), using microarray hybridization (n = 4 per each cell type). (**A**) Discrimination of ovarian follicular compartments by expression profiles of lipid metabolism-related genes, using principal component analysis. (**B**). Heat map representation of differentially expressed genes ($p < 0.05$, Benjamini–Hochberg correction) related to lipid metabolism. (**C**) Examples of differentially expressed genes between ovarian follicular compartments. Bars are the mean values of four independent replicates +/− SEM. Different letters mean significant difference at $p < 0.05$ (ANOVA, Tukey test for multiple comparisons). *LIPA*—Lipase A; *GJA1*—Gap Junction Protein Alpha 1; *SCARB2*—Scavenger Receptor Class B Member 2, *ACSF2*—Acyl-CoA Synthase Family Member 2, *SCD5*—Stearoyl-CoA Desaturase 5, *SCD*—Stearoyl-CoA Desaturase, *OSBP2*—Oxysterol Binding Protein 2, *LPL*—Lipoprotein Lipase, *SCARB1*—Scavenger Receptor Class B Member 1, *APOA1*—Apolipoprotein A1, *FADS2*—Fatty Acid Desaturase 2, *LDLR*—Low Density Lipoprotein Receptor, *STARD7*—StAR (Steroidogenic Acute Regulatory Protein) Related Lipid Transfer Domain Containing 7, *APOO*—Apolipoprotein O, *ELOVL4*—Elongation Of Very Long Chain Fatty Acids Protein 4, *FABP3*—Fatty Acid Binding Protein 3, *CEPT1*—Choline/Ethanolamine Phosphotransferase 1, *HMGCS1*—3-Hydroxy-3-Methylglutaryl-CoA Synthase 1.

The genes that are overexpressed in TH cells (cluster 4) are particularly involved in cholesterol import (*SCARB1*, *STARD5*), bile acid metabolism (*CH25H*), HDL-mediated lipid transport (*APOA1*, *PLTP*, *SCARB1*), lipid degradation (*LPL*, *PLIN5*), and steroidogenesis (*CYP27A*, *CYP7B1*, *TM7SF2*). GO terms enriched in the TH-specific cluster were related to sterol import, the regulation of sequestering of triglycerides and lipid storage, monocarboxylic acid and bile acid biosynthetic processes, and sterol metabolic process. Enriched pathways were related to PPAR

signaling, glycerolipid and primary bile metabolism, phosphatidylinositol, and phospholipase D signaling systems.

Cluster 6 represents the genes that are particularly abundant in oocyte-CC complexes such as intracellular lipid transporter *OSBP2*, and cluster 7 enclosed the genes that are overexpressed in the oocytes. Among the genes of this cluster, we found numerous enzymes transforming lipids such as FA elongases (*ELOVL* genes), desaturases (such as *FADS3*), different phospholipases (phospholipases A and D) and their regulating proteins (*PLAA).* Also, these clusters include the genes that are involved in glycerophospholipid and triacylglycerol synthesis (for example *SPTLC1*, *DGAT2*, *AGPAT*, *GPAT* ...), cholesterol biosynthesis (*HMGCS1*), and sphingolipid synthesis (*SPTLC2*, *ACER*, *CERS2* ...). The oocytes overexpress gene coding for lipid transporters, as FA and oxysterol-binding proteins (*FABP* and *OSBPL* genes, respectively), and apolipoprotein *APOO*. In addition, these clusters enclosed numerous genes that are related to FA mitochondrial and peroxisome oxidation and genes involved in cholesterol and steroid metabolism, as well as in oxidative stress response (*SOD* genes). The most enriched biological process GO terms in clusters 6 and 7 include glycerophospholipid and phosphatidylinositol biosynthetic processes, long-chain fatty-acyl-CoA and acyl-CoA metabolic processes, FA elongation (saturated and unsaturated), FA and lipid phosphorylation, sphingolipid metabolic processes, and membrane lipid biosynthetic processes. Among the pathways enriched in oocyte-related clusters, there were phosphatidylinositol and inositol lipid-mediated signaling, PPAR signaling, FA elongation, FA degradation; GL and GPL metabolism; peroxisome, choline and sphingolipid metabolism; and insulin receptor signaling pathway.

3. Discussion

In the present work, for the first time, using liquid chromatography coupled to high-resolution mass spectrometry, we identified several hundred lipids representing 21 lipid classes in cellular and fluid compartments of bovine ovarian follicles running the terminal part of the folliculogenesis. In addition, MALDI-MS profiling was, for the first time, used to compare lipid fingerprints in the different cell types of individual ovarian follicles. Then, 197 molecular species in the range of 250–1000 m/z were formerly identified in bovine follicular cells, and these identifications implemented the list of lipids that were already annotated in bovine oocytes and cumulus cells [32,33,36,49,50]. By these two approaches, we could identify the major lipids, which were differentially abundant among the somatic compartments: TH, GC, CC, and the oocyte. Although only 1/5 part of m/z peaks detected in MALDI-MS spectra was precisely identified, these analyses coupled to MS imaging enabled localizing the most abundant lipids to ovarian follicular structures.

The majority of identified follicular lipids are known to be involved either in membrane synthesis or energy storage (CE, SL, GPL, GL). In fact, we have analyzed tertiary follicles where somatic follicular cells yet proliferate, and the oocytes, which were close to fully grown and potentially ready to resume meiosis, continued to acquire developmental potential by accumulating molecular reserves [51]. At that stage, the follicles may have strong requirements in energy and building blocks for membranes biosynthesis. During follicular growth up to ovulation, constant bi-directional interplay occurs between the oocyte and surrounding follicular cells. Indeed, the oocyte secretes specific factors GDF9 and BMP15, and thus stimulates follicular cells to proliferate and secrete steroids and other factors, which, in turn, regulate oocyte growth [52,53] and protect it from the harmful environment [54]. Follicular fluid contains molecular factors that were both exuded from blood and follicular secretion [55], and therefore acting as a buffer against adverse blood influence and as a medium of molecular exchanges between follicular cells. Significant proportions of the follicular fluid lipids that were identified here (FA, Cer, DG, lysophospholipids, LPI, LPE, LPC, ..) might exhibit mediator functions [28,56]. FF extracellular vesicles such as exosomes [57] have very specific lipid composition [58], and may participate in these communications inside the follicle.

In order to analyze the lipid distribution through the ovarian follicle, molecular imaging and phenotyping technologies were performed. MSI on bovine ovarian sections allowed the ionization

of numerous lipids, including PC, LPC, SM, and choline molecules. MSI segmentation map clearly discriminated FF from TH and GC layers, similarly to the MSI of porcine ovarian sections [30]. This could be explained by different lipid compositions; for example SM, LPC, and choline molecules were preferentially detected in FF, but also by the different ionization capacity of lipids from either liquid or cellular compartments. The identified PC features were mainly localized to both follicular walls and fluid by MSI. Among the common identified lipids, PC represented 37%, and among the identified MALDI-MS m/z peaks, PC represented more than 50%. PC are the major components of cellular membrane lipids with well-established roles in differentiation and cell proliferation [27]. Therefore, PC localized to the follicular wall may be associated to membrane structures in TH and GC.

MALDI-MS lipid profiling confirmed the higher abundance of PC, as well as other membrane lipids such as PE and PS that feature in GC and TH cells as compared to FF. Overall, the FF lipid profile significantly differed from that of the follicular cells, as was expected from the non-cellular compartment. The TH and GC profiles were partially overlaid, as shown by the principal component analysis of MALDI fingerprints. In fact, although TH and GC are separated by the basal membrane, they are metabolically coupled; thus, many lipids were shared between these layers. However, the increased abundance in several LPC, LPE, SM, and TG in TH compared to GC were sufficient to discriminate these two cell types. A similar approach was performed on human lung where MSI confirmed the specific distribution of three phospholipids (PE, PI, and PG) in different regions of lung slice, illustrating the lipidome differences between alveolar macrophages, bronchial epithelial, and alveolar type II pulmonary cells, which were previously shown by LC-MS/MS [59]. The specific lipid profiling of TH probably reflects its functional structure, which is rich in steroid-secreted cells, blood capillaries, and collagen [60], compared to GC, which is more homogeneous and has smoother tissue.

MSI was not sufficiently resolute to discriminate GC and CC; however, MALDI-MS lipid fingerprints showed significant differences between these cells. Although CC was derived from the GC, the specific functions of CC are conditioned by their physical and metabolic coupling with the enclosed oocyte [61]. Here, GC shared the most of the lipids with other compartments; however, in CC, several not-identified features were particularly abundant and formed a CC-specific cluster. In our previous study, a comparison of GC and CC lipid fingerprints revealed that two LPC, 12 PC, and 12 SM features were up-regulated in CC whereas several features including LPC, four PC, two PE, PS, and Cer were more abundant in GC [62]. The differences between GC and CC lipid concentrations likely reflect the functional differences between these cells [63].

Lipid concentrations in follicular compartments may be predictive for oocyte competence. Indeed, the concentration of several TG, PG, PI, PE and lysophospholipids LPE, LPI, and LPC in human FF demonstrated a strong potential association between the differentially elevated lipids and increased success rate of in vitro fertilization/intracytoplasmic sperm injection outcomes [64]. While CC are physically and metabolically coupled with enclosed oocytes, the MALDI-TOF MS lipid profiling of these cells may also reflect oocyte competence. The differential abundance of several PC was observed in the bovine CC enclosing the oocytes with higher developmental potential after FA (22:6 n-3) supplementation [36]. In human, the MALDI-TOF lipid profiles of CC showed a different abundance of PC species in the pregnant group and PE, PS, and PI features in the non-pregnant group after ICSI [65]. Lipid composition also differed between the oocytes with different competence in bovine [33,36,43], but it is difficult to thoroughly evaluate the roles of each feature in this difference.

Oocytes demonstrated very specific lipid profiles that were distinct from the other follicular compartments; nevertheless, the clustering of differential lipids revealed common features with CC or FF. Among the few identified lipids from oocyte-representative clusters, LPC(13:0) and LPC(18:0) were the most elevated in oocytes, LPC 22:4 was similarly abundant in oocytes and CC, and SM (d32:5) was detected at similar levels in oocytes and FF. Previously, we showed significant variations of several PC, SM, and free FA concentrations in the oocytes during meiotic maturation [34]. This was in line with a decreasing of lipid reserves in mature oocytes as compared to the immature stage [43],

and highlighted the profound changes in both membrane composition and intracellular lipid storage during oocyte maturation.

A relative quantity of total lipids in cellular and fluid compartments was measured using Nile red fluorescent dye in situ targeting mainly the neutral lipids, TG, and cholesteryl esters, which are the main components of lipid droplets (LDs) [23]. GC and TH layers demonstrated intensive fluorescence due to the accumulation of LDs, which may serve as an energy reserve and as precursors of the steroid hormones or secondary messengers produced by GC and TH.

Steroidogenesis in ovarian follicular cells is mediated by a number of well-known enzymes such as, for example, steroidogenic acute regulatory protein STAR, cytochrome P450 side chain cleavage CYP450scc, 3-beta-hydroxysteroid dehydrogenase HSD3β, and CYP450 aromatase in theca and granulosa cells [66]. Here, transcriptome analysis confirmed the expression of genes involved in steroid biosynthesis in TH, GC, and CC, as expected. From the same analysis, expression of numerous genes involved in acyl-CoA, FA, and lipid biosynthesis, including the TG, SL, and GPL families, was evidenced in follicular cells, hypothesizing the existence of ovarian de novo lipogenesis in bovine ovary. It was previously reported that CC could produce cholesterol, and this process is regulated by the oocyte secretion of BMP15/GDF9 in mice [67]. The expression of the key enzymes that are involved in FA synthesis was previously reported in porcine TH and GC [30]. In bovine GC, CC, and oocytes, the expression of lipogenic enzymes FASN and ACC was evidenced at the protein level [35,43,46]. Sterol regulatory element binding transcription factor 1 (*SREBF1*) regulates the genes that were involved in cholesterol and FA biosynthesis [68]. Here, it was detected as ubiquitously expressed in follicular cells, and thus may participate in the regulation of lipid metabolism-related genes.

The accumulation of lipids in LDs by follicular cells is regulated by a number of genes that are strongly expressed in GC, TH, and CC, and are involved in triglyceride biosynthesis (for example, *GPAM*, *GPD1*, *SCD5*, and *ACSBG1)*, lipid storage (*SCARB1*, *SCARB2*, *LPL*, *PLIN2*, and *PLIN5*), and glycerophospholipid metabolism (*PLA2G16*, *GPAM*, *ABHD3*, *PLA2G1B*, and *GPD1*). Correspondent proteins participate in lipoprotein degradation and lipogenesis, leading to the formation of intracellular LDs. In humans, GC accumulate more LDs than CC in vivo [69]. However, CC, which are specialized GC, are also able to rapidly accumulate LDs, especially when exposed to a high concentration of free FA [70,71]. Such a rapid transfer of free FA from FF and their accumulation in the LDs of follicular cells protect the oocyte from lipotoxicity, as was shown in bovine CC [54].

TG, CE, and free FA were also largely represented in FF, although there are no LDs. Indeed, total TG concentrations decreased, and total cholesterol increased in bovine FF along with follicular growth from small to large antral follicles [72]. These lipids may be a part of high density lipoproteins (HDL), which are the smallest lipoproteins that can be transported from blood [24]. Follicular cells may also synthetize lipoproteins, as human GC, which produced very low-density lipoproteins [73]. Among the lipids identified in FF, there were many membrane lipids (PC, PE, PI, PS, and lysophospholipids). These neutral lipids may be a part of FF lipoproteins, similar to human plasma lipoproteins, as analyzed by MALDI-TOF MS [74].

TH and GC cells received nutrients from circulating blood, including different lipoproteins and free FA coupled to albumins. In the present study, the expression of FA transporter *CD36* [75] and scavenger receptors *SCARB1* and *SCARB2* for HDL cholesterol esters uptake [76], which was detected in both TH and GC, supports the exogenous origin of a part of FF neutral lipids. In addition, we showed that the lipoprotein lipase *LPL* gene was highly expressed in TH cells, as well as other lipases in both TH and GC, suggesting that lipoproteins may be rapidly metabolized and liberate TG and CEs, which may be further used for energy storage and steroid synthesis. Follicular fluid also contain the debris of floating atretic GC and extracellular vesicles, which are released from cell membranes [77] and are abundant in bovine FF [57]. Therefore, the PC, as the other membrane phospholipids identified in FF, may originate from both lipoproteins and be membrane-derived, similar to extracellular vesicles, including exosomes [58,78].

On the other hand, several genes coding for apolipoproteins A, E, M, L, and O were strongly expressed in GC, TH, and CC. At the protein level, ApoA1 was shown to be produced and secreted by chicken GC [79]. ApoA1 protein was also evidenced by Western blot in the GC of healthy and polycystic ovary syndrome patients [80]. By immunocytochemistry, the ApoA1 protein was revealed in luteal follicular cells in primates [81]. In our previous work, using top–down proteomics, we have identified ApoA2 and ApoC3 proteins in bovine follicular cells (GC and CC) [82,83]. ApoA1, ApoC3, ApoH, and ApoO were identified using differential detergent fractionation multidimensional protein identification in bovine oocytes and CC [84]. Our present work reported the expression of corresponding genes in follicular cells and oocytes. Therefore, it seems that the bovine follicle is capable of not only degrading, but also synthetizing, the lipoproteins.

In addition, eight free FA, three SM, 28 LPC, and 13 cholesteryl ester features were identified in only FF by LC/HRMS. Around 10% of the total fatty acid concentration that is present in FF is complexed to albumin as free FA, and this pool is the most variable, and depends on the metabolic status of the cow [14,71]. Some of the FF lipids, as LPA or unsaturated FA, can activate peroxisome proliferator-activated receptors PPARs, nuclear transcriptional factors that control the expression of genes that function in lipid and carbohydrate metabolism, vascular development, cell proliferation, and cell differentiation [85]. Our study demonstrated that PPARG is strongly expressed in GC, CC, and oocytes, and may therefore regulate numerous lipid metabolism related genes in all of the compartments, as was here revealed by gene ontology analysis.

Sphingolipids are involved in membrane structure stabilization, cell-to-cell recognition, and cell signaling [86,87]. The preferential location of SM and LPC to FF might be also related to extracellular vesicles, which contain these lipids [58], and to lipoproteins, which contain both SM and lysophospholipids such as LPC [74].

The circulating lysophospholipids are membrane components that are necessary to mediate the synthesis of various phospholipids and embed proteins into cell membranes; however, several lysophospholipids such as LPC and LPI were now recognized as hormone-like signaling molecules acting as the ligands of orphan G protein-coupled receptors, and thus considered as intercellular and intracellular lipid mediators [56]. Therefore, LPC in FF might be involved in intrafollicular signaling and cell-to-cell communication.

LPCs that are derived from the PC are catalyzed either by lecithin-cholesterol acyltransferase LCAT with the formation of a cholesterol ester, or by phospholipases A2. According to our data, the genes *LCAT*, *PLA2G16*, *PLA2G7*, and *PLA2G1B* coding for the correspondent enzymes are expressed in TH, GC, and CC, whereas phospholipase A2-activating protein *PLAA* is overexpressed in oocyte. Therefore, we hypothesize that LPC can be produced by follicular cells, and oocyte may influence this process. Integrated to lipoproteins, the LPC may be then secreted to FF, which therefore should contain the LPC originated from both plasma and follicular cells. Reciprocally, LPC and LPE are transformed to PC or PE by specific acyltransferases, and these enzymes *(LPCAT2* and *MBOAT2*, respectively) were also expressed in follicular cells, with significant overexpression in the oocytes. According to MALDI MS profiling, LPC (16:0) and LPC (18:0) were more detected in the oocyte than in somatic follicular cells, and LPC (22:4) were preferentially detected in oocytes and CC. These LPCs may be either imported from the follicular cells, or locally produced. In addition, oocyte expresses genes to transform LPC to PC (*CEPT1*) or produce lipoproteins (*APOO1*). Several lipid transporters are expressed in the oocyte–cumulus complex and indicate possible exchanges of different lipids between these two compartments, as was shown for FABP3 protein [88], or between OCC and FF.

Within an OCC, a bovine full-grown oocyte exercises low transcriptional activity or is transcriptionally silent [89]. Transcripts are accumulated during oocyte growth and then stored as long as protein synthesis is required. When polyadenylation occurred, mRNA could be translated. By our transcriptomic analysis, only polyadenylated mRNA levels were compared between the follicular cells by microarray; therefore, here, detected overexpressed mRNA could be translated in the oocyte at that stage. Although in this article we did not reported data on protein expression, fatty acyl synthase

FASN, acetyl-CoA carboxylase ACC, FA binding protein FABP3, and lipid-droplet associated perilipin PLIN2 were detected at protein level in bovine immature oocytes recovered from 3–6 mm follicles [35]. Moreover, among 811 proteins identified by proteomics in bovine oocyte, numerous ones are involved in lipid metabolism [84], and the expression of correspondent genes was detected in the present study.

Full-grown bovine oocytes contain many lipid inclusions as LDs and ooplasm vesicles, which could be easily detected and quantified using specific fluorescent dyes such as NR or BODIPY [35,43,71]. In cows, a number of intracellular LDs increased during oocyte growth in vivo [90,91] and decreased during in vitro maturation [43]. Significant correlation between the number of LDs in the oocytes and FA composition in FF was reported in bovine; however, no correlation was found between the number of LDs in the oocytes and the expression level of lipid biosynthesis genes *SCD*, *FADS2*, and *ELOVL5* in GC or CC [92]. According to our transcriptomic data, a set of genes that are involved in the synthesis of glycerolipids *(DGAT2*, *GK*, *AGPAT9*, *MBOAT2*, *PPAP2C*, *AKR1B1*, *GPAT2*, *DGKI)*, sphingolipids (*SPTLC2*, *ACER*, *CERS2*), phospholipids PC and PE (*CEPT1*), lipid storage (*PLIN2*), and FA transport (*FABP3*, *FABP5*) are overexpressed in the oocytes compared to other follicular cells. Expression pattern corroborates with a presence of numerous LDs in the oocyte at that stage and suggest strong lipogenic activity, such as the FA elongation and synthesis of very long-chain fatty acyl-CoA, which is more pronounced in oocytes than in other follicular cells. Oocyte expression pattern also supports its capability to intensive lipolysis and FA oxidation activities, which corroborates with the presence, at protein level, of hormone-sensitive lipase (LIPE protein) in immature oocytes and an increase of LIPE phosphorylation and CPT1 protein abundance in bovine oocytes during maturation [35,43].

In addition, transcriptome analysis revealed the role of the oocyte in PI3 kinase signaling and the synthesis of phosphatidylinositol phosphates (PIP) at the plasma membranes because of the overexpression of the genes that are involved in phosphatidylinositol metabolic processes *(CDS1*, *PI4K2B*, *PLA2G12A*, *PIK3CB*, *PIK3R1*, *PIK3C2A*, *PIK3CA*, *PITPNM1*, *PLCG2*, *PIP4K2A*, *PIK3C3*, *PIP4K2B*, *PIP5K1B*, *PI4KB*, *PIP4K2C*, *PIP5K1C* . . . *).* Indeed, the hydrolysis of PIP_2 and the production of inositol trisphosphate is involved in the triggering of oocyte activation after fertilization [93]. In immature oocytes, which were here analyzed, mRNA may be stocked or partially translated. During oocyte maturation in bovine, protein de novo synthesis occurs in parallel with massive mRNA degradation [94–96]. It is likely that the accumulation of lipid reserves, together with maternal mRNA and protein stocks, may serve to ensure oocyte maturation, fertilization, and zygote activation. The first rapid embryo cleavages require active machinery to produce cell structures from the maternal stock for at least 16 blastomers before relaying to the embryo genome that activates in 8/16-cells stage embryo in bovine [97].

In summary, the provided detailed analysis of lipids and related transcriptional control in the bovine ovarian follicle implies the capacity of bovine follicular cells, especially theca and granulosa cells, to uptake lipoproteins and free FA, metabolize them, and transport lipids. From these blocks, the follicular cells may probably either produce new membrane lipids and lipoproteins or liberate energy through FA oxidation, or constitute lipid droplets as a reserve of energy and precursors of steroid hormones and secondary messengers. The lipid composition of follicular fluid and enclosed oocyte–cumulus complex coupled to a particular gene expression pattern in these cells presumes intensive lipid exchanges between these compartments, and the particular involvement of the oocyte in FA elongation, the synthesis of glycerophospholipids, glycerolipids, and lipid droplet formation. Oocytes thus accumulate lipids and also contain specific metabolic machinery that may be used for energy production, membrane synthesis, and signaling in order to assure meiotic maturation, fertilization, and provide necessary building blocks for the first embryo cells.

Although more investigations at the protein level are required, an analysis of the expression patterns of lipid metabolism-related genes in the follicular cells and the scrutiny of lipid composition in follicular compartments may imply that the ovarian follicle contains complex metabolic machinery for FA uptake and metabolism to assure intrafollicular homeostasis and prepare the oocyte for ovulation.

4. Materials and Methods

4.1. Ethics

Bovine ovaries were obtained from a local commercial slaughterhouse; no experiments on live animals were performed.

4.2. Chemicals

Unless indicated, all of the chemicals were purchased from Sigma-Aldrich (Saint-Quentin Fallavier, France). LC-MS grade water (H_2O) and methanol (MeOH) were from VWR International (Plainview, NY, USA). Internal standard mix for lipid identification was purchased from Avanti Polar Lipids, Inc. (Alabaster, AL, USA).

4.3. Biological Materials

Bovine ovaries were transported from the local slaughterhouse on ice. Follicles of 3–8 mm in length were accurately aspirated in 50-mL Falcon tubes, avoiding blood contamination, on ice. Follicular cells fell down in the bottom of the tube were recovered and centrifuged for 10 min 5000 *g* at 4 °C. The cell pellets were rinsed twice in cold phosphate buffered saline (PBS). Samples of follicular cell pellets and follicular fluid (FF), separated from cell debris, were frozen in liquid nitrogen and used for lipid extraction and identification using liquid chromatography coupled with high-resolution mass spectrometry (LC-HRMS) or tandem high-resolution mass spectrometry (HRMS/MS).

For mass spectrometry imaging (MSI) and liquid extraction surface analysis (LESA) from ovarian sections, ovaries were frozen in nitrogen stream and cut within no longer than four days for lipid analysis.

For lipid profiling by MALDI–TOF MS, individual follicles were dissected in order to separate FF, scraping off granulosa cells (GC), and isolating theca cell layers (TH) from each follicle. Cells were put into cold PBS, centrifuged, and then the pellets were washed twice in Tris-Sucrose buffer (260 mM sucrose 20 mM Tris-HCl pH 6.8). Oocyte–cumulus complexes were recovered from the follicles that were 3–8 mm in size; the oocytes were separated individually from their cumulus cells (CC), and then rinsed with Tris-Sucrose buffer and snap-frozen in liquid nitrogen. Samples were kept at −80 °C and analyzed within no longer than 4 days.

For transcriptomic analysis, pools of GC, TH, CC, and 50 oocytes (n = 4 each) were collected and kept in TriZol reagent (Invitrogen, Cergy Pontoise, France) at −80 °C for RNA extraction.

4.4. Lipid Analysis

4.4.1. Nile Red Staining

Nile red staining of neutral lipids in bovine ovary sections was adapted from original protocol [98]. Bovine ovaries (n = 7) were frozen in nitrogen steam and cut at 10-µm slices using cryostat (MICROM NX70, Walldorf, Germany). Frozen sections were mounted onto Superfrost ®Plus slides (Thermo Scientific, Villebon sur Yvette, France) and air-dried for 10 min. Slides were fixed in 4% (v/v) of paraformaldehyde for 2 min, and then washed in water for 5 min at room temperature. The slides were incubated in 500 ng/µL of Nile red (NR) (Sigma Aldrich, St Louis, MO, USA) water solution for 1 h at room temperature, and then washed for 5 min in water and mounted in a Moveol solution complemented with 1 µg/mL of 4′,6-Diamidine-2′-phenylindole dihydrochloride (DAPI). Sequentially, NR slides were stained by hematoxylin-eosin for the precise identification of histological structures.

NR-treated slides were scanned using an AxioScan.Z1 scanner (Carl Zeiss SAS, Oberkochen, German) at 20×/0.8 magnification and using specific filters to detect blue DAPI fluorescence (excitation and emission wavelength were 335–383 nm and 420–470 nm, respectively) and NR fluorescence (excitation 538–562 nm and emission 570–640 nm) as described. The same exposure time were used for

all of the slides (50 ms to DAPI and 35 ms to NR). Each image was analyzed using Zen Blue version 6.1.7601 software (Carl Zeiss Microscopy, GmbH, German).

In each image, the diameters of the follicles were measured. For each antral follicle, the intensity of NR fluorescence was measured in 25 regions of interest (ROI) positioned in FF, theca (TH), and granulosa cell (GC) layers, representing about 2 mm^2 ROI per compartment. The background was subtracted from the NR fluorescence intensity value, and the resulted value was normalized by the ROI exact area. A comparison of the normalized NR intensities between FF, GC, and TH was performed by one-way ANOVA followed by a Newman-Keuls multiple comparison test using GraphPad Prism version 5.01 (GraphPad Software, La Jolla, CA, USA).

4.4.2. Lipid Identification Using Liquid Chromatography Coupled to High-Resolution Mass Spectrometry (LC-HRMS)

Three samples of 50 µL of FF or 10 mg of ovarian follicular cells were extracted according to a modified Folch method [99]. Briefly, samples were extracted with chloroform/methanol 2:1 (v/v), and 10 µL of internal standard mixture were added. Samples were then reconstituted with 100-fold dilutions of initial volume (50 µL for FF and 100 µL for cells) of MeOH/IPA/H_2O 65:35:5 ($v/v/v$), vortexed for 30 s, and sonicated for 60 s before injection. Samples from follicular cells and FF were analyzed in two separated batches.

Total lipid extracts were separated on HTC PAL-system (CTC Analytics AG, Zwingen, Switzerland) coupled with a Transcend 1250 liquid chromatographic system (ThermoFisher Scientific, Les Ulis, France) using a kinetex C8 2.6 µm 2.1 × 150 mm column (Phenomenex, Sydney, NSW, Australia). Mobile phase A consisted of H_2O/MeOH 60/40 (v/v) and 0.1 % formic acid and mobile phase B of IPA/MeOH 90/10 (v/v) and 0.1 % formic acid. Ammonium formate (10 mM) was added to both mobile phases in the positive ion mode. The gradient program from 32% to 95% of solvent B was established. The flow rate was 400 µL/min, and the column temperature was set to 60 °C.

Mass spectrometry analysis were performed using 10 µL of each sample. After injection, the column effluent was directly introduced into the heated electrospray (HESI) source of a Q-Exactive mass spectrometer (Thermo Scientific, San Jose, CA, USA), and analysis was performed in both ionization modes in two separate runs. Spray voltage was set to 3.7 kV and −3.1 kV in the positive and negative ionization modes, respectively. Mass spectra were recorded in full-scan MS mode from m/z 50 to m/z 2000 at a targeted mass resolution of 140 k, full width at half-maximum at m/z 200, and at a scan speed of 2 Hz.

Data were process as described previously [47]. Peak detection, correction, alignment, and integration were processed using XCMS R package with CentWave algorithm [49]. Features were then annotated thanks to an in silico lipid database and based on accurate measured masses, retention time windows, and relative isotopic abundance (RIA) of lipid species. A comparison of lipid families and lipid classes distributions was performed using Chi-2 following by Fisher exact test. Differences were considered significant at $p < 0.05$.

4.4.3. Lipid Identification Using Tandem High-Resolution Mass Spectrometry (HRMS/MS)

Total lipids were extracted from 100 µL of follicular and environ 100 mg of follicular cells suspension as described [99,100].

From 10 µm, cryosections of freshly frozen bovine ovaries, in situ lipid extraction experiments were performed manually at multiple user-defined points across the tissue targeting follicles. For LESA, 1.5 µL of solvent were dispensed onto the tissue surface using a pipette, incubated for 5 s and reaspirated. Extractions were repeated four times in the same zone, and pooled, using two different extraction solutions as chloroform/methanol/2-isopropanol (1:2:4 $v/v/v$) or methanol 100%.

In order to obtain structural information for fine identifications, all of the lipid extracts were analyzed by tandem high-resolution mass spectrometry (HRMS/MS). All of the samples were infused directly in a dual linear ion trap Fourier Transform Mass Spectrometer (FT-MS) LTQ Orbitrap Velos

(Thermo Fisher Scientific, Bremen, Germany). Data acquisitions were performed with Xcalibur software (version 2.1, Thermo Fisher Scientific, Bremen, Germany). FT-MS spectra were acquired using the profile mode in the 400–2000 m/z mass range, and the FT-MS/MS spectrum using HCD (high-energy collisional dissociation between 25–33%) fragmentation ion mode. Target resolution was set at 100,000 for FT-MS and FT-MS/MS analysis. The selected precursor width for fragmentation was 1.5 m/z.

Folch and LESA extracts were diluted (1:1, v:v) with a solution of 50% methanol/1% formic acid and loaded into a metalized nanoelectrospray needle (PicoTip emitters, New Objective) with a spray voltage of 1.2 kV. Spectra were acquire for 10 min in the positive ion mode from 400 m/z to 2000 m/z, using a method excluding automatically the precursors previously selected for the fragmentation using HCD collision energy of 25% and 33%.

Bligh & Dyer dried extracts were re-solubilized in a solution of 80% methanol/20% H_2O in the presence of 1% formic acid and in a solution of 80% methanol/20% ammonium acetate of 100 mM for MS acquisitions in the positive and negative ion modes, respectively. FT-MS and FT-MS/MS spectra were acquired, over 10 min, in triplicate, using different collision energy levels (20 keV to 60 keV with a step of 5 keV). Data were collected using spectral stitching technique [101] as a series of 100-m/z wide windows that overlap by 5 m/z. Peaks were considered when >500 counts.

The data from FT-MS and FT-MS/MS were converted to Mascot generic format (MGF) using Proteome Discoverer software (version 1.4, ThermoFisher Scientific, San Jose, CA, USA) or MS convert integrated in an R-based tool as LipidMatch software [102]. All of the automatic lipid identifications that were proposed by LipidMatch (mass accuracy of 0.05 Da for precursor and 50 ppm for fragment ions, score = level 1) were confirmed by manual interpretation using LipidBlast 2.0 software. All of the identifications with a score Rev-Dot > 800 were accepted considering the presence of specific fragments ions (error mass accuracy of 0.8 Da) for phospholipids and sphingolipids. For each of the identified lipids, the theoretical mass and formula were obtained through interrogation of the LipidMaps database (http://www.lipidmaps.org/tools/ms/LMSD_search_mass_options.php).

4.4.4. MSI (Mass Spectrometry Imaging) by MALDI-TOF MS

Freshly frozen whole ovaries were cut using a Cryo-Star HM 560 cryostat (Microm, Francheville, France) at −18 °C. The 10-µm thick sections were thaw-mounted onto conductive Indium Tin Oxide-coated microscope slides (Bruker Daltonics, Wissembourg, France). For external mass calibration, 1 µL of a mixture of small molecules and peptides (1 µL of calibrant solution containing Cafein, MRFA peptide, Leu-Enkephalin, Bradykinine 2–9, Glu1-fibrinopeptide B; reserpine; Bradykinine; Angiotensine I) was placed near the tissue section and mixed (1:1 v/v) with the matrix employed for the MALDI MSI.

Ovary sections were scanned before matrix deposition using a histology slide scanner (OpticLab H850 scanner, Plustek, Ahrensburg, Germany). These images were used to overlay the histological and molecular images. Slides were coated with a CHCA (α-cyano-4-hydroxycinnamic acid) matrix sprayed at 7 mg/mL in 60/40 acetonitrile/H_2O, 0.2% trifluoroacetic acid using an Image Prep device (Bruker Daltonik GmbH, Bremen, Germany), and then vacuum-dried. Spectra were acquired using an UltrafleXtreme MALDI-TOF instrument (Bruker Daltonik GmbH, Bremen, Germany) equipped with a Smartbeam laser (Nd:YAG, 355 nm) monitored by the FlexControl 3.4 software (Bruker Daltonics, Bremen, Germany). MSI sequence was performed from one ovarian section targeting several regions of interest (ROIs) corresponding to individual antral follicles (2–6 mm in diameter).

Spectra were acquired in the positive mode, at a 2.0-kHz laser repetition rate, in the 100–1200 m/z range, using a spatial resolution set at 25 µm (medium focus setting) and collecting 500 spectra per pixel as a sum of 50 consecutive laser shots in 10 random walk shot steps. For a better mass accuracy across a tissue section image, raw spectra from all of the datasets were first aligned to a lock mass set at m/z 760.5780 corresponding to $[M + H]^+$ of 34:1 PC. The unprocessed MSI sequence was then imported into the SCiLS Lab software (version 2016b, SCiLS, GmbH, Bremen, Germany). MSI sequence was

loaded and pre-processed, according the used instrument type (TOF). Data were baseline reduced using a convolution algorithm with the setting of 20 for peak width and normalized to the total ion count (TIC). For each ROI (individual follicle), two-dimensional (2D) ion density maps using medium denoising were created from the average projection spectrum, and after data partitioning (bisecting k-Means), a segmentation map was generated.

4.4.5. MALDI-TOF MS Analysis of Lipids on Follicular Cells and Fluid

Frozen oocytes were thawed in ice and placed on the MTP Ground Steel 384 MALDI plate (Bruker Daltonics, Germany) to dry. TH, GC, and CC samples were defrosted in an ice bath, and 5 µl of cell suspension or FF were dried by SpeedVac System (SPD 1010-230, Thermo Savant Eletronic Corporation, France) for 10 min at 45 °C. Pellets were re-suspended in a DHAP (2,5-dihydroxyacetophenone) matrix at 20 mg/mL solubilized in 90% methanol, 2% trifluoroacetic acid in water (4 µl for cells and 8 µL for FF samples). The matrix/sample mixtures were sonicated for four min using an ultrasonic bath sonicator (FisherBrand 15,052, Fisher Scientific) to solubilize the lipids. One microlitrer of the matrix/sample mix was overlaid with 1.5 µL of the same solution as the matrix. Each sample was spotted onto a MALDI plate in three replicates (with the exception of a single oocyte), and then dried at room temperature for 30 min. 3000 spectra per spot (as a sum of 1000 consecutive laser shots in three shot steps) were acquired, using a Bruker UltrafleXtreme MALDI-TOF instrument (Bruker Daltonics, Germany). Spectra were acquired in the positive and negative ion modes using reflecton in the m/z 100–1200 range. External calibration was performed using a mixture of small molecules and peptides (1 µL of calibrant solution containing Cafein, MRFA peptide, Leu-Enkephalin, Bradykinine 2–9, Glu1-fibrinopeptide B; reserpine; Bradykinine; Angiotensine I) and 1 µL of the DHAP matrix. To increase the mass accuracy (mass error < 0.05%), internal calibration was subsequently applied to all of the spectra. Lock mass correction was performed with highest intensity peak, corresponding to the glycerophosphatidylcholine (PC 32:1, m/z 732.556) in the positive mode, and glycerophosphatidylinositol (PI 38:4; m/z 885.5499) in the negative mode, using FlexAnalysis 4.1 software (Bruker). Each spectrum was converted to a .txt file using FlexAnalysis 3.4 software and processed using MALDI Progenesis software version 1.2 (Nonlinear Dynamics, Newcastle upon Tyne, UK). Peaks were automatically detected. The peaks with a signal to background ratio of five, and the isotopes were not considered for analysis. The coefficient of variation (CV%) of intensity values (normalized peak height, NPH) was calculated for all the peaks in three technical replicates per sample, from 12 different follicles for each tissue (Table A2, Appendix A). NPH values were used for a comparative analysis of lipid profiling between the compartments. One-way (ANOVA) and Tukey post-hoc test were used for differential analysis using XLSTAT software (Addinsoft, Paris, France). Differences were considered significant at $p \leq 0.05$.

4.5. Gene Expression Analysis

4.5.1. RNA Extraction

Total RNA was extracted from the pools of isolated TH (n = 4), GC (n = 4), CC (n = 4) and oocytes (four pools of 50 oocytes) using TriZol reagent (Invitrogen, Cergy Pontoise, France) and then treated by RQ1 DNAse (Promega, Charbonnières, France) following the manufacturer's instructions. After isopropanol precipitation, the RNA concentration was determined using a NanoDrop ND-1000 spectrophotometer (Nyxor Biotech, Paris, France), RNA integrity was checked on a Bioanalyzer 2100 (Agilent Technologies, Santa Clara, CA, USA).

4.5.2. Microarray Hybridization and Transcriptome Data Analysist

A customized 60-K bovine microarray (Agilent Technologies, Santa Clara, CA, USA) covering more than 97% of the Ensembl Bos taurus transcripts (genome assembly UMD3.1) was used (GEO number GPL21724). Cyanine-3 (Cy3) labeled cRNA were prepared with 200 ng of total RNA using

the One-Color Low Input Quick Amp Labeling kit following the recommended protocol (Agilent Technologies). Specific activities and cRNA yields were determined using the NanoDrop ND-1000. For each sample, hybridization was performed using 600 ng of Cy3-labeled cRNA (specific activity > 6.0 pmol of Cy3/µg of cRNA) for 17 h at 65 °C, following the manufacturer's protocol at the Animal Biological Resources for Integrative and Digital Genomics facility (INRA Jouy-en-Josas, France, http://crb-gadie.inra.fr/). Slides were washed, air-dried, and scanned immediately using a G2565CA Scanner System with one-color scan setting (Agilent Technologies). The resulting images were analyzed using Feature Extraction Software v10.7.3.1 (Agilent Technologies). Raw data were normalized through intra-array median subtraction and log2 transformation, and then, the expression values were analyzed with a mixture model variance (VarMixt) method (R software). Raw probability values were adjusted using the Benjamini–Hochberg corrections for all of the comparisons; a differential was considered significant at $p < 0.05$. The gene ontology analysis of differential genes was performed using Enrichr gene set enrichment analysis web server application http://amp.pharm.mssm.edu/Enrichr/ [103]. The analysis of differential expression of lipid metabolism-related genes between follicular cells (TH, GC, CC a, d OO) was performed on the normalized expression values of 468 selected genes involved in lipid metabolism by applying ANOVA with Benjamini–Hochberg post-hoc correction of *p*-values. Multiple pair analysis was performed by Tukey test.

4.5.3. Real Time PCR Expression Analysis

Total RNA was extracted as described in Section 4.5.1, from four independent pools of TH, GC, CC, and oocytes ($n = 50$ per pool). Reverse transcription (RT) was performed on 200 ng of extracted RNA from somatic cells and a total yield of oocyte RNA, using the Maxima First Strand cDNA Synthesis kit (Thermo-Fisher Scientific, Courtaboeuf, France) according to the manufacturer's instructions. Real-time PCR reactions were carried out on a CFX96 (Bio-Rad, Marnes-la-Coquette, France) in 20 µL containing primers at a final concentration of 150 nM each, 5 µL of the diluted RT reaction (equivalent of 2 ng cDNA), and qPCR Mastermix Plus for SYBR Green I (Bio-Rad, Marnes-la-Coquette, France) according to the manufacturer's instructions. The efficiency of the primers (Table A3, Appendix A), and standard curve for each gene was deduced from serial dilutions of the correspondent cDNA fragment obtained as a template. The geometric mean of three housekeeping genes (RPL19, RPS9, and GAPDH) was used to normalize gene expression. The relative expression of the genes of interest (RE) in each sample (n = six per cell type) was calculated according to the equation: R = gene E^{-Ct} gene/geometric mean ($RPS9^{E\text{-}Ct\ RPS9}$; $RPL19^{E\text{-}Ct\ RPL19}$; $GAPDH^{E\text{-}Ct\ GAPDH}$), where E is the primer efficiency and Ct the cycle threshold.

Statistics were done using ANOVA followed Tukey post-hoc test. Difference was considered significant at $p < 0.05$.

5. Conclusions

Detailed data on lipid identification and their localization inside of the bovine ovarian follicle coupled with the tissue-specific expression of genes related to lipid turnover, suggest the potential capacity of follicular cells to transform FA from the nutritive uptake and use them to supplement the oocyte and follicular cells with membrane lipids, energy, and signaling mediators, thus maintaining follicular homeostasis. Data on the lipidomics and transcriptomics of ovarian follicular compartments that have been reported here might be useful for better understanding of the mechanisms of lipid metabolism in the oocyte and surrounding follicular cells.

Supplementary Materials: Supplementary materials can be found at http://www.mdpi.com/1422-0067/19/10/3261/s1.

Author Contributions: S.U. and P.S.B. conceived and designed the study, performed the experiments, analyzed the data and wrote paper. A.S. performed lipidomic analysis by LC-HRMS. A.-P.T.-G., V.L. and C.B. were involved in MSI, MALDI MS lipid profiling and identification of lipids. A.V.C. and V.D. performed microarray hybridization and analyzed data. M.-C.B. and L.A.V.C. were involved in analysis of lipids by NR fluorescence and statistics. PP was involved in real-time PCR analysis. V.M. and S.E. were involved in lipidomics, data analysis and contributed in writing the manuscript. All authors read and approved the final manuscript.

Funding: This research was funded by INRA and Val de Loire Region (France), grant APR IR-2014 "Bovomega3". Priscilla Bertevello was funded by University do Estado do Rio Grande do Norte (Brazil).

Acknowledgments: We would like to thank the technical staff of the research (PRC) unit in INRA Val de Loire Centre, Albert Arnould and Thierry Delpuech for collecting the ovaries; students Sawoda Manrouf, Marie Leduc and Magalie Boguenet for help in gene expression analysis and Olfa Ghazouani for help in lipidomic analysis. We are grateful to Marco Moroldo and Jérôme Lecardonnel from Animal Biological Resources for Integrative and digital Genomics facilities (Jouy-en-Josas, France) for the technical assistance of microarray hybridization.

Conflicts of Interest: The authors declare no conflict of interest. The founding sponsors had no role in the design of the study; in the collection, analyses, or interpretation of data; in the writing of the manuscript, and in the decision to publish the results.

Abbreviations

CC	Cumulus cells
Cer	Ceramids
CE	Cholesteryl esters
DG	Diacylglycerols
FA	Fatty acyls
FFA	Free fatty acids
FAC	Fatty acyl carnitines
FF	Folicular fluid
FSH	Follicle Stimulation Hormone
GC	Granulosa cells
GM	Ganglioside
GL	Glycerolipids
GO	Gene Onthology
GP	Glycerophosphates
GPL	Glycerophospholipids
HCer	Hexosylceramide
HDL	High Density Lipoprotein
Hcer	Hexosylceramides
LC/MS	Liquid Chromatography/Mass Spectrometry
LC-HRMS	Liquid Chromatography- High Resolution Mass Spectrometry
LD	Lipid droplet
LDL	Low Density Lipoprotein
LH	Luteinizing Hormone
LPA	Lyso-phatidic acid
LPC	Lyso-phosphatidylcholines
LPE	Lyso-phosphatidylethanolamines
LPI	Lyso-phosphatidylinositols
LPL	Lipoprotein Lipase
m/z	Ion Mass to Ion Charge number ratio
MALDI-TOF	Matrix Assisted Laser Desorption Ionization -Time of Flight
MS	Mass Spectrometry
MSI	Mass Spectrometry Imaging
NEB	Negative Energy Balance
NR	Nile Red

OO	Oocyte
OOC	Oocyte-cumulus complex
PA	Phosphatidic Acid
PC	Phosphatidylcholines
PE	Phosphatidylethanolamines
PG	Phosphatidylglycerols
PI	Phosphatidylinositols
PS	Phosphatidylserines
SL	Sphingolipids
SM	Sphingomyelins
ST	Sterols/Steroid Derivatives
SuSM	Sulfoglycosphingolipids
TG (TAG)	Triacylglycerols
TH	Theca cells

Appendix A

Table A1. Identification of the lipids detected by mass spectrometry imaging (Figure 3B).

Observed *m*/*z*	Exact *m*/*z*	Delta/Da	Lipid Annotation	Ion
104.195	104.173	−0.022	Choline	$[M + H]^+$
184.189	184.152	−0.037	Phosphocholine	$[M + H]^+$
496.434	496.34	−0.0937	LPC 16a:0	$[M + H]^+$
520.427	520.34	−0.0867	LPC 18a:2	$[M + H]^+$
522.429	522.356	−0.073	LPC 18a:1	$[M + H]^+$
524.458	524.372	−0.0864	LPC 18a:0	$[M + H]^+$
534.379	534.296	−0.0834	LPC 16a:0	$[M + K]^+$
544.417	544.3403	0.0767	LPC 20a:4	$[M + H]^+$
560.398	560.3116	−0.0867	LPC 18a:1	$[M + K]^+$
703.64	703.575	−0.0652	SM(d18:1/C16:0)	$[M + H]^+$
706.592	706.539	−0.0533	PC 30a:0	$[M + H]^+$
725.587	725.557	−0.0302	SM(d18:1/C16:0)	$[M + Na]^+$
732.609	732.5543	−0.0547	PC 32a:1	$[M + H]^+$
734.626	734.57	−0.056	PC 32a:0	$[M + H]^+$
741.581	741.5881	0.0071	SM(d18:0/C17:0)	$[M + Na]^+$
746.617	746.57	−0.047	PC 33a:1	$[M + H]^+$
748.625	748.5856	−0.0394	PC 33a:0	$[M + H]^+$
753.628	753.5881	−0.0399	SM(d18:1/C18:0)	$[M + Na]^+$
754.581	754.5357	−0.0453	PC 32a:1	$[M + Na]^+$
755.59	755.5469	−0.0431	SM(d18:1/C17:0)	$[M + K]^+$
756.599	756.5514	−0.0476	PC 32a:0	$[M + Na]^+$
758.621	758.56995	−0.0511	PC 34a:2	$[M + H]^+$
760.617	760.5856	−0.0314	PC 34a:1	$[M + H]^+$
768.598	768.5514	−0.0466	PC 33a:1	$[M + Na]^+$
769.589	769.5626	−0.0264	SM(d18:1/C18:0)	$[M + K]^+$
770.551	770.567	0.016	PC 33a:0	$[M + Na]^+$
772.562	772.5253	0.0367	PC 32a:0	$[M + K]^+$
774.634	774.6013	−0.0327	PE 38:1	$[M + H]^+$
780.578	780.5514	−0.0266	PC 34a:2	$[M + Na]^+$
782.603	782.567	−0.036	PC 34a:1	$[M + Na]^+$
784.602	784.5827	−0.0193	PC 34a:0	$[M + Na]^+$
786.632	786.6013	−0.0307	PC 36a:2	$[M + H]^+$
788.664	788.6169	−0.0471	PC 36a:1	$[M + H]^+$
794.605	794.567	−0.038	PC 35a:2	$[M + Na]^+$
796.562	796.5827	0.0207	PC 35a:1	$[M + Na]^+$

Table A1. *Cont.*

Observed *m/z*	Exact *m/z*	Delta/Da	Lipid Annotation	Ion
798.578	798.5983	0.0203	PC 35a:0	$[M + Na]^+$
806.583	806.567	−0.016	PC 36a:3	$[M + Na]^+$
808.613	808.5827	−0.0303	PC 36a:2	$[M + Na]^+$
810.615	810.5983	−0.0167	PC 36a:1	$[M + Na]^+$
812.592	812.614	0.022	PC 36:0	$[M + Na]^+$
822.567	822.5843	0.0173	PC 36a:3	$[M + K]^+$
824.587	824.5566	−0.0304	PC 36a:2	$[M + K]^+$
826.581	826.572	0.0087	PC 36a:1	$[M + K]^+$

Identifications of the lipids with the lowest delta value (exact m/z –observed m/z) are shown. All of the identifications are available in Supplementary Data (Table S2). Abbreviations: a—acyl; LPC—lyso-glycerophosphocholines; PC—glycerophosphocholines; SM—sphingomyelins. M—mass; Na—sodium ion; K—potassium.

Table A2. Coefficients of variation (%) of normalized peak heights quantification from MALDI-TOF lipid profiles.

Compartment	Positive Mode	Negative Mode
TH	15.9%	16.1%
GC	18.4%	15.8%
FF	18.0%	22.9%
CC	27.6%	21.7%
OO	32.9%	25.3%

Table A3. List of primers used for RT-qPCR analysis of gene expression in bovine ovarian cells.

Gene	Accession Number	Description		Primer's Sequence (5′-3′)	Efficiency, % (E)
ABHD6	NM_001075196	Abhydrolase domain containing 6 (ABHD6)	Fw Rev	ACCCCGAAGGAGATGAGTGA CTGGGAGTTGGCGATTGACT	92.6% (1.93)
AGPAT9	NM_001192514	Acylglycerol-3-phosphate O-acyltransferase 9	Fw Rev	AATGCCTCTCCCATCCGTTG TTATGCTGCACAGTCGGGAA	88.9% (1.89)
CPT1A	FJ415874	Carnitine palmitoyltransferase 1A	Fw Rev	TCCTGGTGGGCTACCAATTA TGCGTCTGTAAAGCAGGATG	95.4% (1.95)
GAPDH	NM_001034034	Glyceraldehyde 3 phosphate dehydrogenase	Fw Rev	TTCAACGGCACAGTCAAGG ACATACTCAGCACCAGCATCAC	100.3% (2.00)
DGAT2	NM_205793.2	Diacylglycerol O-acyltransferase 2	Fw Rev	GTGGCCTCGCTTTGCTTAAC GGGTTCGGGGAACTTCTGTT	92.3% (1.92)
FABP3	NM_174313	Fatty acid binding protein 3	Fw Rev	ATCGTGACGCTGGATGGCGG GCCGAGTCCAGGAGTAGCCCA	104.1% (2.04)
FASN	AY343889	Fatty acid synthase	Fw Rev	CACTCCATCCTCGCTCTCC GCCTGTCATCATCTGTCACC	102.9% (2.02)
LPL	NM_001075120	Lipoprotein lipase	Fw Rev	GGGTTTTGAGCAAGGGTACA GCCACAATGACCTTTCCAGT	87.1% (1.87)
PLIN2	NM_173980	Perilipin 2	Fw Rev	ACAACACACCCCTCAACTGG CTGCCTGCCTACTTCAGACC	97.5% (1.96)
PNPLA2	NM_001046005	Patatin-like phospholipase domain containing 2	Fw Rev	ATGGTGCCCTACACTCTGCC AGCTTCCTCTTGGCGCGTAT	87.6% (1.88)
PPARG	Y12419	Peroxisome proliferator-activated receptor gamma	Fw Rev	CCCTGGCAAAGCATTTGTAT ACTGACACCCCTGGAAGATG	105.1% (2.05)
RPL19	BC102223	Ribosomal protein L19	Fw Rev	AATCGCCAATGCCAACTC CCCTTTCGCTTACCTATACC	98.2% (1.98)
RPS9	BC148016	Ribosomic protein S9	Fw Rev	GGAGACCCTTCGAGAAGTCC GGGCATTACCTTCGAACAGA	85.0% (1.85)

References

1. Butler, W.R.; Smith, R.D. Interrelationships Between Energy Balance and Postpartum Reproductive Function in Dairy Cattle. *J. Dairy Sci.* **1989**, *72*, 767–783. [CrossRef]
2. Staples, C.R.; Thatcher, W.W.; Clark, J.H. Relationship between ovarian activity and energy status during the early postpartum period of high producing dairy cows. *J. Dairy Sci.* **1990**, *73*, 938–947. [CrossRef]
3. Leroy, J.L.; Opsomer, G.; Van Soom, A.; Goovaerts, I.G.; Bols, P.E. Reduced fertility in high-yielding dairy cows: Are the oocyte and embryo in danger? Part I. The importance of negative energy balance and altered corpus luteum function to the reduction of oocyte and embryo quality in high-yielding dairy cows. *Reprod. Domest. Anim.* **2008**, *43*, 612–622. [CrossRef] [PubMed]
4. Van Hoeck, V.; Bols, P.E.; Binelli, M.; Leroy, J.L. Reduced oocyte and embryo quality in response to elevated non-esterified fatty acid concentrations: A possible pathway to subfertility? *Anim. Reprod. Sci.* **2014**, *149*, 19–29. [CrossRef] [PubMed]
5. Bender, K.; Walsh, S.; Evans, A.C.O.; Fair, T.; Brennan, L. Metabolite concentrations in follicular fluid may explain differences in fertility between heifers and lactating cows. *Reproduction* **2010**, *139*, 1047–1055. [CrossRef] [PubMed]
6. Zeron, Y.; Ocheretny, A.; Kedar, O.; Borochov, A.; Sklan, D.; Arav, A. Seasonal changes in bovine fertility: Relation to developmental competence of oocytes, membrane properties and fatty acid composition of follicles. *Reproduction* **2001**, *121*, 447–454. [CrossRef] [PubMed]
7. Fortune, J.E.; Rivera, G.M.; Yang, M.Y. Follicular development: The role of the follicular microenvironment in selection of the dominant follicle. *Anim. Reprod. Sci.* **2004**, *82–83*, 109–126. [CrossRef] [PubMed]
8. Mermillod, P.; Dalbies-Tran, R.; Uzbekova, S.; Thelie, A.; Traverso, J.M.; Perreau, C.; Papillier, P.; Monget, P. Factors affecting oocyte quality: Who is driving the follicle? *Reprod. Domest. Anim.* **2008**, *43* (Suppl. 2), 393–400. [CrossRef]
9. Buratini, J.; Price, C.A. Follicular somatic cell factors and follicle development. *Reprod. Fertil. Dev.* **2011**, *23*, 32–39. [CrossRef] [PubMed]
10. Hsueh, A.J.W.; Kawamura, K.; Cheng, Y.; Fauser, B.C.J.M. Intraovarian control of early folliculogenesis. *Endocr. Rev.* **2015**, *36*, 1–24. [CrossRef] [PubMed]
11. Fortune, J.E. Ovarian follicular growth and development in mammals. *Biol. Reprod.* **1994**, *50*, 225–232. [CrossRef] [PubMed]
12. Dumesic, D.A.; Meldrum, D.R.; Katz-Jaffe, M.G.; Krisher, R.L.; Schoolcraft, W.B. Oocyte environment: Follicular fluid and cumulus cells are critical for oocyte health. *Fertil. Steril.* **2015**, *103*, 303–316. [CrossRef] [PubMed]
13. Gilchrist, R.B.; Lane, M.; Thompson, J.G. Oocyte-secreted factors: Regulators of cumulus cell function and oocyte quality. *Hum. Reprod. Update* **2008**, *14*, 159–177. [CrossRef] [PubMed]
14. Leroy, J.L.M.R.; Vanholder, T.; Mateusen, B.; Christophe, A.; Opsomer, G.; de Kruif, A.; Genicot, G.; Van Soom, A. Non-esterified fatty acids in follicular fluid of dairy cows and their effect on developmental capacity of bovine oocytes in vitro. *Reproduction* **2005**, *130*, 485–495. [CrossRef] [PubMed]
15. Revelli, A.; Piane, L.D.; Casano, S.; Molinari, E.; Massobrio, M.; Rinaudo, P. Follicular fluid content and oocyte quality: From single biochemical markers to metabolomics. *Reprod. Biol. Endocrinol.* **2009**, *7*, 1–13. [CrossRef] [PubMed]
16. Assidi, M.; Dieleman, S.J.; Sirard, M.A. Cumulus cells gene expression following the LH surge in bovine preovulatory follicles: Potential early markers of oocyte competence. *Reproduction* **2010**, *140*, 835–852. [CrossRef] [PubMed]
17. Warzych, E.; Cieslak, A.; Madeja, Z.E.; Pawlak, P.; Wolc, A.; Lechniak, D. Multifactorial Analysis of the Follicular Environment is Predictive of Oocyte Morphology in Cattle. *J. Reprod. Dev.* **2014**, *60*, 1–8. [CrossRef] [PubMed]
18. Matoba, S.; Bender, K.; Fahey, A.G.; Mamo, S.; Brennan, L.; Lonergan, P.; Fair, T. Predictive value of bovine follicular components as markers of oocyte developmental potential. *Reprod. Fertil. Dev.* **2014**, *26*, 337–345. [CrossRef] [PubMed]
19. Bunel, A.; Nivet, A.L.; Blondin, P.; Vigneault, C.; Richard, F.J.; Sirard, M.A. Cumulus cell gene expression associated with pre-ovulatory acquisition of developmental competence in bovine oocytes. *Reprod. Fertil. Dev.* **2014**, *26*, 855–865. [CrossRef] [PubMed]

20. Collado-Fernandez, E.; Picton, H.M.; Dumollard, R. Metabolism throughout follicle and oocyte development in mammals. *Int. J. Dev. Biol.* **2012**, *56*, 799–808. [CrossRef] [PubMed]
21. Ferguson, E.M.; Leese, H.J. A potential role for triglyceride as an energy source during bovine oocyte maturation and early embryo development. *Mol. Reprod. Dev.* **2006**, *73*, 1195–1201. [CrossRef] [PubMed]
22. Sutton-McDowall, M.L.; Gilchrist, R.B.; Thompson, J.G. The pivotal role of glucose metabolism in determining oocyte developmental competence. *Reproduction* **2010**, *139*, 685–695. [CrossRef] [PubMed]
23. Hashemi, H.F.; Goodman, J.M. The life cycle of lipid droplets. *Curr. Opin. Cell Biol.* **2015**, *33*, 119–124. [CrossRef] [PubMed]
24. Grummer, R.R.; Carroll, D.J. A review of lipoprotein cholesterol metabolism: Importance to ovarian function. *J. Anim. Sci.* **1988**, *66*, 3160–3173. [CrossRef] [PubMed]
25. Acosta, T.J.; Miyamoto, A.; Ozawa, T.; Wijayagunawardane, M.P.; Sato, K. Local release of steroid hormones, prostaglandin E2, and endothelin-1 from bovine mature follicles In vitro: Effects of luteinizing hormone, endothelin-1, and cytokines. *Biol. Reprod.* **1998**, *59*, 437–443. [CrossRef] [PubMed]
26. Nuttinck, F.; Gall, L.; Ruffini, S.; Laffont, L.; Clement, L.; Reinaud, P.; Adenot, P.; Grimard, B.; Charpigny, G.; Marquant-Le Guienne, B. PTGS2-Related PGE2 Affects Oocyte MAPK Phosphorylation and Meiosis Progression in Cattle: Late Effects on Early Embryonic Development. *Biol. Reprod.* **2011**. [CrossRef] [PubMed]
27. Van Meer, G.; Voelker, D.R.; Feigenson, G.W. Membrane lipids: Where they are and how they behave. *Nat. Rev. Mol. Cell Biol.* **2008**, *9*, 112–124. [CrossRef] [PubMed]
28. Fernandis, A.Z.; Wenk, M.R. Membrane lipids as signaling molecules. *Curr. Opin. Lipidol.* **2007**, *18*, 121–128. [CrossRef] [PubMed]
29. Sturmey, R.G.; Reis, A.; Leese, H.J.; McEvoy, T.G. Role of fatty acids in energy provision during oocyte maturation and early embryo development. *Reprod. Domest. Anim.* **2009**, *44* (Suppl. 3), 50–58. [CrossRef]
30. Uzbekova, S.; Elis, S.; Teixeira-Gomes, A.P.; Desmarchais, A.; Maillard, V.; Labas, V. MALDI Mass Spectrometry Imaging of Lipids and Gene Expression Reveals Differences in Fatty Acid Metabolism between Follicular Compartments in Porcine Ovaries. *Biology (Basel)* **2015**, *4*, 216–236. [CrossRef] [PubMed]
31. Campbell, D.I.; Ferreira, C.R.; Eberlin, L.S.; Cooks, R.G. Improved spatial resolution in the imaging of biological tissue using desorption electrospray ionization. *Anal. Bioanal. Chem.* **2012**, *404*, 389–398. [CrossRef] [PubMed]
32. Ferreira, C.R.; Saraiva, S.A.; Catharino, R.R.; Garcia, J.S.; Gozzo, F.C.; Sanvido, G.B.; Santos, L.F.A.; Lo Turco, E.G.; Pontes, J.H.F.; Basso, A.C.; et al. Single embryo and oocyte lipid fingerprinting by mass spectrometry. *J. Lipid Res.* **2010**, *51*, 1218–1227. [CrossRef] [PubMed]
33. Silva-Santos, K.; Ferreira, C.; Santos, G.; Eberlin, M.; Siloto, L.; Rosa, C.; Marcantonio, T.; Seneda, M. MALDI-MS Lipid Profiles of Oocytes Recovered by Ovum Pickup from Bos indicus and 1/2 indicus x taurus with High vs Low Oocyte Yields. *Reprod. Domest. Anim.* **2014**, *49*, 711–718. [CrossRef] [PubMed]
34. Bertevello, P.; Ghazouani, O.; Banliat, C.; Elis, S.; Teixeira-Gomes, A.P.; Maillard, V.; Labas, V.; Uzbekova, S. MALDI-TOF mass spectrometry analysis of lipids in single bovine oocytes during IVM. In Proceedings of the 32nd Scientific Meeting of the AETE, Barcelona, Spain, 9–10 September 2016; p. 712.
35. Sanchez-Lazo, L.; Brisard, D.; Elis, S.; Maillard, V.; Uzbekov, R.; Labas, V.; Desmarchais, A.; Papillier, P.; Monget, P.; Uzbekova, S. Fatty Acid synthesis and oxidation in cumulus cells support oocyte maturation in bovine. *Mol. Endocrinol.* **2014**, *28*, 1502–1521. [CrossRef] [PubMed]
36. Elis, S.; Oseikria, M.; Vitorino Carvalho, A.; Bertevello, P.S.; Corbin, E.; Teixeira-Gomes, A.P.; Lecardonnel, J.; Archilla, C.; Duranthon, V.; Labas, V.; et al. Docosahexaenoic acid mechanisms of action on the bovine oocyte-cumulus complex. *J. Ovarian Res.* **2017**, *10*, 74. [CrossRef] [PubMed]
37. Santos, P.H.; Fontes, P.K.; Franchi, F.F.; Nogueira, M.F.; Belaz, K.R.; Tata, A.; Eberlin, M.N.; Sudano, M.J.; Barros, C.M.; Castilho, A.C. Lipid profiles of follicular fluid from cows submitted to ovarian superstimulation. *Theriogenology* **2017**, *94*, 64–70. [CrossRef] [PubMed]
38. Lafontan, M.; Langin, D. Lipolysis and lipid mobilization in human adipose tissue. *Prog. Lipid Res.* **2009**, *48*, 275–297. [CrossRef] [PubMed]
39. Nguyen, P.; Leray, V.; Diez, M.; Serisier, S.; Le Bloc'h, J.; Siliart, B.; Dumon, H. Liver lipid metabolism. *J. Anim. Physiol. Anim. Nutr. (Berl.)* **2008**, *92*, 272–283. [CrossRef] [PubMed]
40. Santos, C.R.; Schulze, A. Lipid metabolism in cancer. *FEBS J.* **2012**, *279*, 2610–2623. [CrossRef] [PubMed]

41. Chmurzynska, A. The multigene family of fatty acid-binding proteins (FABPs): Function, structure and polymorphism. *J. Appl. Genet.* **2006**, *47*, 39–48. [CrossRef] [PubMed]
42. Dunning, K.R.; Russell, D.L.; Robker, R.L. Lipids and oocyte developmental competence: The role of fatty acids and B-oxidation. *Reproduction* **2014**, *148*, R15–R27. [CrossRef] [PubMed]
43. Auclair, S.; Uzbekov, R.; Elis, S.; Sanchez, L.; Kireev, I.; Lardic, L.; Dalbies-Tran, R.; Uzbekova, S. Absence of cumulus cells during in vitro maturation affects lipid metabolism in bovine oocytes. *Am. J. Physiol. Endocrinol. Metab.* **2013**, *304*, E599–E613. [CrossRef] [PubMed]
44. Paczkowski, M.; Silva, E.; Schoolcraft, W.B.; Krisher, R.L. Comparative Importance of Fatty Acid Beta-Oxidation to Nuclear Maturation, Gene Expression, and Glucose Metabolism in Mouse, Bovine, and Porcine Cumulus Oocyte Complexes. *Biol. Reprod.* **2013**, *88*, 111. [CrossRef] [PubMed]
45. Van Hoeck, V.; Leroy, J.L.; Arias-Alvarez, M.; Rizos, D.; Gutierrez-Adan, A.; Schnorbusch, K.; Bols, P.E.; Leese, H.J.; Sturmey, R.G. Oocyte developmental failure in response to elevated non-esterified fatty acid concentrations: Mechanistic insights. *Reproduction* **2013**, *145*, 33–44. [CrossRef] [PubMed]
46. Elis, S.; Desmarchais, A.; Maillard, V.; Uzbekova, S.; Monget, P.; Dupont, J. Cell proliferation and progesterone synthesis depend on lipid metabolism in bovine granulosa cells. *Theriogenology* **2015**, *83*, 840–853. [CrossRef] [PubMed]
47. Aardema, H.; van Tol, H.T.A.; Wubbolts, R.W.; Brouwers, J.; Gadella, B.M.; Roelen, B.A.J. Stearoyl-CoA desaturase activity in bovine cumulus cells protects the oocyte against saturated fatty acid stress. *Biol. Reprod.* **2017**, *96*, 982–992. [CrossRef] [PubMed]
48. Lonergan, P.; Rizos, D.; Gutierrez-Adan, A.; Fair, T.; Boland, M.P. Oocyte and embryo quality: Effect of origin, culture conditions and gene expression patterns. *Reprod. Domest. Anim.* **2003**, *38*, 259–267. [CrossRef] [PubMed]
49. Tata, A.; Sudano, M.J.; Santos, V.G.; Landim-Alvarenga, F.D.; Ferreira, C.R.; Eberlin, M.N. Optimal single-embryo mass spectrometry fingerprinting. *J. Mass Spectrom.* **2013**, *48*, 844–849. [CrossRef] [PubMed]
50. Apparicio, M.; Ferreira, C.R.; Tata, A.; Santos, V.G.; Alves, A.E.; Mostachio, G.Q.; Pires-Butler, E.A.; Motheo, T.F.; Padilha, L.C.; Pilau, E.J.; et al. Chemical Composition of Lipids Present in Cat and Dog Oocyte by Matrix-Assisted Desorption Ionization Mass Spectrometry (MALDI- MS). *Reprod. Domest. Anim.* **2012**, *47*, 113–117. [CrossRef] [PubMed]
51. Fair, T.; Hyttel, P.; Greve, T. Bovine oocyte diameter in relation to maturational competence and transcriptional activity. *Mol. Reprod. Dev.* **1995**, *42*, 437–442. [CrossRef] [PubMed]
52. Gilchrist, R.B.; Ritter, L.J.; Armstrong, D.T. Oocyte-somatic cell interactions during follicle development in mammals. *Anim. Reprod. Sci.* **2004**, *82–83*, 431–446. [CrossRef] [PubMed]
53. Binelli, M.; Murphy, B.D. Coordinated regulation of follicle development by germ and somatic cells. *Reprod. Fertil. Dev.* **2010**, *22*, 1–12. [CrossRef] [PubMed]
54. Lolicato, F.; Brouwers, J.F.; de Lest, C.H.; Wubbolts, R.; Aardema, H.; Priore, P.; Roelen, B.A.; Helms, J.B.; Gadella, B.M. The cumulus cell layer protects the bovine maturing oocyte against fatty acid-induced lipotoxicity. *Biol. Reprod.* **2015**, *92*, 16. [CrossRef] [PubMed]
55. Guerreiro, T.M.; Gonçalves, R.F.; Melo, C.F.O.R.; de Oliveira, D.N.; Lima, E.d.O.; Visintin, J.A.; de Achilles, M.A.; Catharino, R.R. A Metabolomic Overview of Follicular Fluid in Cows. *Front. Vet. Sci.* **2018**, *5*, 1–9. [CrossRef] [PubMed]
56. Drzazga, A.; Sowinska, A.; Koziolkiewicz, M. Lysophosphatidylcholine and lysophosphatidylinosiol–novel promissing signaling molecules and their possible therapeutic activity. *Acta Pol. Pharm.* **2014**, *71*, 887–899. [PubMed]
57. Sohel, M.M.; Hoelker, M.; Noferesti, S.S.; Salilew-Wondim, D.; Tholen, E.; Looft, C.; Rings, F.; Uddin, M.J.; Spencer, T.E.; Schellander, K.; et al. Exosomal and Non-Exosomal Transport of Extra-Cellular microRNAs in Follicular Fluid: Implications for Bovine Oocyte Developmental Competence. *PLoS ONE* **2013**, *8*, e78505. [CrossRef] [PubMed]
58. Skotland, T.; Sandvig, K.; Llorente, A. Lipids in exosomes: Current knowledge and the way forward. *Prog. Lipid Res.* **2017**, *66*, 30–41. [CrossRef] [PubMed]
59. Zemski Berry, K.A.; Murphy, R.C.; Kosmider, B.; Mason, R.J. Lipidomic characterization and localization of phospholipids in the human lung. *J. Lipid Res.* **2017**, *58*, 926–933. [CrossRef] [PubMed]
60. Young, J.M.; McNeilly, A.S. Theca: The forgotten cell of the ovarian follicle. *Reproduction* **2010**, *140*, 489–504. [CrossRef] [PubMed]

61. Tanghe, S.; Van Soom, A.; Nauwynck, H.; Coryn, M.; De Kruif, A. Minireview: Functions of the Cumulus Oophorus during oocyte maturation, ovulation and fertilization. *Mol. Reprod. Dev.* **2002**, *61*, 414–424. [CrossRef] [PubMed]
62. Bertevello, P.; Banliat, C.; Teixeira Gomes, A.P.; Elis, S.; Maillard, V.; Carvalho, A.; Duranthon, V.; Labas, V.; Uzbekova, S. Comparison of lipid profiles and gene expression in granulosa and cumulus cells in bovine. In Proceedings of the 33rd Annual Meeting of the European Embryo Transfer Association (AETE), Bath, UK, 8–9 September 2017; p. 970.
63. Borgbo, T.; Povlsen, B.B.; Andersen, C.Y.; Borup, R.; Humaidan, P.; Grondahl, M.L. Comparison of gene expression profiles in granulosa and cumulus cells after ovulation induction with either human chorionic gonadotropin or a gonadotropin-releasing hormone agonist trigger. *Fertil. Steril.* **2013**, *100*, 994–1001. [CrossRef] [PubMed]
64. Wen, X.; Kuang, Y.; Zhou, L.; Yu, B.; Chen, Q.; Fu, Y.; Yan, Z.; Guo, H.; Lyu, Q.; Xie, J.; et al. Lipidomic Components Alterations of Human Follicular Fluid Reveal the Relevance of Improving Clinical Outcomes in Women Using Progestin-Primed Ovarian Stimulation Compared to Short-Term Protocol. *Med. Sci. Monit.* **2018**, *24*, 3357–3365. [CrossRef] [PubMed]
65. Montani, D.A.; Cordeiro, F.B.; Regiani, T.; Victorino, A.B.; Pilau, E.J.; Gozzo, F.C.; Ferreira, C.R.; Fraietta, R.; Lo Turco, E.G. The follicular microenviroment as a predictor of pregnancy: MALDI-TOF MS lipid profile in cumulus cells. *J. Assist. Reprod. Genet.* **2012**, *29*, 1289–1297. [CrossRef] [PubMed]
66. Bao, B.; Garverick, H.A. Expression of steroidogenic enzyme and gonadotropin receptor genes in bovine follicles during ovarian follicular waves: A review. *J. Anim. Sci.* **1998**, *76*, 1903–1921. [CrossRef] [PubMed]
67. Su, Y.Q.; Sugiura, K.; Wigglesworth, K.; O'Brien, M.J.; Affourtit, J.P.; Pangas, S.A.; Matzuk, M.M.; Eppig, J.J. Oocyte regulation of metabolic cooperativity between mouse cumulus cells and oocytes: BMP15 and GDF9 control cholesterol biosynthesis in cumulus cells. *Development* **2008**, *135*, 111–121. [CrossRef] [PubMed]
68. Shao, W.; Espenshade, P.J. Expanding roles for SREBP in metabolism. *Cell Metab.* **2012**, *16*, 414–419. [CrossRef] [PubMed]
69. Singh, P.; Amin, M.; Keller, E.; Simerman, A.; Aguilera, P.; Briton-Jones, C.; Hill, D.L.; Abbott, D.H.; Chazenbalk, G.; Dumesic, D.A. A novel approach to quantifying ovarian cell lipid content and lipid accumulation in vitro by confocal microscopy in lean women undergoing ovarian stimulation for in vitro fertilization (IVF). *J. Assist. Reprod. Genet.* **2013**, *30*, 733–740. [CrossRef] [PubMed]
70. Aardema, H.; Vos, P.L.; Lolicato, F.; Roelen, B.A.; Knijn, H.M.; Vaandrager, A.B.; Helms, J.B.; Gadella, B.M. Oleic acid prevents detrimental effects of saturated fatty acids on bovine oocyte developmental competence. *Biol. Reprod.* **2011**, *85*, 62–69. [CrossRef] [PubMed]
71. Aardema, H.; Lolicato, F.; van de Lest, C.H.A.; Brouwers, J.F.; Vaandrager, A.B.; van Tol, H.T.A.; Roelen, B.A.J.; Vos, P.L.A.M.; Helms, J.B.; Gadella, B.M. Bovine Cumulus Cells Protect Maturing Oocytes from Increased Fatty Acid Levels by Massive Intracellular Lipid Storage. *Biol. Reprod.* **2013**, *88*, 164. [CrossRef] [PubMed]
72. Leroy, J.L.; Vanholder, T.; Delanghe, J.R.; Opsomer, G.; Van Soom, A.; Bols, P.E.; de Kruif, A. Metabolite and ionic composition of follicular fluid from different-sized follicles and their relationship to serum concentrations in dairy cows. *Anim. Reprod. Sci.* **2004**, *80*, 201–211. [CrossRef]
73. Gautier, T.; Becker, S.; Drouineaud, V.; Ménétrier, F.; Sagot, P.; Nofer, J.-R.; von Otte, S.; Lagrost, L.; Masson, D.; Tietge, U.J.F. Human luteinized granulosa cells secrete apoB100-containing lipoproteins. *J. Lipid Res.* **2010**, *51*, 2245–2252. [CrossRef] [PubMed]
74. Serna, J.; García-Seisdedos, D.; Alcázar, A.; Lasunción, M.Á.; Busto, R.; Pastor, Ó. Quantitative lipidomic analysis of plasma and plasma lipoproteins using MALDI-TOF mass spectrometry. *Chem. Phys. Lipids.* **2015**. [CrossRef] [PubMed]
75. Osz, K.; Ross, M.; Petrik, J. The thrombospondin-1 receptor CD36 is an important mediator of ovarian angiogenesis and folliculogenesis. *Reprod. Biol. Endocrinol.* **2014**, *12*, 21. [CrossRef] [PubMed]
76. Trigatti, B.; Rigotti, A.; Krieger, M. The role of the high-density lipoprotein receptor SR-BI in cholesterol metabolism. *Curr. Opin. Lipidol.* **2000**, *11*, 123–131. [CrossRef] [PubMed]
77. Di Pietro, C. Exosome-mediated communication in the ovarian follicle. *J. Assist. Reprod. Genet.* **2016**, *33*, 303–311. [CrossRef] [PubMed]
78. Record, M.; Silvente-Poirot, S.; Poirot, M.; Wakelam, M.J.O. Extracellular vesicles: Lipids as key components of their biogenesis and functions. *J. Lipid Res.* **2018**, *59*, 1316–1324. [CrossRef] [PubMed]

79. Hermann, M.; Lindstedt, K.A.; Foisner, R.; Morwald, S.; Mahon, M.G.; Wandl, R.; Schneider, W.J.; Nimpf, J. Apolipoprotein A-I production by chicken granulosa cells. *FASEB J.* **1998**, *12*, 897–903. [CrossRef] [PubMed]
80. Choi, D.H.; Lee, W.S.; Won, M.; Park, M.; Park, H.O.; Kim, E.; Lee, K.A.; Bae, J. The apolipoprotein A-I level is downregulated in the granulosa cells of patients with polycystic ovary syndrome and affects steroidogenesis. *J. Proteome Res.* **2010**, *9*, 4329–4336. [CrossRef] [PubMed]
81. Bogan, R.L.; Hennebold, J.D. The reverse cholesterol transport system as a potential mediator of luteolysis in the primate corpus luteum. *Reproduction* **2010**, *139*, 163–176. [CrossRef] [PubMed]
82. Labas, V.; Teixeira-Gomes, A.P.; Bouguereau, L.; Gargaros, A.; Spina, L.; Marestaing, A.; Uzbekova, S. Intact cell MALDI-TOF mass spectrometry on single bovine oocyte and follicular cells combined with top-down proteomics: A novel approach to characterise markers of oocyte maturation. *J. Proteomics* **2018**, *175*, 56–74. [CrossRef] [PubMed]
83. Labas, V.; Teixeira-Gomes, A.P.; Bouguereau, L.; Gargaros, A.; Spina, L.; Marestaing, A.; Uzbekova, S. Data on endogenous bovine ovarian follicular cells peptides and small proteins obtained through Top-down High Resolution Mass Spectrometry. *Data Brief* **2017**, *13*, 175–179. [CrossRef] [PubMed]
84. Peddinti, D.; Memili, E.; Burgess, S.C. Proteomics-based systems biology modeling of bovine germinal vesicle stage oocyte and cumulus cell interaction. *PLoS ONE* **2010**, *5*, e11240. [CrossRef] [PubMed]
85. Wahli, W.; Michalik, L. PPARs at the crossroads of lipid signaling and inflammation. *Trends Endocrinol. Metab.* **2012**, *23*, 351–363. [CrossRef] [PubMed]
86. Zheng, W.; Kollmeyer, J.; Symolon, H.; Momin, A.; Munter, E.; Wang, E.; Kelly, S.; Allegood, J.C.; Liu, Y.; Peng, Q.; et al. Ceramides and other bioactive sphingolipid backbones in health and disease: Lipidomic analysis, metabolism and roles in membrane structure, dynamics, signaling and autophagy. *Biochim. Biophys. Acta* **2006**, *1758*, 1864–1884. [CrossRef] [PubMed]
87. Hannun, Y.A.; Obeid, L.M. Principles of bioactive lipid signalling: Lessons from sphingolipids. *Nat. Rev. Mol. Cell Biol.* **2008**, *9*, 139–150. [CrossRef] [PubMed]
88. Del Collado, M.; Da Silveira, J.C.; Sangalli, J.R.; Andrade, G.M.; Sousa, L.R.D.S.; Silva, L.A.; Meirelles, F.V.; Perecin, F. Fatty Acid Binding Protein 3 and Transzonal Projections Are Involved in Lipid Accumulation during in vitro Maturation of Bovine Oocytes. *Sci. Rep.* **2017**, *7*. [CrossRef] [PubMed]
89. Bettegowda, A.; Smith, G.W. Mechanisms of maternal mRNA regulation: Implications for mammalian early embryonic development. *Front. Biosci.* **2007**, *12*, 3713–3726. [CrossRef] [PubMed]
90. Hyttel, P.F.T.C.H.; Greve, T. Oocyte growth, capacitation and final maturartion in cattle. *Theriogenology* **1997**, *47*, 23–32. [CrossRef]
91. Warzych, E.; Pawlak, P.; Pszczola, M.; Cieslak, A.; Lechniak, D. Prepubertal heifers versus cows—The differences in the follicular environment. *Theriogenology* **2017**, *87*, 36–47. [CrossRef] [PubMed]
92. Warzych, E.; Pawlak, P.; Pszczola, M.; Cieslak, A.; Madeja, Z.E.; Lechniak, D. Interactions of bovine oocytes with follicular elements with respect to lipid metabolism. *Anim. Sci. J.* **2017**, *88*, 1491–1497. [CrossRef] [PubMed]
93. Sanders, J.R.; Jones, K.T. Regulation of the meiotic divisions of mammalian oocytes and eggs. *Biochem. Soc. Trans.* **2018**, *46*, 797–806. [CrossRef] [PubMed]
94. Tomek, W.; Torner, H.; Kanitz, W. Comparative analysis of protein synthesis, transcription and cytoplasmic polyadenylation of mRNA during maturation of bovine oocytes in vitro. *Reprod. Domest. Anim.* **2002**, *37*, 86–91. [CrossRef] [PubMed]
95. Fair, T.; Carter, F.; Park, S.; Evans, A.C.; Lonergan, P. Global gene expression analysis during bovine oocyte in vitro maturation. *Theriogenology* **2007**, *68* (Suppl. 1), S91–S97. [CrossRef]
96. Thelie, A.; Papillier, P.; Perreau, C.; Uzbekova, S.; Hennequet Antier, C.; Dalbies Tran, R. Regulation of bovine oocyte-specific transcripts during in vitro oocyte maturation and after maternal–embryonic transition analyzed using a transcriptomic approach. *Mol. Reprod. Dev.* **2009**, *76*, 773–782. [CrossRef] [PubMed]
97. Graf, A.; Krebs, S.; Heininen-Brown, M.; Zakhartchenko, V.; Blum, H.; Wolf, E. Genome activation in bovine embryos: Review of the literature and new insights from RNA sequencing experiments. *Anim. Reprod. Sci.* **2014**, *149*, 46–58. [CrossRef] [PubMed]
98. Fowler, S.D.; Greenspan, P. Application of Nile red, a fluorescent hydrophobic probe, for the detection of neutral lipid deposits in tissue sections: Comparison with oil red O. *J. Histochem. Cytochem.* **1985**, *33*, 833–836. [CrossRef] [PubMed]

99. Folch, J.; Lees, M.; Stanley, S. A simple method for the isolation and purification of total lipides from animal tissues. *J. biol. Chem.* **1957**, *226*, 497–509. [PubMed]
100. Bligh, E.G.; Dyer, W.J. A Rapid Method of Total Lipid Extraction and Purification. *Can. J. Biochem. Physiol.* **1959**, *37*, 911–917. [CrossRef] [PubMed]
101. Southam, A.D.; Weber, R.J.; Engel, J.; Jones, M.R.; Viant, M.R. A complete workflow for high-resolution spectral-stitching nanoelectrospray direct-infusion mass-spectrometry-based metabolomics and lipidomics. *Nat. Protoc.* **2016**, *12*, 310–328. [CrossRef] [PubMed]
102. Koelmel, J.P.; Kroeger, N.M.; Ulmer, C.Z.; Bowden, J.A.; Patterson, R.E.; Cochran, J.A.; Beecher, C.W.W.; Garrett, T.J.; Yost, R.A. LipidMatch: An automated workflow for rule-based lipid identification using untargeted high-resolution tandem mass spectrometry data. *BMC Bioinform.* **2017**, *18*, 331. [CrossRef] [PubMed]
103. Chen, E.Y.; Tan, C.M.; Kou, Y.; Duan, Q.; Wang, Z.; Meirelles, G.V.; Clark, N.R.; Ma'ayan, A. Enrichr: Interactive and collaborative HTML5 gene list enrichment analysis tool. *BMC Bioinform.* **2013**, *14*, 128. [CrossRef] [PubMed]



© 2018 by the authors. Licensee MDPI, Basel, Switzerland. This article is an open access article distributed under the terms and conditions of the Creative Commons Attribution (CC BY) license (http://creativecommons.org/licenses/by/4.0/).

RESULTS (2)

2. Espèces lipidiques dans les cellules et le liquide folliculaire des follicules de différentes tailles

2.1 Article 2

Bertevello PS, Teixeira-Gomes AP, Labas V, Cordeiro LAV, Blache MC, Duranthon V, Papillier P, and Uzbekova S. . Drastic changes of lipid composition occurs in follicular fluid but not in the enclosed oocyte during final growth of bovine follicle (*to be submitted in Molecular Reproduction and Development)*

Dans les ovaires de mammifères, à chaque cycle, la plupart des follicules meurent et seuls quelques-uns deviennent dominants et peuvent ovuler. La croissance folliculaire nécessite beaucoup d'énergie, qui est produite par les cellules folliculaires à partir de différents substrats énergétiques, y compris les acides gras (AG). Les cellules somatiques folliculaires ovariennes et l'ovocyte possèdent une machinerie moléculaire pour métaboliser des AG afin de produire de l'énergie ou mettre des lipides en réserve. Dans les biotechnologies de la reproduction chez les bovins, les ovocytes issus de grands follicules sont considérés plus compétents pour le développement des embryons *in vitro*, comparés aux follicules de plus petite taille.

L'objectif de notre étude était d'élucider la spécificité de la composition lipidique et du métabolisme des AG dans les follicules de tailles différentes. L'imagerie par spectrométrie de masse de type MALDI-TOF, a permis de cartographier 281 espèces lipidiques dans les compartiments ovariens. Par analyse des lipides par fluorescence (*Nile Red*), nous avons démontré la distribution différentielle des lipides neutres dans les cellules de la granulosa (CG) et de la thèque (TH) en fonction de la taille des follicules. Les empreintes lipidiques des cellules folliculaires isolées et des fluides folliculaires de petits (PF, taille moyenne 5 mm) et de grands follicules (GF, taille moyenne de 13 mm) ont révélé des modifications importantes de leur lipidomes. Plus de 55% des lipides détectés dans les liquides folliculaires ont présenté une variation de plus de deux fois entre GF et PF ($p < 0,05$). Les cellules de la thèque (TH), granulosa (CG) et cumulus (CC) étaient également affectées par la taille folliculaire (environ 5%, 15% et 10% des lipides variaient, respectivement). Au contraire, les ovocytes présentaient moins de 2% de lipides différentiels entre GF et PF.

17% des lipides différentiels ont été identifiés et ont révélé des changements principalement dans les lipides membranaires, à la fois dans les cellules folliculaires somatiques et dans les liquides folliculaires. L'analyse de l'expression de 18 gènes-candidats dans les TH et CG suggère une augmentation significative de la bêta-oxydation des AG et du stress oxydatif dans les GF. Par conséquence, le métabolisme des AG dans les cellules folliculaires se modifie au cours de la croissance folliculaire et change de manière spectaculaire la composition lipidique du liquide folliculaire. La distribution et l'abondance différentielle des lipides peuvent être impliquées dans les processus qui guident les follicules soit vers l'atrésie, soit vers la dominance.

2 Lipid species in follicular cells and fluid in bovine follicles of different sizes

2.1 Article 2

Bertevello PS, Teixeira-Gomes AP, Labas V, Cordeiro LAV, Blache MC, Duranthon V, Papillier P, and Uzbekova S. . Drastic changes of lipid composition occurs in follicular fluid but not in the enclosed oocyte during final growth of bovine follicle (*to be submitted in Molecular Reproduction and Development)*

Abstract.

In mammalian ovary, each cycle among the numerous antral follicles only few become dominant and designated to ovulate. Follicular growth requires a lot of energy, which is produced by follicular cells from different energy substrates, including fatty acids (FA). Ovarian follicular somatic cells and oocyte possess molecular machinery to metabolize FA to produce either energy or lipid storage. In bovine biotechnologies, oocytes from the large follicles are more competent to embryo *in vitro* development compared to small one. The objective of our study was to elucidate specificity of lipid composition and FA metabolism in antral bovine follicles of different size. MALDI-TOF mass spectrometry (MS) imaging allowed the mapping 281 lipid features to ovarian compartments Lipid analysis using Nile Red demonstrated size-dependent differential distribution of neutral lipids in granulosa (GC) and theca (TH) cell layers. Lipid fingerprints of isolated follicular cells and fluid of small (SF, mean size 5 mm) and large follicles (LF, mean size 13 mm) acquired by MALDI-TOF MS revealed drastic changes in follicular fluid lipidome (more than 55% of detected features varied more than two-fold between LF and SF, $p<0.05$). TH, GC and cumulus cells were also affected by follicular size (about 5%, 15% and 10% of lipids varied, respectively) in contrast to oocytes that showed less than 2% of lipids varied. 17% of differential lipids were identified and revealed the major changes in membrane lipids both in somatic follicular cells and FF. Gene expression analysis of 18 candidate genes in TH and GC suggest significant increase of FA beta-oxidation and oxidative stress, respectively, in LF compare to SF. Therefore, FA metabolism in follicular cells changes through follicular growth and significantly modulates follicular fluid lipid composition. Differential distribution and abundance of lipids including signaling molecules may thus influence follicular atresia or dominance.

Article

Lipid species in follicular cells and fluid in bovine follicles of different sizes.

Priscila Silvana Bertevello [1], Ana-Paula Teixeira-Gomes [2,3], Valérie Labas [1,3], Luiz Augusto Vieira Cordeiro [1], Marie-Claire Blache [1], Pascal Papillier [1], *Virginie Maillard [1], Sebastien Elis [1]* and Svetlana Uzbekova [1,3,*]

UMR PRC, INRA 85, CNRS 7247, Université de Tours, IFCE, 37380 Nouzilly, France;
priscila.bertevello@inra.fr (P.S.B.); ana-paula.teixeira@inra.fr (A.-P.T.); valerie.labas@inra.fr (V.L.);
Luiz-Augusto.Viera-Cordeiro@inra.fr (L.A.V.C.); marie-claire.blache@inra.fr (M.-C.B.);
pascal.papillier@inra.fr (P.P.); virginie.maillard@inra.fr (V.M.); sebastien.elis@inra.fr (S.E.)
UMR ISP, INRA 1282, Université de Tours, 37380 Nouzilly, France;
PAIB (Pôle d'Analyse et d'Imagerie des Biomolécules), Plate-forme CIRE (Chirurgie et Imagerie pour la Recherche et l'Enseignement, INRA, Université de Tours, CHRU de Tours, 37380 Nouzilly, France
* Correspondence: svetlana.uzbekova@inra.fr; Tel.: +33-247-427-951

Received:

Abstract:

In mammalian ovary, each cycle among the numerous antral follicles only few become dominant and designated to ovulate. Follicular growth requires a lot of energy, which is produced by follicular cells from different energy substrates, including fatty acids (FA). Ovarian follicular somatic cells and oocyte possess molecular machinery to metabolize FA to produce either energy or lipid storage. In bovine biotechnologies, oocytes from the large follicles are more competent to embryo in vitro development compared to small one. The objective of our study was to elucidate specificity of lipid composition and FA metabolism in antral bovine follicles of different size. MALDI-TOF mass spectrometry (MS) imaging allowed the mapping 281 lipid features to ovarian compartments Lipid analysis using Nile Red demonstrated size-dependent differential distribution of neutral lipids in granulosa (GC) and theca (TH) cell layers. Lipid fingerprints of isolated follicular cells and fluid of small (SF, mean size 5 mm) and large follicles (LF, mean size 13 mm) acquired by MALDI-TOF MS revealed drastic changes in follicular fluid lipidome (more than 55% of detected features varied more than two-fold between LF and SF, $p<0.05$). TH, GC and cumulus cells were also affected by follicular size (about 5%, 15% and 10% of lipids varied, respectively) in contrast to oocytes that showed less than 2% of lipids varied. 17% of differential lipids were identified and revealed the major changes in membrane lipids both in somatic follicular cells and FF. Gene expression analysis of 18 candidate genes in TH and GC suggest significant increase of FA beta-oxidation and oxidative stress, respectively, in LF compare to SF. Therefore, FA metabolism in follicular cells changes through follicular growth and significantly modulates follicular fluid lipid composition. Differential distribution and abundance of lipids including signaling molecules may thus influence follicular atresia or dominance.

Keywords: Lipid metabolism, FA metabolism, follicle-size, mass spectrometry

1. Introduction

A close relationship between the oocyte quality and follicular size has been widely reported; *in vivo*, only large dominant follicles may ovulate; and in bovine biotechnologies, the oocytes from the larger follicles were globally more competent for *in vitro* embryo development than from the smaller ones (Blondin and Sirard 1995; Arlotto et al. 1996; Humblot et al. 2005; Anchamparuthy et al. 2009). Follicular growth is accompanied by morphological, metabolic and biochemical changes of follicular compartments. The granulosa cells (GC) multiply, the antral cavity filled with more follicular fluid (FF). During the folliculogenesis, an oocyte enlarges substantially its size and a part of surrounding GC differentiates into cumulus cells (CC). Specialized stromal layers, the internal and external theca, develop out of the follicular basal lamina. The internal theca (iTH) is composed of capillaries, fibroblasts, immune cells and specialized steroidogenic cells (Young and McNeilly 2010). In antral follicles, somatic cells begin to produce hormones and uptake large amounts of lipids and cholesterol from plasma (Irving-Rodgers et al. 2002). At that stage, follicular growth depends largely on lipid metabolism (Collado-Fernandez, Picton, and Dumollard 2012) and is under the influence of follicle-stimulating hormone (FSH) (Mihm and Bleach 2003). GC only mature in steroidogenic cells during the last 5% of their follicular development, within the weeks leading up to ovulation (Bao and Garverick 1998). At this stage, GC develop the ability to convert androgen-derived of theca into estrogens and GC increased production of estradiol through follicular growth (Hillier 1994; Tajima et al. 2007). Only a few from a cohort of small follicles become dominant and may ovulate whereas most of them disappeared through atresia, where activation of caspase-3 is involved in induction of apoptosis (Namura et al. 1998). Oxidative stress enhances GC death in atretic follicles (H. Yang et al. 2017; Zhang et al. 2014), however there is evidence of framework reversal mediated by antioxidant enzymes released by exosomes (Saeed-Zidane et al. 2017).

The metabolic activity changes significantly during final follicle growth. Transcriptomic analysis performed on GC (Hatzirodos, Hummitzsch, Irving-rodgers, et al. 2014) and theca internal (Hatzirodos, Hummitzsch, Irving-Rodgers, et al. 2014) of small and large (dominant) follicles showed significant differences in gene expression involved in lipid metabolism and related to increased steroidogenic capacity of larger follicles. A number of new markers of antral follicle growth was therefore identified (Hatzirodos et al. 2015). Also, concentrations of cholesterol and triglycerides in follicular fluid (FF) changed from small to large follicles in dairy cows (J.L.M.R Leroy, Vanholder, Delanghe, Opsomer, Van Soom, Bols, Dewulf, et al. 2004).

In ovarian follicular growth, lipid metabolism plays fundamental role; lipids constitute energy supply and involved in steroid production, they are also building blocks for membranes and signalization. Changes in the location and intensity of various lipids, including phosphatidylinositol (PI 38: 4) and arachidonic acid (C20: 4), were observed in the ovary of mice, between the pre-ovulated and post-ovulated stages (Campbell et al. 2012). In bovine, using matrix-assisted laser desorption/ionization time-of-flight mass spectrometry (MALDI-TOF MS) and mass spectrometry imaging (MSI), specific lipids were characterized in different compartments of antral follicles including GC, theca, CC, oocyte and FF (Bertevello et al. 2018).

The objective of this study was to compare lipid composition between the large and small follicles within the same ovary in cows and therefore enlighten the differences in follicular environment enclosing the oocytes with different developmental potential. Analysis of lipids by MALDI MS profiling of oocytes, FF, CC, GC and TH cells in follicles of different size was complemented with expression analysis of several lipid metabolism related genes.

2. Materials and Methods

2.1 Ethics

No experiments on live animals were performed; bovine ovaries were obtained from a local commercial slaughterhouse.

2.2 Chemicals

Unless indicated, all of the chemicals were purchased from Sigma-Aldrich (Saint-Quentin Fallavier, France).

2.3. Biological Materials

Twelve bovine ovaries were transported from a commercial slaughterhouse on ice. Follicle sizes were carefully determined with a caliper rule. The largest and several smaller follicles were isolated from each ovary, measured and photographed. Twenty-four individual follicles of different size (3-20 mm) were dissected in order to separate FF, scraping off granulosa and theca cell layers. An aliquot of FF was clarified by centrifugation (for 10 min 5000g at 4°C), FF supernatant was snap-frozen in liquid nitrogen. GC and TH layers were put into separate tubes with sterile cold phosphate buffered saline (PBS), centrifuged (for 10 min 5000g at 4°C), and then the pellets were washed twice in Tris-Sucrose buffer (260mM sucrose 20mM Tris-HCl pH6.8; TRIS-S). Samples were snap-frozen in liquid nitrogen. Cumulus– oocyte complexes (COC) from a total of 24 ovaries were aspirated - 12 small follicles (SF, 4–6 mm in diameter) and 12 large follicles (LF, >8 mm in diameter) separately - using a 21-gauge needle attached to a 1 or 5 mL syringe, and collected fluids were allocated to independent 15 mL conical tubes for each follicle size. COC with several CC layers were selected. The individual oocytes were separated from their cumulus cells (CC) and rinsed twice in TRIS-Sucrose buffer (Tris-S), and then frozen. The CC were washed in sterile PBS and centrifuged (for 10 min 5000g at 4°C), and the pellets were washed twice in TRIS-S. All samples were snap-frozen in liquid nitrogen and kept at -80°C to analyze within no longer than 4 days.

For qPCR analysis, GC and TH cells from 12 individual follicles per group (SF and LF) were collected and kept in Trizol reagent (Invitrogen, Cergy Pontoise, France) at -80°C for RNA extraction.

For Nile Red Fluorescence staining (NRF), immunohistochemistry (IHC), and mass spectrometry imaging (MSI) analysis, whole ovaries were frozen in nitrogen stream from ovarian sections, and the cuts were made within no longer than four days after for lipid analysis.

2.4 Nile Red Fluorescence

Nile Red staining in bovine ovary sections was mainly performed as described (Bertevello et al. 2018). Briefly, freshly frozen bovine ovaries were cut in 10 µm sections using cryostat (MICROM NX70, Walldorf, Germany) at –18°C. Frozen sections were mounted onto Superfrost ®Plus slides (Thermo Scientific, Villebon sur Yvette, France) and air dried for 10 min. Slides were fixed in 4% (v/v) of paraformaldehyde during 2 min, and then washed in water during 5 min at room temperature. The slides were incubated in 500 ng/µl Nile red (NR) (Sigma Aldrich, St Louis, USA) water solution for 1 hour at room temperature, after washed 5 min in water and mounted in Moveol solution complemented with 1 µG/mL of 4',6-Diamidine-2'-phenylindole dihydrochloride (DAPI). Nile Red Fluorescence (NRF) was used to localize and quantitate neutral lipids, and sequential ovary slides were stained by hematoxylin-eosin for precise identification of histological structures.

The slides were scanned using AxioScan.Z1 scanner (Carl Zeiss SAS, German) at 20x/0.8 magnification. Specific filters were used to detect blue DAPI fluorescence (excitation and emission wavelength were 335-383 nm and 420-470 nm, respectively) and NRF (excitation 538-562nm and emission 570-640 nm). The exposure time were used for all the slides were 50ms to DAPI and 35ms to NRF. Each image was analyzed using Zen Blue version 6.1.7601 software (Carl Zeiss Microscopy GmbH, German). The intensity of fluorescence of NRF and DAPI were measured in three regions of interest (ROI) located to external theca (eTH), internal theca (iTH) and granulosa cell (GC) layers, representing about 2mm² ROI per compartment. Background was subtracted from DAPI and NRF intensity value, respectively, and then resulted value was normalized by cells number in each ROI. NRF intensity in ovarian sections was explored on the surface of each follicular cell compartment, internal and external tissue layers and granulosa cells (iTH, eTH and GC); NRF values were normalized by the mean intensity of the NRF in each ovarian section. For statistical analysis, 43 follicles from 13 ovaries were grouped by size: diameter from 0.66 to 1.16 mm (group F1, 0.88 ± 0.08 mm, n=6); 1.8 to 2.6 mm (group F2, 2.27 ± 0.12 mm, n=6); 3.6 to 4.8 mm (F3, 4.05 ± 0.12 mm, n=11); 5.0 to 7.2 mm (F4, 6.06 ± 0.22 mm, n=12); and 8.3 to 14.2 mm (F5, 12.00 ± 0.82 mm; n=8), defined from 12 images per ovary. Comparison of normalized NRF intensities between GC, iTH and eTH

were performed by one-way ANOVA followed Newman-Keuls multiple comparison test using GraphPad Prism version 5.01 (GraphPad Software).

2.5 Immunohistochemistry (IHC) on ovary sections

Ten µm bovine ovaries frozen sections were fixed in 4% paraformaldehyde buffered (PBS) during 2 min. The slides were rinsed once in TBS for 5 min and then placed in a bath with normal horse serum blocking solution for 20 min. The slides were incubated overnight at 4°C with the primary antibodies anti-Caspase-3 (CASP3, 1:500, rabbit polyclonal, Cusabio, Wuhan Huamei Biotech Co., Hubei Province, China, CSB-PA05689A0Rb), in TBS with 5% non-fat dry milk. In control slides, primary antibody was omitted. Slides were washed 3 times in TBS (5 min), and incubated 2 hours in secondary anti-rabbit biotinylated antibody (1:2000, Biotinylated Universal Antibody, Horse Anti-Mouse/Rabbit IgG, Vector, BA-1400) and rinsed in TBS (5 min). The signal revelation was made with VECTASTAIN ABC-AP Staining Kit (Vector, AK-5000) as recommended by the manufacturer. The sections were counterstained with Papanicolaou stain (Sigma). Coverslips were applied with aqueous mounting medium after dehydration through graded alcohol bath (70%, 80% 95%, 100%; 20 sec each) and in toluene (1 min). Sections were examined using an Axioplan Carl Zeiss microscope. Images were acquired using a digital monochrome camera (Spot-Flex, Diagnostic Instruments) coupled with the SPOT 5.2 imaging software.

2.6 Mass Spectrometry Imaging by MALDI-TOF MS (MSI-MS)

Frozen ovaries were cut using a Cryo-Star HM 560 cryostat (Microm, Francheville, France) at –18°C. The 10µm thick sections were thaw-mounted onto conductive Indium Tin Oxide-coated microscope slides (Bruker Daltonics, Wissembourg, France). Placed near the tissue section, 1µL of a mixture of small molecules and peptides to external mass calibration (1 µL of calibrant solution containing Cafein, MRFA peptide, Leu-Enkephalin, Bradykinine 2–9, Glu1-fibrinopeptide B; reserpine; Bradykinine; Angiotensine I) and mixed (1:1 v/v) with the matrix used for the MALDI MSI.

Using a histology slide scanner (OpticLab H850 scanner, Plustek, Ahrensburg, Germany) the ovary sections were scanned before matrix deposition to overlay the histological and molecular images. Slides were coated with a CHCA (α-cyano-4-hydroxycinnamic acid) matrix sprayed at 7mg/mL in 60/40 acetonitrile/H2O, 0.2% trifluoroacetic acid using an Image Prep device (Bruker Daltonik GmbH, Bremen, Germany), and then vacuum-dried. Spectra were acquired using an UltrafleXtreme MALDI-TOF instrument (Bruker Daltonik GmbH, Bremen, Germany) equipped with a Smartbeam laser (Nd:YAG, 355 nm) monitored by the FlexControl 3.4 software (Bruker Daltonics, Bremen, Germany). MSI sequence was performed from one ovarian section targeting one region of interest (ROI) corresponding to ovary image.

Spectra were acquired in the positive mode, at a 2.0-kHz laser repetition rate, in the 100–1200 m/z range, using a spatial resolution set at 100µm (medium focus setting) and collecting 500 spectra per pixel as a sum of 50 consecutive laser shots in 10 random walk shot steps. For a better mass accuracy across a tissue section image, raw spectra from all of the datasets were first aligned to a lock mass set at m/z 760.5780 corresponding to [M + H]+ of 34:1 PC. The unprocessed MSI sequence was then imported into the SCiLS Lab software (version 2016b, SCiLS, GmbH, Bremen, Germany). MSI sequence was Int. J. Mol. Sci. 2018, 19, 3261 21 of 31 loaded and pre-processed, according the used instrument type (TOF). Data were baseline reduced using a convolution algorithm with the setting of 20 for peak width and normalized to the total ion count (TIC). For ROI (whole ovary section), two-dimensional (2D) ion density maps using medium denoising were created from the average projection spectrum, and after data partitioning (bisecting k-Means), a segmentation map was generated.

2.7 Intact Cells MALDI-TOF MS (ICM MS) Analysis of Lipids on Follicular Cells and Fluid

Lipid profiles were performed on individual frozen oocytes, follicular fluids and follicular somatic cells from individual follicles, divided in two diameter groups: 12 small follicles (SF,4.0 mm to 6.8 mm, mean size 5.0±0.21mm) and 12 large follicles (LF, 8.0 mm to 19mm, mean size 12.9±1.27mm). The oocytes were thawed in ice and placed on the MTP Ground Steel 384 MALDI plate (Bruker Daltonics, Germany) to dry. Other samples were defrosted in an ice bath, and 5 µl of cell suspension or FF were dried by SpeedVac System (SPD 1010-230, Thermo Savant Eletronic Corporation, France) for 10 min at 45 °C. 2,5-dihydroxyacetophenone matrix (DHAP) solution was prepared in concentration 20 mg/mL (DHAP matrix at solubilized in 90% methanol, 2% trifluoroacetic acid in water). Cells pellets and FF samples were re-suspended in 4µl and 8µl of DHAP matrix-

solution, sonicated for four min in ultrasonic bath (FisherBrand 15,052, Fisher Scientific) to solubilize lipids. One microlitrer of the matrix and sample were mixed (1:1 v/v) and 1.5 µL of the same DHAP matrix-solution was added. Each sample was spotted onto a MALDI plate in three replicates (with the exception of a single oocyte), and dried at room temperature for 30 min. External calibration was performed using a mixture of small molecules and peptides (1 µL of calibrant solution containing Cafein, MRFA peptide, Leu-Enkephalin, Bradykinine 2–9, Glu1-fibrinopeptide B; reserpine; Bradykinine; Angiotensine I) mixed with 1 µL of the DHAP matrix-solution. 3000 spectra per spot (as a sum of 1000 consecutive laser shots in three shot steps) were acquired, using a Bruker UltrafleXtreme MALDI-TOF instrument (Bruker Daltonics, Germany). Spectra were acquired in the positive and negative ion modes using reflecton in the m/z 100–1200 range. An internal calibration was subsequently applied to all of the spectra to increase the mass accuracy (mass error < 0.05%). Employing FlexAnalysis 4.1 software (Bruker), lock mass correction was performed with highest intensity peak, corresponding to the glycerophosphatidylcholine (PC 32:1, m/z 732.556) in the positive mode, and glycerophosphatidylinositol (PI 38:4; m/z 885.5499) in the negative mode. Each spectrum was converted to a .txt file using FlexAnalysis 3.4 software and processed using MALDI Progenesis software version 1.2 (Nonlinear Dynamics, Newcastle upon Tyne, UK). Automatically detected peaks were analyzed considering a signal-bottom ratio of five, with exclusion of isotopes. The coefficient of variation (CV%) of intensity values (normalized peak height, NPH) was calculated for all peaks in three technical replicates per sample in 12 different follicles for each tissue (Results: Table 5). For comparative analysis of the lipid profiles between the compartments, the NPH values were used. One-way (ANOVA) and Tukey's post-hoc test were used for differential analysis using XLSTAT software (Addinsoft, Paris, France). The differences were considered significant with $p \leq 0.05$ and fold change >2.

2.7. Lipid Identification

The annotation of m/z features was based on lipid identifications described earlier (Bertevello et al. 2018) and the Lipidmaps.org database.

2.8. Gene Expression Analysis

2.8.1. RNA Extraction and Reverse transcription

Total RNA from GC and TH cells of small and large follicles (SF,3.7mm to 7.0mm, mean size 5.0±0.24mm; LF, 7.2mm to 18mm, mean size 12.8±1.24mm, respectively) from 12 individual ovaries were extracted using TriZol reagent (Invitrogen, Cergy Pontoise, France) and then treated by RQ1 DNAse (Promega, Charbonnières, France) following the manufacturer's instructions. After isopropanol precipitation, the RNA concentration was determined using a NanoDrop ND-1000 spectrophotometer (Nyxor Biotech, Paris, France). Reverse transcription (RT) was performed on 200 ng of extracted RNA from somatic cells, using the Maxima First Strand cDNA Synthesis kit (Thermo-Fisher Scientific, Courtaboeuf, France) according to the manufacturer's instructions.

2.8.2. Real Time PCR Analysis

Real-time PCR reactions were carried out on a CFX96 (Bio-Rad, Marnes-la-Coquette, France) in 20 µL reaction mix containing primers at a final concentration of 150 nM each, 5 µL of the diluted RT reaction (equivalent of 2 ng converted RNA), and qPCR Mastermix Plus for SYBR Green I (Bio-Rad, Marnes-la-Coquette, France) according to the manufacturer's instructions. The efficiency of the primers (Table 1), and standard curve for each gene was deduced from serial dilutions of the correspondent cDNA fragment as a template. The geometric mean of three housekeeping genes (RPL19, RPS9, and GAPDH) was used to normalize gene expression. The relative expression of the genes of interest (RE) was calculated according to the equation: R = gene E^{-Ct} gene/geometric mean ($RPS9^{E\text{-}Ct\ RPS9}$; $RPL19^{E\text{-}Ct\ RPL19}$; $GAPDH^{E\text{-}Ct\ GAPDH}$), where E is the primer efficiency and Ct the cycle threshold. Statistics was done using Mann-Whitney test. Difference was considered significant at $p<0.05$.

Table 1. List of primers used for RT-qPCR analysis of gene expression in bovine ovarian cells.

Gene	Accession Number	Description		Primer's Sequence (5'-3')	Efficiency%(E)
ACACA	NM_174224	Acetyl-CoA Carboxylase Alpha	*Fw* *Rev*	TGCTTCCCATTTGCCATC CTGCCATCCTCACGACCT	103.2% (2.03)
ACADVL	MN_174494	Acyl-CoA Dehydrogenase, Very Long Chain	*Fw* *Rev*	CATCGTCCACCAGGAACTGAG GAACCACCACCATGGCATAGA	103.1% (2.03)
ACOT9	NM_001034560.1	Acyl-CoA Thioesterase 9	*Fw* *Rev*	GTGAGGTGGCCTCTCTTCAG GGGCTTCAACAAGAGCAGTC	114.5% (2.14)
APOA1	NM_174242.3	Apolipoprotein A1	*Fw* *Rev*	TTTGGGAAAACAGCTCAACC CAGGTCCTTGTGCATCTCCT	84.1% (1.84)
CD36	NM_001044622.1	CD36-molecule (Thrombospondin Receptor)	*Fw* *Rev*	TTGGCCTATGAACCGTTTACT CGTTCTGAAGTTGCCAAGCA	119.6% (2.20)
CPT2	NC_037330.1	Carnitine Palmitoyltransferase 2	*Fw* *Rev*	AACCGCAAGTCTGGAGAAGA TGACCGTAACCACCATGAGA	105.1% (2.05)
CYP11A1	NM_176644.1	Cytochrome P450, Family 11, Subfamily A, Polypeptide 1	*Fw* *Rev*	CGGAAAGTTTGTAGGGGACA ACGTTGAGCAGAGGGACACT	100.5% (2.00)
FABP3	NM_174313	Fatty acid binding protein 3	*Fw* *Rev*	ATCGTGACGCTGGATGGCGG GCCGAGTCCAGGAGTAGCCCA	99.8% (1.99)
FABP5	NM_001129805.1	Fatty acid binding protein 5	*Fw* *Rev*	ACGTGTCGAAAGAAGGAGGT ACATCCCAAAGAGCATATCGTA	100.7% (2.00)
GAPDH	NM_001034034	Glyceraldehyde 3 phosphate dehydrogenase	*Fw* *Rev*	TTCAACGGCACAGTCAAGG ACATACTCAGCACCAGCATCAC	100.1% (2.00)
GPX4	NM_174770	Glutathione Peroxidase 4	*Fw* *Rev*	CGATACGCCGAGTGTGGTTTAC ACAGCCGTTCTTGTCAATGAGG	101% (2.01)
HADHA	NM_174335	Hydroxyacyl-CoA Dehydrogenase Trifunctional Multienzyme Complex Subunit Alpha	*Fw* *Rev*	CTGTACGGGGCACAGAAAAT TGCCAGAGTTCGTCTTCCTT	102.2% (2.02)
HSD3B1	NM_174343	Hydroxy-Delta-5-Steroid Dehydrogenase, 3 Beta- and Steroid Delta-Isomerase 1	*Fw* *Rev*	TCCACACCAGCACCATAGAA AAGGTGCCACCATTTTTCAG	102.2% (2.02)
LPL	NM_001075120	Lipoprotein lipase	*Fw* *Rev*	GGGTTTTGAGCAAGGGTACA GCCACAATGACCTTTCCAGT	111.1% (2.11)
PLIN2	NM_173980	Perilipin 2	*Fw* *Rev*	ACAACACACCCCTCAACTGG CTGCCTGCCTACTTCAGACC	95.0% (1.95)
RPL19	BC102223	Ribosomal protein L19	*Fw* *Rev*	AATCGCCAATGCCAACTC CCCTTTCGCTTACCTATACC	101.0% (2.01)
RPS9	BC148016	Ribosomic protein S9	*Fw* *Rev*	GGAGACCCTTCGAGAAGTCC GGGCATTACCTTCGAACAGA	95.8% (1.96)
SCARB1 (SR-BI or CD36L1)	NM_174597.2	Scavenger Receptor Class B, member 1 or CD36 Antigen-Like 1	*Fw* *Rev*	ATGCCCAGTATGTGCTCCTT AAGAAGCGGGGTGTAGGG	100.1% (2.00)
SCARB2 (SR-BII or CD36L2)	NM_001102153.1	Scavenger Receptor Class B, member 2 or CD36 Antigen-Like 2	*Fw* *Rev*	TCCAGGCTTCTCCCACTAGA TTCTGGGCAGCATTCTCTTT	109.6% (2.10)
SLC2A1 (GLUT1)	NM_174602	Solute Carrier Family 2 Member 1 (facilitative glucose transporter)	*Fw* *Rev*	CTGATCCTGGGTCGCTTCAT ACGTACATGGGCACAAAACCA	100% (2.00)
TRIB2	NM_178317.3	Tribbles homolog 2 (Drosophila)	*Fw* *Rev*	GTGGCATGTAGTGCAGACC ACAGGACAAAGCACCAGAG	100.2% (2.00)

3. Results

3.1. Nile Red fluorescence analysis of lipids in bovine ovarian follicles

Spatial distribution of neutral lipids was observed and quantified by Nile Red Fluorescence (NRF) on histological sections of 15 bovine ovaries. Different NRF intensity was observed between different ovarian compartments. Fluorescence intensities of DAPI and NR were measured in GC, internal and external theca layers (iTH and eTH, respectively) of 43 follicles of different sizes.

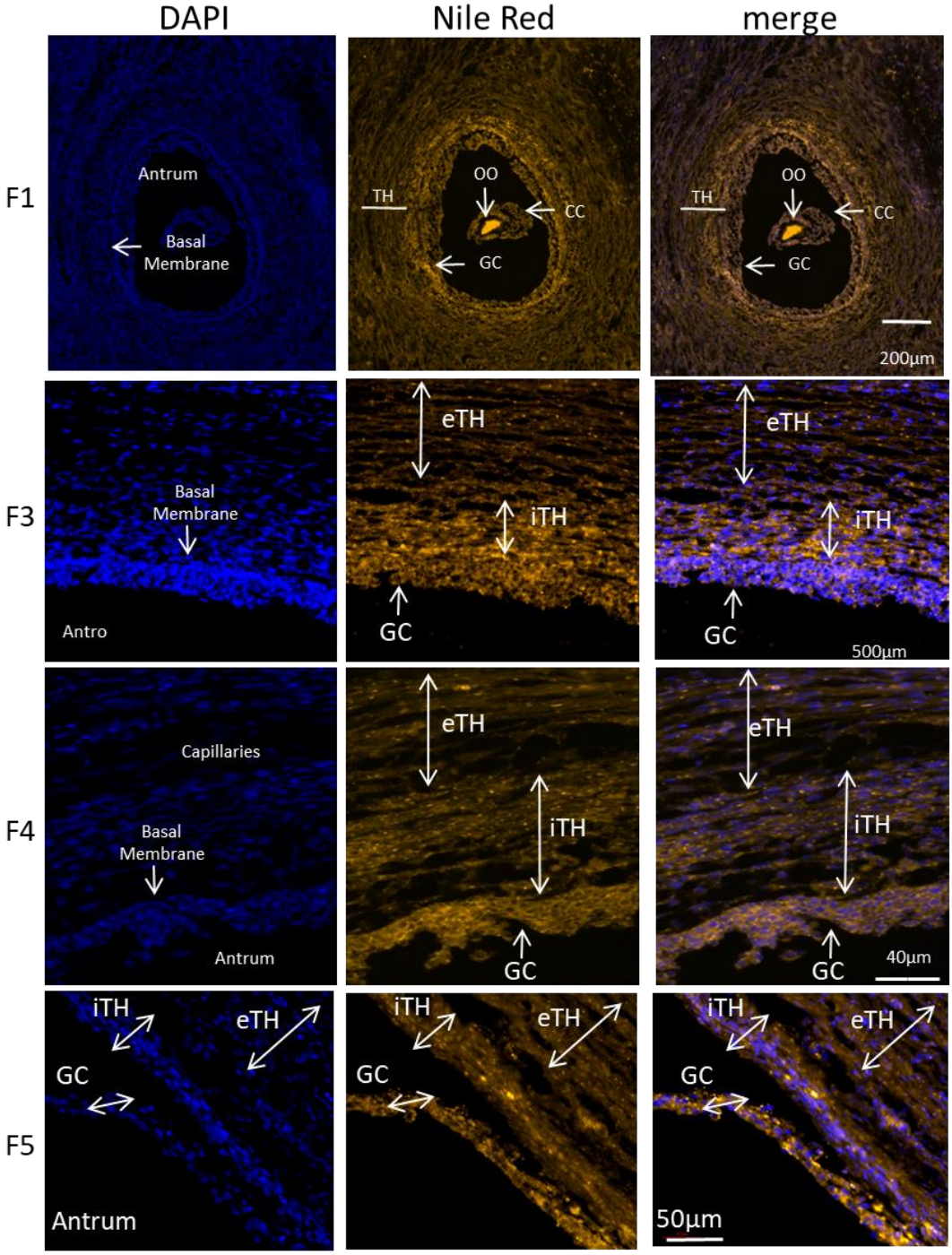


Figure 1. Representative images of Nil Red and DAPI staining in follicles of different size: **F1.** Follicles of 0.88 ± 0.08 mm; **F3.** Follicles of 4.05 ± 0.12 mm; **F4.** Follicles of 6.06 ± 0.22 mm; **F4.** Large Follicles of 12.0 ± 0.82 mm. iTH-internal theca, eTh – externa theca layer, GC – granulosa cells, OO- oocyte.

Follicles were distributed to the five groups, from F1 to F5, dependent on mean follicular size. There groups were as follows: mean size 0.88±0.08 mm (F1, n=6); 2.27±0.12mm (F2, n=6); 4.05±0.12mm (F3, n=11); 6.06±0.22mm (F4, n=12); 12.00±0.82mm (F5, n=8).

The highest NRF levels were observed in somatic cells of the small follicles, particularly in F2 and F3 groups, compared to other follicular size (Figure 2). GC and TH cells of small F2 follicles showed three-fold higher NRF levels than in large F5 follicles (Figure 1 and 2, Supplementary table 01). Globally, there was not significant differences between GC and TH layers, except for F2 and F4 groups where GC showed more NRF compared to eTH (F2) or to both theca layers (F4). In group F4, NRF in iTH was higher than in eTH.

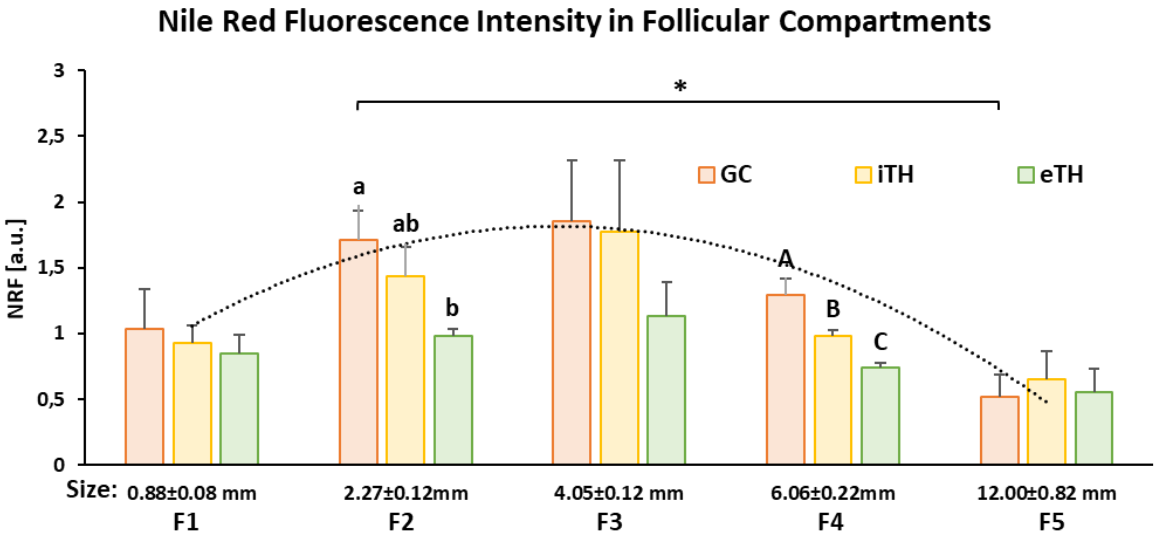


Figure 2. Graphical representation of mean NRF intensity distribution in granulosa (GC), theca interna (iTH) and theca extrena (eTH) layers in five groups of ovarian follicles of different size. Different letters mean significant difference ($p<0.05$) between NRF of different layers. Star denotes significant difference of NRF between GC of small and large follicles (F2 and F5 group, respectively).

3.2. Detection of Caspase-3 in bovine follicles

Follicle atresia was assessed according to morphological characteristics of follicular cell layers. In order to confirm atresia stage in the follicles, serial sections from the ovaries tested by NRF, were immunohistochemically tested in triplicate with anti-caspase-3 antibody, a marker of apoptosis cascade and indicative of atresia (Namura et al. 1998). Immunohistochemistry allowed clear detection of atretic follicles, with strong Caspase-3 labelling (**Figure 3c, e)** and more healthy follicles with faint Caspase-3 labeling (**Figure 3b and e**). From 12 follicles analyzed, five were negative and seven positive for Caspase-3. In the follicles with low caspase-3 labeling, Nile Red staining was less pronounced in GC but higher in iTH, comparing to atretic follicles with more intense caspase-3 labeling of GC and iTH cells (**figure 3f**).

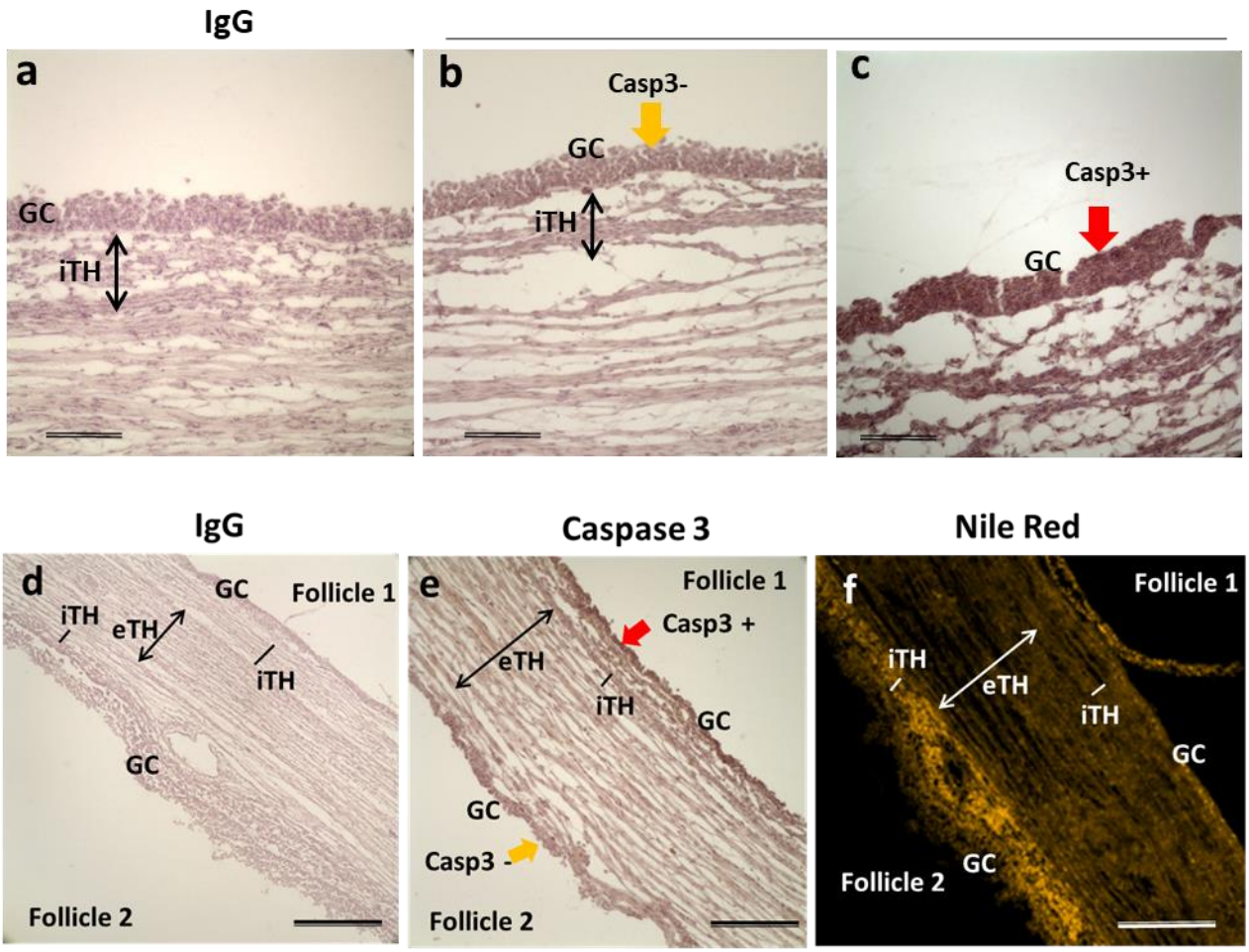


Figure 3. Representative image of immunohistochemistry (IHC) to detect caspase-3 in ovarian follicles, here group F4. IHC without caspase-3 antibody (**a, d**), with caspase-3 antibody (**b, c, e**) and colored by Nile Red (**f**). Caspase-3 labeling was observed in GC of potentially atretic follicles (**c** and **e** – Follicle 1). GC with no positive Caspase-3 labeling **(b** and **e-** Follicle 2). Bars 200 µm (a, b, c) and 400 µm (d, e, f). **Abbreviations:** Casp3 - caspase-3, GC - granulosa cells, iTH - internal theca cells, eTH - external theca layer, yellow arrow – caspase-3 negative labeling; red arrow – caspase-3 positive labeling.

3. 3 Mass Spectrometry Imaging by MALDI-TOF MS (MSI-MS)

MALDI-TOF mass spectrometry imaging (MSI) allowed the mapping of 281 molecular species with variable intensity in the mass range 100–1000 m/z within the analyzed section; the skyline projection spectra was generated from all the detected ion signals (**Figure 4A, Supplementary table 2**). All the ion signal profiles (some of them are presented here as molecular images of ion density maps, **figure 4C**) were grouped par similarity using unsupervised hierarchical cluster analysis. The most specific clusters were selected to generate representative molecular reconstruction of ovarian tissue sections (MSI segmentation map, **Figure 4B**, left image). Follicles and interstitial stroma compartments are distinguished on this MSI segmentation map in coherence with histological digital image of the same section **Figure 4B**, right image). The different colors in the segmented map (Figure 4B) represent differences in lipid composition between the zones throughout ovarian section and between different follicles. Different colors in ion density maps (**Figure 4C**) represents different abundance of this ion in the spectra (color bar: increasing from blue to red).

Data on lipid identification in bovine ovarian follicles reported in previous study (Bertevello et al. 2018) allowed the annotation of 53 m/z features (18.8% from total detected features); the most of them were either protonated ($[M+H]^+$) lipid species or salt adducts as sodium $[M+Na]^+$ and potassium $[M+K]^+$. Identified lipids represented the following classes: phosphatidylcholines (PC) - 55.6%; lyso-phosphatidylcholine (LPC) - 7.4%; sphingomyelin (SM) - 16.7%; ceramide (Cer) - 1.9%; cholesteryl esters (CE) - 5.6%; diacylglycerol (DG) - 1.9%; triacylglycerol (TG) - 9.3% (Supplementary-table 3). According to ion density maps, there are a homogeneous distribution of lipids PC, SM, CE, and DG. Those lipids were globally observed in the interstitial stroma of the bovine ovary histological sections (Figure 4C). Some LPC lipids were more abundant inside the follicles, probably in FF, were identified as m/z 496.43 (LPC 16:0); m/z 518.39 (LPC 18:3); m/z 520.45 (LPC 18:2), and also several PC, such as m/z 703.992 (unknown); m/z 758.628 (PC 34:2/ PC 35:1), m/z 760.87 (PC 34:1), m/z 824.658 (PC 36:2). While, other lipid species located by MSI showed diffuse and heterogeneous distributed throughout the ovary, as m/z 703.580 (SM 34:1), m/z 732.683 (PC 32:1), m/z 851.702 (SM 42:2) and 872.568 (PC 40:6) (Supplementary Table 3).

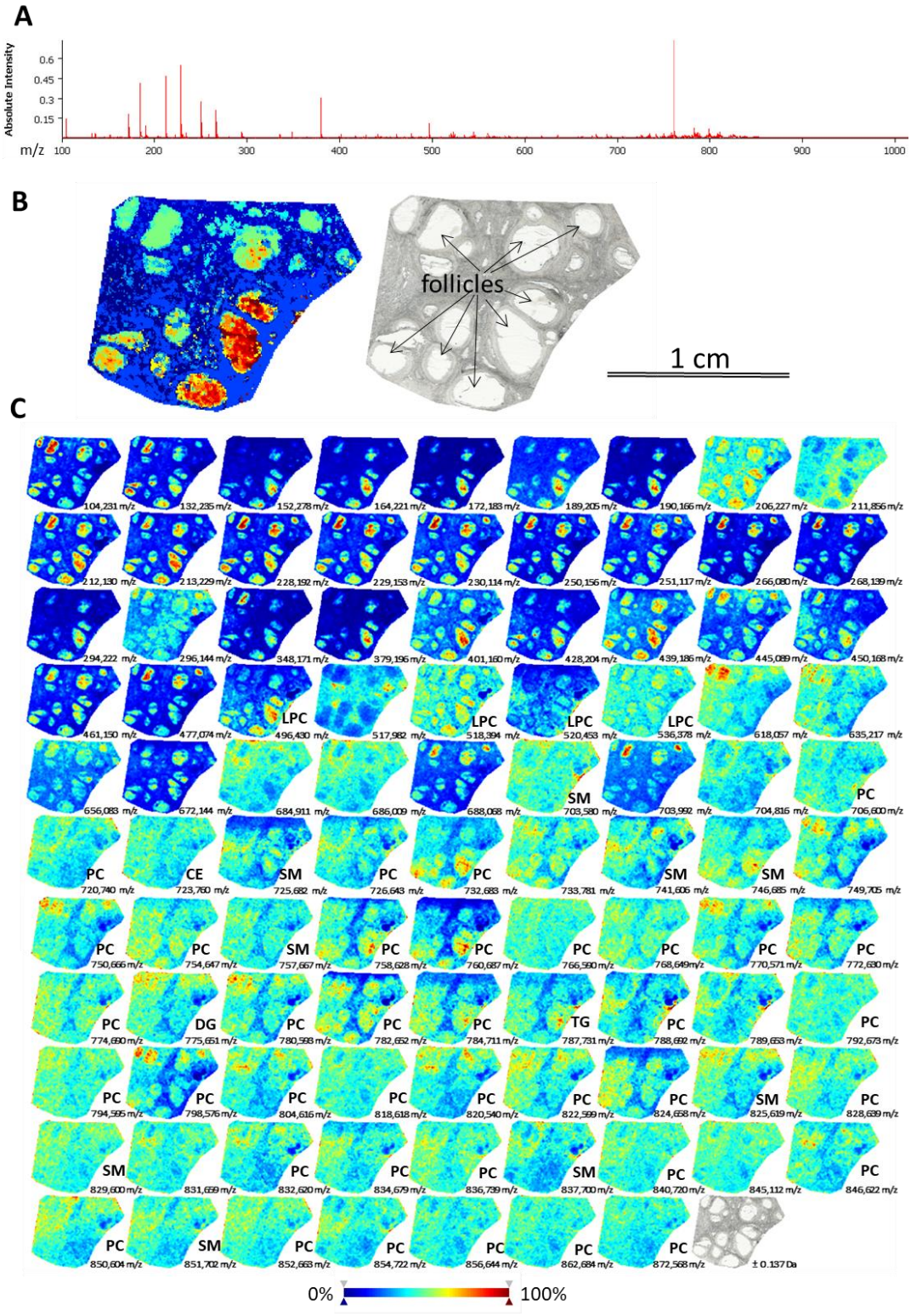


Figure 04. Detection of lipid species in bovine ovary using high-resolution mass spectrometry imaging (MSI). 281 m/z species detected from bovine ovarian section with follicles from 1 to 4 mm in diameter**. A.** Skyline projection spectrum of molecular species in the 100–1000 m/z range. **B**. Spatial segmentation map (left picture) was obtained by hierarchical clustering using the bisecting k-means algorithm. Light scan of the same section (right picture). **C.** Ion density maps of detected m/z species through ovarian section, lipid classes of 53 identified m/z are shown. PC – phosphatidylcholine; LPC-phosphatidylcholine, SM – sphingomyelin, TG – triacylglycerol.

3. 4 Comparison of Lipid Profiling in Follicular Cells and Fluid of small and large follicles

In order to compare lipid composition between small and large follicles (Figure 5A), we analyzed lipid profiles of their follicular cells (GC, TH, CC and oocyte) and follicular fluid (Figure 5B) obtained using MALDI-TOF MS in positive and negative acquisition modes (Figure 5C).

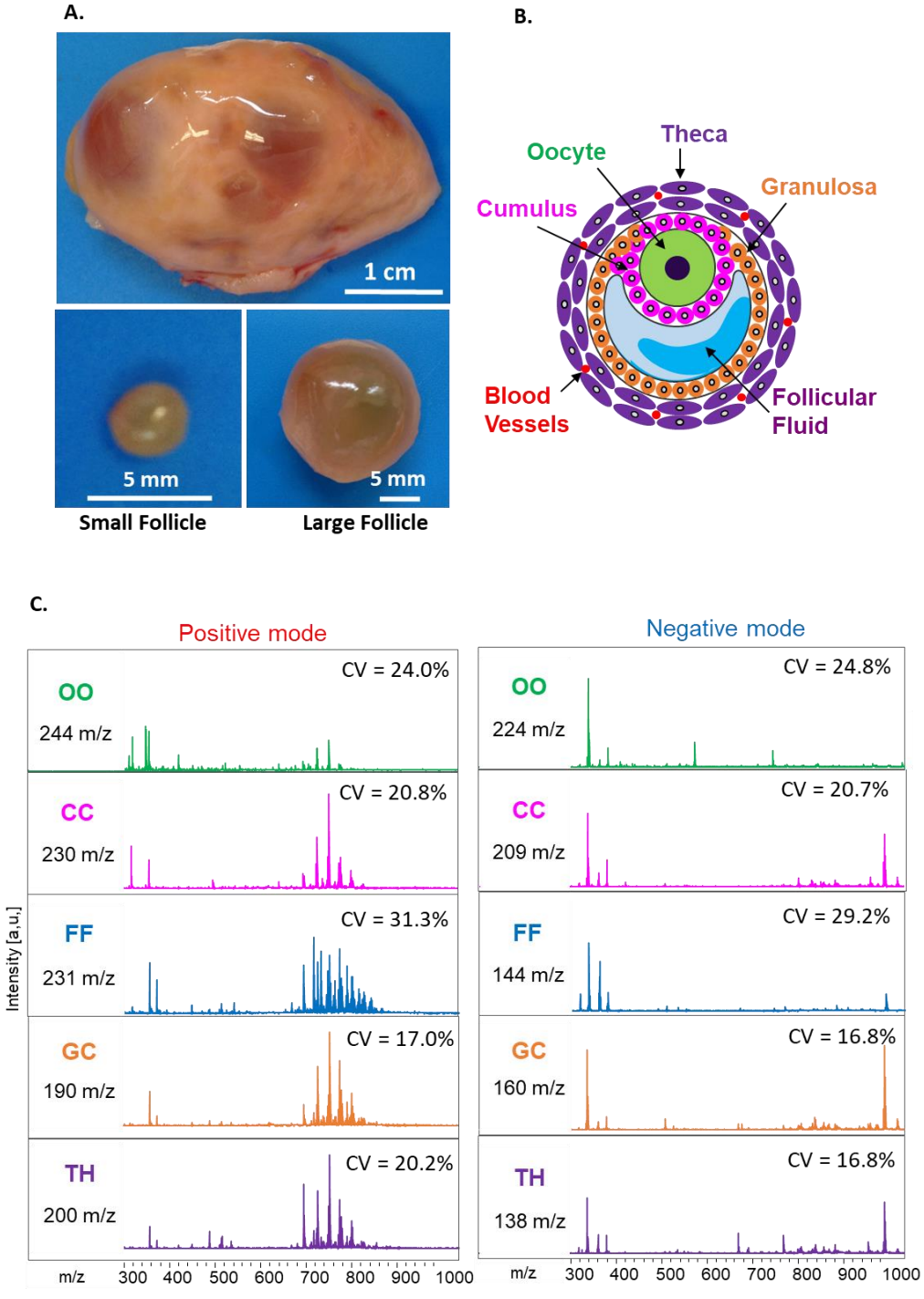


Figure 5. Illustrative image of ovary and small and large follicles used in analyzes (A). Schematic representation of ovarian follicle compartments (B). Representative MALDI-TOF MS spectra of bovine oocytes, cumulus cells (CC), granulosa (GC) and theca cells (TH) and follicular fluid (FF) in positive and negative acquisition modes, m/z range of 300 to 1000. Number of features (m/z) detected and mean coefficient of variation of their abundance (CV, %) are indicated for each tissue/mode.

The number of differently abundant features between SF and LF significantly varied per compartment (**Table 2**). In oocytes and TH, only 1.7% m/z and 5.3% species, respectively, differed between LF and SF ($p<0.05$, fold change >2); in CC and GG the percentage of differential species was 9.9% and 14.9%, respectively. In the same time, in FF more than half of the peaks (55.5%) significantly changed their abundance in LF as compare to SF.

Table 2. Detection and differential analysis of lipids in follicular cells and fluids between large and small follicles

Follicular compartment	Total m/z number detected	Differentially abundant features, n (%)	LF vs SF	
			Up-regulated	Down-regulated
OO	468	8 (1.7%)	2	6
CC	439	43 (9.8%)	41	2
FF	375	208 (55.5%)	111	97
GC	350	52 (14.9%)	35	17
TH	338	18 (5.3%)	15	3

Lipids detected in positive and negative modes in the range 300-1000 m/z were compared between LF and SF ($p<0.05$; fold change >2). Abbreviations: m/z-mass to charge; LF-Large Follicle; SF-Small Follicle

Using expression values of the differentially abundant features, Principal Component Analysis (PCA) was performed for each compartment. Globally, the two groups of follicles, LF and SF, were discriminated by lipid profiles of their enclosed oocytes or follicular cells (**Figure 6A**), however the most discriminant were lipid profiles in correspondent follicular fluids (**Figure 6B**). The mean values of relative abundance of 111 up-regulated and 97 down regulated differential lipid species in FF of the LF as compared to SF is here presented as a heatmap (**Figure 6C)**.

All the ions detected as differential and their respective annotations are presented in the supplementary data (supplementary table 4). In the tables 3-7, presented below, the annotation was done with present lipid species with the closer delta of m/z detected by MALDI-TOF MS.

In FF, among the 48 annotated differential lipids (**Table 3**), mainly PC and LPC were more abundant in large follicles (9 PC, 5 LPC, 2 CE, 1 LPE, 1 PE, and 1 SM), whereas DG, SM, PE and PI were over-represented in smaller follicles (12 PC, 8 PE, 3 PI, 3 DG, 2 SM, 2 PS and 1 LPC). In addition, the incidence of lipids including polyunsaturated FAs in FF was higher in small follicles (35%) than in large ones (20%), as much as 15% saturated fatty acids and 17% monounsaturated fatty acids in SF.

In the oocytes, three peaks up-regulated in small follicles were identified, 2 PC and 1 SM (**table 4**). In CC, among 43 differential lipid species, 15 PC, 2 SM and 1 TG significantly more abundant in LF compared to SF were identified; 44% of these lipids contain very long chain polyunsaturated carbons (**Table 5**). In GC, among 35 differential peaks more abundant in LF, only one was annotated as PI 36: 2. Among the lipids, over-represented in the SF, we annotated C18:0 carnitine, 3 LPC, 2 PC, 1 SM and 1 PE, and 55% of them showed the presence of medium or long-chain polyunsaturated FAs (**table 6**). In TH, 4 annotated m/z, more abundant in LF, corresponded to identified lipids (TG 38:4) and PE (34:2 and 38:7) (**table 7**).

338 **Table 3**. Differential lipids in FOLLICULAR FLUID of large and small follicles

m/z	p-value	Ratio LF vs SF	Lipid ion (carbons : unsaturation [add])	Lipid Class
m/z502.218+	3,15E-03	0,46	LPC 16p:0 $[Na]^+$	LPC
m/z506.197+	1,33E-06	3,90	LPC 14a:0 $[K]^+$	LPC
m/z518.223+	2,88E-04	2,56	LPC 18a:3 $[H]^+$	LPC
m/z524.310+	6,21E-07	5,21	LPE 20:4 $[Na]^+$ or LPC 18a:0 $[H]^+$	LPE/LPC
m/z544.283+	4,55E-06	2,46	LPC 18a:1 $[Na]^+$	LPC
m/z546.293+	5,84E-07	6,14	LPC 18a:0 $[Na]^+$	LPC
m/z605.487+	3,98E-05	0,48	DG 32a:1 $[K]^+$	DG
m/z669.576+	5,15E-05	2,34	CE 18:3 $[Na]^+$	CE
m/z671.543+	7,21E-05	3,99	CE 18:2 $[Na]^+$	CE
m/z683.450+	1,44E-03	0,48	DG 38a:4 $[K]^+$	DG
m/z706.527+	1,20E-07	0,33	PC 30a:0 $[H]^+$	PC
m/z707.525+	2,32E-07	0,29	DG 40a:6 $[K]^+$	DG
m/z711.516+	1,80E-04	2,36	SM 33:1 $[Na]^+$	SM
m/z716.424+	1,87E-04	2,01	PC 28a:0 $[K]^+$	PC
m/z716.652-	3,02E-06	0,27	PE 34a:1 $[H]^-$	PE
m/z734.551+	3,02E-12	0,16	PC 32a:0 $[H]^+$	PC
m/z741.510+	5,38E-10	0,30	SM 34:1 $[K]^+$	SM
m/z742.641-	1,97E-08	0,10	PE 36a:2 $[H]^-$	PE
m/z744.664-	8,79E-12	0,07	PE 36a:1 $[H]^-$	PE
m/z748.537+	6,20E-04	0,43	PC 33a:0 $[H]^+$	PC
m/z750.654-	6,63E-06	0,27	PE 38e:5 or PE 38p:4 $[H]^-$	PE
m/z760.606-	2,60E-05	0,10	PE 38a:7 $[H]^-$	PE
m/z762.576+	3,23E-10	0,31	PC 34a:0 $[H]^+$	PC
m/z769.515+	8,65E-09	0,30	SM 36:1 $[K]^+$	SM
m/z770.517+	1,12E-12	0,32	PC 32a:1 $[K]^+$	PC
m/z772.501+	4,55E-13	0,21	PC 32a:0 $[K]^+$	PC
m/z774.645-	1,45E-10	0,14	PE 40e:7 or PE 40p:6 $[H]^-$	PE
m/z788.619+	6,14E-06	2,43	PC 36a:1 $[H]^+$	PC
m/z788.660-	1,92E-09	0,02	PE 40a:7 $[H]^-$	PE
m/z790.629+	2,34E-05	2,07	PC 38e:7 or PC 38p:6 $[H]^+$	PC
m/z794.668-	1,21E-09	0,38	PE 40a:4 $[H]^-$	PE
m/z798.517+	1,51E-11	0,23	PC 34a:1 $[K]^+$	PC
m/z800.540+	7,12E-10	0,37	PC 34a:0 $[K]^+$	PC
m/z808.592+	2,73E-05	2,74	PC 38a:5 $[H]^+$	PC
m/z810.601+	2,75E-08	2,82	PC 38a:4 $[H]^+$	PC
m/z812.625+	2,32E-07	2,37	PC 38a:3 $[H]^+$	PC
m/z826.575+	2,98E-02	0,46	PC 36a:1 $[K]^+$	PC
m/z832.584+	1,47E-06	2,39	PC 40a:7 $[H]^+$ or PC 38a:4 $[Na]^+$	PC
m/z834.607-	9,57E-07	0,43	PS 40a:6 $[H]^-$	PS
m/z836.624-	4,67E-08	0,10	PS 40a:5 $[H]^-$	PS
m/z846.501+	2,10E-02	0,41	PC 38a:5 $[K]^+$	PC
m/z846.658-	2,45E-11	0,23	PS 42p:6 $[H]^-$	PS
m/z858.613+	1,02E-04	3,49	PC 42a:8 $[H]^+$ or PC 40a:5 $[Na]^+$	PC
m/z860.595+	7,80E-05	3,31	PC 42a:7 $[H]^+$ or PC 40a:4 $[Na]^+$	PC
m/z870.506+	7,08E-11	0,41	PC 40a:7 $[K]^+$	PC
m/z872.530+	1,44E-02	0,49	PC 40a:6 $[K]^+$	PC
m/z883.624-	2,32E-08	0,09	PI 38a:5 $[H]^-$	PI
m/z885.652-	9,09E-10	0,11	PI 38:4 $[H]^-$	PI
m/z887.662-	1,23E-07	0,30	PI 38:3 $[H]^-$	PI

339

Table 4. Differential lipids in OOCYTES of large and small follicles

m/z	p-value	Ratio LF vs SF	Lipid ion (carbons : unsaturation [add])	Lipid Class
m/z702.431+	3,66E-02	0,43	PC 31e:2 or PC 31p:1 $[H]^+$	PC
m/z713.467+	2,28E-02	0,39	SM 32:1 $[K]^+$	SM
m/z728.456+	3,41E-02	0,43	PC 29a:1 $[K]^+$	PC

Table 5. Differential lipids in CUMULUS CELLS of large and small follicles

m/z	p-value	Ratio LF vs SF	Lipid ion (carbons : unsaturation [add])	Lipid Class
m/z714.352+	2,93E-05	4,65	PC 29a:0 $[Na]^+$	PC
m/z721.406+	2,38E-02	2,00	SM 34:3 $[Na]^+$	SM
m/z725.533+	9,83E-03	2,06	SM 34:1 $[Na]^+$	SM
m/z734.595+	7,08E-03	2,90	PC 32a:0 $[H]^+$	PC
m/z744.522+	1,57E-03	2,01	PC 31e:0 $[K]^+$	PC
m/z748.593+	6,23E-05	2,06	PC 33a:0 $[H]^+$	PC
m/z786.626+	1,97E-03	2,33	PC 36a:2 $[H]^+$ or PC 33a:0 $[K]^+$	PC
m/z788.634+	1,28E-03	2,06	PC 36a:1 $[H]^+$	PC
m/z800.647+	7,75E-03	2,49	PC 34a:0 $[K]^+$ or PC 37a:2 $[H]^+$	PC
m/z802.659+	3,46E-02	2,02	PC 37a:1 $[H]^+$	PC
m/z808.598+	4,51E-04	2,57	PC 38a:5 $[H]^+$	PC
m/z810.634+	2,96E-04	2,45	PC 38a:4 $[H]^+$	PC
m/z813.701+	8,74E-05	2,78	TG 47:1 $[Na]^+$	TG
m/z824.744+	3,46E-05	2,45	PC 40e:4 or PC 40p:3 $[H]^+$	PC
m/z826.754+	7,79E-03	2,34	PC 39a:3$[H]^+$	PC
m/z828.758+	2,28E-03	2,57	PC 39a:2 $[H]^+$	PC
m/z834.642+	2,54E-05	2,35	PC 40a:6 $[H]^+$ or PC 38a:3 $[Na]^+$	PC
m/z836.677+	3,26E-04	2,13	PC 40a:5 $[H]^+$ or PC 38a:2 $[Na]^+$	PC

Table 6. Differential lipids in GRANULOSA CELLS of large and small follicles

m/z	p-value	Ratio LF vs SF	Lipid ion (carbons : unsaturation [add])	Lipid Class
m/z428.379+	8,21E-04	0,37	C18:0 Carnitine $[H]^+$	FAC
m/z534.302+	3,84E-03	0,38	LPC 16a:0 $[K]^+$	LPC
m/z560.274+	3,70E-03	0,49	LPC 18a:1 $[K]^+$	LPC
m/z582.303+	1,22E-02	0,40	LPC 20a:4 $[K]^+$	LPC
m/z722.463-	8,16E-04	0,45	PE 36e:5 or PE 36p:4 $[H]^-$	PE
m/z844.546+	1,03E-04	0,50	PC 38a:6 $[K]^+$	PC
m/z848.559+	1,01E-04	0,46	PC 38a:4 $[K]^+$	PC
m/z861.431-	5,83E-03	2,81	PI 36a:2 $[H]^-$	PI
m/z863.704+	2,54E-02	0,47	SM 44:2 $[Na]^+$	SM

Table 7. Differential lipids in THECA CELLS of large and small follicles

m/z	p-value	Ratio LF vs SF	Lipid ion (carbons : unsaturation [add])	Lipid Class
m/z683.481+	2,14E+00	2,14	DG 38a:4 $[K]^+$	DG
m/z667.572+	2,20E+00	2,20	DG 38a:4 $[Na]^+$	DG
m/z714.550-	2,02E+00	2,02	PE 34a:2 $[H]^-$	PE
m/z760.544-	2,08E+00	2,08	PE 38a:7 $[H]^-$	PE

Abbreviations: phospholipids with a lower case a, diacyl; d, dihydroxyl; e, plasmanyl; p, plasmalogen subspecies respectively; FAC, fatty acyl carnitines; LPC, lyso-phosphatidylcholine; PC, phosphatidylcholine; LPE, lyso-phosphatidylethanolamines; PE, phosphatidylethanolamine; PS, phosphatidylserines; PI, phosphatidylinositol; CE, cholesteryl esters; SM, sphingomyelins; Cer, ceramides; HexCer, hexosylceramides; DG, diacylglycerol; TG, triacylglycerol.

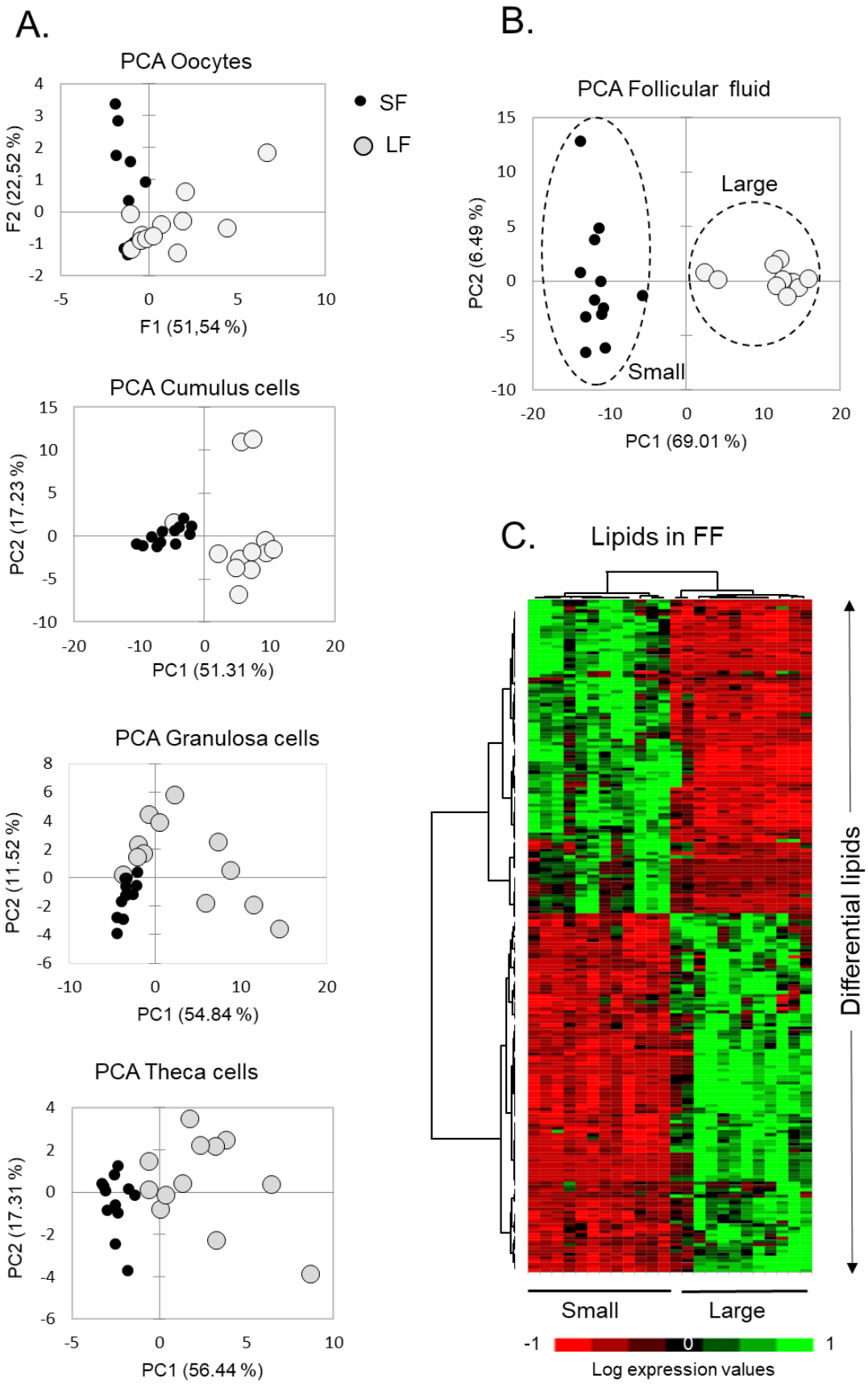


Figure 6. Principal Component Analysis (PCA) show the difference between small and large follicles lipid profiles in oocyte, CC, GC and theca cells (A) and follicular fluid (B). Abundance of differential lipids in FF presented as a heatmap (C).

3.5. Gene Expression Analysis

Expression of eighteen genes involved in different functions related to lipid transport (*APOA1, CD36, CPT2, FABP3, FABP5, SCARB1, SCARB2*), glucose transport (*GLUT1*), lipid metabolism (*ACACA, ACADVL, ACOT9, HADHA, LPL, PLIN2, TRIB2*), lipid antioxidant (GPX4), steroidogenesis (*CYP11A1 and HSD3B1),* relative to that of house-keeping genes *RPL19, GAPDH* and *RPS9*, was quantified in TH and GC of small and large follicles (n=12 per group) by real-time PCR (**Table 7**).

Relative expression of *HSD3B1* was twice lower in TH of large follicles, whereas *CYP11A1* increased 6-fold in GC as compared to small follicles ($p<0.05$). In theca cells, genes *ACOT9*, *PLIN2* and *TRIB2* were significantly higher expressed in SF than in LF ($p<0.05$), *CD36, CPT2* and *LPL* tended to this over-expression in SF ($p<0.1$), whereas no difference was observed in GC. In GC, relative expression of *GPX4* is significantly higher and that of *ACADVL, HADHA* showed tendency to be higher in LF as compared to SF. Gene *FABP3* tended to higher expression in TH and lower in GC of SF compared to LF.

Table 7. Gene expression analysis in TH and GC from small and large follicles.

	Theca cells		Granulosa cells	
Genes	**Small follicle**	**Large follicle**	**Small follicle**	**Large follicle**
ACACA	1579±373	1044±246	986±309	906.59±325.81
ACADVL	1634±739	1092±165	***1692±816***	***4716 ±1635***
ACOT9	**12.5±3.25 (a)**	**3.8±1.5 (b)**	0.8±0.2	1.03±0.17
APOA1	0.41±0.22	0.31±0.1	0.21±0.03	0.42±0.24
CD36	**253 ±69 (a)**	**89.99±48.05 (b)**	2302 ±979	1820 ±778
CPT2	***13528 ±5502***	***4561 ±1236***	8687 ±2408	8464. ±3618
CYP11A1	1956 ±1344	6044 ±3285	**1583 ±547 (A)**	**9277 ±3107 (B)**
FABP3	***3376 ±1681***	***1278 ±270***	***859 ±241***	***1629 ±540***
FABP5	7271 ±2614	4073 ±2641	547 ±272	1646 ±1043
GLUT1	973 ±289	941 ±303	13126 ±5844	44136 ±23953
GPX4	3269 ±1186	13407 ±7815	**11672 ±3132 (A)**	**34370 ±8799 (B)**
HADHA	917 ±258	883 ±156	***885 ±137***	***1229 ±130***
HSD3B1	**1060 ±331 (a)**	**566 ±189 (b)**	885 ±291	1387 ±330
LPL	177636 ±63479	79488 ±38902	973 ±388	1055 ±424
PLIN2	**19.49±7.3 (a)**	**3.91±1.75 (b)**	5.96±2.6	2.71±0.61
SCARB1	10.8±4.2	15.6±4.6	16.2±8.1	18.5±5.0
SCARB2	2.7±2	3.1±1.3	7.7±3.1	11.4±4.7
TRIB2	**5.2±1.4 (a)**	**1.9±0.5 (b)**	1.9±0.8	3.9±1.8

Mean ± SD values of 12 samples per group are shown. Differential expression values are bold: different letters mean significant difference at $p<0.05$; tendency to significance ($p<0.1$) is marked in italics. **Abbreviations:** ACACA: Acetyl-CoA Carboxylase Alpha; ACADVL: Acyl-CoA Dehydrogenase, Very Long Chain; ACOT9: Acyl-CoA Thioesterase 9;APOA1: Apolipoprotein A1; CD36: CD36-molecule (Thrombospondin Receptor) ; CPT2: Carnitine Palmitoyltransferase 2; CYP11A1: Cytochrome P450, Family 11, Subfamily A, Polypeptide 1; FABP3: Fatty acid binding protein 3; FABP5: Fatty acid binding protein 5; GPX4: Glutathione Peroxidase 4; HADHA: Hydroxyacyl-CoA Dehydrogenase Trifunctional Multienzyme Complex Subunit Alpha; HSD3B1: Hydroxy-Delta-5-Steroid Dehydrogenase, 3 Beta- and Steroid Delta-Isomerase 1; LPL: Lipoprotein lipase; PLIN2: Perilipin 2; SCARB1 (SR-BI or CD36L1) : Scavenger Receptor Class B, member 1 or CD36 Antigen-Like 1; SCARB2 (SR-BII or CD36L2): Scavenger Receptor Class B, member 2 or CD36 Antigen-Like 2; SLC2A1 (GLUT1): Solute Carrier Family 2 Member 1 (facilitative glucose transporter); TRIB2: Tribbles homolog 2 (Drosophila); GAPDH: Glyceraldehyde 3 phosphate dehydrogenase; RPL19: Ribosomal protein L19; RPS9: Ribosomic protein S9.

4. Discussion

We have here reported analysis of lipid content in the individual oocytes and their follicular environment derived from the bovine ovarian follicles of different sizes. In fact, mass spectrometry imaging, performed in these work on bovine ovary sections, demonstrated that the FF inside the follicles of the same ovary had different lipid composition, which significantly distinguished from lipid content of other ovarian structures, as it was previously reported in mice and porcine ovaries (Campbell et al. 2012; Uzbekova et al. 2015). Ovarian follicles are very dynamic structures and by this study, we demonstrated that follicular lipid signatures also change during follicle growth and could reflect physiological state of the follicle, and thus future oocyte competence. Stain of total lipid inclusions by Nile Red revealed the distribution of intracellular neutral lipids in lipid droplets (LDs) through the ovary. Except corpus luteum, that was extremely rich in lipids due to high steroid production (Quirk, Cowan, and Harman 2013), the follicles accumulate LDs mostly in GC and internal theca layers, and in comparison, external TH and interstitial stroma contain fewer lipids. Globally, small and intermediate follicles (2-6 mm, F2-F4 groups) showed the most intense lipid accumulation in mural follicular layers (GC and iTH) in comparing to similar compartments of very small F1 follicles (< 1mm) or large F5 follicles (>10 mm). And, total lipid quantity in GC of F2 antral follicles (2 mm) was significantly higher than in GC of large F5 follicles. This may be due to an increase of steroidogenic activity of GC in growing antral follicles that requires more lipid reserves (Monniaux et al. 2014). In addition, in 2-6 mm follicles neutral lipids were significantly more abundant in GC than in vascularized external TH layer. This may be due to constant intense transfer of lipids from TH to other follicle cells and fluids (Young and McNeilly 2010), and supports the higher activity of lipid consumption in TH that was shown by expression pattern of correspondent enzymes in TH cells from the antral follicles of these sizes (Bertevello et al. 2018). In very small and very large follicles, neutral lipids were less abundant than in intermediate-sized and LDs are distributed homogeneously through GC, iTH and eTH cells. Interestingly, that spatial distribution of LDs in GC and iTH seems to be influenced not only by follicular size but also by the degree of follicular atresia. In fact, GC are the first undergoing apoptosis in atretic follicles before the oocytes and TH, and thus may initiate follicular atresia (Inoue et al. 2011; Jiang et al. 2003; Tajima et al. 2007). Nile red staining showed more intense in iTH of healthy follicles and in GC of atretic follicles. GC from atretic follicles recently reported the presence of lysophosphatidic acid (LPA, bioactive glycerophospholipid produced from the cellular membrane phospholipids), LPA participates in apoptotic initiation through the regulation of TNF-alpha-dependent and caspase-induced pathways (Sinderewicz et al. 2017). From the other hand, sphingosine-1-phosphate, signaling sphingolipid, blocked follicle atresia in human ovarian cortical fragments in vitro, improved their steroidogenic activity and decreased caspase-3 protein level thus protecting cells from apoptosis (Guzel, Bildik, and Oktem 2018). Dautel and colleagues (2017) demonstrated healthy and apoptotic tissues have different lipid composition (Dautel et al. 2017). The ovary, as a peculiar tissue, has most of the follicles show a different degree of apoptosis, and that may explain the variability of lipid content in different follicles of similar size, both in cells and FF.

MSI provided distribution of lipids within ovarian sections and inside the follicles. This technology allowed the ionization of numerous lipid species, such as LPC, PC, SM, CE, DG and choline molecules (Zemski Berry et al. 2011). MSI segmentation map clearly discriminated interstitial stroma from TH and GC layers and FF due to their different lipid composition and/or different ionization capacity of lipids from liquid or cellular compartments, similarly to MSI of porcine ovarian sections (Uzbekova et al. 2015). By MSI MS, we observed singular distribution of the identified lipid species in a global view and in detail in the follicles. In general, most PC were located in the interstitial stroma and somatic cells (TH and GC), while several SM and LPC (16:0; 18:3 and 18:2) were located preferentially in FF. For many features, this location was confirmed by the MALDI MS lipid profiles performed on intact follicular cells and FF.

Metabolic composition of FF reflects that of blood plasma (Jo L.M.R. Leroy et al. 2005; Renaville et al. 2010; Aardema et al. 2013). During follicular growth and development, the follicular cells together with the oocyte undergo many dynamic changes which also include lipid metabolism (reviewed by (Paulini et al. 2014). The neutral lipids, triacylglycerols, steryl esters as well as other lipids, which may be the precursors of, for example, hormones or secondary messengers, also are crucial source of energy (Hashemi and Goodman 2015). Studies *in vivo*, reported changes in contents of metabolites of FF during follicular growth as decrease of TG and lactate concentration, and increased of glucose, β-hydroxybutyrate, and total cholesterol in bovine (J.L.M.R Leroy, Vanholder, Delanghe, Opsomer, Van Soom, Bols, and de Kruif 2004; Shabankareh, Kor, and Hajarian 2013) and ovine (Nandi et al. 2007)**.** The follicular fluid composition of previously mentioned metabolites during follicular growth suggests that follicular cells consume proportionally more lipids than glucose as an energy source. The decrease of lactate in FF from large follicles suggests a decrease in the anaerobic pathway of glucose, while an increase in β-hydroxybutyrate reveals an increase in oxidation of acyl and acetyl CoA (FA subunits) obtained from the breakdown of lipid molecules such as TG. A total cholesterol increased could be explained by a temporary halt in steroid synthesis, the follicle remains in the "static phase" before becoming dominant or atretic (Dadarwal et al. 2015). Partly the glucose-fatty acid cycle, or Randle cycle, can explain the reduction in glucose uptake and utilization that occurs in tissues when fatty acid oxidation is intense. In this phenomenon, the fatty acid oxidation produces acetyl-CoA from which citrate is generated by the action of citrate synthase. High values of acetyl-CoA/CoA and NADH/NAD+ ratios stimulate PDH kinase, which phosphorylates and inactivates PDH. ATP and citrate inhibit phosphofructokinase, with the accumulation of substrates from previous stages, including G-6-P, which has an inhibitory effect on hexokinase. This depresses glycolysis. This mechanism allows for preserving glucose into the cells, instead of using fatty acids, in cells or tissues who depend on glucose for energy (Randle 1998; Warzych et al. 2017). Explain the increased ability of the COC to utilize fatty acids as energy substrates may decrease the need for the COC to metabolize glucose, or allow glucose to be stored or participate in other essential pathways (Warzych et al. 2017).

Considering that follicles are responsible for the metabolism of huge amounts of lipids and cholesterol, for primary production of sex hormones (and other lipid-metabolites) and widely used as an energy source, glucose could drive a gene expression program characterized by activating genes involved in its metabolism, in part, by increasing acetate-derived histone acetylation. The repressing both glucose and glutamine metabolism, McDonnell and colleagues (2016) found fatty acid oxidation reprograms cellular metabolism leading to increased lipid-derived acetyl-CoA (i.e., acetate) leading to epigenetic events that control gene expression (McDonnell et al. 2016). Studies on the detection of nutrients such as lipids used in dietary manipulation are integrated by epigenetic events that control gene expression. It is a new perspective to obtain answers about oocyte quality or negative energy balance in postpartum, and even metabolic diseases.

The other lipid role can be involved in the cross-talk and signalizations between somatic cells and oocyte. According to our MALDI MS analysis of lipids in follicular cells and fluid from follicles of different sizes, showed more than a half of all lipid features (55%) have changed their FF concentrations in large follicles (mean size 12.9 mm) as compared to smaller ones (mean size 5.0 mm). Among the lipid species identified, lipids as PI and PS decrease during follicular growth (Jiang et al. 2003), and lipid species like LPC, DG, and SM increase, which suggests a **go/no-go atresia**.

In FF, the lipid profiling showed that the LPC was composted, mainly, by saturated or mono-unsaturated FAs (LPC 14:0, 18:0, 20:0, 18:1) and that these lipids species were more abundant in LF. Verified by imaging MS MS, some LPCs were located near the blood vessels in the region close to the follicles demonstrated the occurrence of lipid transports between plasma and follicle. One of the more abundant lipid species observed was the LPC 16:0, but this lipid showed a particular expression in specific follicles, demonstrating their difference from the other ones. Low concentrations of LPC are associated with pathology such as obesity in humans (review by (Lapid and Graff 2017) and high

concentrations were correlated to negative energy balance in dairy cows (J.L.M.R Leroy, Vanholder, Delanghe, Opsomer, Van Soom, Bols, and de Kruif 2004), with low reproductive rate in both cases. Thus, over-abundance of some specific lipid species might determine the lower quality of the enclosed oocyte. LPC was associated to activate several second messengers, including extracellular-signal-regulated kinases and protein kinase C, which have been shown to be involved in the regulation of follicular development and oocyte maturation (Wen et al. 2018). Others numerous LPC observed in FF which also can be derived from the extracellular vesicles (Silveira et al. 2018) or lipoproteins (Serna et al. 2015) and still may be involved in intra-follicular signaling and cell-to-cell communication (Drzazga, Sowińska, and Koziołkiewicz 2014; Bertevello et al. 2018). It has been discovered that LPC functions as a major mediator in both inflammation and apoptotic cell death, with recognized effects on multiple immune cell types. The leading role of LPC as an attraction signal in the process of programmed cell death has been shown by Lauber and colleagues (2003), who found that the disposal of apoptotic cells is initiated by the secretion of LPC as a chemotactic signal that induces the recruitment of phagocytes (Lauber et al. 2003). Moreover, Zurgil and colleagues (2007) suggested that LPC triggers apoptosis in activated peripheral blood lymphocytes, in association with an increased generation of reactive oxygen species (ROS) and an increase in the Bax/Bcl-2 ratio (Zurgil et al. 2007). Actually, LPC induces apoptotic cell death not only of lymphocytes but also of other cells. LPC stimulates several intracellular signaling events: activation of caspase-3, Ca2+ influx, phosphorylation of MAP kinases, and production of ROS, all of which can lead to apoptosis (Matsubara and Hasegawa 2005). Moreover, a novel interaction between LPC and pro-apoptotic Bid protein has been shown to prime mitochondria for the release of apoptogenic factors (Goonesinghe et al. 2005). LPC could represent a novel strategy for the inhibition of the progression of cell death. Cells commonly use membrane lipids to modulate the function of ion channels. The interaction of ion channels with membrane lipids can be highly specific and is often important for the fully functional and structural integrity of ion channels (Hunte and Richers 2008). The literature reveals that some agonists, despite their direct effect on ion channels, may also influence functions of ion channels via cellular lipid metabolism. For instance, phosphatidylinositol bisphosphate to diacylglycerol not only contributes to the membrane surface potential but also affects the functional properties of some channels (from the opened state to the closed state of the channels) (Minke and Cook 2002). Also, in several types of cells, sphingosine-1-phosphate (S1P) promotes cellular proliferation and survival, whereas ceramide (CER) triggers cell death, and the S1P/CER ratio may determine the fate of the cell. A study suggest that S1P plays a role in follicle health, increasing cellular proliferation and survival. In contrast, reduction of S1P and the S1P/CER in the antral follicle could trigger cellular death and atresia in the bovine (Hernández-Coronado et al. 2014) and S1P improves follicle survival in human ovarian cortical samples by decreasing apoptosis under *in vitro* conditions (Guzel, Bildik, and Oktem 2018). All of these mechanisms of lipid metabolism reported above lead to cell death or not (**go/no-go atresia**).

In contrast, lipid changes in the correspondent oocytes were not so dramatic: less than 2% of lipid features were differential between the oocytes from SF and LF, among them PC and SM lipids. This data are corroborated with a recent study showing some variations in only a few phospholipids (PC and SM) between the oocytes from LF and SF (Annes et al. 2018). In large dominant follicles structural changes as decrease of Golgi complexes size, peripheral location of cortical granules and increase of lipid deposit occurs compared to smaller subordinate ones (Assey et al. 1994; Fair 2003), even as an enrichment and translocation of mitochondria (Dadarwal et al. 2015). However, we only observed faint fluctuations in the phospholipid profiles between the oocytes from LF and SF. This demonstrates that membrane integrity of immature oocyte is highly protected from changing FF lipid environment during terminal stages of follicular growth.

The cross-talk between follicular cells is clearly observed through by MALDI MS profiling analysis. Directly contact the FF and somatic cells demonstrated more significant modulations of their lipid profiles, about 15% in the GC and 10% in the CC showed differential lipids between LF and SF, while in the TH about 5% of lipids changed. These variations suggest that GC and CC actively

transformed lipids and thus enclosed oocyte may be preserved from potentially harmful FF environment. In fact, it was shown, that when FF became lipotoxic due to accumulation of free FA, cumulus transform them in TG and increased the number of intracellular lipid droplets (Aardema et al. 2013; Lolicato et al. 2015) and also desaturate the potentially toxic stearic acid into oleic acid via SCD activity (Aardema et al. 2017).

The higher abundance of SM, PI, and DG in FF of small follicles could be a clue to another way of communication and signalization. Sphingolipids are involved not only in the stabilization of membrane structure, but also in cell signaling and cell-cell recognition (Milhas, Clarke, and Hannun 2011; Melendez 2008; Hannun and Obeid 1995). This signaling system is evolutionarily conserved, analogous to conventional systems, such as the cAMP and phosphoinositide pathways. The SM pathway use ceramide (generated from SM) as a second messenger. Ceramide signaling is a stress response system older than cell death by caspases, also transduces signals mediating differentiation, growth, cytokine biosynthesis and secretion, and a variety of other cellular functions (Mathias, Pena, and Kolesnick 1998; Ohanian and Ohanian 2001; Melendez 2008; Sanllehí et al. 2016). Phosphatidylinositols are minor acid phospholipids present in cell membranes, but play a major role in interacting and regulating the activity of integral membrane proteins via PI signaling (Falkenburger et al. 2010). Several PI are maintained at stable levels in the plasma membrane internal leaflet and through a continuous and sequential series of phosphorylation and dephosphorylation reactions by specific kinases and phosphatases, respectively, are regulated and/or reallocated through cell surface receptors to extracellular ligands (PI3K signaling). The 1,2-DG species are the cellular intermediates in the biosynthesis and degradation of TG, and the protein kinase C is their major effector. The binding of DG to a conserved C1 domain in PKC leads to its activation, cell cycle modulating, cellular survival, malignant transformation, and apoptosis (Wang 2006). In fact, genes involved in PI3K signaling were differentially expressed in GC of large and small follicles (Hatzirodos, Hummitzsch, Irving-rodgers, et al. 2014) indicating significant involvement of this pathway in follicular growth.

Changes in membrane lipid composition observed between SF and LF shows ability in lipid influence to some metabolism processes through scramble and translocase phospholipids realized by protein transporters (e.g. ABC transporters) (Y. Yang, Lee, and Fairn 2018; Van Meer, Voelker, and Feigenson 2008), and/or lipid elongation made by elongases (Kihara 2012). Glycerophospholipids enriched in polyunsaturated FA and largely represented in follicular somatic cells and FF may be are involved in the activity of elongases (ELOVL) and desaturases (SCD) present in somatic cells (Warzych et al. 2017; Bertevello et al. 2018). In CC, genes *ELOVL1* and *ELOVL*5 were over-expressed after maturation comparing to the immature stage (Sanchez-Lazo et al. 2014). Follicle size-specific variations of *ELOVL5* and *ELOVL6* were also observed along follicular growth (Annes et al. 2018).

Plasticity in intra- and inter-cellular communication is fundamental in several mechanisms, such as energy production, hormone and immunological activity, facilitated by transporters and signaling mediated by the presence of certain membrane lipids. A dispute between survival and stress signaling determine follicular dominance. The presence of these lipid species in FF and somatic cells suggests that there is high differentiation activity and follicular growth influenced by the composition of somatic cell membranes. Thus, folliculogenesis shows several mechanisms of communication and intrafollicular signaling mediated by lysophospholipids system (such as LPC), sphingolipids (ceramides) pathway, phosphatidylinositol signal-mechanism, and diacylglycerol signaling (**go/no-go atresia**). Among the somatic cells, theca showed the smallest differences in the abundance of molecular species between small and large follicles. Considering TH cells importance to follicle functioning, such as nutrient transport, hormone production, and signaling transmission, a few lipid changes during follicular development, maybe indicating stability for the follicle.

Metabolic activity of follicular somatic cells can greatly influence the lipid composition of FF. Globally, all somatic follicular cells possess enzymatic machinery to uptake and transform FAs,

synthesize and degrade lipids and lipoproteins, and each cell type has specific expression pattern regulating lipid metabolism in TH, GC or CC (Bertevello et al. 2018). From comparative transcriptomic studies performed on GC and TH of small and large follicles, data on differential expression of numerous lipid metabolism genes were reported, both between follicular compartments (Hatzirodos et al. 2015) and size-dependent (Hatzirodos, Hummitzsch, Irving-Rodgers, et al. 2014; Hatzirodos, Hummitzsch, Irving-rodgers, et al. 2014). Our gene expression analysis by real-time PCR revealed variations in expression levels in GC and TH between the individual follicles, which may be due to different atresia degree. Nevertheless, over-expression of lipid metabolism-related genes ACOT9, CD36, CPT2, TRIB2, and PLIN2 was observed in TH of smaller follicles, whereas in GC, ACADVL and GPX4 were overexpressed in large follicles, along with expected expression pattern of CYP11A1 and HSD3B1 transcripts, which encode key enzymes of steroid hormone biosynthesis in TH and GC.

Mitochondrial beta-oxidation of fatty acyl-CoA is the major route of FA degradation, but very-long-chain FAs and branched-chain FAs are poorly oxidized in mitochondria and easily in peroxisomes (Demarquoy 2015). Thus, numerous acyl-CoA thioesterases (ACOT) reverse this reaction, despite the high-energy cost of acyl-CoA synthesis. ACOTs promote acyl-CoA synthesis and oxidation, to provide the very high requirement for free CoASH within mitochondria, so it is possible that ACOT9 operates to ensure sufficient free CoASH to maintain optimal mitochondrial function (Grevengoed, Klett, and Coleman 2014). ACADVL (Acyl-CoA Dehydrogenase Very Long Chain) is targeted to the inner mitochondrial membrane where it catalyzes the first step of the mitochondrial FA beta-oxidation pathway specifically to long-chain and very-long-chain FAs. CPT2, carnitine palmitoyltransferase II, is also involved in FA beta-oxidation and together with CPT1, it oxidizes long-chain FAs in the mitochondria. When FA beta-oxidation was inhibited during *in vitro* maturation of bovine cumulus-oocyte complexes, expression of *TRIB2*, *CD36, CPT2,* ACADVL in CC were significantly changed (Sanchez-Lazo et al. 2014; Brisard et al. 2014), showing their involvement on FA oxidation process. The over-expression of these genes in TH of the small follicles may indicate increased activity in mitochondrial FA beta-oxidation, associated to higher lipid uptake from plasma, considering higher expression of *LPL* (coding for lipase responsible for the uptake of plasma lipids) and *FABP3* and *5* (membrane and intracellular FA transporters) in TH compared to GC.

Strong expression of glutathione peroxidase 4 (GPX4) in both GC and TH showed the importance of this antioxidant enzyme that has the capacity to scavenge free radicals. Over-expression in GC of large follicles may help to prevent lipid peroxidation and maintain intracellular homeostasis as well as redox balance. Inhibition of glutathione peroxidase 4 (GPX4) could be the key to regulated cell death by an iron-dependent accumulation of lipid peroxides (Lei, Bai, and Sun 2019). GPX genes were up-regulated in small atretic follicles with respect to healthy follicles (Hatzirodos, Hummitzsch, Irving-rodgers, et al. 2014). Furthermore, Elis and colleagues (Elis et al. 2017) observed a tendency of a decrease in *GPX4* expression in cumulus cells supplemented with docosahexaenoic acid (C22:2), suggesting a reduced oxidative stress environment after treatment. In our study an increase in GPX4 expression suggest higher oxidative stress with increasing of the follicular size that might be related to the control between survival or cell death of the follicles.

The most of follicles in mammalian ovaries undergo a degenerative process, atresia, and thus only a limited number of ovarian follicles actually ovulate after full growth and development (Tajima et al. 2007). The precise and systematic molecular mechanisms of steroidogenesis enzymes involved in atresia are unclear yet. Expression of a steroidogenic acute regulatory protein, CYP11, CYP17, 3β-hydroxysteroid dehydrogenase (3β-HSD), CYP19, as well as related pituitary and ovarian hormone receptors were quantified during the follicular atresia in porcine ovaries. Significant correlations were observed between the expression of steroidogenic enzymes and their receptors in follicular fluid. These results suggest that CYP19 plays a role during early atresia by regulating the production of E2, whereas CYP11 and 3β-HSD increased atresia progression by increasing progesterone levels (Pan et al. 2012). The 3β-HSD are responsible to catalyze the conversion of pregnenolone to progesterone

specifically in lutein cells (corpus luteum) or polycystic ovary. But the abundance in TH cells from small follicles can suggest the DNA methylation, particular chemical modifications of histones, such as methylation, acetylation, or phosphorylation, can are involved in chromatin modulation (Grunstein, 1997; Nan et al., 1998; Jenuwein and Allis, 2001). The promoter methylation might be involved in the LH surge-induced down-regulation of genes of steroidogenesis, CYP19A1, CYP17A1, and HSD3B1 in the preovulatory follicles of the cow has been recently rebutted by experimental evidence (Vanselow et al., 2010). There are few examples, however, indicating that chromatin condensation and DNA methylation are not necessarily connected (Garrick et al., 1996). This epigenetic mechanism might be involved in the pre-ovulatory down-regulation of genes HSD3B1 transcripts, which encode enzymes of steroid hormone biosynthesis. This epigenetic mechanism might be involved in the pre-ovulatory down-regulation of genes HSD3B1 transcripts, which encode enzymes of steroid hormone biosynthesis. Nimz and colleagues (2010) related that LH induces cell type- and gene-specific chromatin condensation in the pre-ovulatory bovine follicle. The abundance of HSD3B1 transcripts was similar in the granulosa and theca of E2-active large dominant follicles, whereas down-regulation of HSD3B1 was significant only in the theca, but not in the granulosa. The access of fragment H3 (histone 3) in HSD3B1, include the TATA-Boxes, suggestively, one binding of the transcription initiation complex and may require a highly accessible structure of the local chromatin. Our data suggest that the epigenetic mechanism might be involved in the pre-ovulatory bovine follicle regulation of genes, which theca cells from small follicles showed a significantly negative correlation in transcript genes of steroidogenesis enzymes and granulosa cells from large follicles; these results suggest a process of atresia.

In general, the lipid fingerprint found in follicle compartments of large size showed store of long-chain and very long chain FAs. As those lipids are poorly metabolized by mitochondria to immediate energy, this probably indicates that there are stored for future use in benefit of progesterone production by post-ovulation body-luteum, whose goal will be the maintenance of gestation.

In conclusion, during antral follicle terminal growth, lipid composition significantly changed in both somatic cells and fluid as revealed by mass spectrometry lipidomics. Among all the compartments, FF is the most variable whereas enclosed immature oocyte is preserved from significant lipid variations. Theca and granulosa cell layers seem to regulate intra-follicular lipid metabolism dependently from follicle vascularization, apoptotic degree and follicular size, thus leading to strong modulation of FF lipid composition. Turnover and accumulation of specific lipids are essential to the maintenance of plasma membrane integrity, signaling and molecular communication necessary to determine follicular dominance.

5. References

Aardema, Hilde, Francesca Lolicato, Chris H A Van De Lest, Jos F Brouwers, Arie B Vaandrager, Helena T A Van Tol, Bernard A J Roelen, Peter L A M Vos, J Bernd Helms, and Bart M Gadella. 2013. "Bovine Cumulus Cells Protect Maturing Oocytes from Increased Fatty Acid Levels by Massive Intracellular Lipid Storage." *BIOLOGY OF REPRODUCTION* 88164 (6): 1–15. https://doi.org/10.1095/biolreprod.112.106062.

Aardema, Hilde, Helena T. A. van Tol, Richard W. Wubbolts, Jos F. H. M. Brouwers, Bart M. Gadella, and Bernard A. J. Roelen. 2017. "Stearoyl-CoA Desaturase Activity in Bovine Cumulus Cells Protects the Oocyte against Saturated Fatty Acid Stress." *Biology of Reproduction* 96 (5): 982–92. https://doi.org/10.1095/biolreprod.116.146159.

Anchamparuthy, Vahida M., Arindam Dhali, Whitney M. Lott, Ronald E. Pearson, and Francis C. Gwazdauskas. 2009. "Vitrification of Bovine Oocytes: Implications of Follicular Size and Sire on the Rates of Embryonic Development." *Journal of Assisted Reproduction and Genetics* 26 (11–12): 613–19. https://doi.org/10.1007/s10815-009-9362-2.

Annes, Kelly, Diego B Muller, Jorge A P Vilela, Roniele S Valente, Diana P Caetano, Francielli W S Cibin, Marcella P Milazzotto, and Mateus J Sudano. 2018. "Influence of Follicle Size on Bovine Oocyte Lipid Composition , Follicular Metabolic and Stress Markers , Embryo Development and Blastocyst Lipid Content." *Reproduction, Fertility and Development*. https://doi.org/10.1071/RD18109.

Arlotto, T., J-L. Schwartz, N.L. First, and M.L. Leibfried-Rutledge. 1996. "Aspects of Follicle and Oocyte Stage That Affect in Vivtro Maturation an Development of Bovine Oocytes." *Theriogenology* 45: 943–56.

Assey, R. J., P. Hyttel, T. Greve, and B. Purwantara. 1994. "Oocyte Morphology in Dominant and Subordinate Follicles." *Molecular Reproduction and Development* 37 (3): 335–44. https://doi.org/10.1016/S0021-9673(03)00538-7.

Bao, Bagna, and H. Allen Garverick. 1998. “Expression of Steroidogenic Enzyme and Gonadotropin Receptor Genes in Bovine Follicles during Ovarian Follicular Waves: A Review.” *Journal of Animal Science* 76 (7): 1903–21. https://doi.org/10.2527/1998.7671903x.

Bertevello, Priscila Silvana, Alexandre Seyer, Anaïs Vitorino Carvalho, Valérie Labas, Marie-claire Blache, Charles Banliat, Luiz Augusto, et al. 2018. “Lipid Identification and Transcriptional Analysis of Controlling Enzymes in Bovine Ovarian Follicle.” *International Journal of Molecular Sciences*. https://doi.org/10.3390/ijms19103261.

Blondin, Patrick, and Marc-André Sirard. 1995. “Oocyte and Follicular Morphology as Determining Characteristics for Developmental Competence in Bovine Oocytes.” 62: 54–62.

Brisard, Daphné, Alice Desmarchais, Jean Luc Touzé, Lionel Lardic, Sandrine Freret, Sebastien Elis, Fabienne Nuttinck, Sylvaine Camous, Joelle Dupont, and Svetlana Uzbekova. 2014. “Alteration of Energy Metabolism Gene Expression in Cumulus Cells Affects Oocyte Maturation via MOS-Mitogen-Activated Protein Kinase Pathway in Dairy Cows with an unfavorable ‘Fertil-’ Haplotype of One Female Fertility Quantitative Trait Locus.” *Theriogenology*. https://doi.org/10.1016/j.theriogenology.2013.11.013.

Campbell, Dahlia I., Christina R. Ferreira, Livia S. Eberlin, and R. Graham Cooks. 2012. “Improved Spatial Resolution in the Imaging of Biological Tissue Using Desorption Electrospray Ionization.” *Analytical and Bioanalytical Chemistry* 404 (2): 389–98. https://doi.org/10.1007/s00216-012-6173-6.

Collado-Fernandez, Esther, Helen M. Picton, and Rémi Dumollard. 2012. “Metabolism throughout Follicle and Oocyte Development in Mammals.” *Int. J. Dev. Biol.* 56: 799–808. https://doi.org/10.1387/ijdb.120140ec.

Dadarwal, D., G. P. Adams, P. Hyttel, G. M. Brogliatti, S. Caldwell, and Jaswant Singh. 2015. “Organelle Reorganization in Bovine Oocytes during Dominant Follicle Growth and Regression.” *Reproductive Biology and Endocrinology* 13 (1). Reproductive Biology and Endocrinology: 1–11. https://doi.org/10.1186/s12958-015-0122-0.

Dautel, Sydney E., Jennifer E. Kyle, Geremy Clair, Ryan L. Sontag, Karl K. Weitz, Anil K. Shukla, Son N. Nguyen, et al. 2017. “Lipidomics Reveals Dramatic Lipid Compositional Changes in the Maturing Postnatal Lung.” *Scientific Reports* 7 (February). Nature Publishing Group: 1–12. https://doi.org/10.1038/srep40555.

Demarquoy, Jean. 2015. “Crosstalk between Mitochondria and Peroxisomes.” *World Journal of Biological Chemistry* 6 (4): 301. https://doi.org/10.4331/wjbc.v6.i4.301.

Drzazga, Anna, Agata Sowińska, and Maria Koziołkiewicz. 2014. “Lysophosphatidylcholine and Lysophosphatidylinosiol Novel Promissing Signaling Molecules and Their Possible Therapeutic Activity.” *Acta Poloniae Pharmaceutica - Drug Research* 71 (6): 887–99.

Elis, Sebastien, Mouhamad Oseikria, Anais Vitorino Carvalho, Priscila Silvana Bertevello, Emilie Corbin, Ana Paula Teixeira-Gomes, Jérôme Lecardonnel, et al. 2017. “Docosahexaenoic Acid Mechanisms of Action on the Bovine Oocyte-Cumulus Complex.” *Journal of Ovarian Research* 10 (1). https://doi.org/10.1186/s13048-017-0370-z.

Fair, Trudee. 2003. “Follicular Oocyte Growth and Acquisition of Developmental Competence” 78: 203–16. https://doi.org/10.1016/S0378-4320(03)00091-5.

Falkenburger, Björn H., Jill B. Jensen, Eamonn J. Dickson, Byung Chang Suh, and Bertil Hille. 2010. “Phosphoinositides: Lipid Regulators of Membrane Proteins.” *Journal of Physiology* 588 (17): 3179–85. https://doi.org/10.1113/jphysiol.2010.192153.

Garrick D, Sutherland H, Robertson G, Whitelaw E. 1996. Variegated expression of a globin transgene correlates with chromatin accessibility but not methylation status. Nucleic Acids Res 24:4902–4909.

Goonesinghe, Alexander, Elizabeth S. Mundy, Melanie Smith, Roya Khosravi-Far, Jean Claude Martinou, and Mauro D. Esposti. 2005. “Pro-Apoptotic Bid Induces Membrane Perturbation by Inserting Selected Lysolipids into the Bilayer.” *Biochemical Journal* 387 (1): 109–18. https://doi.org/10.1042/BJ20041389.

Grevengoed, Trisha J, Eric L Klett, and Rosalind A Coleman. 2014. “Acyl-CoA Metabolism and Partitioning.” *Annu Rev Nutr* 34: 1–30. https://doi.org/10.1146/annurev-nutr-071813-105541.

Grunstein M. 1997. Histone acetylation in chromatin structure and transcription. Nature 389:349–352.

Guzel, Yilmaz, Gamze Bildik, and Ozgur Oktem. 2018. “Sphingosine-1-Phosphate Protects Human Ovarian Follicles from Apoptosis in Vitro.” *European Journal of Obstetrics Gynecology and Reproductive Biology* 222. Elsevier Ireland Ltd: 19–24. https://doi.org/10.1016/j.ejogrb.2018.01.001.

Hannun, Yusuf A, and Lina M Obeid. 1995. “Ceramide: An Intracellular Signal for Apoptosis,” no. February: 0–4.

Hashemi, Hayaa F., and Joel M. Goodman. 2015. “The Life Cycle of Lipid Droplets.” *Current Opinion in Cell Biology* 33. Elsevier Ltd: 119–24. https://doi.org/10.1016/j.ceb.2015.02.002.

Hatzirodos, Nicholas, Katja Hummitzsch, Helen F. Irving-Rodgers, and Raymond J. Rodgers. 2014. “Transcriptome Profiling of the Theca Interna in Transition from Small to Large Antral Ovarian Follicles.” *PLoS ONE* 9 (5). https://doi.org/10.1371/journal.pone.0097489.

———. 2015. “Transcriptome Comparisons Identify New Cell Markers for Theca Interna and Granulosa Cells from Small and Large Antral Ovarian Follicles.” *PLoS ONE* 10 (3): 1–13. https://doi.org/10.1371/journal.pone.0119800.

Hatzirodos, Nicholas, Katja Hummitzsch, Helen F Irving-rodgers, Margaret L Harland, Stephanie E Morris, and Raymond J Rodgers. 2014. “Transcriptome Profiling of Granulosa Cells from Bovine Ovarian Follicles during Atresia.” *BMC Genomics* 14. https://doi.org/10.1186/1471-2164-15-24.

Hernández-Coronado, C. G., A. Guzmán, R. Espinosa-Cervantes, M. C. Romano, J. R. Verde-Calvo, and A. M. Rosales-Torres. 2014. “Sphingosine-1-Phosphate and Ceramide Are Associated with Health and Atresia of Bovine Ovarian Antral Follicles.” *Animal* 9 (2): 308–12. https://doi.org/10.1017/S1751731114002341.

Hillier, S. G. 1994. “Current Concepts of the Roles of Follicle Stimulating Hormone and Luteinizing Hormone in Folliculogenesis.” *Human Reproduction* 9 (2): 188–91. https://doi.org/10.1093/oxfordjournals.humrep.a138480.

Humblot, P., P. Holm, P. Lonergan, C. Wrenzycki, A. S. Lequarré, C. Guyader Joly, D. Herrmann, et al. 2005. “Effect of Stage of Follicular Growth during Superovulation on Developmental Competence of Bovine Oocytes.” *Theriogenology* 63 (4): 1149–66. https://doi.org/10.1016/j.theriogenology.2004.06.002.

Hunte, Carola, and Sebastian Richers. 2008. “Lipids and Membrane Protein Structures.” *Current Opinion in Structural Biology* 18 (4): 406–11. https://doi.org/10.1016/j.sbi.2008.03.008.

Inoue, Naoko, Fuko Matsuda, Yasufumi Goto, and Noboru Manabe. 2011. “Role of Cell-Death Ligand-Receptor System of Granulosa Cells in Selective Follicular Atresia in Porcine Ovary.” *Journal of Reproduction and Development* 57 (2): 169–75. https://doi.org/10.1262/jrd.10-198e.

Irving-Rodgers, Helen F, Ross A D Bathgate, Richard Ivell, Roger Domagalski, and Raymond J Rodgers. 2002. “Dynamic Changes in the Expression of Relaxin-Like Factor (Insl3), Cholesterol Side-Chain Cleavage Cytochrome P450, and 3℀L-Hydroxysteroid Dehydrogenase in Bovine Ovarian Follicles During Growth and Atresia.” *Biology of Reproduction* 66: 934–43. https://doi.org/10.1095/biolreprod66.4.934.

Jenuwein T, Allis CD. 2001. Translating the histone code. Science 293:1074–1080. Vanselow J, P€ohland R, F€urbass R. 2005. Promoter 2 derived Cyp19 expression in bovine granulosa cells coincides with gene-specific DNA hypo-methylation. Mol Cell Endocrinol 233:57–64.

Jiang, Jin-yi, Carmen K M Cheung, Yifang Wang, and Benjamin K Tsang. 2003. “REGULATION OF CELL DEATH AND CELL SURVIVAL GENE EXPRESSION DURING OVARIAN FOLLICULAR DEVELOPMENT AND ATRESIA Jin-Yi Jiang, Carmen K.M. Cheung, Yifang Wang, Benjamin K. Tsang.” *Obstetrics & Gynecology*, no. 1: 222–37.

Kihara, Akio. 2012. “Very Long-Chain Fatty Acids: Elongation, Physiology and Related Disorders.” *Journal of Biochemistry* 152 (5): 387–95. https://doi.org/10.1093/jb/mvs105.

Lapid, Kfir, and Jonathan M. Graff. 2017. “Form(ul)ation of Adipocytes by Lipids.” *Adipocyte* 6 (3): 176–86. https://doi.org/10.1080/21623945.2017.1299298.

Lauber, Kirsten, Erwin Bohn, Stefan Martin Kröber, Yi Jin Xiao, Sibylle G. Blumenthal, Ralph K. Lindemann, Patrizia Marini, et al. 2003. “Apoptotic Cells Induce Migration of Phagocytes via Caspase-3-Mediated Release of a Lipid Attraction Signal.” *Cell* 113 (6): 717–30. https://doi.org/10.1016/S0092-8674(03)00422-7.

Lei, Pengxu, Tao Bai, and Yuling Sun. 2019. “Mechanisms of Ferroptosis and Relations With Regulated Cell Death: A Review.” *Frontiers in Physiology* 10 (February): 1–13. https://doi.org/10.3389/fphys.2019.00139.

Leroy, J.L.M.R, T Vanholder, J.R Delanghe, G Opsomer, A Van Soom, P.E.J Bols, J Dewulf, and A de Kruif. 2004. “Metabolic Changes in Follicular Fluid of the Dominant Follicle in High-Yielding Dairy Cows Early Post Partum.” *Theriogenology* 62 (6): 1131–43. https://doi.org/10.1016/j.theriogenology.2003.12.017.

Leroy, J.L.M.R, T Vanholder, J.R Delanghe, G Opsomer, A Van Soom, P.E.J Bols, and A de Kruif. 2004. “Metabolite and Ionic Composition of Follicular Fluid from Different-Sized Follicles and Their Relationship to Serum Concentrations in Dairy Cows.” *Animal Reproduction Science* 80 (3): 201–11. https://doi.org/10.1016/S0378-4320(03)00173-8.

Leroy, Jo L.M.R., T. Vanholder, B. Mateusen, A. Christophe, G. Opsomer, A. de Kruif, G. Genicot, and A. Van Soom. 2005. “Non-Esterified Fatty Acids in Follicular Fluid of Dairy Cows and Their Effect on Developmental Capacity of Bovine Oocytes in Vitro.” *Reproduction* 130 (4): 485–95. https://doi.org/10.1530/rep.1.00735.

Lolicato, Francesca, Jos F Brouwers, Chris H A Van De Lest, Richard Wubbolts, Hilde Aardema, Paola Priore, Bernard A J Roelen, J Bernd Helms, and Bart M Gadella. 2015. “The Cumulus Cell Layer Protects the Bovine Maturing Oocyte Against Fatty Acid- Induced Lipotoxicity.” *BIOLOGY OF REPRODUCTION* 9216 (1): 1–16. https://doi.org/10.1095/biolreprod.114.120634.

Mathias, S, L A Pena, and R N Kolesnick. 1998. “SIGNAL TRANSDUCTION OF STRESS VIA CERAMIDE [Review].” *Biochemical Journal* 335 (Part 3): 465–80.

Matsubara, Masahiro, and Kazuhide Hasegawa. 2005. “Benidipine, a Dihydropyridine-Calcium Channel Blocker, Prevents Lysophosphatidylcholine-Induced Injury and Reactive Oxygen Species Production in Human Aortic Endothelial Cells.” *Atherosclerosis* 178 (1): 57–66. https://doi.org/10.1016/j.atherosclerosis.2004.08.020.

McDonnell, Eoin, Scott B. Crown, Douglas B. Fox, Betül Kitir, Olga R. Ilkayeva, Christian A. Olsen, Paul A. Grimsrud, and Matthew D. Hirschey. 2016. “Lipids Reprogram Metabolism to Become a Major Carbon Source for Histone Acetylation.” *Cell Reproduction* 17 (6): 1463–72. https://doi.org/10.1016/j.celrep.2016.10.012.

Meer, Gerrit Van, Dennis R. Voelker, and Gerald W. Feigenson. 2008. “Membrane Lipids: Where They Are and How They Behave.” *Nature Reviews Molecular Cell Biology* 9 (2): 112–24. https://doi.org/10.1038/nrm2330.

Melendez, Alirio J. 2008. “Sphingosine Kinase Signalling in Immune Cells: Potential as Novel Therapeutic Targets.” *Biochimica et Biophysica Acta - Proteins and Proteomics* 1784 (1): 66–75. https://doi.org/10.1016/j.bbapap.2007.07.013.

Mihm, M., and E. C.L. Bleach. 2003. “Endocrine Regulation of Ovarian Antral Follicle Development in Cattle.” *Animal Reproduction Science* 78 (3–4): 217–37. https://doi.org/10.1016/S0378-4320(03)00092-7.

Milhas, Delphine, Christopher J Clarke, and Yusuf A Hannun. 2011. “Sphingomyelin Metabolism at the Plasma Membrane: Implications for Bioactive Sphingolipids.” *NIH FEBS Lett.* 584 (9): 1887–94. https://doi.org/10.1016/j.febslet.2009.10.058.Sphingomyelin.

Minke, Baruch, and Boaz Cook. 2002. “TRP Channel Proteins and Signal Transduction.” *Physiological Reviews* 82 (2): 429–72. https://doi.org/10.1152/physrev.00001.2002.

Monniaux, Danielle, Frederique Clelent, Rozen Dalbies-Tran, Anthony Estienne, Stephane Fabre, Camille Mansanet, and Philippe Monget. 2014. “Minireview The Ovarian Reserve of Primordial Follicles and the Dynamic Reserve of Antral Growing Follicles: What Is the

Link?" *Biology of Reproduction* 90 (March): 1–11. https://doi.org/10.1095/biolreprod.113.117077.

Namura, Shobu, Jinmin Zhu, Klaus Fink, Matthias Endres, Anu Srinivasan, Kevin J. Tomaselli, Junying Yuan, and Michael A. Moskowitz. 1998. "Activation and Cleavage of Caspase-3 in Apoptosis Induced by Experimental Cerebral Ischemia." *The Journal of Neuroscience* 18 (10): 3659–68. https://doi.org/10.1523/jneurosci.18-10-03659.1998.

Nandi, S., V. Girish Kumar, B. M. Manjunatha, and P. S.P. Gupta. 2007. "Biochemical Composition of Ovine Follicular Fluid in Relation to Follicle Size." *Development Growth and Differentiation* 49 (1): 61–66. https://doi.org/10.1111/j.1440-169X.2007.00901.x.

Nan X, Ng H-H, Johnson CA, Laherty CD, Turner BM, Eisenman RN, Bird A. 1998. Transcriptional repression by the methyl-CpG-binding protein MeCP2 involves a histone deacetylase complex. Nature 393:386–389.

Nimz M, Spitschak M, Fürbass R, Vanselow J.. The Pre-Ovulatory Luteinizing Hormone Surge Is Followed by Down-Regulation of CYP19A1, HSD3B1, and CYP17A1 and Chromatin Condensation of the Corresponding Promoters in Bovine Follicles. Mol. Reprod. Dev. 77: 1040–1048, 2010.

Ohanian, J, and V Ohanian. 2001. "Cellular and Molecular Life Sciences Sphingolipids in Mammalian Cell Signalling." *Cellular and Molecular Life Sciences* 58 (14): 2053–68. https://doi.org/10.1007/PL00000836.

Paulini, Fernanda, Renata Carvalho Silva, José Luiz Jivago de Paula Rôlo, and Carolina Madeira Lucci. 2014. "Ultrastructural Changes in Oocytes during Folliculogenesis in Domestic Mammals." *Journal of Ovarian Research* 7 (1): 1–12. https://doi.org/10.1186/s13048-014-0102-6.

Pan Z, Zhang J, Lin F, Ma X, Wang X, Liu H. Expression profiles of key candidate genes involved in steroidogenesis during follicular atresia in the pig ovary. Mol Biol Rep. 2012 Dec;39(12):10823-32. doi: 10.1007/s11033-012-1976-2.

Quirk, Susan M., Robert G. Cowan, and Rebecca M. Harman. 2013. "Role of the Cell Cycle in Regression of the Corpus Luteum." *Reproduction* 145 (2): 161–75. https://doi.org/10.1530/REP-12-0324.

Randle, Philip J. 1998. "Regulatory Interactions between Lipids and Carbohydrates: The Glucose Fatty Acid Cycle after 35 Years." *Diabetes/Metabolism Reviews* 14 (4): 263–83. https://doi.org/10.1002/(SICI)1099-0895(199812)14:4<263::AID-DMR233>3.0.CO;2-C.

Renaville, B., N. Bacciu, A. Comin, M. Motta, I. Poli, G. Vanini, and A. Prandi. 2010. "Plasma and Follicular Fluid Fatty Acid Profiles in Dairy Cows." *Reproduction in Domestic Animals* 45 (1): 118–21. https://doi.org/10.1111/j.1439-0531.2008.01264.x.

Saeed-Zidane, Mohammed, Lea Linden, Dessie Salilew-Wondim, Eva Held, Christiane Neuhoff, Ernst Tholen, Michael Hoelker, Karl Schellander, and Dawit Tesfaye. 2017. "Cellular and Exosome Mediated Molecular Defense Mechanism in Bovine Granulosa Cells Exposed to Oxidative Stress." *PLoS ONE* 12 (11): 1–24. https://doi.org/10.1371/journal.pone.0187569.

Sanchez-Lazo, Laura, Daphné Brisard, Sébastien Elis, Virginie Maillard, Rustem Uzbekov, Valérie Labas, Alice Desmarchais, Pascal Papillier, Philippe Monget, and Svetlana Uzbekova. 2014. "Fatty Acid Synthesis and Oxidation in Cumulus Cells Support Oocyte Maturation in Bovine." *Molecular Endocrinology* 28 (9): 1502–21. https://doi.org/10.1210/me.2014-1049.

Sanllehí, Pol, José Luis Abad, Josefina Casas, and Antonio Delgado. 2016. "Inhibitors of Sphingosine-1-Phosphate Metabolism (Sphingosine Kinases and Sphingosine-1-Phosphate Lyase)." *Chemistry and Physics of Lipids* 197: 69–81. https://doi.org/10.1016/j.chemphyslip.2015.07.007.

Serna, Jorge, David García-Seisdedos, Alberto Alcázar, Miguel Ángel Lasunción, Rebeca Busto, and Óscar Pastor. 2015. "Quantitative Lipidomic Analysis of Plasma and Plasma Lipoproteins Using MALDI-TOF Mass Spectrometry." *Chemistry and Physics of Lipids*. https://doi.org/10.1016/j.chemphyslip.2015.05.005.

Shabankareh, Hamed Karami, Nasroallah Moradi Kor, and Hadi Hajarian. 2013. "The Influence of the Corpus Luteum on Metabolites Composition of Follicular Fluid from Different Sized Follicles and Their Relationship to Serum Concentrations in Dairy Cows." *Animal Reproduction Science* 140 (3–4). Elsevier B.V.: 109–14. https://doi.org/10.1016/j.anireprosci.2013.06.018.

Silveira, Juliano C da, Ana Clara F C M de Ávila, Hannah L Garrett, Jason E Bruemmer, Quinton A Winger, and Gerrit J Bouma. 2018. "Cell-Secreted Vesicles Containing microRNAs as Regulators of Gamete Maturation." *Journal of Endocrinology* 236 (1): R15–27. https://doi.org/10.1530/JOE-17-0200.

Sinderewicz, Emilia, Katarzyna Grycmacher, Dorota Boruszewska, Ilona Kowalczyk-Zieba, Joanna Staszkiewicz, Tomasz ŚleZak, and Izabela Woclawek-Potocka. 2017. "Expression of Factors Involved in Apoptosis and Cell Survival Is Correlated with Enzymes Synthesizing Lysophosphatidic Acid and Its Receptors in Granulosa Cells Originating from Different Types of Bovine Ovarian Follicles." *Reproductive Biology and Endocrinology* 15 (1): 1–15. https://doi.org/10.1186/s12958-017-0287-9.

Tajima, Kimihisa, Makoto Orisaka, Takahide Mori, and Fumikazu Kotsuji. 2007. "Ovarian Theca Cells in Follicular Function." *Reproductive BioMedicine Online* 15 (5): 591–609. https://doi.org/10.1016/S1472-6483(10)60392-6.

Uzbekova, Svetlana, Sebastien Elis, Ana-Paula Teixeira-Gomes, Alice Desmarchais, Virginie Maillard, and Valerie Labas. 2015. "MALDI Mass Spectrometry Imaging of Lipids and Gene Expression Reveals Differences in Fatty Acid Metabolism between Follicular Compartments in Porcine Ovaries." *Biology* 4 (1): 216–36. https://doi.org/10.3390/biology4010216.

Wang, Qiming J. 2006. "PKD at the Crossroads of DAG and PKC Signaling." *Trends in Pharmacological Sciences* 27 (6): 317–23. https://doi.org/10.1016/j.tips.2006.04.003.

Warzych, Ewelina, Piotr Pawlak, Marcin Pszczola, Adam Cieslak, Zofia E. Madeja, and Dorota Lechniak. 2017. "Interactions of Bovine Oocytes with Follicular Elements with Respect to Lipid Metabolism." *Animal Science Journal* 88 (10): 1491–97. https://doi.org/10.1111/asj.12799.

Wen, Xiaowei, Yanping Kuang, Lixia Zhou, Baofeng Yu, Qiuju Chen, Yonglun Fu, Zheng Yan, et al. 2018. "Lipidomic Components Alterations of Human Follicular Fluid Reveal the Relevance of Improving Clinical Outcomes in Women Using Progestin-Primed Ovarian Stimulation Compared to Short-Term Protocol." *Medical Science Monitor : International Medical Journal of Experimental and*

Clinical Research 24: 3357–65. https://doi.org/10.12659/MSM.906602.

Yang, Hongyan, Yan Xie, Dongyu Yang, and Decheng Ren. 2017. "Oxidative Stress-Induced Apoptosis in Granulosa Cells Involves JNK, p53 and Puma." *Oncotarget* 8 (15): 25310–22. https://doi.org/10.18632/oncotarget.15813.

Yang, Yanbo, Minhyoung Lee, and Gregory D. Fairn. 2018. "Phospholipid Subcellular Localization and Dynamics." *Journal of Biological Chemistry* 293 (17): 6230–40. https://doi.org/10.1074/jbc.R117.000582.

Young, J. M., and A. S. McNeilly. 2010. "Theca: The Forgotten Cell of the Ovarian Follicle." *Reproduction* 140 (4): 489–504. https://doi.org/10.1530/REP-10-0094.

Zemski Berry, Karin A., Joseph A. Hankin, Robert M. Barkley, Jeffrey M. Spraggins, Richard M. Caprioli, and Robert C. Murphy. 2011. "MALDI Imaging of Lipid Biochemistry in Tissues by Mass Spectrometry." *Chemical Reviews* 111 (10): 6491–6512. https://doi.org/10.1021/cr200280p.

Zhang, Jia Qing, Ming Shen, Cheng Cheng Zhu, Feng Xiang Yu, Ze Qun Liu, Nazim Ally, Shao Chen Sun, Kui Li, and Hong Lin Liu. 2014. "3-Nitropropionic Acid Induces Ovarian Oxidative Stress and Impairs Follicle in Mouse." *PLoS ONE* 9 (2): 1–12. https://doi.org/10.1371/journal.pone.0086589.

Zurgil, Naomi, Elena Afrimzon, Yana Shafran, Ora Shovman, Boris Gilburd, Haim Brikman, Yehuda Shoenfeld, and Mordechai Deutsch. 2007. "Lymphocyte Resistance to Lysophosphatidylcholine Mediated Apoptosis in Atherosclerosis." *Atherosclerosis* 190 (1): 73–83. https://doi.org/10.1016/j.atherosclerosis.2006.02.013.

RESULTS (3)

3. Modulation des profils lipidiques des ovocytes bovins

Lors de ces études, réalisées sur les ovocytes bovins individuels, nous avons développé la méthodologie d'analyse des lipides par la spectrométrie de masse MALDI-TOF sur cellules entières (ICM-MS) et comparé les profils lipidiques entre les ovocytes aux différents états physiologiques.

3.1. Analyse des lipides dans les ovocytes bovins au cours de la maturation *in vitro*

Au cours de la maturation, l'ovocyte reprend sa première division méiotique accompagnée par la réorganisation structurale et biochimique de l'ooplasm (maturation cytoplasmique). L'ovocyte bovin est riche en lipides intracellulaires et la quantité totale de lipides change entre l'ovocyte immature (stade de prophase-I) et mature (stade de métaphase-II). L'objectif de cette étude a été de comparer les profils lipidiques des ovocytes avant et après maturation *in vitro* (MIV) par ICM-MS.

L'analyse différentielle des profils lipidiques a révélé un changement significatif de l'abondance relative de 101 masses sur 564 espèces moléculaires détectées, entre les ovocytes immatures et ceux maturés *in vitro* ($p<0.05$, différence supérieure à 2 fois). Parmi ces pics différentiels, nous avons identifiés des lipides de différentes classes: fatty acids (FA), lysophosphatidylcholine (LPC), phosphatidylethanolanime (PE), phosphatidylcholine (PC), sphingomyéline (SM), parmi lesquels les PCs sont les plus représentées. Ces différences de composition lipidique discriminant les ovocytes immatures des ovocytes matures par leur empreintes lipidiques, reflètent les changements membranaires et intracellulaires de l'ovocyte, dus à la fois à la modification de l'environnement ovocytaire et au métabolisme des acides gras propre à l'ovocyte.

Publication : **Bertevello P**, Ghazouani O, Banliat C, Elis S, Teixeira-Gomes AP, Maillard V, Labas V and Uzbekova S (2016). **MALDI-TOF mass spectrometry analysis of lipids in single bovine oocytes during IVM** 32. Scientific meeting of the AETE, Brazilian College of Animal Reproduction, Barcelone pp. 712 – *Prix meilleur poster*

3.2. Effet des AGPI n-3 sur les profils lipidiques des ovocytes bovins

Le traitement des complexes ovocyte-cumulus par l'acide docosahexaenoic (1µM DHA, C22 :6, acide gras polyinsaturé n-3) pendant les 24h de la MIV a amélioré la compétence de l'ovocyte au développement embryonnaire *in vitro* (Oseikria *et al.*, 2016). L'objectif de cette étude a été de déterminer les changements lipidiques des ovocytes et CC après ce traitement pour mieux comprendre le mécanisme d'action du DHA sur la qualité ovocytaire.

Les analyses par ICM-MS des lipides dans les ovocytes traités ou non par 1µM DHA pendant 24h de MIV n'ont révélées que peu de changement dans les ovocytes (3 espèces lipidiques sur 700 m/z) et les cellules de cumulus (7 sur 698 m/z). Néanmoins, l'abondance différentielle de certaines PC dans le cumulus et des FA, SM et LPC dans l'ovocyte permet de discriminer les groupes traités des non-traités. Nous avons posé l'hypothèse de l'action directe du DHA mais les voies de signalisation impliquées nécessitent plus d'investigations.

Publication: Elis S, Oseikria M, Vitorino Carvalho A, **Bertevello PS**, Corbin E, Teixeira-Gomes AP, Lecardonnel J, Archilla C, Duranthon V, Labas V, Uzbekova S. **Docosahexaenoic acid mechanisms of action on the bovine oocyte-cumulus complex**. J Ovarian Res. 2017 Nov 9;10(1):74. doi: 10.1186/s13048-017-0370-z.

3 Lipid profiling modulations in bovine oocytes

3.1 MALDI-TOF mass spectrometry analysis of lipids in single bovine oocytes during IVM

During this first study, we have developed the methodology of lipid analysis in single bovine oocytes using MALDI-TOF mass spectrometry. The experimental results reported here have been presented in 32nd Annual Scientific Meeting of European Embryo Technology Association (AETE) in 2016 in Barcelona (Spain) and received award of best poster presentation.

Bertevello P, Ghazouani O, Banliat C, Elis S, Teixeira-Gomes AP, Maillard V, Labas V and Uzbekova S (2016). 32. Scientific meeting of the AETE, Brazilian College of Animal Reproduction, Barcelone pp. 712

3.1.1 Abstract

During maturation, an oocyte resumes first meiotic division and passes through cytoplasm maturation. Bovine oocyte is rich in intracellular lipids which serve as energy storage, membrane structure and in signaling. We have recently showed that level of neutral lipids containing in lipid droplets was diminished during IVM (Auclair *et al.*, 2013). Our previous studies also revealed that Intact Cell Matrix-assisted laser desorption/ionization time of flight Mass Spectrometry (ICM-MS) was effective in determination of differential lipid profiling in bovine cumulus cells and allowed the discrimination of immature and mature oocytes (Sanchez-Lazo *et al.*, 2014). The objectives of this work were to adapt ICM-MS technology to single bovine oocytes and to compare their lipid profiles before and after *in vitro* maturation (IVM). Bovine oocyte-cumulus complexes were recovered from 4-6 mm ovarian follicles and 24h IVM was performed in maturation medium containing 10% of fatty acid-free fetal bovine serum, gonadotrophins and growth factors. Immature and mature oocytes were separated from cumulus cells, washed in PBS and kept in Tris-sucrose buffer at -80°C. Before analysis, individual oocytes were deposited on a MALDI sample plate, recovered with fresh 2,5-dihydroxyacetophenone (DHAP) matrix solution and air dried. Lipid spectral profiles (3000 shots per spectra) were acquired for each oocyte using an UltrafleXtreme MALDI-TOF/TOF instrument (Bruker) in negative and positive reflector ion mode. Spectra were processed and analyzed using Progenesis MALDI™ (Nonlinear Dynamics). M/z peaks were detected in the range of 160 to 1000 m/z and quantified using the values of normalized peak

heights. Coefficient of variation (CV %) was calculated for each m/z peak from 3 technical replicates using 20 immature oocytes. Multivariate Principal Component Analysis (PCA) and Student test were performed for hunting of lipid content variations between immature and mature oocytes (n=24). A total of 266 and 296 distinct peaks ranging from m/z 163.27 to 951.62 were detected in positive and negative mode, respectively. Mean CV% calculated for all the peaks was 32%. Considering a differential at $P < 0.01$ and a Fold Change >2, from positive mode, 72 peaks were differential (38 up- and 34 down-regulated during IVM). From negative mode, 29 peaks significantly changed their relative abundance during IVM (20 up- and 9 down-regulated). Immature and mature oocyte groups were therefore clearly discriminated by PCA. Several peaks could be annotated and belong to glycerophospholipid and sphingomyelin lipid categories. In conclusion, oocyte lipid content significantly varies during maturation and thus may reflect dynamics of lipid metabolism (synthesis, lipolysis) and structural modulations inside of the oocyte.

3.1.2 Introduction

Capacity of female germ cell, an oocyte, to be fertilized and to develop to viable embryo is acquired throughout meiotic maturation during pre-conceptual period in mammals. Transcription does not occur in the oocyte during this period, however significant modifications occur in the oocyte cytoplasm at protein and metabolite levels. A lot of energy is required to assure oocyte meiosis from prophase-I to metaphase-II and then early embryo development after fertilization. Bovine oocyte is rich in intracellular lipids concentrated in lipid droplets (LD), vesicles and membranes and these lipids are involved in membrane composition, intracellular signaling and energy storage. Lipid metabolism in oocyte-cumulus cell complex is very important for oocyte maturation and competence (Auclair *et al.*, 2013). Intact Cell Matrix-assisted laser desorption/ionization time of flight Mass Spectrometry (ICM-MS) analysis of lipid profiles of cumulus cells was able to discriminate immature and mature oocytes (Sanchez-Lazo *et al.*, 2014). The objective of this work was to adapt ICM-MS technology to single bovine oocyte and to compare lipid contents in the oocytes before and after *in vitro* maturation (IVM).

3.1.3 Materials and methods

Ethics

The approved experimental protocols by the local ethics committee were required (CEEA VdL, reference number of the protocol 2012-10-4 and 01607.02-Prolific project; and the protocol 2015-100115278976-v5-Bovomega3 Project), according to the directives of the French Council for animals protection.

Chemicals

All chemicals were purchased from Sigma-Aldrich (Saint-Quentin Fallavier, France). Internal standard mix for lipid identification was purchased from Avanti Polar Lipids, Inc (Alabaster, AL). Exceptions were indicated in the description of materials and methods.

Oocyte collection and *in vitro* maturation

Bovine ovaries were obtained from a commercial slaughterhouse and kept in a water bath at 37°C. Cumulus– oocyte complexes (COC) were recovery from bovine ovaries, washed with saline (0.9% w/v NaCl) at 37°C to remove blood and debris. Follicles were aspirated with a used 18-gauge needle attached controlled vacuum system (30mmHg) and the fluids allocated in independent 50 mL conical tubes. COCs were allowed to settle for 15 min and selected according to the cytoplasm aspect and number of cell layers. Only oocytes with homogeneous cytoplasm and more than three layers of cumulus cells were selected and denuded by repeated pipetting. Immature oocytes were separated individually from their cumulus cells (CC) by repetitive aspirating-ejecting movements using a P100 Gilson pipette in 100-µl drops under observation with a stereomicroscope, then rinsed twice in Tris-sucrose. The immature oocytes samples were snap-frozen in liquid nitrogen and kept at -80°C.

Selected COCs were washed several times in TCM199/HEPES medium supplemented with 50 mg/l gentamycin and 0.1% BSA. IVM was performed at 38.8°C for 22 h in a humidified atmosphere containing 5% CO2 in 500 µl of TCM199-enriched medium containing recombinant human (rh) epidermal growth factor (EGF, 10 ng/ml), rh insulin-like growth factor-I (IGF-I, 19 ng/ml), rh basic fibroblast growth factor (2.2 ng/ml), human chorionic gonadotropin (hCG, 5 IU/ml; Intervet, Beaucouze, France), pregnant mare serum gonadotropin (PMSG, 10 IU/ml; Intervet), rh insulin (5 µg/ml), rh transferrin (5 µg/ml), sodium selenite (5 ng/ml), L-cystein (90 µg/ml), β-mercaptoethanol (0.1 mM), ascorbic acid (75 µg/ml), glycine (720 µg/ml), glutamine (0.1 mg/ml), and pyruvate (110 µg/ml) as described (Donnay *et al.*, 2004). After IVM, the oocytes were stripped from CC, washed in Tris-sucrose as described. Oocytes were snap-frozen in liquid nitrogen and kept at -80°C. Analysis of immature and mature oocytes was performed together within no longer than 4 days after collection.

MALDI-TOF MS Analysis of lipids in immature and mature bovine oocytes.

Oocytes (n=12 per group) were thawed in ice and individually placed on the MTP Ground Steel 384 MALDI plate (Bruker Daltonics, Germany) to dry with 2.5µl of DHAP (2,5-dihydroxyacetophenone) matrix at 20 mg/mL solubilized in 90% methanol, 2% trifluoroacetic acid in water. Also spotted on plate an external calibration was performed using a mixture of small molecules and peptides (1 µL of calibrant solution containing Cafein, MRFA peptide, Leu-Enkephalin, Bradykinine 2-9, Glu1-fibrinopeptide B;

reserpine; Bradykinine; Angiotensine I) and mix in 1 µL of DHAP matrix. 3000 spectra per spot (as a sum of 1000 consecutive laser shots in 3 shot steps) were acquired, using Bruker UltrafleXtreme MALDI-TOF instrument (Bruker Daltonics, Germany). Spectra were acquired in positive ion modes using reflectron, in the m/z 160 – 1000 range. To increase mass accuracy (mass error < 0.05%), internal calibration was subsequently applied to all spectra. Lock mass correction was performed with highest intensity peak, corresponding to the glycerophosphocholine (PC 32:1, m/z 732.556) in positive mode, using FlexAnalysis 4.1 software (Bruker). Spectra (*.txt) were background subtracted, smoothed, aligned and normalized by the Total Ion Current (Progenesis MALDI™ software, Nonlinear Dynamics, Newcastle upon Tyne, UK). Peaks were detected with a signal/noise > 2.5. ANOVA was applied to log values of normalized peak heights. Differentially expressed m/z peaks were established to a probability value < 0.01. All molecular species with a differential fold change (FC) > 2 were selected for a principal components analysis (PCA).

3.1.4 Results and discussion

Lipid profiling on individual oocytes was performed and showed repeatability with low variability between the replicates (Figure 22). 266 peaks were detected; mean coefficient of variation calculated from all the peaks in all the samples was 32 %.

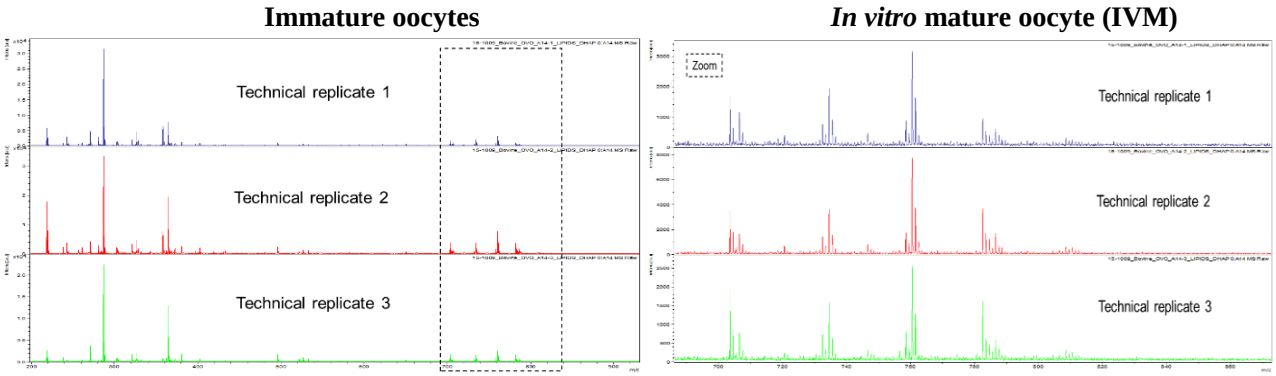


Figure 22. Lipid fingerprints of single bovine oocyte in the range 200-1000 m/z.

By differential analysis of lipid species abundance, 38 molecular species (m/z) increased in immature oocytes and 34 m/z in the oocytes after IVM as shown in a heatmap (**Figure 23**).

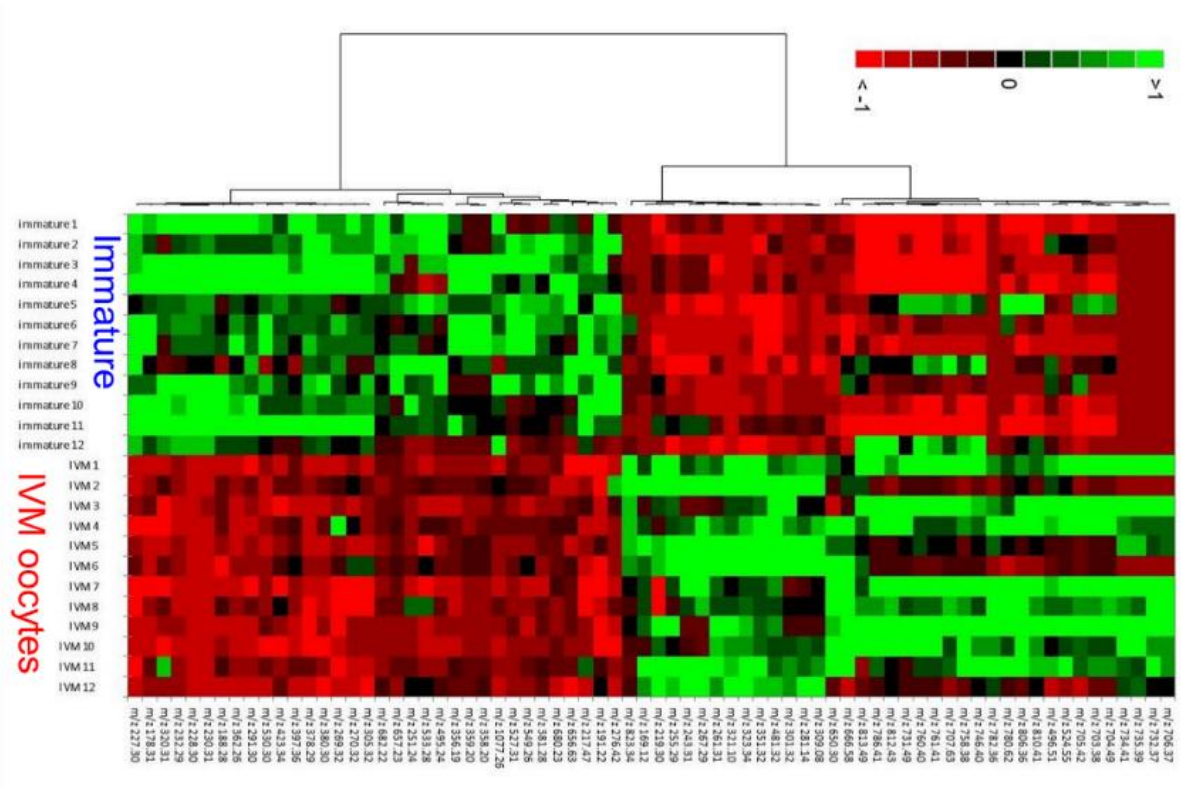


Figure 23. Heat map representation of differently abundant lipids in the oocytes before (immature, n=12) and after 22h IVM (n=12).

Principle Component Analysis shows that immature and mature oocytes were discriminated by their differential lipids **(Figure 24).**

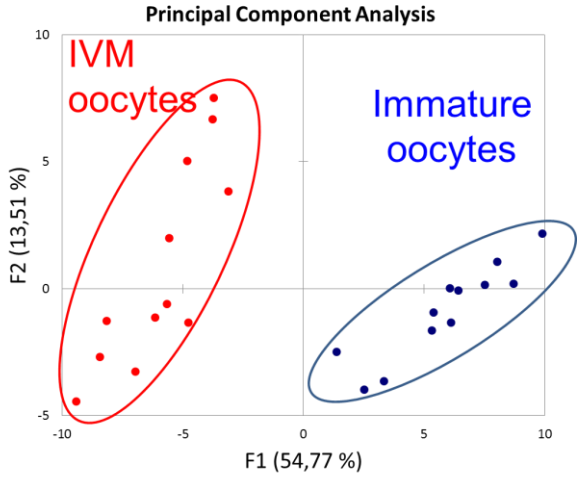


Figure 24. PCA of differently abundant lipids in immature and mature (22h IVM) bovine oocytes.

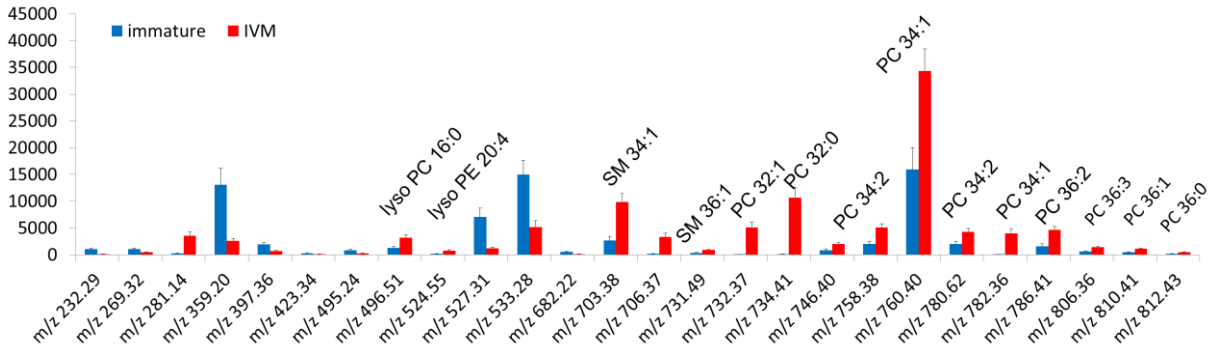


Figure 25. Relative abundance and identification of differential lipids detected in single immature and mature oocytes by ICM-MS lipid profiling.

Lipid ions that contributed to the separation of groups include phosphatidylcholines (PC) and sphingomyelins (SM) (m / z 700-1000), and fatty acids (FA) and lyso-phosphatidylcholines (LPC) (m / z 200-500). This shows that immature oocytes have smaller molecules and after IVM the lipid species found were more complex. Several major lipids were identified (top-down fragmentation of extracted lipids) and/or annotated (Lipid Maps); the identifications of differential lipids are shown in the table 1. Lipids over-represented in immature oocytes are in blue, and those more abundant after IVM are in red.

Table 3. Annotations of oocyte lipid species differently abundant during *in vitro* maturation

Ions	Lipid ID	Ions	Lipid ID
m/z 255,294 -	C16:0 Palmitic acid	**m/z 734,414 +**	PC 32:0 $[H]^+$
m/z 281,132 -	C18:1 Oleic acid	**m/z 746,398 +**	PE 36:1$[H]^+$ or PE35:5$[Na]^+$ or PC33:1$[H]^+$
m/z 283,283 -	Stearic acid	**m/z 758,382 +**	PC 34:2$[H]^+$ or PC33:6$[Na]^+$
m/z 303,107 -	Arachidonic acid	**m/z 760,393 +**	PC 34:1$[H]^+$
m/z 331,023 -	Adrenic acid	**m/z 766,573 -**	PE 38:4 $[H]^-$
m/z 496,514 +	LPC 16:0 $[H]^+$	**m/z 780,621 +**	PC 34:2$[Na]^+$
m/z 524,543 +	LPE 20:4 $[Na]^+$	**m/z 782,365 +**	PC36:4$[H]^+$ or PC 34:1$[Na]^+$
m/z 703,382 +	SM 34:1 $[H]^+$	**m/z 786,41 +**	PC 36:2$[H]^+$
m/z 706,371 +	PC 30:0 $[H]^+$	**m/z 806,375 +**	PC 36:3$[Na]^+$ or PC 38:6$[H]^+$
m/z 731,428 +	SM 36:1 $[H]^+$	**m/z 810,407 +**	PC 38:4$[H]^+$ or PS 36:2$[Na]^+$ or PC 36:1$[Na]^+$
m/z 732,377 +	PC 32:1 $[H]^+$	**m/z 812,43 +**	PC 38:3$[H]^+$ or PS 36:2$[H]^+$ or PC 36:0$[Na]^+$

Arachidonic acid and adrenic acid are deposited on phospholipid membranes. The enzymatic removal of linoleic acid hydrogens, an essential n-6 (linoleic acid; C18H32O2) produces these FAs, which have as its main function the anti-inflammatory responses by the biosynthesis of prostaglandins, thromboxanes and leukotrienes (Brown 2011). Abundance of this FAs in immature oocytes may indicate an alternative pathway of eicosanoid synthesis and therefore can be explored in ovarian physiology. The circulating lysophospholipids (LPC and LPE) are membrane components that are necessary to mediate the synthesis of various phospholipids and embed proteins into cell membranes (Drzazga 2014).

3.1.5 Conclusion

In conclusion, MALDI-TOF MAS **lipid profiling** on single bovine oocytes allowed discrimination of the oocytes in relation to their **maturation** state. A number of **lipid markers** related to oocyte meiotic maturation was reported in individual oocytes. Significant variation of lipid content in the oocytes before or after IVM may be due to both changes of oocyte environment and to proper intracellular FA composition leading to structural modifications in the oocyte during maturation.



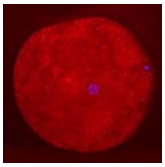
Bovine mature oocyte

MALDI-TOF mass spectrometry analysis of lipids in single bovine oocytes during IVM

Priscila Bertevello, Olfa Ghazouani, Sebastien Elis, Charles Banliat, Ana-Paula Teixeira-Gomes, Virginie Maillard, Valerie Labas and Svetlana Uzbekova

Physiologie de la Reproduction et des Comportements INRA, CNRS, Université de Tours, IFCE, F-37380 Nouzilly, France

Contact : svetlana.uzbekova@tours.inra.fr


Lipids in bovine mature oocyte (Nile Red staining)

INTRODUCTION

Capacity of female germ cell, an **oocyte**, to be fertilized and to develop to viable embryo is acquired throughout **meiotic maturation** during pre-conceptual period in mammals. Transcription doesn't occur in the oocyte during this period, however significant modifications occur in the oocyte cytoplasm at protein and metabolite levels. High energy production is required to assure oocyte meiosis from prophase-I to metaphase-II and then early embryo development after fertilization. Bovine oocyte is rich in **intracellular lipids** (Figure 1) concentrated in lipid droplets, vesicles and membranes and these lipids are involved in membrane composition, intracellular signaling and energy storage. **Lipid metabolism** in **oocyte-cumulus cell complex** is very important for oocyte **maturation** and competence (**1).* Intact Cell Matrix-assisted laser desorption/ionization time of flight Mass Spectrometry (**ICM-MS**) analysis of **lipid profiles** of **cumulus cells** was able to discriminate immature and mature oocytes *(*2).*

The **objective** of this work was to adapt ICM-MS technology to **single bovine oocyte** and to compare lipid contents in the oocytes before and after *in vitro* maturation (IVM).

EXPERIMENTAL APPROACHES AND RESULTS

Biological samples : bovine oocytes

Immature bovine oocytes were obtained by aspiration of ovarian follicles .

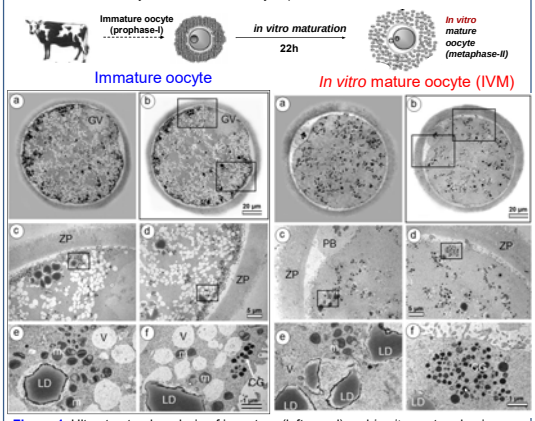
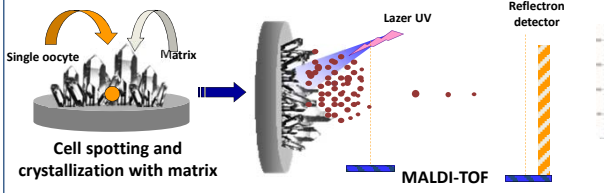


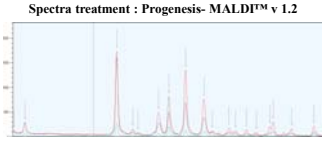
Figure 1. Ultrastructural analysis of immature (left panel) and *in vitro* mature bovine oocytes (right panel). (a) Representative image of semi-thin section of oocyte stained with toluidine blue and captured with a confocal microscope. (b) One of the following ultrathin section of the same oocyte obtained by the assembly of several electron microscopy microphotographs. Outlined rectangle surfaces are magnified in (c) and (d); (e) and (f) – magnification of outlined areas from (c) and (d) pictures, respectively. GV - germinal vesicle; PB – polar body; ZP – zona pelucida, **V – vesicle, LD - lipid droplet**, m – mitochondrion, CG – cortical granules. Bars: 20µm (a, b), 5 µm (c, d) and 1µm (e,f). (*From Auclair et al 2013 (*1*).

Lipid profiling : Intact Cell MALDI-TOF Mass Spectrometry on single oocyte



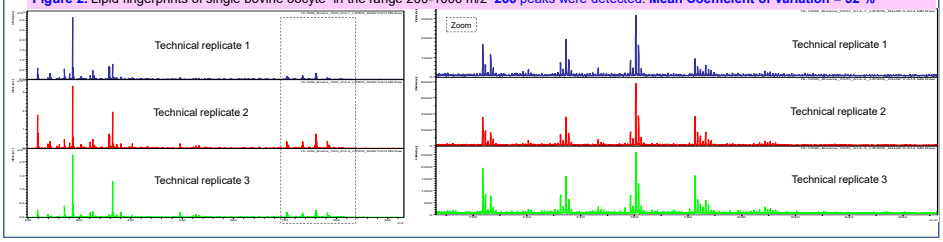
a) Oocytes were stripped from surrounded cells, washed in Tris-sucrose buffer and individually deposited on MALDI plate with 20 mg/mL DHAP / 90% methanol / 2% TFA / 8% H_2O

b) **Mass spectra** were recorded using a UltrafleXtreme MALDI-TOF/TOF instrument (Bruker Daltonics) in positive and reflectron ion mode. Spectral profiles were collected in the mass range **160-1000 m/z** with 3x1000 scans per spectrum and processed using FlexAnalysis version 3.4 (**Figure 2**)



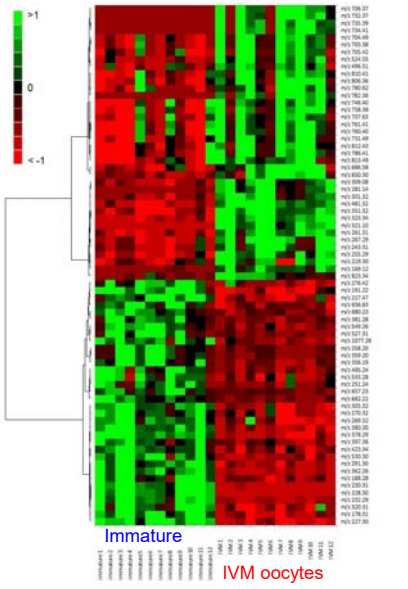
c) Spectra (*.txt) were background subtracted, smoothed, aligned and normalized by the Total Ion Current (Progenesis MALDI™ software, Nonlinear Dynamics). Peaks were detected with a signal/noise > 2.5. ANOVA was applied to log values of normalized peak heights. Differentially expressed m/z peaks were established to a probability value < 0.01. All molecular species with a differential fold change (FC) > 2 were selected for a principal components analysis (PCA).

Figure 2. Lipid fingerprints of single bovine oocyte in the range 200-1000 m/z **266** peaks were detected. **Mean Coefficient of Variation = 32 %**



Lipid markers of oocyte maturation : differential analysis of lipid species between immature and mature oocytes using lipid fingerprints by ICM-MS

Figure 3. Heat map representation of differently abundant lipids in the oocytes before (immature, n=12) and after 22h IVM (n=12)



- 38 molecular species (m/z) increased and 34 m/z during IVM (**Figure 3**)
- Immature and mature oocytes are discriminated by differential lipids (**Figure 4**)
- Several major lipids were identified (top-down fragmentation of extracted lipids) and/or annotated (Lipid Maps) (**Figure 5**)

Figure 4. PCA of differently abundant lipids in immature and mature (22h IVM) bovine oocytes

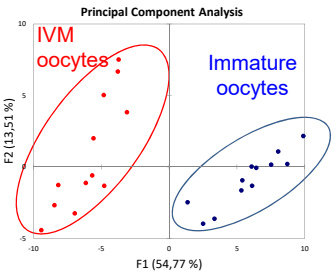
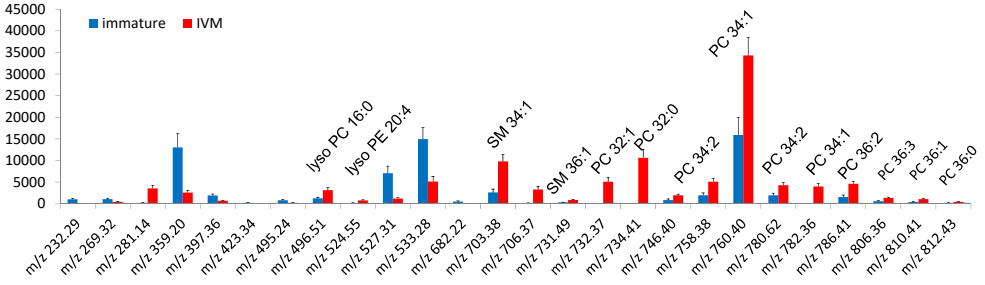


Figure 5. Relative abundance and identification of differential lipids detected in single immature and mature oocytes by ICM-MS lipid profiling



CONCLUSIONS

In conclusion, ICM-MS **lipid profiling** approach on single bovine oocyte allowed discrimination of the oocytes in relation to their **maturation** state. A number of **lipid markers** were revealed as m/z peaks which can be quantified in individual oocytes.

Lipid content significantly varied in the oocytes before or after IVM may be due to both changes of oocyte follicular environment and to proper intracellular fatty metabolism leading to structural modifications in the oocyte.

REFERENCES.

*1. Auclair, S, Uzbekov, R., Elis, S., Sanchez, L., Lardic, L., Dalbies-Tran, R. and **Uzbekova, S.** Absence of cumulus cells during in vitro maturation affected lipid metabolism in bovine oocyte. *Am J of Physiology Endocrinology and Metabolism* **2013** Mar 15;304(6):E599-613

*2. Sanchez-Lazo L, Brisard D, Elis S, Maillard V, Uzbekov R, Labas V, Desmarchais A, Papillier P, Monget P, **Uzbekova S**. Fatty acid synthesis and oxidation in cumulus cells support oocyte maturation in bovine. Mol Endocrinol. **2014** Sep;28(9):1502-21.

Centre de recherche Val de Loire,
UMR Physiologie de la Reproduction et des Comportements
37380 Nouzilly, France
www.val-de-loire.inra.fr
http://www7.tours.inra.fr/physiologie_reproduction_comportements

Funding :
- INRA, Region Centre Val-de-Loire subvention, project BOVOMEGA3
- Fellowship P.Bertevello : University do Estado do Rio Grande do Norte (Brazil)

2016

3.2 Effect of n-3 PUFA on lipid profiles on bovine oocytes as detected by MALDI-TOF mass spectrometry

3.2.1 Article 3

Elis S, Oseikria M, Vitorino Carvalho A, **Bertevello PS**, Corbin E, Teixeira-Gomes AP, Lecardonnel J, Archilla C, Duranthon V, Labas V, Uzbekova S. **Docosahexaenoic acid mechanisms of action on the bovine oocyte-cumulus complex**. J Ovarian Res. 2017 Nov 9;10(1):74. doi: 10.1186/s13048-017-0370-z.

In the present work, performed by Sebastien Elis and colleagues (Bovomega3 project), my goal was to compare MALDI MS lipid profiles between the oocytes and surrounding cumulus cells (CC) of the cumulus-oocyte complexes (COC) treated *in vitro* with low concentration of n-3 PUFA, 1 µM of docosahexaenoic acid (DHA, C22:6), during IVM. This 24 h DHA-treatment of COCs during IVM improved oocyte quality in terms of *in vitro* embryo development by increasing blastocyst rate from 17.6% to 30.6% in control and DHA-treated groups, respectively (Oseikria *et al.*, 2016) One of the objectives of this work was to see if lipid composition changes in the oocytes and CC during this treatment.

Comparative analysis of the lipid profiles was performed using MALDI-TOF mass spectrometry on individual intact oocytes and corresponding CC after 24 h IVM in the presence or absence of DHA 1 µM. Using positive acquisition mode (200-1000 m/z), 324 and 406 peaks were detected in CC and in the oocytes, respectively. Using negative acquisition mode (200-1000 m/z), 374 (in CC) and 294 peaks (in oocytes) were detected. Using differential analysis of lipid spectra (both positive and negative modes) between control and DHA-treated oocytes (n=15 per condition), only three peaks out 700 (m/z 387.24, 518.42 and 725.57) showed significantly lower abundance in DHA-treated oocytes ($p < 0.01$, $FC > 1.5$) and m/z 965.47 increased in DHA-treated oocytes: (**Figure 26A**). Peaks with m/z 518.42 and m/z 725.57 were formerly identified as LPC 16:0+Na+ and SM 34:1+Na+ and m/z 387.24 was annotated as potentially being an unsaturated fatty acyl. Principle component analysis discriminated the control and DHA groups; however, they partially overlapped (**Figure 26B**).

Lipid profiles of CC differed in seven peaks between the two groups (n=4 pools of CC per group), from 698 m/z detected ($p < 0.01$, fold-change > 1.5). The relative abundance of these seven lipids was

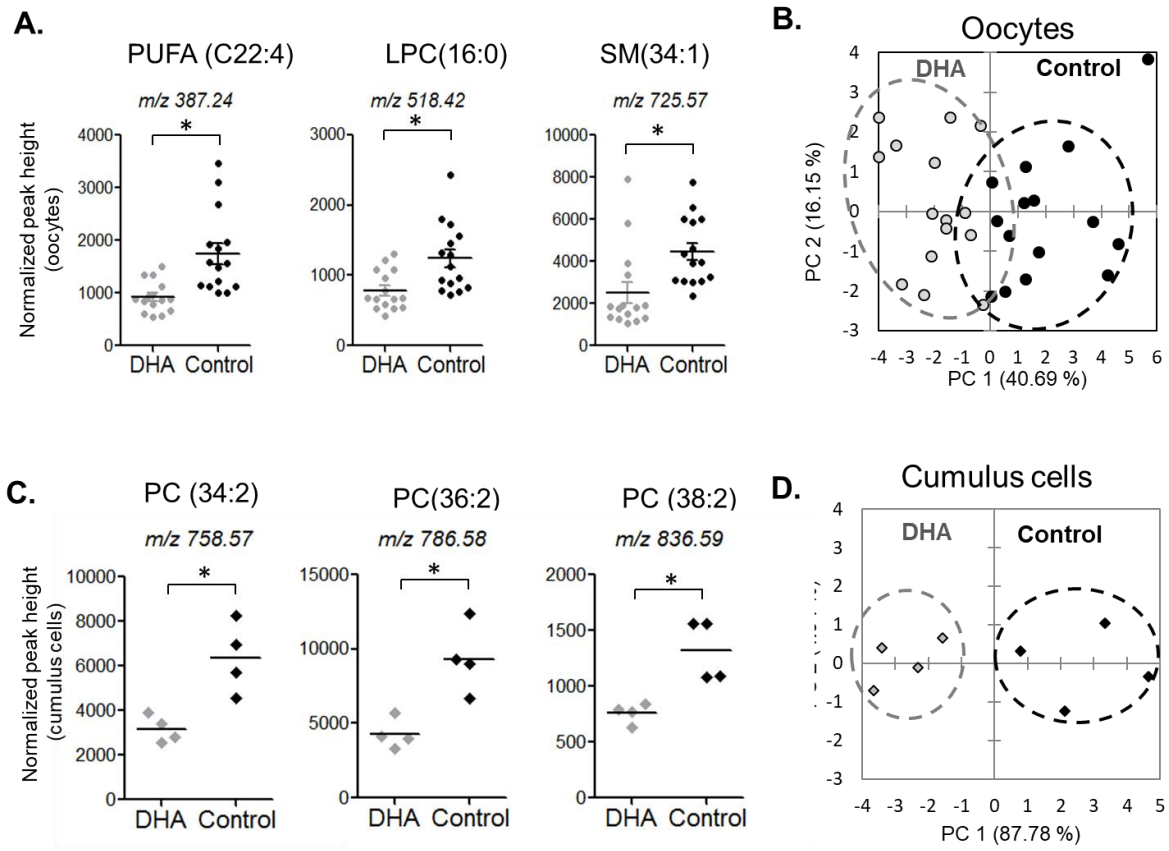


Figure 26. Analysis of lipid composition using MALDI-TOF mass spectrometry profiling in bovine oocytes and cumulus cells after 24h IVM with or without DHA 1 µM treatment. Individual oocytes (15 per group) and triplicates of pools of CC (4 per group) were analyzed. Relative abundance of lipid species in DHA-treated and control oocytes (A) and cumulus cells (C). Principle component analysis and scatter-plots of differential lipids in control vs. DHA-treated oocytes (B) and in cumulus cells (D).

significantly lower in DHA-treated cumulus cells compared to control (**Figure 26C**). The four most abundant m/z were previously identified as polyunsaturated phosphatidylcholine (PC): m/z 758.57 PC 34:2 +H+, m/z 784.56 as PC 34:0+Na+, m/z 786.58 as PC 36:2+H+ and m/z 836.59 as PC 38:2+Na+. Control and DHA groups were clearly discriminated by PCA (**Figure 26D**).

By comparing mature oocytes and their CC with or without DHA treatment during IVM, some modifications in the lipid composition were observed. In fact, we have previously shown that CC lipid fingerprints changed through IVM and were also affected by the inhibition of FA oxidation (Sanchez-Lazo *et al.*, 2014).

In this study, the reduction in lysophosphatidylcholine (LPC) observed in DHA treated oocytes may be relevant to a potential increase in a lysophosphatidic acid (LPA), as LPC is a precursor of LPA. It has been reported that DHA could inhibit LPA-induced proliferation in breast or prostate cancer cells (Liu *et al.*, 2014; Hopkins *et al.*, 2016). It has already been described that LPA can improve bovine oocyte maturation (Boruszewska *et al.*, 2015). A potential increase in LPA could, therefore, explain some of the beneficial effects of DHA on oocyte quality. Globally, the changes observed in the lipid composition of CC and oocytes were limited, which could be explained by the very similar lipid composition (mainly brought by the calf serum) of the medium and exhibiting only a 1 µM DHA difference.

Conclusion

Overall, despite functional differences between DHA-treated and control oocytes, only moderate changes in the oocyte and CC lipid composition were observed. These results may support the hypothesis of a direct effect on signaling pathways, notable through binding with free fatty acid receptor 4, largely investigated in this study (Elis *et al.*, 2017).

Elis et al. Journal of Ovarian Research (2017) 10:74
DOI 10.1186/s13048-017-0370-z

Journal of Ovarian Research

RESEARCH Open Access

Docosahexaenoic acid mechanisms of action on the bovine oocyte-cumulus complex

Sebastien Elis[1*†], Mouhamad Oseikria[1†], Anais Vitorino Carvalho[1,2], Priscila Silvana Bertevello[1], Emilie Corbin[1], Ana-Paula Teixeira-Gomes[3,4], Jérôme Lecardonnel[5], Catherine Archilla[2], Véronique Duranthon[2], Valérie Labas[1,4] and Svetlana Uzbekova[1,4]

Abstract

Background: Supplementation of bovine oocyte-cumulus complexes during in vitro maturation (IVM) with 1 μM of docosahexaenoic acid (DHA), C22:6 n-3 polyunsaturated fatty acid, was reported to improve in vitro embryo development. The objective of this paper was to decipher the mechanisms of DHA action.

Results: Transcriptomic analysis of 1 μM DHA-treated and control cumulus cells after 4 h IVM showed no significant difference in gene expression. MALDI-TOF mass spectrometry analysis of lipid profiles in DHA-treated and control oocytes and cumulus cells after IVM showed variations of only 3 out of 700 molecular species in oocytes and 7 out of 698 species in cumulus cells ($p < 0.01$).
We showed expression of free fatty acid receptor *FFAR4* in both oocytes and cumulus cells, this receptor is known to be activated by binding to DHA. FFAR4 protein was localized close to the cellular membrane by immunofluorescence. Functional studies demonstrated that supplementation with FFAR4 agonist TUG-891 (1 μM or 5 μM) during IVM led to an increased blastocyst rate (39.5% ± 4.1%, 41.3% ± 4.1%), similar to DHA 1 μM treatment (39.2% ± 4.1%) as compared to control (25.2% ± 3.6%).
FFAR4 activation via TUG-891 led to beneficial effect on oocyte developmental competence and might explain in part similar effects of DHA.

Conclusions: In conclusion, we suggested that low dose of DHA (1 μM) during IVM might activate regulatory mechanisms without evident effect on gene expression and lipid content in oocyte-cumulus complexes, likely through signaling pathways which need to be elucidated in further studies.

Keywords: Bovine, Oocyte-cumulus complex, FFAR4, DHA, Oocyte maturation

Background

Polyunsaturated fatty acids (PUFA) belong to a family of biologically active fatty acids (FA) known to have numerous health benefits [1]. Among them, n-3 PUFA, α-linolenic acid (ALA, C18:3 n-3), eicosapentaenoic acid (EPA, C20:5 n-3) and docosahexaenoic acid (DHA, C22:6 n-3) are essential FA, especially because mammals cannot produce ALA, which is the precursor of EPA and DHA. DHA, the longest member of this family, can be produced from ALA and EPA; however, the efficiency of the necessary elongation and desaturation reactions in mammals is low, and the most extensive source of DHA is therefore the diet, particularly seafood [2, 3]. In several organisms, DHA has been described as exerting pleiotropic effects at both the central and peripheral levels (i.e. brain, heart, inflammation) [4–6].

Among their physiological roles, n-3 PUFA affect reproduction in cattle [7, 8]. Indeed, an n-3 PUFA-enriched diet led to a significant increase or a tendency toward a higher presumptive conception rate [9–11] or reduced early embryo loss in cows [8–10, 12]. Moreover, an n-3 PUFA diet also directly affected the cleavage rate and tended to increase the blastocyst rate after in vitro maturation (IVM) and in vitro fertilization (IVF) in cows [13, 14]. We also reported in a previous

* Correspondence: sebastien.elis@inra.fr
†Equal contributors
[1]UMR PRC, CNRS, IFCE, INRA, Université de Tours, 37380 Nouzilly, France
Full list of author information is available at the end of the article

BioMed Central

© The Author(s). 2017 **Open Access** This article is distributed under the terms of the Creative Commons Attribution 4.0 International License (http://creativecommons.org/licenses/by/4.0/), which permits unrestricted use, distribution, and reproduction in any medium, provided you give appropriate credit to the original author(s) and the source, provide a link to the Creative Commons license, and indicate if changes were made. The Creative Commons Public Domain Dedication waiver (http://creativecommons.org/publicdomain/zero/1.0/) applies to the data made available in this article, unless otherwise stated.

RESULTS (4)

4. Modulation des profils lipidiques des cellules folliculaires somatiques

4.1. Comparaison des profils lipidiques et de l'expression des gènes dans les cellules de la granulosa et les cellules du cumulus chez le bovin.

Les cellules de cumulus (CC) sont des cellules spécialisées issues des cellules de la granulosa (CG). Les deux types cellulaires contribuent à la régulation de l'ovogenèse et peuvent refléter la qualité des ovocytes.

L'objectif de cette étude était de comparer les lipides intracellulaires et l'expression de gènes régulant le métabolisme des lipides entre ces 2 compartiments. 15% des espèces moléculaires détectées changent significativement leur abondance en fonction du type cellulaire et parmi ces lipides on trouve les sphingomyélines (SM) et différents glycerophospholipides (PC, LPC, PS, PE).

L'analyse transcriptomique a mis en évidence l'expression différentielle de nombreux gènes du métabolisme des carbohydrates et des lipides entre les CG et CC.

Ces deux analyses soulignaient des différences fonctionnelles entre ces deux types cellulaires, qui pourraient être en partie dues à la proximité de l'ovocyte pour les CC et de la thèque vascularisée pour les CG. Les CG pourraient utiliser ces phospholipides et le cholestérol pour les structures membranaires et la signalisation afin de guider le développement du follicule vers l'atrésie ou la dominance folliculaire, tandis que les CC conservent leur fonction de nutrition et de protection de l'ovocyte qui l'entoure.

Publication : **Bertevello, P**., Banliat C, Teixeira-Gomez Ap, Elis S, Maillard V, Carvalho, A, Duranthon V, Labas V, Uzbekova S. (2017). **Comparison of lipid profiles and gene expression in granulosa and cumulus cells in bovine**. 33th Annual Meeting of the European Embryo Transfer Association (AETE). Bath, Brazilian College of Animal Reproduction. **14 (3):** 970.

4.2. Analyse des lipides dans les cellules de la granulosa des vaches laitières en post-partum avec régimes de différents niveaux d'énergie.

Cette étude nous a permis de comparer les cellules de granulosa récupérées *in vivo* chez les vaches en lactation, nourries avec des régimes à apports énergétiques différents. Ces régimes n'ont pas changé la majorité des variables de la fonction reproductive chez ces vaches, sauf l'activité lutéale après la première mise bas (Mellouk et al., 2017; Ntallaris et al., 2017).

La comparaison des profils lipidiques des CG obtenus par ICM-MS n'a pas révélé de changement significatif entre les groupes d'animaux suivant ces différents régimes, une forte variabilité des échantillons pourrait en être une des causes.

Publication : **Bertevello P**, Labas V, Dalbies-Tran R, Touze JL, Dupont M, Briant E, Papillier P, Corbin E, and Uzbekova S. **Analysis of lipid profiling by MALDI-TOF mass spectrometry in granulosa cells of postpartum Holstein dairy cows**, 18th International Congress on Animal Reproduction (ICAR) 2016 – Tours, France, 28th to 30th June 2016

4 Lipid profiling modulations in somatic cells

4.1 Comparison of lipid profiles and gene expression in granulosa and cumulus cells in bovine.

Bertevello, P., et al. (2017). Comparison of lipid profiles and gene expression in granulosa and cumulus cells in bovine. 33th Annual Meeting of the European Embryo Transfer Association (AETE). Bath, Brazilian College of Animal Reproduction. **14 (3):** 970.

Abstract

In order to decipher more differences between originally related the cumulus and granulosa cells, we performed m/z detection and differential analysis on CC and GC fingerprints, obtained by MALDI-TOF MS. In fact, CC derive from GC during follicular growth and antrum formation and are coupled with an oocyte. Fatty acid (FA) synthesis and oxidation in GC impact cell proliferation and steroidogenesis (Elis *et al.*, 2015) whereas in CC these processes are crucial for oocyte maturation (Sanchez-Lazo *et al.*, 2014). Both GC and CC contribute to oogenesis and reflect oocyte quality.

The objective of this study was to compare intracellular lipids and lipid related transcripts between these compartments. Lipid profiles obtained using MALDI-TOF mass spectrometry were compared between GC from individual follicles (n=12) and pools of CC (n=12) aspirated from 4-5 mm follicles of slaughtered cows. Freshly isolated cells were analyzed using UltrafleXtreme MALDI-TOF/TOF instrument (Bruker) in positive (+) and negative (-) reflector mode, with 2,5-dihydroxyacetophenone matrix. Peaks were detected in 100 -1000 m/z range and values of the normalized peak heights (NPH) were quantified using Progenesis MALDI™ (Nonlinear Dynamics). Student test were applied to NPH values for hunting lipid content variations between GC and CC. Peaks were annotated using MS/MS fragmentation confronted to lipid databases.

Lipid fingerprints from CC and GC gathered 462 peaks in (+) and 486 peaks in (-) modes, with coefficients of variation = 27% for CC and 18% for GC. 143 species were significantly upregulated in CC ($p<0.01$, fold change >2.0). Among them, 2 lyso-phosphatidylcholines (LPC 20:4 and 20:3) 12

phosphatidylcholines (PC), and 12 sphingomyelins (SM) were identified. Among 44 molecular forms which were more abundant in GC, we identified LPC (14:0), 4 PC, ceramide (22:1), SM (15:1), phosphatidylethanolamines (28:0 and 38:7) and phosphatidylserine (29:0). 4 m/z were annotated as triglycerides.

Gene expression in pools of CC (n=4) and GC (n=4) was analyzed using a customized 60K bovine microarray (Agilent technology, 61326 probes). Differential analysis revealed 2009 differentially expressed genes (DEG) which were up-regulated in CC and 694 in GC ($p<0.05$, Benjamini-Hochberg correction). DEG showed significant enrichment in the pathways related to carbon metabolism, glycolysis /gluconeogenesis, ATP-binding cassette transporters, amino acid and O-glycan biosynthesis, thyroid hormone, PI3K-Akt signaling, p53 and PPAR signaling pathway (corrected $p \leq 0.05$). Among the DEG related to lipid metabolism and regulated by PPARs, genes *ACOX2, LPL, SCD, PPARG, FABP3, FADS2, ACADL, SLC27A2* were up-regulated in CC and *CPT1A, CPT1B, SCD5, PLTP* were more expressed in GC. Ten sphingolipid metabolism genes were over-expressed in CC.

In conclusion, all these differences underlined functional differences between these two cell types, which may be influenced by the proximity of the oocyte for CC and vascularized theca layers for GC. Metabolically, the GC are the suppliers of phospholipids of membrane and cholesterol, indicative of signaling mediation for the development of the follicle, among them atresia and follicular dominance, while CC maintain their function of nutrition and protection of the developing enclosed oocyte.

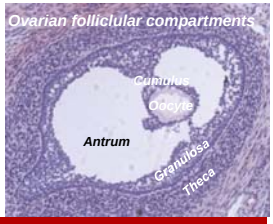
COMPARISON OF LIPID PROFILES AND GENE EXPRESSION IN GRANULOSA AND CUMULUS CELLS IN BOVINE

Priscila Bertevello[1], **Charles Banliat**[1], **Ana-Paula Teixeira-Gomes**[1], **Sebastien Elis**[1], **Virginie Maillard**[1], **Anaïs Vitorino Carvalho**[2], **Véronique Duranthon**[2], **Valérie Labas**[1], **and Svetlana Uzbekova**[1].

[1] *INRA, UMR Physiologie de la Reproduction et des Comportements F-37380 Nouzilly, France*

[2] *INRA, UMR Biologie du Développement et de la Reproduction, F-78352 Jouy en Josas, France*

Contact : *priscila.bertevello@inra.fr*
svetlana.uzbekova@inra.fr



INTRODUCTION

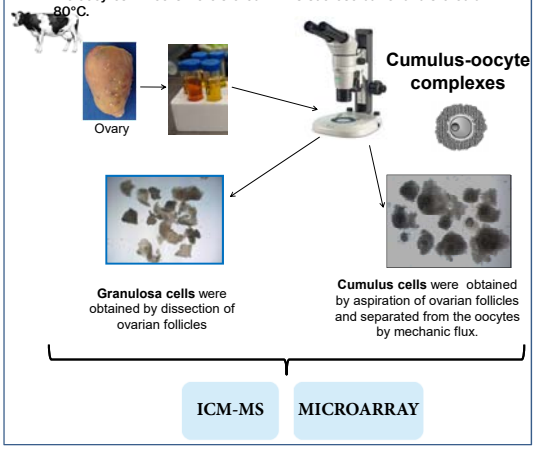
Cumulus cells (CC) derive from granulosa cells (GC) during follicular growth and antrum formation and are coupled with an oocyte. Fatty acid (FA) synthesis and oxidation in GC impact cell proliferation and steroidogenesis [*1] whereas in CC these processes are crucial for oocyte maturation [*2]. Both GC and CC contribute to oogenesis and reflect oocyte quality. **Lipid metabolism** in **cumulus cell** regulate oocyte metabolisation of **intracellular lipids** concentrated in lipid droplets, vesicles and membranes. These lipids are involved in energy storage, membrane composition and intracellular signaling [*3]. In-depth delineation of lipid metabolism in GC and CC is significant to open new insights into physiology and energy metabolism, and provide potential biomarkers with greater accuracy for improved characterization of follicle.

The **objective** of this work was to compare intracellular lipids using Intact Cell Matrix-assisted laser desorption/ionization time of flight Mass Spectrometry (**ICM-MS**) and lipid metabolism related transcripts between these compartments. Here, we performed lipidomic and transcriptomic analysis of granulosa and cumulus in order to identify potential lipid and transcript markers discriminating these cells in bovine follicles.

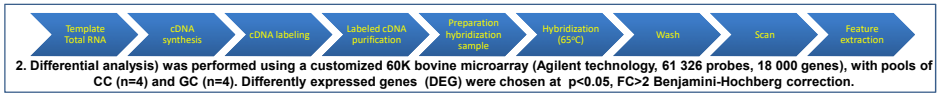
EXPERIMENTAL APPROACHES AND RESULTS

Biological samples : bovine cells

Bovine ovaries were collected from slaughterhouse. Follicles of 8 to 12 mm were dissected to obtain Granulosa cells (GC). Cumulus-oocyte complexes were recovered from fluid aspirated using a vacuum system from the follicles of 3-8 mm. Cumulus cells (CC) were separated from the oocytes. All cells were stored in Tris-sucrose buffer and stored at -80°C.

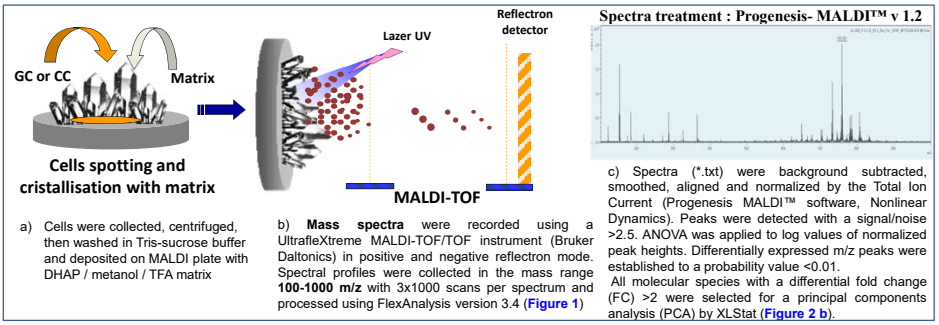


Workflow for sample preparation and array processing



2. Differential analysis) was performed using a customized 60K bovine microarray (Agilent technology, 61 326 probes, 18 000 genes), with pools of CC (n=4) and GC (n=4). Differently expressed genes (DEG) were chosen at p<0.05, FC>2 Benjamini-Hochberg correction.

Lipid profiling : Intact Cells MALDI-TOF Mass Spectrometry on cells



a) Cells were collected, centrifuged, then washed in Tris-sucrose buffer and deposited on MALDI plate with DHAP / metanol / TFA matrix

b) **Mass spectra** were recorded using a UltrafleXtreme MALDI-TOF/TOF instrument (Bruker Daltonics) in positive and negative reflectron mode. Spectral profiles were collected in the mass range **100-1000 m/z** with 3x1000 scans per spectrum and processed using FlexAnalysis version 3.4 (**Figure 1**)

c) Spectra (*.txt) were background subtracted, smoothed, aligned and normalized by the Total Ion Current (Progenesis MALDI™ software, Nonlinear Dynamics). Peaks were detected with a signal/noise >2.5. ANOVA was applied to log values of normalized peak heights. Differentially expressed m/z peaks were established to a probability value <0.01.
All molecular species with a differential fold change (FC) >2 were selected for a principal components analysis (PCA) by XLStat (**Figure 2 b**).

Figure 1. Lipid fingerprints of bovine somatics cells in the range 100-1000 m/z. Spectra were generated in positive (a.) and negative (b.) mode. 462 (+) and 486 (-) peaks were detected, showing the most abundant lipid species (showed below):

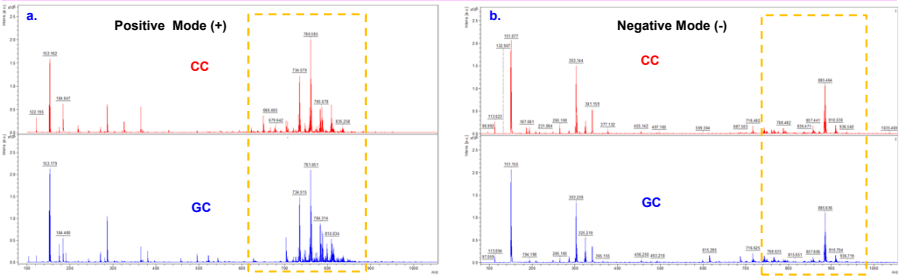


Figure 2. PCA discriminated CC and GC using differently abundant in **a. lipids species** (by ICM-MS) and **b. genes** (by Microarray) in bovine follicles.

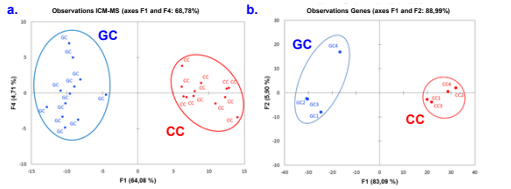


Figure 3. Heat map representation of differently abundant : **a.** 147 **lipid species by ICM-MS** (n=12) ;**b. 96 lipid metabolism genes** from µarray analysis differently expressed between **CC** and **CG** (n=4)

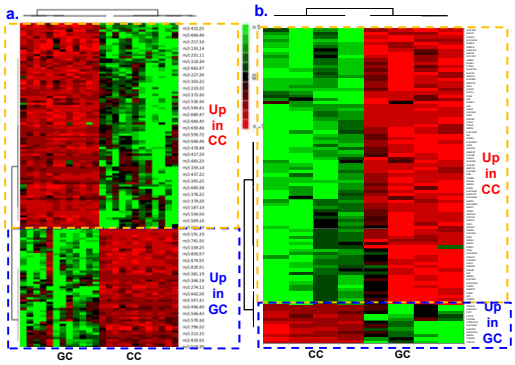
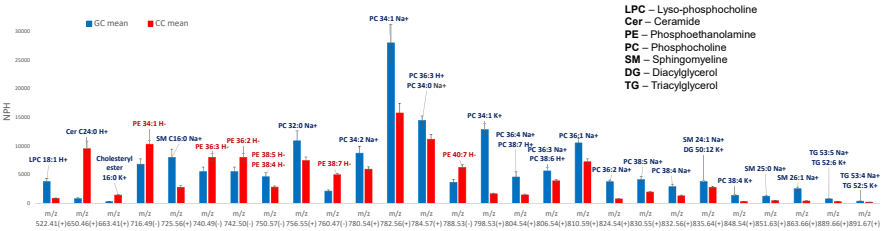


Figure 4.
Relative abundance of several identified differential lipids (p< 0.01). PC, SM and TG are more presented in GC whereas Cer, Cholesterol ester and PE were more abundant in CC.



GO analysis of differentially expressed genes (750 genes up-regulated in CC and 276 in GC) :

- DEGs up-regulated **in CC** showed significant enrichment in glycolytic process, response to hypoxia, lipid transport and pathways related to carbon metabolism and synthesis of amino acids, 109 DEGs were related to lipid metabolism.
- DEGs up-regulated **in GC** showed significant enrichment in the pathways related to extracellular matrix formation, regulation of GTPase activity, PI3K-Akt and MAPK3/1 signaling pathways, and 25 DEGs were related to lipid metabolism.

CONCLUSIONS

In conclusion, differential analysis of lipid profiles and gene expression between granulosa and cumulus bovine cells allowed clear discrimination of these types of ovarian follicular cells. A series of **gene and lipid markers** revealed that CC may function to metabolize glucose and glycerol to produce lipids for membranes and energy reserve to an oocyte. GC showed more abundance in TG possibly as energy reserve to steroids production. More abundant PC, SM coupled to overexpression of the genes related to secretion and signaling in GC highlighting their involvement in membrane production and maintenance.

REFERENCES:
*1. Elis S, Desmarchais A, Maillard V, Uzbekova S, Monget P, Dupont J., 2015 **Cell proliferation and progesterone synthesis depend on lipid metabolism in bovine granulosa cells.** Theriogenology. **2015**, 83(5):840-53
*2. Sanchez-Lazo L, Brisard D, Elis S, Maillard V, Uzbekov R, Labas V, Desmarchais A, Papillier P, Monget P, Uzbekova S. **Fatty acid synthesis and oxidation in cumulus cells support oocyte maturation in bovine.** Mol Endocrinol. **2014** Sep;28(9):1502-21.
*3. Auclair, S, Uzbekov, R., Elis, S., Sanchez, L., Lardic, L., Dalbies-Tran, R. and Uzbekova, S. **Absence of cumulus cells during in vitro maturation affected lipid metabolism in bovine oocyte.** *Am J of Physiology Endocrinology and Metabolism* **2013** Mar 15;304(6):E599-613

Centre de recherche Val de Loire,
UMR Physiologie de la Reproduction et des Comportements
37380 Nouzilly, France
www.val-de-loire.inra.fr
http://www7.tours.inra.fr/physiologie_reproduction_comportements

Funding :
- INRA, Region Centre Val-de-Loire subvention, project BOVOMEGA3
- Fellowship P.Bertevello : University do Estado do Rio Grande do Norte (Brazil)

2017

4.2 Analysis of lipids in granulosa cells of postpartum Holstein dairy cows fed with diets with differing energy levels.

Bertevello P, Labas V, Dalbies-Tran R, Touze JL, Dupont M, Briant E, Papillier P, Corbin E, and Uzbekova S. Analysis of lipid profiling by MALDI-TOF mass spectrometry in granulosa cells of postpartum Holstein dairy cows, 18th International Congress on Animal Reproduction (ICAR) 2016 – Tours, France, 28th to 30th June 2016

This work was a part of PROLIFIC project (coordinated by Joelle Dupont), and the aim of my work was lipidomic analysis of biological material obtained by ovum pick up from the cows fed with nutriments of different energy uptake.

During lactation, dairy cows present negative energy balance which could in part explain their suboptimal fertility through postpartum period. Ovarian activity may be affected through this period by modulating fatty acid (FA) metabolism inside the follicle whereas follicular environment is crucial for developmental potential of enclosed oocyte. FA metabolism play an important role in follicular granulosa cells (GC) functionality and these cells can accumulate lipids (Elis *et al.*, 2015).

We recently showed that Intact Cell Matrix-assisted laser desorption/ionization time of flight Mass Spectrometry (ICM-MS) was effective in determination of differential lipid profiling in bovine cumulus cells and thus allowed the discrimination of immature and mature oocytes (Sanchez-Lazo *et al.*, 2014).

The objective was to adapt this MS technology to bovine granulosa cells (GC) and to compare GC lipid fingerprints between Holstein dairy cows receiving either high or low energy diets (HE or LE), respectively.

Cows from one month before calving and during two lactation were fed either HE diet calculated to yield 35 kg of milk/cow per day (n = 17) or a LE diet calculated to yield 25 kg of milk/cow per day (n = 22). Immature 4-10 mm follicles were aspirated by ovum pick up from lactating cows at 80-100 days postpartum receiving either HE or LE diets, bearing 25% difference in energy supply. Healthy mural granulosa biopsies from HE (n=11) and LE (n=18) cows were recovered and kept at -80°C. GC biopsies were sonicated in matrix solution containing 2,5-dihydroxyacetophenone/ methanol and trifluoroacetic acid, deposited on a MALDI plate and recovered with fresh matrix. Lipid spectral profiles (5000 spectra per technical replicate) were acquired using an UltrafleXtreme MALDI-TOF/TOF instrument (Brucker)

first in positive and then in negative reflector ion mode. Spectra were analyzed using Progenesis MALDI™ (Nonlinear Dynamics). M/z peaks were detected in the range of m/z 160 to m/z 1000 and quantified using the values of normalized peak heights. Coefficient of variation (CV %) was calculated for each m/z peak as (SD/mean)*100 of 6 technical replicates in all GC samples (n=29). Multivariate Principal Component Analysis (PCA) and Student test was performed for hunting of lipid content variations between conditions.

A total of 146 and 190 distinct peaks ranging from m/z 163.22 to 965.95 were detected in positive and negative mode, respectively. Mean CV% calculated for all the peaks from all GC samples was 36.4 % for positive and 32.5% for negative mode. Considering a differential at $p<0.01$ and a fold change >2, no lipid species in m/z range (m/z 400-1000) showed significantly higher abundance in HE group compared to LE diet group. However, five differential peaks in low m/z range (m/z 192.65, 264.33, 300.35, 302.37 and 340.43; $p<0.05$, fold change >2) were observed, but principle component analysis failed to discriminate clearly the HE and LE groups, indicating faint differences of lipid composition between the diet groups.

Analysis of production and reproductive variables of HE and LE cows were reported (Mellouk et al., 2017; Ntallaris et al., 2017). In fact, dry matter intake and energy balance in animals fed a LE diet were significantly lower than that of animals fed a HE diet in the first lactation. Body weight, milk production, back fat thickness, and plasma concentrations of FAs, glucose, and insulin were not affected by diet, whereas plasma leptin and adiponectin concentrations were lower and plasma resistin concentrations higher in animals fed the LE diet. No effect of diet was found on reproductive variables between HE and LE groups. Our lipidomic analysis of ovarian GC also did not revealed significant changes between HE and LE diet groups. However, the commencement of luteal activity after first calving occurred sooner and the frequency of LH pulses was higher in the HE group than in the LE group. It was suggested that dietary energy content in the range applied here can alter the resumption of ovarian activity and LH pulsatility without affecting fat mobilization (Mellouk et al., 2017; Ntallaris et al., 2017).

Thus, no significant effect of employed energy diets on lipid content of granulosa cells was observed in postpartum cows that suggests that follicular cells were not differently affected by HE and LE diets. Possible lipid oxidation during relatively long storage of the samples at -80°C (due to a longue period of numerous OPU sessions) could also influence the integrity of lipid composition of GC, and therefore mask the eventual differences. Therefore, further studies are necessary to determine how influences of diets with different energy intake may influence the metabolism of other follicular compartments and possibly in animal reproduction.

Analysis of lipid profiling by MALDI-TOF mass spectrometry in granulosa cells of postpartum Holstein dairy cows

Bertevello PS, Labas V, Dalbies-Tran R, Dupont J, Touze JL, Dupont M, Briant E, Papillier P, Corbin E. and Uzbekova S.

UMR PRC INRA - CNRS - Université de Tours - IFCE,
Team « BINGO-Biologie Intégrative de l'Ovaire » & Mass Spectrometry Laboratory
(*Platform PAIB² « Analyse Integrative des Biomolécules et Phénomique des Animaux d'Intérêt Bio-agronomique »*)
F-37380, Nouzilly, FRANCE

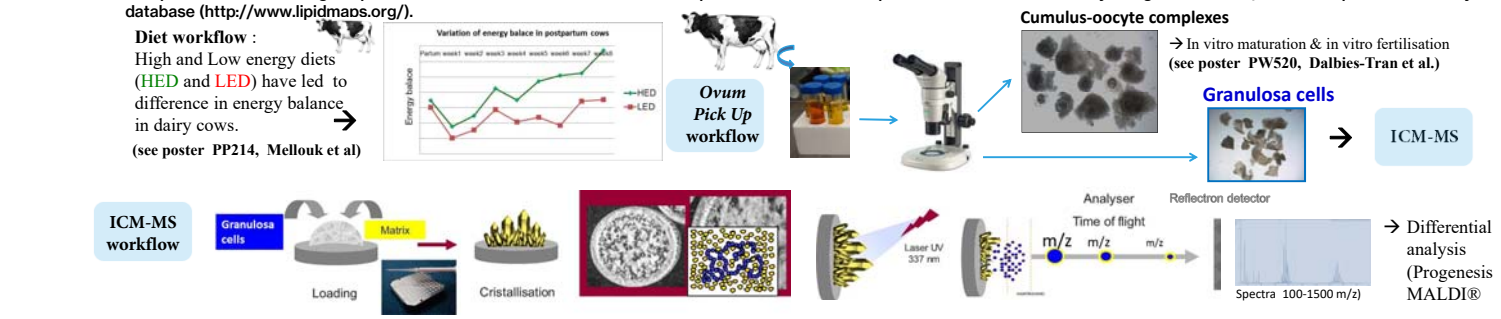
INTRODUCTION

During lactation, dairy cows present **negative energy balance** which could in part explain their suboptimal fertility through postpartum period. Ovarian activity may be affected through this period by modulating fatty acid (FA) metabolism inside the follicle whereas follicular environment is crucial for developmental potential of enclosed oocyte. Lipids play diverse biological roles as energy source, cell signaling mediators and the constituents of plasma and organelle membranes. **FA metabolism** plays an important role in follicular **granulosa cells (GC)** functionalities as cell proliferation and estradiol synthesis, thus potentially affecting follicular growth and viability; GC can also accumulate neutral lipids [1]. We recently showed that Intact Cell Matrix-assisted laser desorption/ionization time of flight Mass Spectrometry **(ICM-MS)** may be used for determination of differential **lipid profiling** in bovine cumulus cells and thus allowed the discrimination of immature and mature oocytes [2].

The objective of this study was to adapt this **ICM-MS technology to bovine granulosa cells** and to compare their lipid fingerprints between **dairy cows** receiving either **high or low energy diets** bearing 25% difference in energy supply.

MATERIALS AND METHODS

Immature 4-10 mm follicles were aspirated by ovum pick up after ovarian stimulation from Holstein lactating cows at 80-100 days postpartum (see details in poster *PW520*). These cows received either High Energy Diet (**HED**) or Low Energy Diet (**LED**) diets (25% difference in energy supply) during more than 1 year (see details in poster *PP214*). Healthy **mural granulosa biopsies** from HED (n=11) and LED (n=18) cows were recovered and kept at -80°C. To perform **ICM-MS**, GC were sonicated in matrix solution containing 2,5-dihydroxyacetophenone/ methanol and trifluoroacetic acid, deposited on a MALDI plate and recovered with fresh matrix. **Lipid spectral profiles** (5000 spectra per technical replicate) were acquired using an UltrafleXtreme MALDI-TOF/TOF instrument (Brucker) in positive and then in negative reflector ion mode. Spectra were analyzed using Progenesis MALDI™ (Nonlinear Dynamics). M/z peaks were detected in the range of m/z 160 to m/z 1000 and quantified using the values of normalized peak heights. Coefficient of variation (CV %) was calculated for each m/z peak as (SD/mean)*100 of 6 technical replicates in all GC samples (n=29). Multivariate Principal Component Analysis (PCA) and Student test was performed for hunting of lipid content variations between conditions. Lipids were identified in lipid extract from bovine GC by using nano-LC-MS/MS and "Lipidomic Gateway" database (http://www.lipidmaps.org/).



RESULTS

1. Specific reproducible lipid fingerprints were obtained by ICM-MS of GC **(Figure1)**. A total of 146 and 190 distinct peaks ranging from m/z 163.22 to 965.95 were detected in positive **(PR)** and negative **(NR)** mode, respectively. **Mean CV%** for all the peaks was **36.4** % for PR and **32.5%** for NR mode.

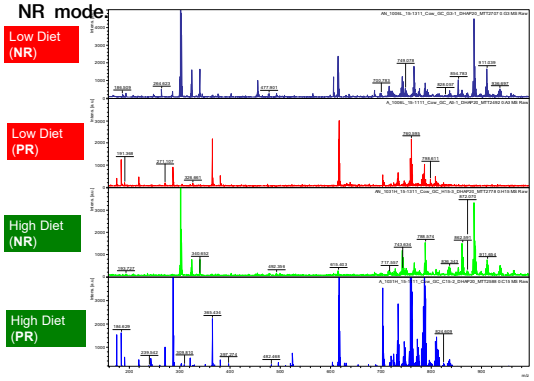


Figure 1. Representative ICM-MS spectra of bovine GC from LED and HED diet cows, in positive (PR) and negative NR) mode. For quantitative analysis, each peak height was normalized by global intensity in m/z range 160-1000.

2. Differential analysis: only few peaks showed significantly differential abundance in granulosa cells of HED compared to LED cows **(P<0.01, Fold Change >2, Fig.2)**. Using these m/z, PCA could not properly discriminate the cows of HED and LED groups **(Fig. 3)**

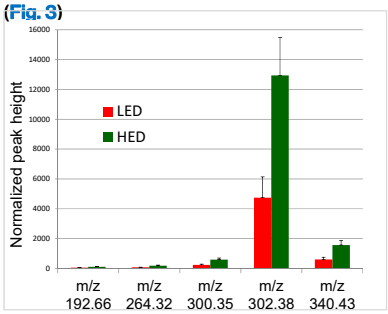


Figure 2. Differential lipids in GC from the LED and HED diet cows. ICM-MS was performed in NR mode.

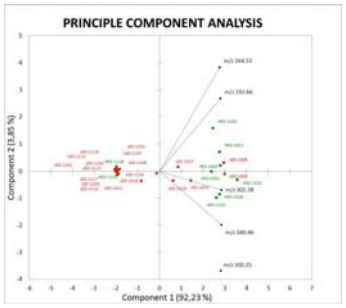


Figure 3. PCA bi-plot representation of HED and LED groups and differential peaks (m/z).

3. Lipid annotation. Several major lipid species in the range m/z 600-900 could be identified and may correspond to phosphatidylethanolamines (**PE**, m/z 786.66=**PE**(O-40:2), m/z 782.63=PE(O-40:4)), sphingomyelins (**SM**, m/z 725.63=SM(16:0)), diacylglycerols (DG, 725.63=DG(44:6)) and phosphatidylcholines (**PC**, m/z 760.65=PC(O-35:1), m/z 808.63=PC(38:5), m/z 798.60=PC(37:3). However, differential peaks having lower m/z (192.66-340.43 m/z range, Fig. 2), corresponding likely **to fatty acyls** or other metabolites, could not be unanimously annotated.

CONCLUSIONS

- Employed **energy diets had no significant effect of lipid content in granulosa cells** in spite of different energy balance in postpartum cows .
- **Intact Cell MALDI Mass Spectrometry** was adapted to analysis of lipids in **bovine granulosa cells** and produced reproducible spectra bearing major lipid species which could be then identified

REFERENCES

1. Elis S, Desmarchais A, Maillard V, Uzbekova S, Monget P, Dupont J. Cell proliferation and progesterone synthesis depend on lipid metabolism in bovine granulosa cells. Theriogenology 2015;83: 840-853.
2. Sanchez-Lazo L, Brisard D, Elis S, Maillard V, Labas V, Uzbekova S. et al. Fatty acid synthesis and oxidation in cumulus cells support oocyte maturation in bovine. Mol Endocrinol 2014;28: 1502-1521.

FINANCIAL SUPORT

P.Bertevello : Universidade do Estado do Rio Grande do Norte
Funding : FP7-KBBE-2012-6-311776-PROLIFIC
European Union Seventh Framework Program (FP7/2007-2013), project "PROLIFIC" (grant agreement n°311776)

Contact : svetlana.uzbekova@tours.inra.fr
Centre de recherche Val de Loire,
UMR Physiologie de la Reproduction et des Comportements
37380 Nouzilly, France
www.val-de-loire.inra.fr
http://www7.tours.inra.fr/physiologie_reproduction_comportements

DISCUSSION

DISCUSSION

For the first time, we have characterized and compared lipid composition of different compartments in bovine ovarian follicles, including follicular fluid, mural cell layers (TH and GC) and cumulus with the enclosed oocytes, using original MS approaches as molecular fingerprints and imaging of lipids by MALDI-TOF. MSI is a rapidly evolving methodology for monitoring the spatial distribution and abundance of molecular species in tissue sections that allows direct and simultaneous analysis of hundreds of different compounds in a label-free manner. Up today, only few studies have reported MSI analysis of ovarian lipids: for studying ovarian maturation cycle in banana shrimp (Chansela *et al.*, 2012), lipid distribution in porcine ovary (Uzbekova *et al.*, 2015), and analysis of healthy and cancerous ovarian tissues in hens (Nazari and Muddiman, 2016). Lipid profiling on ovarian cells was recently applied to analysis of follicular fluid, cumulus cells and the oocytes in human, bovine and equine (Montani *et al.*, 2014; Sessions-Bresnahan *et al.*, 2015; Alessandra A Vireque *et al.*, 2017; Elis *et al.*, 2017; Santos *et al.*, 2017; Cordeiro *et al.*, 2018). In the present work, we have identified the most abundant lipids in bovine ovary and demonstrated that each ovarian compartment had specific lipid signature. Nevertheless, many lipids were common between the different types of somatic follicular cells (TH, GC, and CC), oocytes and FF. Among these common features, the most were assigned to lipid classes forming membrane components and energy reserves due to multitudes of membrane structures in the cells and FF and strong energy requirement to assume rapid follicular growth. Different types of ovarian somatic follicular cells have their specific functions (Monniaux, 2014), and our data supported this specificity by differential lipid composition and gene expression patterns in ovarian compartments.

1 Lipid metabolism in follicular wall cells.

More than a half of follicular cell lipids were identified by LC-HRMS as glycerophospholipids, among them the PC was the major class. Among the identified peaks detected by MALDI MS, the PC represented 37%. PC are the main component of cell membrane lipids, with well-established roles in cell differentiation and proliferation (Van Meer, Voelker and Feigenson, 2008). Spatial molecular localization of the lipids by MSI MS showed the higher abundance of PC in the interstitial stroma and follicular walls. Therefore, these PC may be associated with cell membrane structures, including that of TH and GC. Follicular wall cells shared many common lipids that explained the partial overlay of TH

and GC in MSI segmentation map. In fact, although TH and GC are separated by basal membrane they are metabolically coupled. However, the increased abundance in several LPC, LPE, SM and TG in TH compared to GC, allowed discrimination of these two cell types by PCA. A similar approach was performed on human lung where MSI confirmed specific distribution of three phospholipids (PE, PI, and PG) in different regions of lung slice, illustrating lipidome differences between alveolar macrophages, bronchial epithelial and alveolar type II pulmonary cells that were previously shown by LC-MS/MS (Zemski Berry *et al.*, 2017). Specific lipid profiling of TH probably reflects its functional structure that is rich in steroid-secreted cells, blood capillaries and collagen (Young and McNeilly, 2010), compared to GC that is more homogeneous and smooth tissue (Tajima *et al.*, 2007). Along with follicle growth, lipid distribution in wall follicular cells seems to change, and GC showed more lipids that are differential between large and small follicles as compared to TH.

Lipid metabolism of TH is largely related to androstenedione production, essential for follicular development and fertility (review by (Young and McNeilly, 2010). TH layer is the first permeable barrier between the vascular and follicular system, responsible in part for the control of nutrient transport, required to maintain cellular activities during follicular growth (Tajima *et al.*, 2007; Hatzirodos, Hummitzsch, Irving-Rodgers, *et al.*, 2014). Our results show that lipids distribution in both internal and external TH cell layers is regulated during follicular growth and may depend to different causes. Despite the faint alterations of neutral lipid accumulation as revealed by Nile Red staining through follicular growth, it is plausible to suggest that follicular atresia affects lipid composition in both TH and GC, as it occurs in mice lung tissues (Dautel *et al.*, 2017). Transcriptomic data showed that TH of small follicles over-expressed the genes associated to FA uptake via lipoprotein lipase, LPL; and cholesterol, through lipoproteins, via scavenger receptor class B transporters. Thus TH may liberate TG and CE from the lipoproteins and modulate cholesterol metabolism and, consequently, steroid synthesis. Strong expression of genes coding for different lipases and apolipoproteins A, E, M, L, and O may indicate that TH as other follicular cells are capable of not only degrading but also synthesizing the lipoproteins (Gautier et al., 2010), and even of the microsomal triglyceride transfer protein (MTP) (Hussain et al., 2012). The role of lipids and cholesterol in fertility has been demonstrated in specific murine knockout (KO) models, suggesting that HDL metabolism may play an important role in fertility, since (1) female mice without SR-BI are completely infertile by developmental block the zygote or two-cell stage (Trigatti *et al.*, 1999), and (2) ATP-binding cassette KO (ABCA1) as well as (3) Liver X-Receptor KO (LXR) mice are subfertile , with reduced litter size (Christiansen-Weber *et al.*, 2000; Steffensen *et al.*, 2006). The fertility is reduced by an effect on HDL general metabolism and HDL particle composition,

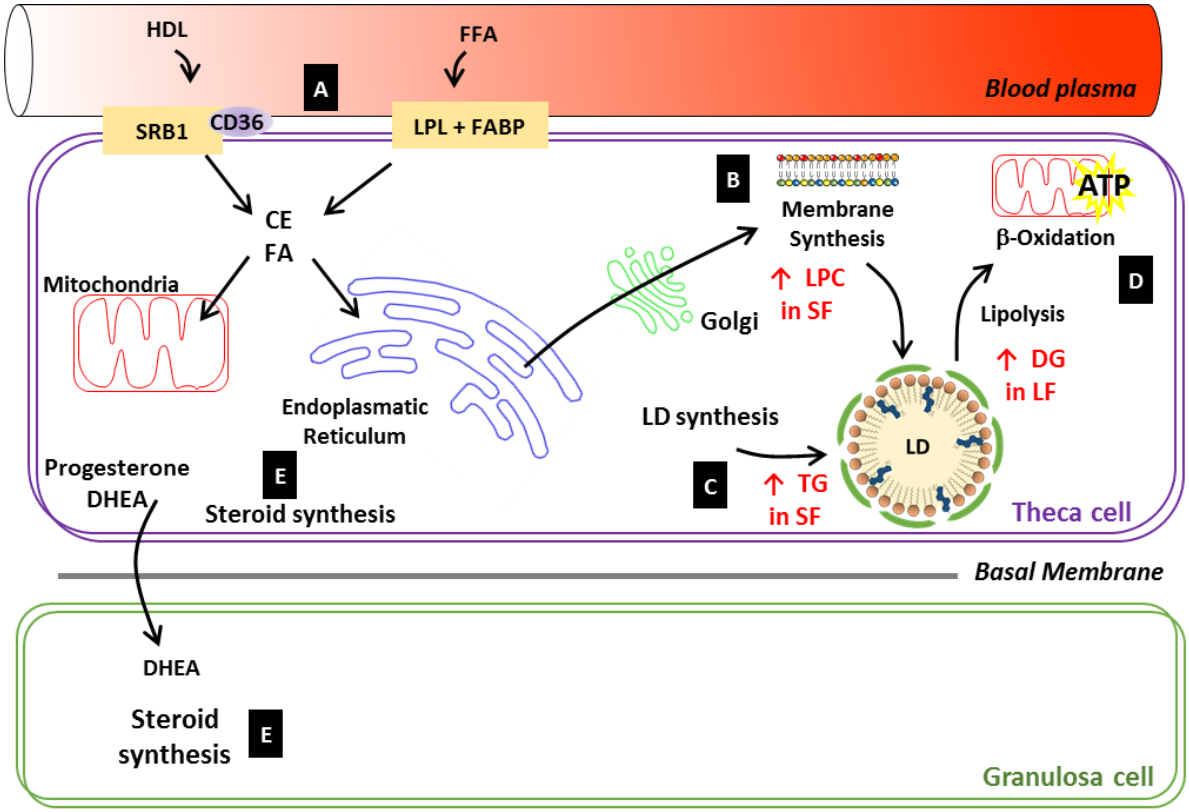


Figure 27. Scheme of lipid content and metabolic lipid pathways in theca cells of bovine ovarian follicles. (A) Intense uptake of cholesterol by the scavenger receptor class B transporters (SRB1 and CD36), and FA, mediated by lipoprotein lipase (LPL) and fatty acids binding transporters (FABPs); **(B)** membrane synthesis, mediated by the abundance of **LPC in SF**, and cellular response to oxidative stress; **(C)** lipogenesis process to lipid droplets production; and **(D)** lipolysis and FA b-oxidation, maintaining the balance between energy storage and delivering. **(E)** Steroid production in collaboration with GC. **Abbreviation:** CE: cholesteryl esters; HDL: high-cholesterol lipoprotein; FA: fatty acids; FFA: free fatty acids, SRB1: scavenger receptor class B transporters type 1; CD36: CD36-molecule (Thrombospondin Receptor); LPC: lysophosphatidylcholine; DG: diacylglycerol; TG: triacylglycerol; SF: small follicles; LF: large follicles; DHEA: dehydroepiandrosterone; LD: lipid droplets; LPL: lipoprotein lipase; FABP: Fatty acids binding protein; ATP: adenosine triphosphate.

as the transfer of ovaries SR-BI$^{-/-}$ to wild mice restored fertility (Miettinen, Rayburn and Krieger, 2001). However studies on the effects of extremely altered lipoprotein levels within ovarian cell programming are not known.

The importance of HDL in fertility were observed in several studies. Velasco et al. (2006) made use of the natural variation in SR-BI expression in granulosa cells of in vitro fertilization (IVF) patients to correlate SR-BI expression to clinical parameters related to infertility. The baseline and low plasma estradiol levels are lower when the level of SR-BI expression was in the lowest rather than the highest quartile. The number of retrieved and fertilized oocytes was also reduced (Velasco *et al.*, 2006). Certain polymorphisms within SR-BI gene may also play a role in fertility. In fact, some single-nucleotide polymorphisms are related to altered FF progesterone levels and a reduction in the number of ongoing pregnancies (Yates *et al.*, 2011). And also, studies on FF collected during ovum pick up in an IVF treatment show that concentrations of HDL and its lipoprotein apoA1 are inversely related to embryo fragmentation (Browne *et al.*, 2008), but also to embryo cleavage, blastocyst formation, and embryo quality (Valckx *et al.*, 2012; Wallace *et al.*, 2012), resulting in a reduced implantation potential. Typical lipoprotein lipid species, like CE, TG, SM, LPC, and PC have been identified in human plasma lipoproteins (Zschörnig *et al.*, 2005; Hidaka *et al.*, 2007), as well as were found in this work in different follicular compartments. Among the differential lipid species identified, LPC and TG were predominant lipid species in TH in comparison to the other compartments, corroborating these transcriptomic data. On the other hand, large follicles showed the higher abundance of some lipids including DG species - metabolites of lipid oxidation.

Therefore, TH cells may ensure the species lipid and cholesterol transport, also cholesterol resynthesize to production of androgens, and the production of energy reserves in order to generate ATP to manage all these activities. More specifically, in antral follicles, TH cells safeguard a massive uptake of FA and cholesterol used for androgens production, assure lipid transport to GC and FF, and guarantee energy reserves by the production and consume of lipid droplets. TH layer from the larger follicles have probably higher activity in FA transport and oxidation, but those activities appear to depend on the state of follicular atresia or dominance.

Figure 27 represents hypothetical scheme of lipid metabolism in TH cells in relation with blood circulation and neighboring GC.

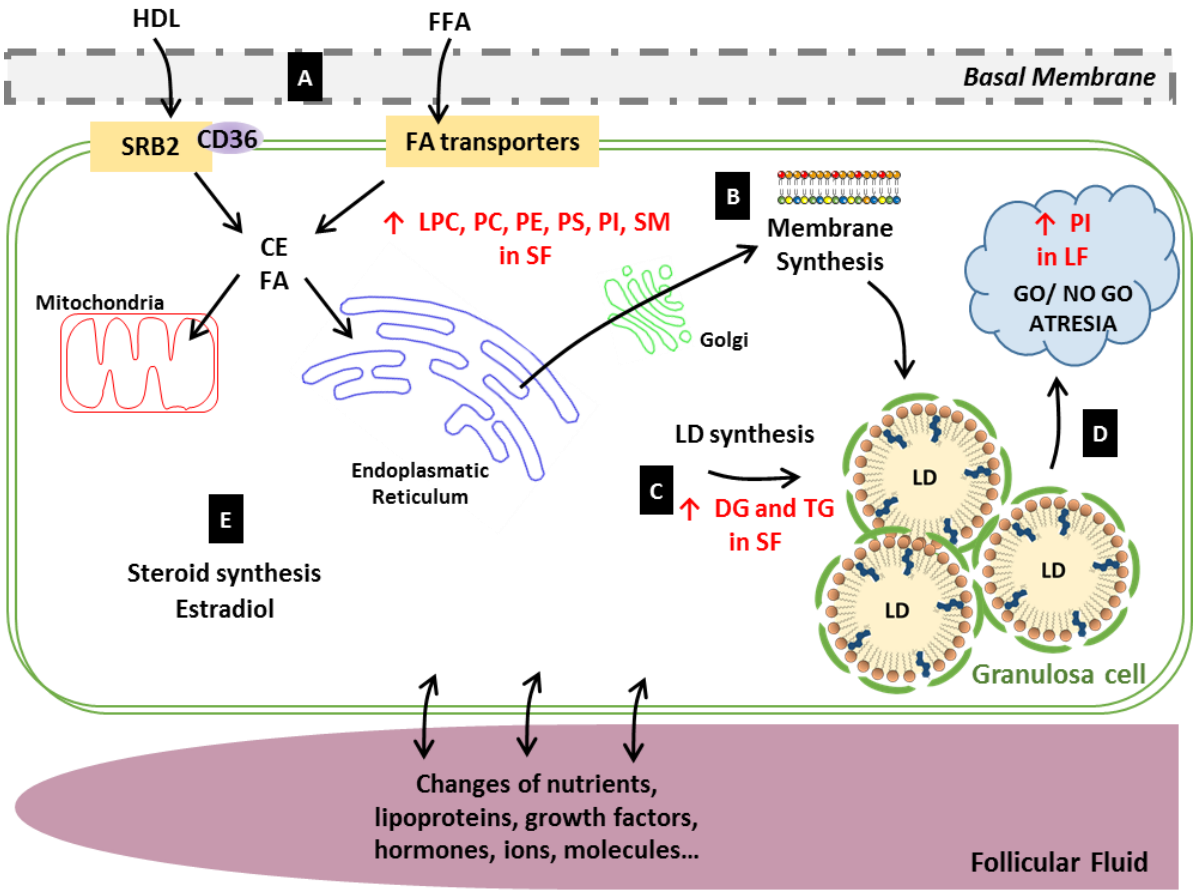


Figure 28. Scheme of lipid content and metabolic lipid pathways in granulosa cells of bovine ovarian follicles. (A) Intense uptake of cholesterol by the scavenger receptor class B transporters (SRB2 and CD36), and FA mediated by FA transporters (fatty acids binding transporters, FABP) from blood plasma. Small solutes can diffuse through basal membrane; **lipogenesis process (B)** accentuated membrane synthesis, mediated by presence of **LPC, PC, PE, PS, PI, and SM in SF**, and **(C)** production of lipid droplets. **(D)** Cellular response to oxidative stress to atresia or follicular dominance. **(E)** Steroid production in collaboration with theca cells. **Abbreviation:** HDL: high-cholesterol lipoprotein; CE: cholesteryl esters; FA: fatty acids; FFA: free fatty acids, SRB1: scavenger receptor class B transporters type 1; CD36: CD36-molecule (Thrombospondin Receptor); LPC: lysophosphatidylcholine; PC: phosphatidylcholine, PE: phosphatidylethanolamine; PS: phosphatidylserine; PI: phosphatidylinositol; SM: sphingomyeline; DG: diacylglycerol; TG: triacylglycerol; SF: small follicles; LF: large follicles; LD: lipid droplets.

Granulosa cell layers are a major site of estrogen production and a variety of locally produced growth factors related with gonadotrophin action on follicular function (Kol and Adashi, 1995). Correlations between the highly differentiated mesenchymal-derived TH cells and epithelial-derived GC, which both ensure a constant supply of various steroid hormones, are well-coordinated for the success of the ultimate purpose of generating fertilizable oocytes with sufficient developmental potency (Tajima *et al.*, 2007). The mobilization of stored CEs is probably the most rapid way to support the "acute" stimulation of steroidogenesis (Stocco, 2000) by *de novo* lipogenesis (Stocco, 2000; Azhar and Reaven, 2002; Azhar *et al.*, 2006), and this process requires considerable energy reserves, thus accumulation of LDs in internal TH of growing follicles were observed.

Early secondary follicular development is related to angiogenesis, which provides numerous plasma nutrients and growth factors (Tajima *et al.*, 2007) and increased steroidogenic GC activity that also requires more lipid reserves (Monniaux *et al.*, 2014). In GC of 2-6 mm follicles, neutral lipids were significantly more abundant than in the vascularized external TH layer. It is probably explained by the diffusion and transport of fat, nutrients and other factors from plasma, since these changes are more intense and constant with vascularization (Young and McNeilly, 2010). The increase of FA consumption by TH is supported by expression pattern of corresponding enzymes, as those realized to FA uptake and mitochondrial oxidation. Interestingly, we found the increase of lipid accumulation in GC and iTH of intermediate-sized follicles, which seems to be influenced not only by follicular size but also by the degree of follicular atresia. In fact, GC are the first to undergo apoptosis in atresic follicles prior to oocytes and TH, and thus may initiate follicular death via atresia (Jiang *et al.*, 2003; Tajima *et al.*, 2007; Inoue *et al.*, 2011). Also, follicular atresia induces accumulation of LDs in the ooplasm (Dadarwal *et al.*, 2015). This reinforces the idea of bi-directional signaling between the oocytes and somatic cells, and these interactions play a key role in pre-antral folliculogenesis and atresia mediated loss of the follicles (Cortvrindt and Smitz, 2001). In atresic follicles, GC apoptosis has recently been linked to the role of lysophosphatidic acid (LPA, bioactive glycerophospholipid produced from cell membrane phospholipids). LPA participates in apoptotic initiation through the regulation of TNF-alpha-induced and caspase-induced pathways (Emilia Sinderewicz *et al.*, 2017a)(E. Sinderewicz *et al.*, 2017b). Meanwhile, sphingosine-1-phosphate signaling is involved in blocking of follicular atresia in ovarian cortical fragments *in vitro*, it improved steroidogenic activity, and decreased caspase-3 protein levels, thus protecting cells against apoptosis (Guzel, Bildik and Oktem, 2018). Healthy and apoptotic tissues have different lipid composition (Dautel *et al.*, 2017). The variability of lipid content in GC of different follicles of similar size, both in cells and FF, may be explained by different degree of apoptosis between the follicles.

The plasticity of the plasma membranes may occur in the follicles of different sizes. These processes include scramble and translocase of phospholipids performed by ABC transporters (Yang, Lee and Fairn, 2018), lipid elongation by elongases (Kihara, 2012; Sanchez-Lazo *et al.*, 2014; Annes *et al.*, 2018), and inclusion of unsaturation in FA by desaturases (Warzych *et al.*, 2017). Also, the increase of LPC and SM relative abundance in small follicles, and PI and DG in the large follicles, may reflect the different signaling mechanisms that could regulate the maintenance of follicular homeostasis. In fact, go/no-go atresia choice may be mediated by lysophospholipids system (Makide *et al.*, 2009; Drzazga, Sowińska and Koziołkiewicz, 2014), sphingolipids (ceramides) pathway (Zheng *et al.*, 2006), phosphatidylinositol signal-mechanism (Sanders and Jones, 2018), and diacylglycerol signaling (Wang, 2006).

Granulosa cells are involved in maintenance of follicular homeostasis through several lipids metabolism processes, such as elongation and desaturation of FA, and also may influence entry in follicular atresia or dominance.

The putative lipid metabolism in GC in relation with follicular fluid is represented in **Figure 28**.

2 Lipids in follicular fluid.

The lipid composition of FF is influenced by several factors, among them the nutrients that arrive through the blood plasma or secreted from follicular cells (Guerreiro *et al.*, 2018), debris of GC cells and extracellular vesicles (Sohel *et al.*, 2013), exosomes and lipoproteins (Gautier *et al.*, 2010; Skotland, Sandvig and Llorente, 2017; Record *et al.*, 2018).

Described previously, the lipoproteins are presents in FF. Although (V)LDL/apoB are present in FF at much lower levels compared with HDL, a potential effect on fertility should not be neglected, especially since in an evolutionary context apoB-containing lipoproteins represent the significantly older system of cholesterol transport compared with HDL (Palm et al. 2012). Moreover, LDLR expression in human oocytes increases during development. In a single study, although on a rather small group of individuals, the number of top-quality embryos and the pregnancy rate in patients with an FF apoB level above the median were substantially higher compared with the group with lower FF apoB levels (Gautier et al. 2010).

Metabolic activity of follicular somatic cells can greatly influence the lipid composition of FF (**Figure 29**). According to our data, different somatic follicular cells possess enzymatic machinery to uptake and transform FAs, synthesize and degrade lipids and lipoproteins, and each cell type (TH, GC or CC) has their own specific expression pattern regulating lipid metabolism.

By MALDI MS lipid profiling, as was expected for non-cellular compartment, the FF lipid profile has significantly differed from follicular cells. The differential analysis based on quantitative profiles of the MALDI MSI corroborates the images of ion density maps of differential lipid species. Lipid species presented different distribution between the follicles with a specific location in either FF or mural follicular cells. Specific and distinct lipid profiles of FF also corroborated MALDI MS fingerprints from small and large follicles. In fact, the molecular image of these follicles may also indicate the developmental state or atresia follicular. By MS analysis of FF we identified lipids of different classes including FA, Cer, DG, lysophospholipids (LPC, LPE, LPI ...), SM, CE, and TG. Significant proportions of FF lipids identified as Cer, DG, lysophospholipids, and SM might exhibit mediator functions (Fernandis and Wenk, 2007; Drzazga, Sowińska and Koziołkiewicz, 2014). FF contains microsomal triglyceride transfer protein (MTP) a major cellular protein capable of transferring neutral lipids between membrane vesicles (Hussain *et al.*, 2012) and extracellular vesicles like exosomes (Sohel *et al.*, 2013), which content a very specific lipid composition (Skotland, Sandvig and Llorente, 2017) and may

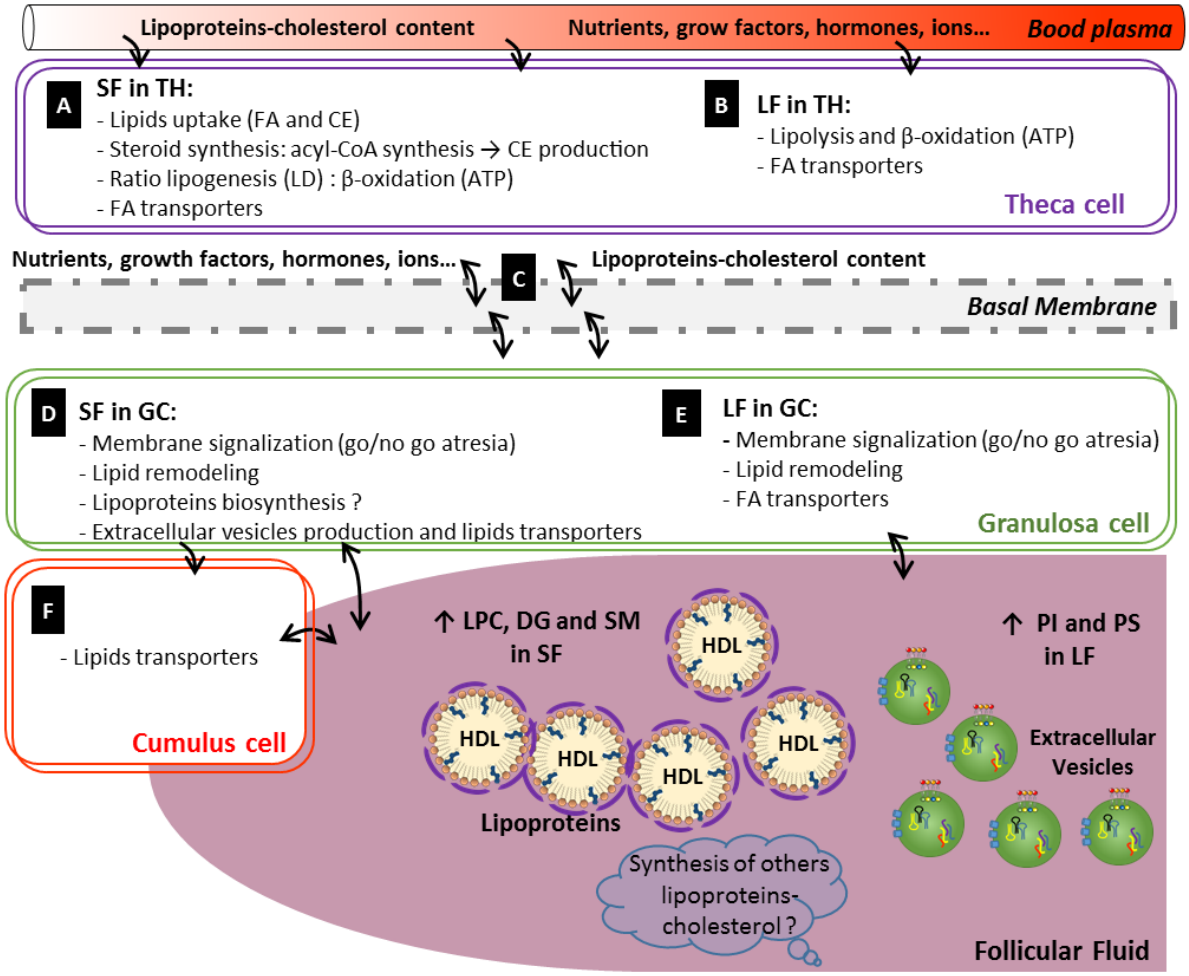


Figure 29. Hypothetical scheme of lipid content in follicular fluid and interactions between the compartments in bovine ovarian follicles. The scheme shows the presence of extracellular vesicles and HDL-cholesterol lipoprotein in the follicular fluid, besides representing the abundant lipid species such as LPC, DG and SM detected in small follicles; and in large follicles the composition changes for lipid species such as phospholipids (PI and PS), both associated with signaling (go/no go atresia). Massive uptake of plasma lipids and cholesterol by theca layers, lipid metabolism and inter- and intracellular transport: **(A)** predominant theca cells actions in small follicles; **(B)** predominant theca cells actions in large follicles; **(C)** basal membrane allows the passage of small plasma molecules, including HDL-cholesterol lipoprotein, and molecules synthesis by somatic cells; **(D)** predominant granulosa cells actions in small follicles; **(E)** predominant granulosa cells actions in large follicles; **(F)** lipids transporters by cumulus cells; **arrows**: exchanges and transport of lipids and other substances. **Abbreviations:** SF: small follicles; LF: large follicles; TH: theca cells; GC: granulosa cells; FA: fatty acids; CE: cholesteryl esters; HDL: high-cholesterol lipoprotein; LPC: lysophosphatidylcholine; SM: sphingomyelin; DG: diacylglycerol; PI: phosphatidylinositol; PS: phosphatidylserine.

participate in these communications inside the follicle. TG, CE and free FA were largely represented in FF although there are no visible lipid droplets. These lipids may be a part of high density-(HDL) lipoproteins, the smallest lipoproteins, which could be transported from blood (Grummer and Carroll, 1988). According to our data on expression of genes coding for apolipoproteins, follicular cells may also synthesize lipoproteins, as was shown for human GC, which produced very low-density lipoproteins (Gautier *et al.*, 2010). These neutral lipids may be a part of FF lipoproteins, similarly to human plasma lipoproteins as analyzed by MALDI-TOF MS (Serna *et al.*, 2015).

Our study demonstrated, that PPARγ is strongly expressed in GC, CC, and oocytes and therefore may regulate numerous lipid metabolism-related genes in all compartments, as was revealed by Gene Ontology analysis. Some of FF lipids, as LPA or unsaturated FA, can activate peroxisome proliferator-activated receptors PPARs, nuclear transcriptional factors, controller of genes expression associated with lipid and carbohydrate metabolism, angiogenesis, cell proliferation and differentiation (Peddinti, Memili and Burgess, 2010).

Somatic cells expressed the genes encoding phospholipases A2 (*LCAT, PLA2G16, PLA2G7, PLA2G1B*) and the enzymes related to the formation of cholesteryl esters. All these enzymes use PC-derived LPCs, which were found abundant in FF. According to our data, different LPCs can be produced by follicular cells, and the oocyte can influence this process. Specifically, LCAT is associated with lipoprotein metabolism. Lysophospholipids are also involved in membrane synthesis (e.g. PC and PE). Genes from the enzyme acyltransferases (*LPCAT2* and *MBOAT2*) are also highly expressed in follicular cells. Therefore, LPC found in FF man be imported from the circulating lipoproteins or produced by the cells.

The comparison of FF lipids to other compartments showed a preferential location of free FA, and several SM. Those might reflect the presence in FF of extracellular vesicles (Skotland, Sandvig and Llorente, 2017), and the lipoproteins (Serna *et al.*, 2015). According to our analysis of lipids in the follicles of different sizes, more than a half of all lipid features (55%) changed their relative abundance in FF of growing follicles as compared to smaller ones. Among the lipid species identified here, several PI and PS decreased during follicular growth (Jiang *et al.*, 2003), while LPC, DG, and SM increased. Those lipids are involved not only in the stabilization of membrane structure, but also in cell signaling and cell-cell recognition (Hannun and Obeid, 1995; Melendez, 2008; Milhas, Clarke and Hannun, 2011). The higher levels of DG signalization, generated by hormone-activated phospholipases, is attenuated by mechanisms that include lipolysis or phospholipid re-synthesis (review by (Igal *et al.*, 2001). Also, the LPC, cell signaling molecules produced by the action of phospholipases from membrane phospholipids, are involved in acute and chronic inflammation (Schmitz and Ruebsaamen, 2010). Acute inflammation

is required for normal folliculogenesis and ovulation, and its associated tissue remodeling mediated by prostaglandins, predominantly E2, and eicosanoids (phospholipids derived) that enhance the inflammatory reaction, promoting angiogenesis, and hyperemia and activate collagenases and other proteolytic enzymes. While chronic inflammation is associated with pathological reproduction dysfunctions (review by (Boots and Jungheim, 2015)). Also sphingolipids are involved in membrane structure stabilization and cell-to-cell recognition and signaling (Zheng *et al.*, 2006; Wahli and Michalik, 2012). Several lysophospholipids like LPC and LPI were now recognized as hormone-like signaling molecules and thus considered as inter- and intracellular lipid mediators (Drzazga, Sowińska and Koziołkiewicz, 2014); that may be therefore the mediators of inter-cellular communication inside the ovarian follicles.

FF lipid composition depends on nutrients, lipoproteins, growth factors, hormones, ions, and other molecules coming from the blood plasma and also from the synthesis of different factors by follicular cells. These factors are involved in autocrine and paracrine communication between the somatic cells and oocytes. The quality of enclosed oocyte is influenced by the lipid content of FF or culture medium (Leroy, Vanholder, Delanghe, Opsomer, Van Soom, Bols and de Kruif, 2004; Jo L.M.R. Leroy *et al.*, 2005). In women, the concentration of several lipids FF demonstrated a strong potential association between the differentially elevated lipids and increased success rate of *in vitro* fertilization and intracytoplasmic sperm injection outcomes (ICSI) (Wen *et al.*, 2018).

Metabolic activity of follicular cells plays the important role in follicular growth and influences lipid composition of enclosed follicular fluid.

3 Lipid content and regulation in Cumulus-Oocyte Complex (COC)

An oocyte is physically attached to *cumulus oophorus*. Although CC are derived from the granulosa layer, specific functions of these cells are conditioned by their physical and metabolic coupling with the enclosed oocyte (Tanghe *et al.*, 2002). We revealed very significant differences in both lipid and transcript signatures between cumulus and granulosa cells, that likely reflect the functional differences between these cells (Borgbo *et al.*, 2013).

During follicular growth up to ovulation, constant bi-directional communication occurs between the oocyte and surrounding follicular cells. Specific oocyte-secreted factors stimulates follicular cells to proliferate and to secrete steroids and other factors, which, in turn, proper regulate growth (Gilchrist, Ritter and Armstrong, 2004; Binelli and Murphy, 2010). The major phospholipids identified in CC were PC and SM. In small follicles, the CCs showed lipids species with low molecular weight, and the larger ones contained lipids species with large molecular weight, observed by mass spectrometry analyses. We found an increase of 30% of long-chain and very-long-chain FA in large follicles analyses. Complex oocyte-cumulus is bathed in FF, therefore these compartments share several lipid species, mostly the LPC. In addition, oocytes express genes to transform LPC into PC (CEPT1). Intense changes of different lipids between the COC and FF were reported as indicative of the presence of several lipid transporters expressed in these cells (Peddinti, Memili and Burgess, 2010). The changes in m/z, or mass size of lipid species identified in different size follicles can be explained by (1) FF composition changes with follicle growth, maybe caused by several different species molecule synthetized in collaboration of theca and granulosa cell (p.ex. lipoproteins, membrane vesicles, exosomes, etc); as well as (2) the action of fatty acid remodeling enzymes, elongases, and desaturases, present in the CCs. The genes of this enzymes were observed by transcriptomics data analyzed published in the first paper of this thesis. In COCs exposed to saturated free fatty acids during maturation, the cumulus cells showed capable of converts saturated into monounsaturated fatty acids activity provides by enzyme stearoyl-CoA desaturase (SCD) (Aardema *et al.*, 2017).

CC protect the enclosed oocytes from potentially toxic environment. Rapid transfer of free FA from FF and their accumulation in LDs of follicular cells protect the oocyte from lipotoxicity (Lolicato *et al.*, 2015).The high capacity in accumulating LDs was observed in bovine CC, especially when exposed to a high concentration of free FA (Aardema *et al.*, 2011, 2013). We have observed that the changes of CC lipid composition in response to environmental modulations of FA concentrations are much more significant compared to oocytes (Elis *et al.*, 2017). In addition, follicular growth have modulated lipid

composition of GC and CC significantly more than oocyte lipid fingerprints, which were only slightly affected by the follicular size. In fact, both large and small follicles taken in the study, contained immature oocytes, blocked at germinal vesicle stage. Immature oocyte showed the majority of identified lipids involved in steroidogenesis, membrane synthesis or energy storage (CE, SL, GPL, GL) and demonstrated very similar phospholipid profiles making difficulties to a clear differentiation of each follicular size. Indeed, the oocyte in this stage is near to full-grown and potentially ready to continue meiosis, but persistent in accumulation of molecular reserves for the acquisition of developmental potential, while somatic follicular cells continue proliferation and thus require more lipids for membrane building (Fair, Hyttel and Greve, 1995; Dadarwal *et al.*, 2015). In the oocytes from the large dominant follicles, structural changes as decreasing of Golgi complexes size, peripheral location of cortical granules, enrichment and translocation of mitochondria and increasing of lipid deposit occur as compared to smaller subordinate ones (Assey *et al.*, 1994; Fair, 2003; Dadarwal *et al.*, 2015). However, it seems that immature oocytes retain the lipid integrity probably maintained by the CC, even by influence by FF and other somatic cells. Interestingly, immature oocytes demonstrated a very specific and distinct lipid profile from the other follicular compartments by MALDI MS analysis; however, clustering of differential lipids revealed the common features with CC or FF. All this demonstrates that the membrane integrity of immature oocyte is highly protected from the changes of FF lipid environment during terminal stages of follicular growth in physiological conditions.

In contrast, meiotic maturation significantly changed lipid fingerprints of both CC (Sanchez-Lazo *et al.*, 2014) and the oocytes (this study). After meiotic maturation, significant variations of PC, SM and free FA were detected in the oocyte as compared to immature ones. This was consistent with total lipids changes in the mature oocyte compared to the immature stage (Auclair *et al.*, 2013; Annes *et al.*, 2018) and highlighted the profound changes in membrane composition and storage of intracellular lipids during oocyte maturation.

Gene expression analysis showed specific capacity of CC to FA beta-oxidation using acyl-CoA dehydrogenase, steroid synthesis, glycerophospholipid biosynthesis, FA catabolism, regulation of cholesterol metabolism, and phosphatidylinositol signaling. Cluster of genes expressed in CC and OO was enriched in genes involved in glycerophospholipid and phosphatidylinositol synthesis; long-chain fatty-acyl-CoA biosynthesis and acyl-CoA metabolic process, elongation of saturated and unsaturated FA, lipid phosphorylation, membrane lipid biosynthesis through sphingolipid, GL and GPL metabolism, phosphatidylinositol (predominantly in CC) and inositol lipid-mediated signaling (predominantly in OO); PPAR signaling, FA degradation, peroxisome oxidation, and choline metabolism. In addition,

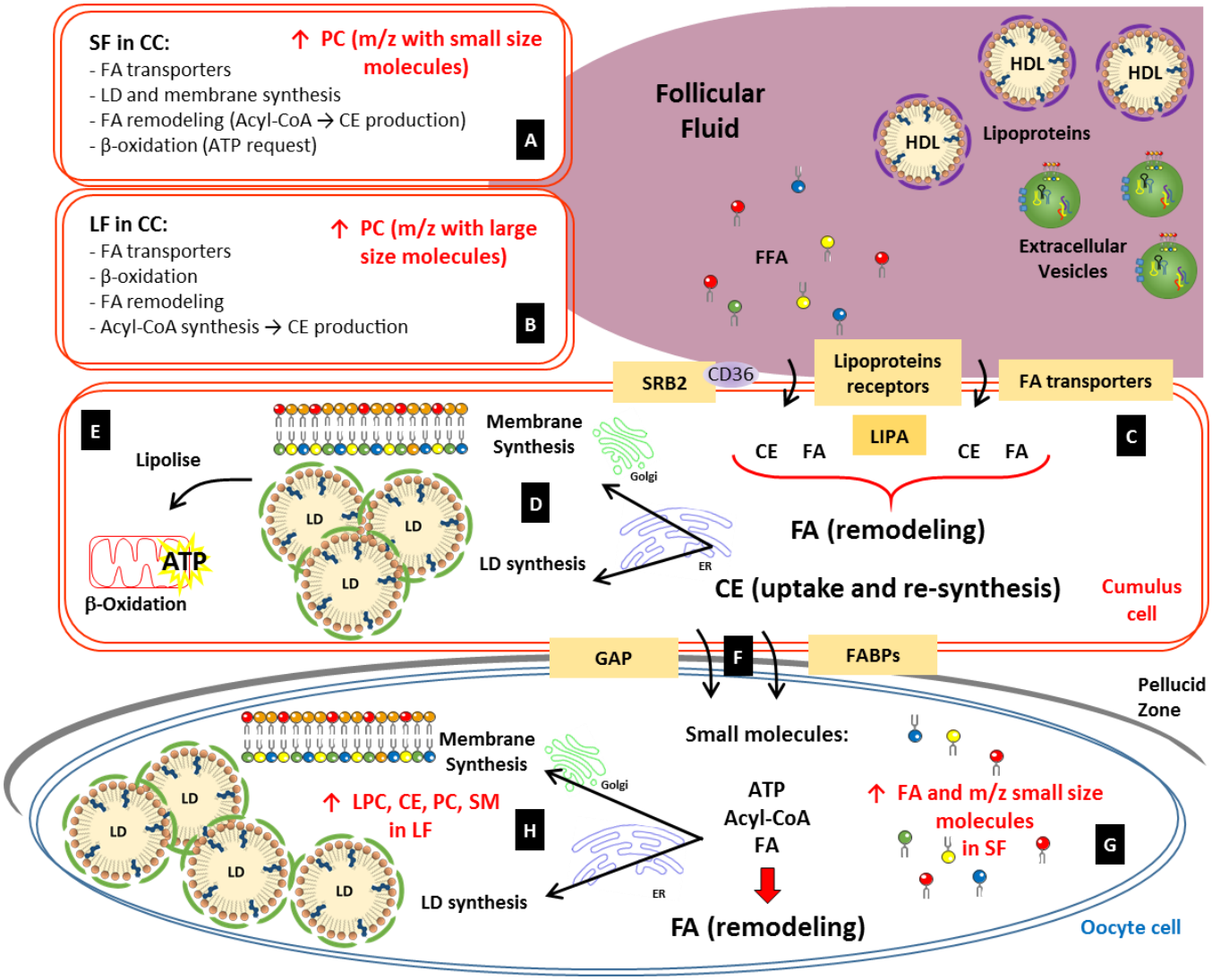


Figure 30. Hypothetical scheme of lipid metabolism related in oocyte-cumulus complex, and interactions between the compartments in bovine ovarian follicle.

(A) predominant cumulus cells actions and lipid content phospholipids and phosphoglycerolipids with m/z with small size in small follicles; **(B)** predominant cumulus cells actions and lipid content phospholipids and phosphoglycerolipids with m/z with large size (probably long- and very long-chain fatty acids; LCFA and VLCFA, respectively) in large follicles; **(C)** uptake and transport of lipids from FF, by enzymes actions (like as lipase, elongases and desaturases) the FA are remodeling and CE are re-synthesis; **(D)** lipogenesis process: membrane synthesis and lipid droplets synthesis; **(E)** to ATP request occurs lipolysis and b-oxidation to energy supply for CC and might also in oocyte. **(F)** From CC small molecules are transfer into oocyte, by action of GAP-junctions and FABPs; **(G)** in small follicles, lipid contents are abundant in lipid species identified with m/z of small size and FA; **(H)** growing follicles maybe remodeling this FA by actions of elongases and desaturases, and make a lipid reserve in droplets and membranes. **Abbreviations:** SF: small follicles; LF: large follicles; CC: cumulus cells; FA: fatty acids; FFA: free fatty acids; CE: cholesteryl esters; HDL: high-cholesterol lipoprotein; LPC: lysophosphatidylcholine; PC: phosphatidylcholine; SM: sphingomyelin; SRB2: scavenger receptor class B transporters type 2; CD36: CD36-molecule (Thrombospondin Receptor); FABP: fatty acids binding transporters; LD: lipid droplets; LIPA: lipase A, Lysosomal Acid Type.

transcriptome analysis revealed that oocyte over-expressed the genes involved in phosphatidylinositol metabolic processes. The fact, hydrolysis of PIP2 and the production of inositol trisphosphate is involved in triggering of oocyte activation after fertilization (Warzych *et al.*, 2017). In mature oocytes, protein synthesis can occur in parallel with the massive degradation of mRNA (Tomek, Torner and Kanitz, 2002; Fair *et al.*, 2007; Sanders and Jones, 2018). Probably, the accumulation of lipid reserves, together with maternal mRNA and protein stores, can probably serve to ensure oocyte maturation, fertilization, and zygote activation (Thelie *et al.*, 2009) and lipids are required for energy and membrane biosynthesis.

According to Dunning and coworkers, oocytes are devoid of cholesterol receptors and respective metabolizing enzymes (Dunning *et al.*, 2012). Therefore they are dependent on the *de novo* synthesis of cholesterol provided by cumulus cells (Su *et al.*, 2008), thus cholesterol and acetate molecules (precursors for cholesterol synthesis and fatty acids) are transported to the oocyte and stored in lipid droplets. From our transcriptomic analysis, the oocytes showed elevated mRNA concentrations of precursors genes of *de novo* cholesterol synthesis, FA elongation and transport of FA. Together with complex lipid composition of the oocytes, these highly abundant transcripts demonstrate that an oocyte have a potential to metabolize FA and stored lipids to obtain energy and building blocks for the future embryo.

Glucose metabolism is considered crucial in determining oocyte development potential (Sutton-McDowall, Gilchrist and Thompson, 2010), as well as intrafollicular lipid metabolism, essential for farm animals reproduction (Leroy, Vanholder, *et al.*, 2008). Lipid oxidation depends on the availability of oxalacetate produced by glucose metabolism (Garrett and Grisham, 2000). The key to high developmental competence of the oocyte seems to be intrinsic to CC metabolism, because of lipid flexibility in metabolic pathways, i.e. availability for protection, biosynthesis, and energy production, allowing oocyte growth and maturation. Lipid composition differed also between the oocytes with different competence in bovine (Auclair *et al.*, 2013; Silva-Santos *et al.*, 2014; Elis *et al.*, 2017).

Lipid profiles in CC may reflect the physiological state or quality of the enclosed oocyte. Differential abundance of several PC was observed in bovine CC enclosing the oocytes with higher developmental potential after omega-3 FA supplementation (Elis *et al.*, 2017). In human, MALDI-TOF lipid profiles of CC showed a different abundance of PC species in the pregnant group and PE, PS and PI feature in the non-pregnant group after ICSI (Montani *et al.*, 2012). Therefore, in addition to the availability of lipids for oocyte development competency, lipids quality are also critical to the process.

During follicular growth, CC change lipid profiling. The onset, the lipids species of molecular weight smaller is consistent with the over-expressed transcripts of elongation and desaturation genes in CC (Sanchez-Lazo *et al.*, 2014; Aardema *et al.*, 2017). Long carbon chain FAs have a tendency to decrease oxidative rate in mitochondria and in this way a long-term metabolic storage characteristic (Garrett and Grisham, 2000; Gurr et al., 2002). CC can store lipids and thus support the oocytes during a period of fertilization after ovulation. Recapitulative scheme representing lipid metabolism in cumulus cells and enclosed oocyte is shown in **Figure 30**.

CONCLUSIONS

CONCLUSIONS ET PERSPECTIVES

L'analyse du contenu lipidique dans le follicule ovarien bovin et du contrôle transcriptionnel associé impliquent la capacité potentielle des cellules de thèque et de granulosa à absorber des lipoprotéines et des acides gras (AG) libres, à les métaboliser et à transporter ces lipides. Les cellules folliculaires ont la capacité d'effectuer la lipolyse, la lipogenèse, l'oxydation des AG dans les mitochondries ou peroxisomes, et de stocker des lipides dans les gouttelettes lipidiques. Ce métabolisme des lipides au sein des follicules peut donc assurer la production des précurseurs des hormones stéroïdiennes, et probablement effectuer la synthèse des esters de cholestérol et de lipoprotéines. Ainsi, ces mécanismes assurent la biosynthèse membranaire dans les cellules somatiques et dans les ovocytes et la production des messagers secondaires responsables de la communication entre les cellules folliculaires. L'expression des transporteurs des AG dans les cellules folliculaires indique des échanges entre la circulation sanguine et la paroi des follicules, ainsi qu'entre le liquide folliculaire et le complexe cumulus-ovocyte. Les profils lipidiques spécifiques aux follicules de grande taille montrent un stockage des AG à longues et très longues chaînes. Au cours de la croissance folliculaire terminale, la composition lipidique change de manière significative à la fois dans le liquide folliculaire et dans les cellules somatiques, comme le révèle l'analyse des profils de lipides par spectrométrie de masse. Le liquide folliculaire présente un énorme changement de la composition lipidique dans les grands follicules par rapport aux plus petits, sans fluctuations notables entre les profils lipidiques des ovocytes quelle que soit la taille des follicules dont ils proviennent. Cependant, l'ovocyte a la capacité d'accumuler des lipides et possède également des mécanismes moléculaires spécifiques qui peuvent être utilisés pour la production d'énergie, la synthèse des membranes et la signalisation afin d'assurer la maturation méiotique, la fécondation et de fournir les blocs de construction nécessaires aux premières cellules embryonnaires. Couplées aux différences de composition lipidique observées dans les cellules somatiques de follicules dominants de grande taille, ces données pourraient suggérer l'accumulation par le follicule de réserves lipidiques pour une utilisation future par les cellules folliculaires restantes après l'ovulation, afin de favoriser la production de progestérone par le corps jaune pour le maintien de la gestation.

En conclusion, des recherches plus approfondies sur la localisation et l'identification des lipides dans les différents compartiments du follicule ovarien au cours des différentes phases de la croissance folliculaire pourraient permettre de mieux comprendre comment et où les lipides peuvent impacter la reproduction des femelles chez les ruminants.

En perspective, l'identification d'espèces lipidiques détectées dans différents compartiments folliculaires et à différents stades de la folliculogenèse nous permettrait d'approfondir nos connaissances sur les interactions métaboliques au sein du follicule, en corrélation avec le métabolisme de la vache et avec des activités pertinentes pour la synthèse et la dégradation des lipides. À travers les lipides, il est probablement possible de réguler des processus importants tels que, la synthèse des membranes, des lipoprotéines, cholestérol et stéroïdes, ainsi que la signalisation entre cellules, et peut-être ainsi fournir un équilibre énergétique propice pour la reproduction. Pour cela, de nouvelles études *in vitro* et *in vivo* plus détaillées sont encore nécessaires. Les programmes d'étude sur la stratégie d'alimentation et de supplémentation des AG chez les bovins doivent encore être approfondis, car la qualité de la nutrition pourrait affecter la santé et la reproduction des vaches laitières.

Il est également possible d'étendre les recherches sur la localisation et l'identification par l'imagerie des lipides par spectrométrie de masse sur les coupes ovariennes des différentes espèces de mammifères, sous l'influence de différents traitements, tels que la supplémentation en acides gras.

CONCLUSIONS

Analysis of lipids content and related transcriptional control in bovine ovarian follicle imply the potential capacity of bovine theca and granulosa cells to uptake lipoproteins and free FA, metabolize and transport them. From these lipid-blocks, the follicular cells have the capacity to perform lipolysis, lipogenesis, mitochondrial and peroxisomal FA oxidation and store lipids by LDs production. Lipid metabolism may therefore assure membrane biosynthesis in somatic cells and particularly in the oocyte, precursors of steroid hormones, secondary messengers, and probably perform synthesis of cholesteryl esters and lipoprotein cholesterol. Expression of FA transporters indicate the exchanges between blood circulation and follicular cells wall and between FF and cumulus-oocyte complex. Lipid fingerprints found in large-size follicle compartments suggested the storage of molecules with large mass per charge (m/z), an increase in lipids species of long-chain and very-long-chain FAs. During antral follicle terminal growth, lipid composition significantly changed in both somatic cells and fluid as revealed by mass spectrometry lipidomics. The follicular fluid showed huge diversity in the lipid composition along with follicular growth, without notable fluctuations in the lipid profiles of the oocytes from the follicles of different sizes. However, the oocyte has the ability to accumulate lipids and also contains specific metabolic machinery that can be used for energy production, membrane synthesis and signaling in order to ensure meiotic maturation, fertilization and provide building blocks needed for the first embryonic cells. Coupled with the differences in lipid composition observed in somatic cells of dominant large size follicles, these data may suggest the accumulation by the follicle of lipid reserves for future use by the remnant-follicular cells after ovulation to benefit the production of progesterone by corpus luteum for gestation maintenance.

The lipid and transcriptomic signatures of the theca, granulosa, and cumulus cells, as well as the oocyte, are consistent with their specific functions. They reflect the cooperation between these cells to metabolize fatty acids and the existence of molecular exchanges via the follicular fluid, to maintain follicle homeostasis and protect the oocyte. And thus, the accumulation of different classes of lipids in the oocyte and its transcript stock suggest its ability to provide energy, membrane lipids, and signaling, to support its maturation, fertilization, and the first embryonic cleavages.

The identification of lipid species detected in different follicular compartments and at different stages of folliculogenesis would allow us to deepen our knowledge about the metabolic interactions within the follicle, in correlation with cow metabolism and with activities relevant for lipid synthesis and degradation. Through lipids, it is probably possible to regulate important processes such as membrane synthesis, lipoprotein, cholesterol, steroids and de novo producing lipids during the initial to terminal

folliculogenesis, as well as signaling between cells, and perhaps thus provide a favorable energy balance for reproduction.

In this work, it was possible to identify that the lipid metabolism is directly correlated to the negative energy balance of farm animals. In order to deepen and prove several hypotheses raised here, I suggest for future research (1) Further analysis of the proteins in follicular cells, such as the enzymatic regulation of lipid transformation; lipoprotein production by somatic cells; analysis of modulated pathways during follicular growth (elongation, oxidation, oxidative stress, etc.). (2) A study the link between follicular atresia state and its lipid content, through analyzed by P4/E2 assay on individual follicles of different sizes; cytomorphological and immunological evaluation of granulosa atresia; associated with ICM-MS profiling in well-characterized follicles. (3) Multi-omic analyzes of follicular compartments, by classical proteomics, MALDI-TOF lipid profiles in follicular cells and fluid and lipid imaging on ovarian sections correlate to well-characterized follicles; and use of bioinformatics tools to integrate lipidome/proteome data. (4) Functional analysis in well-characterized follicles by (a) *in vitro*: use of inhibitors/activators of different stages of lipid metabolism and lipid analyzes; and (b) *in vivo*: follicular cell/fluid analyzes of animals with different conditions, as supplementation with different kind of fatty acids, and/or under influence of different nutritional treatments.

This thesis made it possible to establish a new approach to the analysis of lipid species identified in different compartments of antral follicles and the correlation between the physiological conditions of the various processes of lipid metabolism during the growth of ovarian follicles and oocytes. However, these discoveries raise new questions that are investigated in our laboratory.

.

BIBLIOGRAPHY

BIBLIOGRAPHY

Aardema, H. *et al.* (2011) 'Oleic Acid Prevents Detrimental Effects of Saturated Fatty Acids on Bovine Oocyte Developmental Competence', *Biology of Reproduction*, 85(1), pp. 62–69. doi: 10.1095/biolreprod.110.088815.

Aardema, H. *et al.* (2013) 'Bovine Cumulus Cells Protect Maturing Oocytes from Increased Fatty Acid Levels by Massive Intracellular Lipid Storage', *BIOLOGY OF REPRODUCTION*, 88164(6), pp. 1–15. doi: 10.1095/biolreprod.112.106062.

Aardema, H. *et al.* (2017) 'Stearoyl-CoA desaturase activity in bovine cumulus cells protects the oocyte against saturated fatty acid stress', *Biology of Reproduction*, 96(5), pp. 982–992. doi: 10.1095/biolreprod.116.146159.

Aardema, H., Vos, P. L. A. M. and Gadella, B. M. (2018) 'Cumulus cells protect the oocyte against saturated free fatty acids', *Animal Reproduction*, 15(Suppl. 1), pp. 737–750. doi: 10.21451/1984-3143-ar2018-0063.

Acuña, M. *et al.* (2016) 'Structural and functional analysis of the ASM p.Ala359Asp mutant that causes acid sphingomyelinase deficiency', *Biochemical and Biophysical Research Communications*, 479(3), pp. 496–501. doi: 10.1016/j.bbrc.2016.09.096.

Adamiak, S. J. *et al.* (2006) 'Body composition, dietary carbohydrates and fatty acids determine post-fertilisation development of bovine oocytes in vitro', *Reproduction*, 131(2), pp. 247–258. doi: 10.1530/rep.1.00871.

Ambrose, D. J. *et al.* (2006) 'Lower Pregnancy Losses in Lactating Dairy Cows Fed a Diet Enriched in α-Linolenic Acid', *Journal of Dairy Science*. Elsevier, 89(8), pp. 3066–3074. doi: 10.3168/jds.s0022-0302(06)72581-4.

Ami, D. *et al.* (2011) 'Biochimica et Biophysica Acta FTIR spectral signatures of mouse antral oocytes : Molecular markers of oocyte maturation and developmental competence', *BBA - Molecular Cell Research*. Elsevier B.V., 1813(6), pp. 1220–1229. doi: 10.1016/j.bbamcr.2011.03.009.

Annes, K. *et al.* (2018) 'Influence of follicle size on bovine oocyte lipid composition , follicular metabolic and stress markers , embryo development and blastocyst lipid content', *Reproduction, Fertility and Development*. doi: 10.1071/RD18109.

De Antueno, R. J. *et al.* (2001) 'Activity of human Δ5 and Δ6 desaturases on multiple n-3 and n-6 polyunsaturated fatty acids', *FEBS Letters*, 509(1), pp. 77–80. doi: 10.1016/S0014-5793(01)03135-0.

Assey, R. J. *et al.* (1994) 'Oocyte morphology in dominant and subordinate follicles', *Molecular Reproduction and Development*, 37(3), pp. 335–344. doi: 10.1016/S0021-9673(03)00538-7.

Assidi, M., Dieleman, S. J. and Sirard, M. A. (2010) 'Cumulus cell gene expression following the LH surge in bovine preovulatory follicles: Potential early markers of oocyte competence', *Reproduction*, 140(6), pp. 835–852. doi: 10.1530/REP-10-0248.

Attie, A. D. (2006) 'A liver-high-density lipoprotein-ovarian axis of fertility', *Endocrinology*, 147(4), pp. 1575–1576. doi: 10.1210/en.2006-0093.

Auclair, S. *et al.* (2013) 'Absence of cumulus cells during in vitro maturation affects lipid metabolism in bovine oocytes', *Am J Physiol Endocrinol Metab*, 15(67), pp. E599–E613. doi: 10.1152/ajpendo.00469.2012.

Azhar, S. *et al.* (2006) 'LDL and cAMP cooperate to regulate the functional expression of the LRP

in rat ovarian granulosa cells.', *Journal of lipid research*, 47(11), pp. 2538–50. doi: 10.1194/jlr.M600349-JLR200.

Azhar, S. and Reaven, E. (2002) 'Scavenger receptor class BI and selective cholesteryl ester uptake: Partners in the regulation of steroidogenesis', *Molecular and Cellular Endocrinology*, 195(1–2), pp. 1–26. doi: 10.1016/S0303-7207(02)00222-8.

Azhar, S., Tsai, L. and Reaven, E. (1990) 'Uptake and utilization of lipoprotein cholesteryl esters by rat granulosa cells', *Biochimica et Biophysica Acta (BBA)/Lipids and Lipid Metabolism*, 1047(2), pp. 148–160. doi: 10.1016/0005-2760(90)90041-U.

Baarine, M. *et al.* (2012) 'Evidence of oxidative stress in very long chain fatty acid - Treated oligodendrocytes and potentialization of ROS production using RNA interference-directed knockdown of ABCD1 and ACOX1 peroxisomal proteins', *Neuroscience*, 213, pp. 1–18. doi: 10.1016/j.neuroscience.2012.03.058.

Bauchart, D. (1993) 'Lipid Absorption and Transport in Ruminants', *Journal of Dairy Science*. Elsevier, 76(12), pp. 3864–3881. doi: 10.3168/jds.S0022-0302(93)77728-0.

Beever, D. E. (2006) 'The impact of controlled nutrition during the dry period on dairy cow health, fertility and performance', *Animal Reproduction Science*, 96(3–4), pp. 212–226. doi: 10.1016/j.anireprosci.2006.08.002.

Bennabi, I., Terret, M. E. and Verlhac, M. H. (2016) 'Meiotic spindle assembly and chromosome segregation in oocytes', *Journal of Cell Biology*, 215(5), pp. 611–619. doi: 10.1083/jcb.201607062.

Binelli, M. and Murphy, B. D. (2010) 'Coordinated regulation of follicle development by germ and somatic cells', *Reproduction, Fertility and Development*, 22(1), pp. 1–12. doi: 10.1071/RD09218.

Bionaz, M. *et al.* (2013) 'Functional role of PPARs in ruminants: Potential targets for fine-tuning metabolism during growth and lactation', *PPAR Research*. doi: 10.1155/2013/684159.

Blasiole, D. A., Davis, R. A. and Attie, A. D. (2007) 'The physiological and molecular regulation of lipoprotein assembly and secretion', *Molecular BioSystems*, 3(9), pp. 608–619. doi: 10.1039/b700706j.

Boland, N. I. *et al.* (1994) 'Characterization of follicular energy metabolism', *Human Reproduction*, 9(4), pp. 604–609.

Bonen, A. *et al.* (2004) 'Regulation of fatty acid transport by fatty acid translocase/CD36', *Proceedings of the Nutrition Society*, 63(2), pp. 245–249. doi: 10.1079/PNS2004331.

Boots, C. and Jungheim, E. (2015) 'Inflammation and Human Ovarian Follicular Dynamics', *Seminars in Reproductive Medicine*, 33(4), pp. 270–275. doi: 10.1055/s-0035-1554928.

Borgbo, T. *et al.* (2013) 'Comparison of gene expression profiles in granulosa and cumulus cells after ovulation induction with either human chorionic gonadotropin or a gonadotropin-releasing hormone agonist trigger', *Fertility and Sterility*. Elsevier Inc., 100(4), p. 994–1001.e2. doi: 10.1016/j.fertnstert.2013.05.038.

Boruszewska, D. *et al.* (2015) 'The effect of lysophosphatidic acid during in vitro maturation of bovine cumulus-oocyte complexes: Cumulus expansion, glucose metabolism and expression of genes involved in the ovulatory cascade, oocyte and blastocyst competence', *Reproductive Biology and Endocrinology*. ???, 13(1), pp. 1–18. doi: 10.1186/s12958-015-0044-x.

Brown, M. S. and Goldstein, J. L. (1986) 'M58 A receptor-mediated pathway for cholesterol

homeostasis.', *Science (New York, N.Y.)*, 232(4746), pp. 34–47. doi: 10.1126/science.3513311.

Browne, R. W. *et al.* (2008) 'Distributions of high-density lipoprotein particle components in human follicular fluid and sera and their associations with embryo morphology parameters during IVF', *Human Reproduction*, 23(8), pp. 1884–1894. doi: 10.1093/humrep/den183.

Buratini, J. and Price, C. A. (2011) 'Follicular somatic cell factors and follicle development', *Reproduction, Fertility and Development*, 23(1), pp. 32–39. doi: 10.1071/RD10224.

Campbell, B. K. and Baird, D. T. (2001) 'Inhibin A is a follicle stimulating hormone-responsive marker of granulosa cell differentiation , which has both autocrine and paracrine actions in sheep', pp. 333–345.

Cetica, P. *et al.* (2002) 'Activity of key enzymes involved in glucose and triglyceride catabolism during bovine oocyte maturation in vitro', *Reproduction*, 124, pp. 675–681.

Chang, T.-Y. *et al.* (2017) 'Cellular cholesterol homeostasis and Alzheimer's disease', *Journal of Lipid Research*, 58(12), pp. 2239–2254. doi: 10.1194/jlr.R075630.

Chansela, P. *et al.* (2012) 'Composition and localization of lipids in penaeus merguiensis ovaries during the ovarian maturation cycle as revealed by imaging mass spectrometry', *PLoS ONE*. doi: 10.1371/journal.pone.0033154.

Chaurand, P. *et al.* (2011) 'From Whole-body Sections Down to Cellular Level, Multiscale Imaging of Phospholipids by MALDI Mass Spectrometry* □ S', *Molecular & Cellular Proteomics*, pp. 1–11. doi: 10.1074/mcp.O110.004259.

Childs, S. *et al.* (2008) 'Effect of level of dietary n-3 polyunsaturated fatty acid supplementation on systemic and tissue fatty acid concentrations and on selected reproductive variables in cattle', 70, pp. 595–611. doi: 10.1016/j.theriogenology.2008.04.002.

Chmurzyńska, A. (2006) 'The multigene family of fatty acid-binding proteins (FABPs): Function, structure and polymorphism', *Journal of Applied Genetics*, 47(1), pp. 39–48. doi: 10.1007/BF03194597.

Christian, B. E. and Spremulli, L. L. (2012) 'Mechanism of protein biosynthesis in mammalian mitochondria', *Biochimica et Biophysica Acta - Gene Regulatory Mechanisms*. Elsevier B.V., 1819(9–10), pp. 1035–1054. doi: 10.1016/j.bbagrm.2011.11.009.

Christiansen-Weber, T. A. *et al.* (2000) 'Functional Loss of ABCA1 in Mice Causes Severe Placental Malformation, Aberrant Lipid Distribution, and Kidney Glomerulonephritis As Well As High- Density Lipoprotein Cholesterol Deficiency', *The American Journal of Pathology*, 157(3), pp. 1017–1029. doi: 10.1016/S0002-9440(10)64614-7.

Christie, W. W. (2003) *Isolation, Separation, Identification and Structural Analysis of Lipids in Lipid Analysis.* 3 Edition. Edited by W. W. Christie. Bridgwater: The Oily Press.

Cinti, D. L. *et al.* (1992) 'The fatty acid chain elongation system of mammalian endoplasmic reticulum', *Progress in Lipid Research*, 31(1), pp. 1–51. doi: 10.1016/0163-7827(92)90014-A.

Clark, A. R. and Stokes, Y. M. (2011) 'Follicle Structure Influences the Availability of Oxygen to the Oocyte in Antral Follicles', *Computational and Mathematical Methods in Medicine*. doi: 10.1155/2011/287186.

Del Collado, M. *et al.* (2017) 'Fatty Acid Binding Protein 3 and Transzonal Projections Are Involved in Lipid Accumulation during in Vitro Maturation of Bovine Oocytes', *Scientific Reports*, 7(1). doi: 10.1038/s41598-017-02467-9.

Collado, M. del *et al.* (2018) 'Contributions from the ovarian follicular environment to oocyte function', *Animal Reproduction*, 15(3), pp. 261–270. doi: 10.21451/1984-3143-AR2018-.

Collado-Fernandez, E., Picton, H. M. and Dumollard, Ré. (2012) 'Metabolism throughout follicle and oocyte development in mammals', *Int. J. Dev. Biol.*, 56, pp. 799–808. doi: 10.1387/ijdb.120140ec.

Comin, A. *et al.* (2002) 'The effect of an acute energy deficit on the hormone profile of dominant follicles in dairy cows', *Theriogenology*, 58(5), pp. 899–910. doi: 10.1016/S0093-691X(02)00922-6.

Cordeiro, F. B. *et al.* (2018) 'Ovarian environment aging: follicular fluid lipidomic and related metabolic pathways', *Journal of Assisted Reproduction and Genetics*. Journal of Assisted Reproduction and Genetics, 35(8), pp. 1385–1393. doi: 10.1007/s10815-018-1259-5.

Cortvrindt, R. and Smitz, J. (2001) 'Review In vitro Follicle Growth : Achievements in Mammalian Species In vivo folliculogenesis : morphology', *Journal of Reproduction and Fertility*, 9, pp. 3–9.

Cui, X. *et al.* (2007) 'Maternal Gene Transcription in Mouse Oocytes : Genes Implicated in Oocyte Maturation and Fertilization', 53(2).

Curry, T. E. and Smith, M. F. (2006) 'Impact of extracellular matrix remodeling on ovulation and the folliculo-luteal transition', *Seminars in Reproductive Medicine*, 24(4), pp. 228–241. doi: 10.1055/s-2006-948552.

Dadarwal, D. *et al.* (2015) 'Organelle reorganization in bovine oocytes during dominant follicle growth and regression', *Reproductive Biology and Endocrinology*. Reproductive Biology and Endocrinology, 13(1), pp. 1–11. doi: 10.1186/s12958-015-0122-0.

Dautel, S. E. *et al.* (2017) 'Lipidomics reveals dramatic lipid compositional changes in the maturing postnatal lung', *Scientific Reports*. Nature Publishing Group, 7(February), pp. 1–12. doi: 10.1038/srep40555.

Dewailly, D. *et al.* (2016) 'Interactions between androgens , FSH , anti-Müllerian hormone and estradiol during folliculogenesis in the human normal and polycystic ovary Androgens-FSH-AMH', *Human Reproduction Update*, 22(6), pp. 709–724. doi: 10.1093/humupd/dmw027.

Dirandeh, E. *et al.* (2013) 'Effects of different polyunsaturated fatty acid supplementations during the postpartum periods of early lactating dairy cows on milk yield, metabolic responses, and reproductive performances', *Journal of Animal Science*, 91(2), pp. 713–721. doi: 10.2527/jas.2012-5359.

Donald B. Jump (2009) 'Mammalian Fatty Acid Elongases', *Methods Mol Biol.*, pp. 375–389. doi: 10.1007/978-1-60761-322-0_19.

Donnay, I. *et al.* (2004) 'Effect of prematuration, meiosis activating sterol and enriched maturation medium on the nuclear maturation and competence to development of calf oocytes', *Theriogenology*, 62(6), pp. 1093–1107. doi: 10.1016/j.theriogenology.2003.12.019.

Drzazga, A., Sowińska, A. and Koziołkiewicz, M. (2014) 'Lysophosphatidylcholine and lysophosphatidylinosiol novel promissing signaling molecules and their possible therapeutic activity', *Acta Poloniae Pharmaceutica - Drug Research*, 71(6), pp. 887–899.

Dunning, K. R. *et al.* (2010) 'Beta-Oxidation Is Essential for Mouse Oocyte Developmental Competence and Early Embryo Development 1', *Biology of reproduction*, 83, pp. 909–918. doi: 10.1095/biolreprod.110.084145.

Dunning, K. R. *et al.* (2012) 'Molecular Filtration Properties of the Mouse Expanded Cumulus

Matrix: Controlled Supply of Metabolites and Extracellular Signals to Cumulus Cells and the Oocyte1', *Biology of Reproduction*, 87(4), pp. 1–10. doi: 10.1095/biolreprod.111.096271.

Dunning, K. R. *et al.* (2014) 'Regulation of fatty acid oxidation in mouse cumulus-oocyte complexes during maturation and modulation by PPAR agonists', *PLoS ONE*, 9(2), pp. 1–11. doi: 10.1371/journal.pone.0087327.

Dunning, K. R., Russell, D. L. and Robker, R. L. (2014) 'Lipids and oocyte developmental competence: The role of fatty acids and B-oxidation', *Reproduction*, 148(1). doi: 10.1530/REP-13-0251.

Eberlin, L. S. *et al.* (2011) 'DESI then MALDI mass spectrometry imaging of lipid and protein distributions in single tissue sections', *November*, 15(8322), pp. 8366–8371. doi: 10.1021/ac202016x.

Elis, S. *et al.* (2015) 'Cell proliferation and progesterone synthesis depend on lipid metabolism in bovine granulosa cells', *Theriogenology*. Elsevier Inc, 83(5), pp. 840–853. doi: 10.1016/j.theriogenology.2014.11.019.

Elis, S. *et al.* (2016) 'Effect of a long-chain n-3 polyunsaturated fatty acid–enriched diet on adipose tissue lipid profiles and gene expression in Holstein dairy cows', *Journal of Dairy Science*. Elsevier, 99(12), pp. 10109–10127. doi: 10.3168/jds.2016-11052.

Elis, S. *et al.* (2017) 'Docosahexaenoic acid mechanisms of action on the bovine oocyte-cumulus complex', *Journal of Ovarian Research*, 10(1). doi: 10.1186/s13048-017-0370-z.

Fadeel, B. and Xue, Di. (2009) 'Membrane : Roles in Health and Disease', *Crit Rev Biochem Mol Biol*, 44(5), pp. 264–277. doi: 10.1080/10409230903193307.The.

Fahy, E. *et al.* (2005) 'A comprehensive classification system for lipids', *Journal of Lipid Research*, 46(5), pp. 839–862. doi: 10.1194/jlr.E400004-JLR200.

Fahy, E. *et al.* (2009) 'Update of the LIPID MAPS comprehensive classification system for lipids', *Journal of Lipid Research*, 50(Supplement), pp. S9–S14. doi: 10.1194/jlr.R800095-JLR200.

Fair, T. (2003) 'Follicular oocyte growth and acquisition of developmental competence', 78, pp. 203–216. doi: 10.1016/S0378-4320(03)00091-5.

Fair, T. *et al.* (2007) 'Global gene expression analysis during bovine oocyte in vitro maturation', *Theriogenology*, 68(SUPPL. 1), pp. 91–97. doi: 10.1016/j.theriogenology.2007.04.018.

Fair, T., Hyttel, P. and Greve, T. (1995) 'Bovine oocyte size in relationship to follicular diameter, maturational competence and rna synthesis', *Theriogenology*, 43, p. 209. doi: 10.1016/0093-691X(95)92363-E.

Favari, E. *et al.* (2009) 'Small discoidal pre-β1 HDL particles are efficient acceptors of cell cholesterol via ABCA1 and ABCG1', *Biochemistry*, 48(46), pp. 11067–11074. doi: 10.1021/bi901564g.

Fernandis, A. Z. and Wenk, M. R. (2007) 'Membrane lipids as signaling molecules', *Current Opinion in Lipidology*, 18, pp. 121–128.

Ferreira, C. R. *et al.* (2010) 'Single embryo and oocyte lipid fingerprinting by mass spectrometry', *The Journal of Lipid Research*, 51(5), pp. 1218–1227. doi: 10.1194/jlr.D001768.

Ferreira, E. M. *et al.* (2009) 'Cytoplasmic maturation of bovine oocytes: Structural and biochemical modifications and acquisition of developmental competence', *Theriogenology*, 71(5), pp. 836–848. doi: 10.1016/j.theriogenology.2008.10.023.

Fouladi-nashta, A. A. *et al.* (2007) 'Impact of Dietary Fatty Acids on Oocyte Quality and Development in Lactating Dairy Cows 1', *Biology of reproduction*, 17(March), pp. 9–17. doi: 10.1095/biolreprod.106.058578.

Fowler, S. D. and Greenspan, P. (1985) 'Application of Nile red, a fluorescent hydrophobic probe, for the detection of neutral lipid deposits in tissue sections: Comparison with oil red O', *Journal of Histochemistry and Cytochemistry*, 33(8), pp. 833–836. doi: 10.1177/33.8.4020099.

Fraser, H. M. (2006) 'Regulation of the ovarian follicular vasculature', *Reproductive Biology and Endocrinology*, 4, pp. 1–9. doi: 10.1186/1477-7827-4-18.

Friggens, N. C. *et al.* (2009) 'Invited review: Body condition score and its association with dairy cow productivity, health, and welfare', *Journal of Dairy Science*. Elsevier, 92(12), pp. 5769–5801. doi: 10.3168/jds.2009-2431.

Fuchs, B. and Schiller, J. (2008) 'MALDI-TOF MS Analysis of Lipids from Cells, Tissues and Body Fluids', *Lipids in Health and Disease*, pp. 541–565. doi: 10.1007/978-1-4020-8831-5_21.

Fujimoto, V. Y. *et al.* (2009) 'High-density lipoprotein metabolism and the human embryo', *Human Reproduction Update*, 16(1), pp. 20–38. doi: 10.1093/humupd/dmp029.

Garrett, R. h. and Grisham, C. M. (2000) *Biochimie*. 2th Editio. Paris: Sauders College Publishing.

Gautier, T. *et al.* (2010) 'Human luteinized granulosa cells secrete apoB100-containing lipoproteins', *Journal of Lipid Research*, 51(8), pp. 2245–2252. doi: 10.1194/jlr.M005181.

Genicot, G. *et al.* (2005) 'The use of a fluorescent dye , Nile red , to evaluate the lipid content of single mammalian oocytes', *Theriogenology*, 63, pp. 1181–1194. doi: 10.1016/j.theriogenology.2004.06.006.

Gentile, L. *et al.* (2004) 'Single-cell quantitative RT-PCR analysis of Cpt1b and Cpt2 gene expression in mouse antral oocytes and in preimplantation embryos', *Genome in Development and Cloning*, pp. 215–221. doi: 10.1159/000078191.

Gibellini, F. and Smith, T. K. (2010) 'The Kennedy pathway-de novo synthesis of phosphatidylethanolamine and phosphatidylcholine', *IUBMB Life*, 62(6), pp. 414–428. doi: 10.1002/iub.337.

Gilchrist, R. B., Ritter, L. J. and Armstrong, D. T. (2004) 'Oocyte-somatic cell interactions during follicle development in mammals', *Animal Reproduction Science*, 82–83, pp. 431–446. doi: 10.1016/j.anireprosci.2004.05.017.

Glatz, J. F. C. and Luiken, J. (2017) 'From fat to FAT (CD36/SR-B2): Understanding the regulation of cellular fatty acid uptake', *Biochimie*. Elsevier Ltd, 136, pp. 21–26. doi: 10.1016/j.biochi.2016.12.007.

Goldstein, J. L. and Brown, M. S. (2009) 'History of DIscovery: The LDL receptor.', *Arteriosclerosis, thrombosis, and vascular biology*, 29(4), pp. 431–8. doi: 10.1161/ATVBAHA.108.179564.History.

González-Serrano, A. F. *et al.* (2013) 'Desorption Electrospray Ionization Mass Spectrometry Reveals Lipid Metabolism of Individual Oocytes and Embryos', *PLoS ONE*, 8(9), pp. 1–11. doi: 10.1371/journal.pone.0074981.

Goodenough, D. A. and Paul, D. L. (2009) 'Gap junctions.', *Cold Spring Harbor perspectives in biology*, 1(1), pp. 1–19. doi: 10.1101/cshperspect.a002576.

Goto-Inoue, N. *et al.* (2011) 'Imaging mass spectrometry for lipidomics', *BBA - Molecular and Cell*

Biology of Lipids, 1811, pp. 961–969. doi: 10.1016/j.bbalip.2011.03.004.

Grevengoed, T. J., Klett, E. L. and Coleman, R. A. (2014) 'Acyl-CoA Metabolism and Partitioning', *Annu Rev Nutr*, 34, pp. 1–30. doi: 10.1146/annurev-nutr-071813-105541.

Griffiths, W. J. *et al.* (2001) 'Electrospray and tandem mass spectrometry in biochemistry', *Biochem. J*, 355, pp. 545–561.

Grummer, R. R. and Carroll, D. J. (1988) 'A review of lipoprotein cholesterol metabolism: importance to ovarian function.', *Journal of animal science*, 66(12), pp. 3160–3173. doi: 10.2527/jas1988.66123160x.

Gu, L. *et al.* (2015) 'Metabolic control of oocyte development:linking maternal nutrition and reproductive outcomes', *Cell Mol Life Sci.*, 72(2), pp. 251–271. doi: 10.1007/s00018-014-1739-4.Metabolic.

Guerreiro, T. M. *et al.* (2018) 'A Metabolomic Overview of Follicular Fluid in Cows', *Frontiers in Veterinary Science*, 5(February), pp. 1–9. doi: 10.3389/fvets.2018.00010.

Guillou, H. *et al.* (2010) 'The key roles of elongases and desaturases in mammalian fatty acid metabolism: Insights from transgenic mice', *Progress in Lipid Research*. Elsevier Ltd, 49(2), pp. 186–199. doi: 10.1016/j.plipres.2009.12.002.

Gunter, J. (2016) *Steroidogenesis, Intravaginal DHEA Isn't An 'Alternative' To Estrogen It's The Prodrug*. Available at: https://drjengunter.wordpress.com/2016/01/11/ (Accessed: 11 January 2016).

Gurr, M. I., Harwood, J. L. and Frayn, K. N. (2002) *Lipid Biochemistry*. 5th Editio. Blackwell Science: Malden. doi: 10.1002/9780470774366.

Gustafsson, J. O. R. *et al.* (2011) 'MALDI imaging mass spectrometry (MALDI-IMS)-application of spatial proteomics for ovarian cancer classification and diagnosis', *International Journal of Molecular Sciences*, 12(1), pp. 773–794. doi: 10.3390/ijms12010773.

Guzel, Y., Bildik, G. and Oktem, O. (2018) 'Sphingosine-1-phosphate protects human ovarian follicles from apoptosis in vitro', *European Journal of Obstetrics Gynecology and Reproductive Biology*. Elsevier Ireland Ltd, 222, pp. 19–24. doi: 10.1016/j.ejogrb.2018.01.001.

Hall, J. E. and Guyton, A. C. (2016) *Guyton and Hall textbook of medical physiology.* Philadelphia: Elsevier.

Han, X. (2016) 'Lipidomics for studying metabolism', *Nature Publishing Group*. Nature Publishing Group, 12(11), pp. 668–679. doi: 10.1038/nrendo.2016.98.

Hannun, Y. A. and Obeid, L. M. (1995) 'Ceramide: an intracellular signal for apoptosis', (February), pp. 0–4.

Harris, S. E. *et al.* (2007) 'Carbohydrate metabolism by murine ovarian follicles and oocytes grown in vitro', *Reproduction*, 134, pp. 415–424. doi: 10.1530/REP-07-0061.

Harris, S. E., Leese, H. J. and Gosden, R. G. (2009) 'Pyruvate and Oxygen Consumption Throughout the Growth and Development of Murine Oocytes', 238, pp. 231–238. doi: 10.1002/mrd.20945.

Hashemi, H. F. and Goodman, J. M. (2015) 'The life cycle of lipid droplets', *Current Opinion in Cell Biology*. Elsevier Ltd, 33, pp. 119–124. doi: 10.1016/j.ceb.2015.02.002.

Hatzirodos, N., Hummitzsch, K., Irving-rodgers, H. F., *et al.* (2014) 'Transcriptome profiling of granulosa cells from bovine ovarian follicles during atresia', *BMC Genomics*, 14. doi:

10.1186/1471-2164-15-24.

Hatzirodos, N., Hummitzsch, K., Irving-Rodgers, H. F., *et al.* (2014) 'Transcriptome profiling of the theca interna in transition from small to large antral ovarian Follicles', *PLoS ONE*, 9(5). doi: 10.1371/journal.pone.0097489.

Hidaka, H. *et al.* (2007) 'Analysis of human serum lipoprotein lipid composition using MALDI-TOF mass spectrometry', *Annals of Clinical and Laboratory Science*, 37(3), pp. 213–221.

Holthuis, J. C. M. and Menon, A. K. (2014) 'Lipid landscapes and pipelines in membrane homeostasis', *Nature*, 510(7503), pp. 48–57. doi: 10.1038/nature13474.

Hopkins, M. *et al.* (2016) 'Eicosopentaneoic Acid and Other Free Fatty Acid Receptor Agonists Inhibit Lysophosphatidic Acid- and Epidermal Growth Factor-Induced Proliferation of Human Breast Cancer Cells', *Journal of Clinical Medicine*, 5(2), p. 16. doi: 10.3390/jcm5020016.

Hsueh, A. J. W. *et al.* (2015) 'Intraovarian control of early folliculogenesis', *Endocrine Reviews*, 36(1), pp. 1–24. doi: 10.1210/er.2014-1020.

Hussain, M. M. *et al.* (2012) 'Multiple functions of microsomal triglyceride transfer protein', *Nutrition and Metabolism*, 9, pp. 1–16. doi: 10.1186/1743-7075-9-14.

Hutt, K. J., McLaughlin, E. A. and Holland, M. K. (2006) 'Kit ligand and c-Kit have diverse roles during mammalian oogenesis and folliculogenesis', *Molecular Human Reproduction*, 12(2), pp. 61–69. doi: 10.1093/molehr/gal010.

Hyttel, P., Fair, T., Callesen, H. and G. T. . (1997) 'OOCYTE GROWTH, CAPACITATION AND FINAL MATURATION IN CATTLE', *Science*, (96), pp. 23–32.

Igal, R. a *et al.* (2001) 'Diacylglycerol generated in CHO cell plasma membrane by phospholipase C is used for triacylglycerol synthesis.', *Journal of lipid research*, 42(1), pp. 88–95. Available at: http://www.ncbi.nlm.nih.gov/pubmed/11160369.

Inoue, N. *et al.* (2011) 'Role of Cell-Death Ligand-Receptor System of Granulosa Cells in Selective Follicular Atresia in Porcine Ovary', *Journal of Reproduction and Development*, 57(2), pp. 169–175. doi: 10.1262/jrd.10-198e.

Ireland, J. J. *et al.* (2000) 'Historical Perspective of Turnover of Dominant Follicles During the Bovine Estrous Cycle: Key Concepts, Studies, Advancements, and Terms', *Journal of Dairy Science*, 83(7), pp. 1648–1658. doi: 10.3168/jds.S0022-0302(00)75033-8.

Jackson, S. N., Wang, H. Y. J. and Woods, A. S. (2005) 'In situ structural characterization of phosphatidylcholines in brain tissue using MALDI-MS/MS', *Journal of the American Society for Mass Spectrometry*. doi: 10.1016/j.jasms.2005.08.014.

Jagerstrom, S. *et al.* (2009) 'Lipid droplets interact with mitochondria using SNAP23', *Cell Biology International*, 33, pp. 934–940. doi: 10.1016/j.cellbi.2009.06.011.

Jakobsson, A., Westerberg, R. and Jacobsson, A. (2006) 'Fatty acid elongases in mammals: Their regulation and roles in metabolism', *Progress in Lipid Research*, 45(3), pp. 237–249. doi: 10.1016/j.plipres.2006.01.004.

Jiang, J. *et al.* (2003) 'REGULATION OF CELL DEATH AND CELL SURVIVAL GENE EXPRESSION DURING OVARIAN FOLLICULAR DEVELOPMENT AND ATRESIA Jin-Yi Jiang, Carmen K.M. Cheung, Yifang Wang, Benjamin K. Tsang', *Obstetrics & Gynecology*, (1), pp. 222–237.

Jorritsma, R. *et al.* (2003) 'Acute fasting in heifers as a model for assessing the relationship between

plasma and follicular fluid NEFA concentrations', 60, pp. 151–161. doi: 10.1016/S0093-691X(02)01358-4.

Jungheim, E. S. *et al.* (2011) 'Associations between free fatty acids, cumulus oocyte complex morphology and ovarian function during in vitro fertilization', 95(6), pp. 1970–1974. doi: doi:10.1016/j.fertnstert.2011.01.154.

Junqueira, L. C. U. and Carneiro, J. (2010) *Basic histology : text & atlas*. New York: McGraw-Hill.

Kallen, C. B. *et al.* (1998) 'Unveiling the mechanism of action and regulation of the steroidogenic acute regulatory protein', *Molecular and Cellular Endocrinology*, 145(1–2), pp. 39–45. doi: 10.1016/S0303-7207(98)00167-1.

Kent, C. (1995) 'Eukaryotic phospholipid biosynthesis', *Annual Review of Biochemistry*, 64, pp. 315–343.

Khor, V. K. *et al.* (2014) 'The Proteome of Cholesteryl-Ester-Enriched Versus Triacylglycerol-Enriched Lipid Droplets', 9(8), pp. 1–11. doi: 10.1371/journal.pone.0105047.

Khrameeva, E. *et al.* (2018) 'Lipidome evolution in mammalian tissues', *Molecular Biology and Evolution*, 35(8), pp. 1947–1957. doi: 10.1093/molbev/msy097.

Kidder, G. M. and Mhawi, A. A. (2002) 'Gap junctions and ovarian folliculogenesis', *Reproduction*, 123(5), pp. 613–620. doi: 10.1530/reprod/123.5.613.

Kihara, A. (2012) 'Very long-chain fatty acids: Elongation, physiology and related disorders', *Journal of Biochemistry*, 152(5), pp. 387–395. doi: 10.1093/jb/mvs105.

Kim, J. Y. *et al.* (2001) 'Lipid and fatty acid analysis of fresh and frozen-thawed immature and in vitro matured bovine oocytes', *Reproduction*, 122(1), pp. 131–138. doi: 10.1530/reprod/122.1.131.

Kol, S. and Adashi, E. Y. (1995) 'Intraovarian factors regulating ovarian function', *Current Opinion in Obstetrics and Gynecology*, 7, pp. 209–213.

Koonen, D. P. Y. *et al.* (2005) 'Long-chain fatty acid uptake and FAT/CD36 translocation in heart and skeletal muscle', *Biochimica et Biophysica Acta - Molecular and Cell Biology of Lipids*, 1736(3), pp. 163–180. doi: 10.1016/j.bbalip.2005.08.018.

Kumari, A. (2018) 'Beta Oxidation of Fatty Acids', *Sweet Biochemistry*, pp. 17–19. doi: 10.1016/0005-2760(91)90015-A.

Lagarrigue, M. *et al.* (2011) 'Matrix-Assisted Laser Desorption/Ionization Imaging Mass Spectrometry: A Promising Technique for Reproductive Research1', *Biology of Reproduction*, 86(3), pp. 1–11. doi: 10.1095/biolreprod.111.094896.

Lam, S. M. and Shui, G. (2013) 'Lipidomics as a Principal Tool for Advancing Biomedical Research', *Journal of Genetics and Genomics*. Elsevier Limited and Science Press, 40(8), pp. 375–390. doi: 10.1016/j.jgg.2013.06.007.

Leij, F. R. Van Der *et al.* (1999) 'Cytological evidence that the C-terminus of carnitine palmitoyltransferase I is on the cytosolic face of the mitochondrial outer membrane', 341, pp. 777–784.

Leroy, J. L. M. ., Vanholder, T., Delanghe, J. ., Opsomer, G., Van Soom, A., Bols, P. E. ., Dewulf, J., *et al.* (2004) 'Metabolic changes in follicular fluid of the dominant follicle in high-yielding dairy cows early post partum', *Theriogenology*, 62(6), pp. 1131–1143. doi: 10.1016/j.theriogenology.2003.12.017.

Leroy, J. L. M. ., Vanholder, T., Delanghe, J. ., Opsomer, G., Van Soom, A., Bols, P. E. . and de

Kruif, A. (2004) 'Metabolite and ionic composition of follicular fluid from different-sized follicles and their relationship to serum concentrations in dairy cows', *Animal Reproduction Science*, 80(3), pp. 201–211. doi: 10.1016/S0378-4320(03)00173-8.

Leroy, J. L. M. R. *et al.* (2005) 'Non-esterified fatty acids in follicular fluid of dairy cows and their effect on developmental capacity of bovine oocytes in vitro', *Reproduction*, 130(4), pp. 485–495. doi: 10.1530/rep.1.00735.

Leroy, J. L. M. R. *et al.* (2005) 'Short Communication Evaluation of the Lipid Content in Bovine Oocytes and Embryos with Nile Red : a Practical Approach', *Reproduction in domestic animals = Zuchthygiene*, 40(1), pp. 76–78. doi: 10.1111/j.1439-0531.2004.00556.x.

Leroy, J. L. M. R., Vanholder, T., *et al.* (2008) 'Nutrient Prioritization in Dairy Cows Early Postpartum: Mismatch Between Metabolism and Fertility?', *Reproduction in Domestic Animals*, 43(SUPPL.2), pp. 96–103. doi: 10.1111/j.1439-0531.2008.01148.x.

Leroy, J. L. M. R., Opsomer, G., *et al.* (2008) 'Reduced fertility in high-yielding dairy cows: Are the oocyte and embryo in danger? Part I. The importance of negative energy balance and altered corpus luteum function to the reduction of oocyte and embryo quality in high-yielding dairy cows', *Reproduction in Domestic Animals*, 43(5), pp. 612–622. doi: 10.1111/j.1439-0531.2007.00960.x.

Leroy, J. L. M. R. *et al.* (2014) 'Dietary fat supplementation and the consequences for oocyte and embryo quality: Hype or significant benefit for dairy cow reproduction?', *Reproduction in Domestic Animals*, 49(3), pp. 353–361. doi: 10.1111/rda.12308.

Liebisch, G. *et al.* (2013) 'Shorthand notation for lipid structures derived from mass spectrometry', *Journal of Lipid Research*, 54(6), pp. 1523–1530. doi: 10.1194/jlr.M033506.

Liu, Z. *et al.* (2014) 'Omega-3 Fatty Acids and Other FFA4 Agonists Inhibit Growth Factor Signaling in Human Prostate Cancer Cells', *Journal of Pharmacology and Experimental Therapeutics*, 352(2), pp. 380–394. doi: 10.1124/jpet.114.218974.

Lizardo, D. Y. *et al.* (2018) 'Noncanonical Roles of Lipids in Different Cellular Fates', *Biochemistry*, 57(1), pp. 22–29. doi: 10.1021/acs.biochem.7b00862.

Lolicato, F. *et al.* (2015) 'The Cumulus Cell Layer Protects the Bovine Maturing Oocyte Against Fatty Acid- Induced Lipotoxicity', *BIOLOGY OF REPRODUCTION*, 9216(1), pp. 1–16. doi: 10.1095/biolreprod.114.120634.

Makarov, A. *et al.* (2006) 'Performance Evaluation of a Hybrid Linear Ion Trap / Orbitrap Mass Spectrometer', *Anal. Chem.*, 78(7), pp. 2113–2120. doi: 10.1021/ac0518811.

Makide, K. *et al.* (2009) 'Emerging lysophospholipid mediators, lysophosphatidylserine, lysophosphatidylthreonine, lysophosphatidylethanolamine and lysophosphatidylglycerol', *Prostaglandins and Other Lipid Mediators*, 89(3–4), pp. 135–139. doi: 10.1016/j.prostaglandins.2009.04.009.

Malviya, R. *et al.* (2010) 'High Performance Liquid Chromatography: A Short Review', *Journal of Global Pharma Technology*, 2(May), pp. 22–26.

Man, W. C. *et al.* (2006) 'Colocalization of SCD1 and DGAT2: implying preference for endogenous monounsaturated fatty acids in triglyceride synthesis', *Journal of Lipid Research*, 47(9), pp. 1928–1939. doi: 10.1194/jlr.M600172-JLR200.

Manzanares-Meza, L. D., Gutiérrez-Román, C. I. and Medina-Contreras, O. (2017) 'Imagenología por MALDI: más allá del diagnóstico clásico', *Boletin Medico del Hospital Infantil de Mexico*. Hospital Infantil de México Federico Gómez, 74(3), pp. 212–218. doi:

10.1016/j.bmhimx.2017.03.004.

Mao, L. *et al.* (2014) 'Behaviour of cytoplasmic organelles and cytoskeleton during oocyte maturation', *Reproductive BioMedicine Online*. Reproductive Healthcare Ltd., 28(3), pp. 284–299. doi: 10.1016/j.rbmo.2013.10.016.

Marei, W. F., Wathes, D. C. and Fouladi-Nashta, A. A. (2009) 'The Effect of Linolenic Acid on Bovine Oocyte Maturation and Development1', *Biology of Reproduction*, 81(6), pp. 1064–1072. doi: 10.1095/biolreprod.109.076851.

Masini, E. *et al.* (2008) 'Ceramide : a Key Signaling Molecule in a Guinea Pig Model of Allergic Asthmatic Response and Airway Inflammation', 324(2), pp. 548–557. doi: 10.1124/jpet.107.131565.these.

Matoba, S. *et al.* (2014) 'Predictive value of bovine follicular components as markers of oocyte developmental potential', *Reproduction, Fertility and Development*, 26(2), pp. 337–345. doi: 10.1071/RD13007.

Mattos, R., Staples, C. R. and Thatcher, W. W. (2000) 'Effects of dietary fatty acids on reproduction in ruminants Digestion and absorption of fats', *Reviews of Reproduction*, 5, pp. 38–45. Available at: http://ror.reproduction-online.org/cgi/reprint/5/1/38.pdf.

McEvoy, T. G. *et al.* (2000) 'Fatty acid composition of lipids in immature cattle, pig and sheep oocytes with intact zona pellucida', *Journal of Reproduction and Fertility*, 118, pp. 163–170.

Van Meer, G., Voelker, D. R. and Feigenson, G. W. (2008) 'Membrane lipids: Where they are and how they behave', *Nature Reviews Molecular Cell Biology*, 9(2), pp. 112–124. doi: 10.1038/nrm2330.

Meikle, A. *et al.* (2001) 'Endometrial mRNA expression of oestrogen receptor alpha, progesterone receptor and insulin-like growth factor-I (IGF-I) throughout the bovine oestrous cycle.', *Animal reproduction science*, 68(1–2), pp. 45–56. Available at: http://www.ncbi.nlm.nih.gov/pubmed/11600273.

Melendez, A. J. (2008) 'Sphingosine kinase signalling in immune cells: Potential as novel therapeutic targets', *Biochimica et Biophysica Acta - Proteins and Proteomics*, 1784(1), pp. 66–75. doi: 10.1016/j.bbapap.2007.07.013.

Mellouk, N. *et al.* (2017) 'Involvement of plasma adipokines in metabolic and reproductive parameters in Holstein dairy cows fed with diets with differing energy levels', *Journal of Dairy Science*, 100(10), pp. 8518–8533. doi: 10.3168/jds.2017-12657.

Meriaux, C. *et al.* (2010) 'Liquid ionic matrixes for MALDI mass spectrometry imaging of lipids', *Journal of Proteomics*. doi: 10.1016/j.jprot.2010.02.010.

Mermillod, P. *et al.* (2008) 'Factors Affecting Oocyte Quality: Who is Driving the Follicle?', *Reproduction in Domestic Animals*, 43(SUPPL.2), pp. 393–400. doi: 10.1111/j.1439-0531.2008.01190.x.

Merrill, A. H. (2002) 'Biosynthesis : A Necessary , but Dangerous , Pathway *', *THE JOURNAL OF BIOLOGICAL CHEMISTRY*. doi: 10.1074/jbc.R200009200.

Metwally, M. *et al.* (2007) 'Effect of increased body mass index on oocyte and embryo quality in IVF patients', *Reproductive BioMedicine Online*, 15(5), pp. 532–538. doi: 10.1016/S1472-6483(10)60385-9.

Michel, V., Yuan, Z. and Ramsubir, S. (2006) 'Choline Transport for Phospholipid Synthesis', *Society for Experimental Biology and Medicine*, pp. 490–504.

Miettinen, H. E., Rayburn, H. and Krieger, M. (2001) 'Abnormal lipoprotein metabolism and reversible female infertility in HDL receptor (SR-BI)– deficient mice', *J Clin Invest*, 108, pp. 1717–1722. doi: 10.1172/JCI200113288.Introduction.

Milhas, D., Clarke, C. J. and Hannun, Y. A. (2011) 'Sphingomyelin metabolism at the plasma membrane: implications for bioactive sphingolipids', *NIH FEBS Lett.*, 584(9), pp. 1887–1894. doi: 10.1016/j.febslet.2009.10.058.Sphingomyelin.

Miller, W. L. (2017) 'Steroidogenesis: Unanswered Questions', *Trends in Endocrinology and Metabolism*. Elsevier Ltd, 28(11), pp. 771–793. doi: 10.1016/j.tem.2017.09.002.

Moallem, U. *et al.* (2013) 'Dietary α-linolenic acid from flaxseed oil improved folliculogenesis and IVF performance in dairy cows, similar to eicosapentaenoic and docosahexaenoic acids from fish oil', *Reproduction*, 146(6), pp. 603–614. doi: 10.1530/REP-13-0244.

Monniaux, D. *et al.* (2014) 'Minireview The Ovarian Reserve of Primordial Follicles and the Dynamic Reserve of Antral Growing Follicles: What Is the Link?', *Biology of Reproduction*, 90(March), pp. 1–11. doi: 10.1095/biolreprod.113.117077.

Monniaux, D. (2016) 'Driving folliculogenesis by the oocyte-somatic cell dialog: Lessons from genetic models', *Theriogenology*. Elsevier Inc, 86(1), pp. 41–53. doi: 10.1016/j.theriogenology.2016.04.017.

Monniaux, D. *et al.* (2018) 'Folliculogenesis', in *Reference Module in Biomedical Sciences*. Elsevier 978-0-12-801238-3, pp. 1–22. Available at: https://prodinra.inra.fr/record/423846.

Montani, D. A. *et al.* (2012) 'The follicular microenviroment as a predictor of pregnancy: MALDI-TOF MS lipid profile in cumulus cells', *Journal of Assisted Reproduction and Genetics*. doi: 10.1007/s10815-012-9859-y.

Montani, D. A. ntunes *et al.* (2014) 'Hyaluronidase alters the lipid profile of cumulus cells as detected by MALDI-TOF MS and multivariate analysis', *Lipids*. doi: 10.1007/s11745-014-3931-6.

van Montfoort, A. P. A. *et al.* (2014) 'Impact of maternal cholesterol metabolism on ovarian follicle development and fertility', *Journal of Reproductive Immunology*. doi: 10.1016/j.jri.2014.04.003.

Montigny, C. *et al.* (2016) 'Biochimica et Biophysica Acta On the molecular mechanism of fl ippase- and scramblase-mediated phospholipid transport ☆', *BBA - Molecular and Cell Biology of Lipids*. Elsevier B.V., 1861(8), pp. 767–783. doi: 10.1016/j.bbalip.2015.12.020.

Montjean, D., Entezami, F. and Lichtblau, I. (2012) 'Carnitine content in the follicular fluid and expression of the enzymes involved in beta oxidation in oocytes and cumulus cells', *J Assist Reprod Genet*, pp. 1221–1225. doi: 10.1007/s10815-012-9855-2.

Moore, K. L., Persaud, T. and Torchia, M. (2016) *The developing human: clinically oriented embryology*. 10th edn. Philadelphia: Elsevier.

Moran, L. A. *et al.* (2012) *Structure and function: Lipids and membrane, in Principles of Biochemestry*. 5th Editio. Edited by L. A. Moran et al. Boston: Pearson Editions.

Mu, Y. *et al.* (2001) 'Saturated FFAs, Palmitic Acid and Stearic Acid, Induce Apoptosis in Human Granulosa Cells', *Endocrinology*, 142(8), pp. 3590–3597.

Murphy, R. C., Hankin, J. A. and Barkley, R. M. (2009) 'Imaging of lipid species by MALDI mass spectrometry', *Journal of Lipid Research*, 50(Supplement), pp. S317–S322. doi: 10.1194/jlr.R800051-JLR200.

Nakamura, M. T. and Nara, T. Y. (2003) 'Essential fatty acid synthesis and its regulation in mammals', *Prostaglandins Leukotrienes and Essential Fatty Acids*, 68(2), pp. 145–150. doi: 10.1016/S0952-3278(02)00264-8.

Nakamura, M. T. and Nara, T. Y. (2004) 'Structure, Function, and Dietary Regulation of Δ6, Δ5, and Δ9 Desaturases', *Annual Review of Nutrition*, 24(1), pp. 345–376. doi: 10.1146/annurev.nutr.24.121803.063211.

Nazari, M. and Muddiman, D. C. (2016) 'Polarity Switching Mass Spectrometry Imaging of Healthy and Cancerous Hen Ovarian Tissue Sections by Infrared MatrixAssisted Laser Desorption Electrospray Ionization (IR-MALDESI)', 21(141), pp. 595–605. doi: 10.1039/c5an01513h.

Nes, W. D. (2011) 'Biosynthesis of cholesterol and other sterols', *Chemical Reviews*, 111(10), pp. 6423–6451. doi: 10.1021/cr200021m.

Niemann, B. and Rohrbach, S. (2016) *Chapter 3 – Metabolically Relevant Cell Biology – Role of Intracellular Organelles for Cardiac Metabolism*, *The Scientist's Guide to Cardiac Metabolism*. Elsevier Inc. doi: 10.1016/B978-0-12-802394-5.00003-0.

Ntallaris, T. *et al.* (2017) 'Effect of energy balance profiles on metabolic and reproductive response in Holstein and Swedish Red cows', *Theriogenology*. Elsevier Ltd, 90, pp. 276–283. doi: 10.1016/j.theriogenology.2016.12.012.

Okazaki, T. *et al.* (1990) 'Role of Ceramide as a Lipid Mediator of l (r , 25-Dihydroxyvitamin D & nduced HL-60 Cell Differentiation *', 265(26).

Osei, P. *et al.* (1989) 'Topography of rat hepatic microsomal enzymatic components of the fatty acid chain elongation system', *Journal of Biological Chemistry*, 264(12), pp. 6844–6849.

Oseikria, M. *et al.* (2016) 'N-3 polyunsaturated fatty acid DHA during IVM affected oocyte developmental competence in cattle', *Theriogenology*. Elsevier Inc, 85(9), p. 1625–1634.e2. doi: 10.1016/j.theriogenology.2016.01.019.

Ospina, P. A. *et al.* (2010a) 'Associations of elevated nonesterified fatty acids and β-hydroxybutyrate concentrations with early lactation reproductive performance and milk production in transition dairy cattle in the northeastern United States', *Journal of Dairy Science*. Elsevier, 93(4), pp. 1596–1603. doi: 10.3168/jds.2009-2852.

Ospina, P. A. *et al.* (2010b) 'Evaluation of nonesterified fatty acids and β-hydroxybutyrate in transition dairy cattle in the northeastern United States: Critical thresholds for prediction of clinical diseases', *Journal of Dairy Science*. Elsevier, 93(2), pp. 546–554. doi: 10.3168/jds.2009-2277.

Paczkowski, M. *et al.* (2013) 'Comparative Importance of Fatty Acid Beta-Oxidation to Nuclear Maturation, Gene Expression, and Glucose Metabolism in Mouse, Bovine, and Porcine Cumulus Oocyte Complexes 1', *BIOLOGY OF REPRODUCTION*, 88111(5), pp. 1–11. doi: 10.1095/biolreprod.113.108548.

Paton, C. M. and Ntambi, J. M. (2009) 'Biochemical and physiological function of stearoyl-CoA desaturase', *AJP: Endocrinology and Metabolism*, 297(1), pp. E28–E37. doi: 10.1152/ajpendo.90897.2008.

Peddinti, D., Memili, E. and Burgess, S. C. (2010) 'Proteomics-based systems biology modeling of bovine germinal vesicle stage oocyte and cumulus cell interaction', *PLoS ONE*, 5(6). doi: 10.1371/journal.pone.0011240.

Pflege, B. F., Fowler, Z. L. and Koffa, M. (2010) *Future Applications of Metabolic Engineering, in The metabolic pathway engineering handbook: Tools and Apllications*. CRC Press. Edited

by C. D. Smolke. New York: Taylor & Francis Group.

Pulfer, M. and Murphy, R. C. (2003) 'Electrospray mass spectrometry of phospholipids', *Mass Spectrometry Reviews*. doi: 10.1002/mas.10061.

Qu, Q. *et al.* (2016) 'Fatty acid oxidation and carnitine palmitoyltransferase I : emerging therapeutic targets in cancer', pp. 1–9. doi: 10.1038/cddis.2016.132.

Ramasamy, I. (2014) 'Recent advances in physiological lipoprotein metabolism', *Clinical Chemistry and Laboratory Medicine*, 52(12), pp. 1695–1727. doi: 10.1515/cclm-2013-0358.

Raphael, W. and Sordillo, L. M. (2013) 'Dietary polyunsaturated fatty acids and inflammation: The role of phospholipid biosynthesis', *International Journal of Molecular Sciences*, 14(10), pp. 21167–21188. doi: 10.3390/ijms141021167.

Ratnayake, W. M. N. and Galli, C. (2009) 'Fat and fatty acid terminology, methods of analysis and fat digestion and metabolism: A background review paper', *Annals of Nutrition and Metabolism*, 55(1–3), pp. 8–43. doi: 10.1159/000228994.

Reader, K., Stanton, J.-A. and Juengel, J. (2017) 'The Role of Oocyte Organelles in Determining Developmental Competence', *Biology*, 6(4), p. 35. doi: 10.3390/biology6030035.

Record, M. *et al.* (2018) 'Extracellular vesicles: lipids as key components of their biogenesis and functions', *Journal of Lipid Research*, 59(8), pp. 1316–1324. doi: 10.1194/jlr.e086173.

Redding, G. P., Bronlund, J. E. and Hart, A. L. (2007) 'Mathematical modelling of oxygen transport-limited follicle growth', *Reproduction*, 133, pp. 1095–1106. doi: 10.1530/REP-06-0171.

Renaville, B. *et al.* (2010) 'Plasma and follicular fluid fatty acid profiles in dairy cows', *Reproduction in Domestic Animals*, 45(1), pp. 118–121. doi: 10.1111/j.1439-0531.2008.01264.x.

Richards, J. S. and Pangas, S. A. (2010) 'The ovary : basic biology and clinical implications', *The Journal of Clinical Investigation*, 120(4), pp. 963–972. doi: 10.1172/JCI41350.critical.

Rigotti, A., Miettinen, H. E. and Krieger, M. (2003) 'The role of the high-density lipoprotein receptor SR-BI in the lipid metabolism of endocrine and other tissues', *Endocrine Reviews*, 24(3), pp. 357–387. doi: 10.1210/er.2001-0037.

Roberts, R. *et al.* (2004) 'Energy Substrate Metabolism of Mouse Cumulus-Oocyte Complexes : Response to Follicle-Stimulating Hormone Is Mediated by the Phosphatidylinositol 3-Kinase Pathway and Is Associated with Oocyte Maturation 1', *Biology of reproduction*, 71(March), pp. 199–209. doi: 10.1095/biolreprod.103.023549.

Robker, R. L., Wu, L. L. Y. and Yang, X. (2011) 'Inflammatory pathways linking obesity and ovarian dysfunction', *Journal of Reproductive Immunology*. Elsevier Ireland Ltd, 88(2), pp. 142–148. doi: 10.1016/j.jri.2011.01.008.

Roelen, B. A. J. *et al.* (2015) 'Free fatty acid levels in fluid of dominant follicles at the preferred insemination time in dairy cows are not affected by early postpartum fatty acid stress', *Journal of Dairy Science*. Elsevier, 98(4), pp. 2322–2336. doi: 10.3168/jds.2014-7970.

Roux, A. *et al.* (2011) 'Applications of liquid chromatography coupled to mass spectrometry-based metabolomics in clinical chemistry and toxicology : A review', *Clinical Biochemistry*. The Canadian Society of Clinical Chemists, 44(1), pp. 119–135. doi: 10.1016/j.clinbiochem.2010.08.016.

Roy, S. K. and Terada, D. M. (1999) 'Activities of Glucose Metabolic Enzymes in Human Preantral Follicles : In Vitro Modulation by Follicle-Stimulating Hormone , Luteinizing Hormone ,

Epidermal Growth Factor , Insulin-Like Growth Factor I , and Transforming Growth Factor β 1', *Biology of reproduction*, 60, pp. 763–768.

Rudenko, G. *et al.* (2011) 'Structure of the LDL Receptor Extracellular Domain at Endosomal pH -- Rudenko et al_, 10_1126-science_1078124 -- Science', 2353(2002), pp. 2353–2359. doi: 10.1126/science.1078124.

Rufer, A. C., Thoma, Æ. R. and Hennig, Æ. M. (2009) 'Structural insight into function and regulation of carnitine palmitoyltransferase', pp. 2489–2501. doi: 10.1007/s00018-009-0035-1.

Russell, D. L. *et al.* (2016) 'Bidirectional communication between cumulus cells and the oocyte: Old hands and new players?', *Theriogenology*. Elsevier Inc, 86(1), pp. 62–68. doi: 10.1016/j.theriogenology.2016.04.019.

Sánchez, F. and Smitz, J. (2012) 'Molecular control of oogenesis', *Biochimica et Biophysica Acta - Molecular Basis of Disease*. Elsevier B.V., 1822(12), pp. 1896–1912. doi: 10.1016/j.bbadis.2012.05.013.

Sanchez-Lazo, L. *et al.* (2014) 'Fatty Acid Synthesis and Oxidation in Cumulus Cells Support Oocyte Maturation in Bovine', *Molecular Endocrinology*, 28(9), pp. 1502–1521. doi: 10.1210/me.2014-1049.

Sanders, J. R. and Jones, K. T. (2018) 'Regulation of the meiotic divisions of mammalian oocytes and eggs', *Biochemical Society Transactions*, 46(4), pp. 797–806. doi: 10.1042/bst20170493.

Santander, N. *et al.* (2018) 'Transcriptional profiling of embryos lacking the lipoprotein receptor SR-B1 reveals a regulatory circuit governing a neurodevelopmental or metabolic decision during neural tube closure', *BMC Genomics*. BMC Genomics, 19(1), p. 731. doi: 10.1186/s12864-018-5110-2.

Santos, P. H. *et al.* (2017) 'Lipid profiles of follicular fluid from cows submitted to ovarian superstimulation', *Theriogenology*. Elsevier Inc., 94, pp. 64–70. doi: 10.1016/j.theriogenology.2017.02.002.

Saponaro, C. *et al.* (2015) 'The subtle balance between lipolysis and lipogenesis: A critical point in metabolic homeostasis', *Nutrients*, 7(11), pp. 9453–9474. doi: 10.3390/nu7115475.

Sata, R. *et al.* (1999) 'Fatty Acid Composition of Bovine Embryos Cultured in Serum-Free and Serum-Containing Medium during Early Embryonic Development.', *Journal of Reproduction and Development*, 45(1), pp. 97–103. doi: 10.1262/jrd.45.97.

Sato, S. *et al.* (2006) 'Proteomic Profiling of Lipid Droplet Proteins in Hepatoma Cell Lines Expressing Hepatitis C Virus Core Protein', 930, pp. 921–930. doi: 10.1093/jb/mvj104.

Schiller, J. *et al.* (2006) 'Recent applications of MALDI-TOF mass spectrometry and P NMR spectroscopy in phospholipid research Recent applications of MALDI-TOF mass spectrometry and 31 P NMR spectroscopy in phospholipid research', *Future Lipidol.*, 1(1), pp. 115–125. doi: 10.2217/17460875.1.1.115.

Schiller, J. and Arnold, K. (2002) 'Application of high resolution 31 P NMR spectroscopy to the characterization of the phospholipid composition of tissues and body fluids – a methodological review', 8(11), pp. 205–223.

Schmitz, G. and Ruebsaamen, K. (2010) 'Metabolism and atherogenic disease association of lysophosphatidylcholine', *Atherosclerosis*, 208(1), pp. 10–18. doi: 10.1016/j.atherosclerosis.2009.05.029.

Schrader, M. *et al.* (2015) 'Peroxisome-mitochondria interplay and disease', *Journal of Inherited*

Metabolic Disease, 38(4), pp. 681–702. doi: 10.1007/s10545-015-9819-7.

Schrader, M. and Fahimi, H. D. (2008) 'The peroxisome: Still a mysterious organelle', *Histochemistry and Cell Biology*, 129(4), pp. 421–440. doi: 10.1007/s00418-008-0396-9.

Schuchman, E. H. *et al.* (1991) 'Human Acid Sphingomyelinase', 266, pp. 8531–8539.

Schuhmann, K. *et al.* (2011) 'Bottom-Up Shotgun Lipidomics by Higher Energy Collisional Dissociation on LTQ Orbitrap Mass Spectrometers', *Analytical Chemistry*, 83, pp. 5480–5487. doi: 10.1021/ac102505f.

Schwudke, D. *et al.* (2011) 'Shotgun Lipidomics on High Resolution Mass Spectrometers', *Cold Spring Harb Perspect Biol 2011;3:a004614*, 3, pp. 1–13.

Serna, J. *et al.* (2015) 'Quantitative lipidomic analysis of plasma and plasma lipoproteins using MALDI-TOF mass spectrometry', *Chemistry and Physics of Lipids*. doi: 10.1016/j.chemphyslip.2015.05.005.

Sessions-Bresnahan, D. R. *et al.* (2015) 'Effect of Obesity on the Preovulatory Follicle and Lipid Fingerprint of Equine Oocytes1', *Biology of Reproduction*, 94(1), pp. 1–12. doi: 10.1095/biolreprod.115.130187.

Shen, W. J., Azhar, S. and Kraemer, F. B. (2016) 'Lipid droplets and steroidogenic cells', *Experimental Cell Research*. doi: 10.1016/j.yexcr.2015.11.024.

Silva-Santos, K. C. *et al.* (2014) 'MALDI-MS lipid profiles of oocytes recovered by ovum pickup from Bos indicus and 1/2 indicus × taurus with high vs low oocyte yields', *Reproduction in Domestic Animals*, 49(5), pp. 711–718. doi: 10.1111/rda.12352.

Sinderewicz, E. *et al.* (2017) 'Expression of factors involved in apoptosis and cell survival is correlated with enzymes synthesizing lysophosphatidic acid and its receptors in granulosa cells originating from different types of bovine ovarian follicles', *Reproductive Biology and Endocrinology*, 15(1), pp. 1–15. doi: 10.1186/s12958-017-0287-9.

Sinderewicz, E. *et al.* (2017) 'Lysophosphatidic acid expression in theca cells depends on the type of bovine ovarian follicle', *Reproduction in Domestic Animals*. doi: 10.1111/rda.12790.

Sirard, M. A. *et al.* (2006) 'Contribution of the oocyte to embryo quality', *Theriogenology*, 65(1), pp. 126–136. doi: 10.1016/j.theriogenology.2005.09.020.

Skotland, T., Sandvig, K. and Llorente, A. (2017) 'Lipids in exosomes: Current knowledge and the way forward', *Progress in Lipid Research*. The Authors, 66, pp. 30–41. doi: 10.1016/j.plipres.2017.03.001.

Smith, S. and Tsai, S. (2008) 'The type I fatty acid and polyketide synthases: a tale of two megasynthases', 24(5), pp. 1041–1072.

Sohel, M. M. H. *et al.* (2013) 'Exosomal and non-exosomal transport of extra-cellular microRNAs in follicular fluid: Implications for bovine oocyte developmental competence', *PLoS ONE*, 8(11). doi: 10.1371/journal.pone.0078505.

Staples, C. R., Burke, J. M. and Thatcher, W. W. (1998) 'Influence of Supplemental Fats on Reproductive Tissues and Performance of Lactating Cows', *Journal of Dairy Science*. Elsevier, 81(3), pp. 856–871. doi: 10.3168/jds.s0022-0302(98)75644-9.

Steffensen, K. R. *et al.* (2006) 'Reduced fertility and inability of oocytes to resume meiosis in mice deficient of the Lxr genes', *Molecular and Cellular Endocrinology*, 256(1–2), pp. 9–16. doi: 10.1016/j.mce.2006.03.044.

Steinmetz, A. *et al.* (1990) 'Human apolipoprotein A-IV binds to apolipoprotein A-I/A-II receptor

sites and promotes cholesterol efflux from adipose cells', *Journal of Biological Chemistry*, 265(14), pp. 7859–7863.

Stocco, D. M. (2000) 'Intramitochondrial cholesterol transfer', *Biochimica et Biophysica Acta - Molecular and Cell Biology of Lipids*, 1486(1), pp. 184–197. doi: 10.1016/S1388-1981(00)00056-1.

Stocco, D. M. (2001) 'StAR Protein and the Regulation of Steroid Hormone Biosynthesis', *Annual Review of Physiology*, 63(1), pp. 193–213. doi: 10.1146/annurev.physiol.63.1.193.

Stoeckli, M. *et al.* (2001) 'Imaging mass spectrometry: A new technology for the analysis of protein expression in mammalian tissues', *Nature Medicine*, 7(4), pp. 493–496. doi: 10.1038/86573.

Sturmey, R. G. *et al.* (2009) 'Role of Fatty Acids in Energy Provision During Oocyte Maturation and Early Embryo Development', 44, pp. 50–58. doi: 10.1111/j.1439-0531.2009.01402.x.

Su, Y. *et al.* (2007) 'Selective degradation of transcripts during meiotic maturation of mouse oocytes', *Dev Biol.*, 302(1), pp. 104–117.

Su, Y. *et al.* (2008) 'Oocyte regulation of metabolic cooperativity between mouse cumulus cells and oocytes : BMP15 and GDF9 control cholesterol biosynthesis in cumulus cells', 121, pp. 111–121. doi: 10.1242/dev.009068.

Su, Y.-Q. *et al.* (2007) 'Oocyte regulation of metabolic cooperativity between mouse cumulus cells and oocytes: BMP15 and GDF9 control cholesterol biosynthesis in cumulus cells', *Development*, 135(1), pp. 111–121. doi: 10.1242/dev.009068.

Sutton, M. L. *et al.* (2003) 'Influence of oocyte-secreted factors and culture duration on the metabolic activity of bovine cumulus cell complexes', *Reproduction*, 126, pp. 27–34.

Sutton-mcdowall, M. L. *et al.* (2012) 'Utilization of endogenous fatty acid stores for energy production in bovine preimplantation embryos', *Theriogenology*. Elsevier Inc., 77(8), pp. 1632–1641. doi: 10.1016/j.theriogenology.2011.12.008.

Sutton-mcdowall, M. L., Gilchrist, R. B. and Thompson, J. G. (2004) 'Cumulus expansion and glucose utilisation by bovine cumulus– oocyte complexes during in vitro maturation: the influence of glucosamine and follicle-stimulating hormone', *Reproduction*, 128, pp. 313–319. doi: 10.1530/rep.1.00225.

Sutton-McDowall, M. L., Gilchrist, R. B. and Thompson, J. G. (2010) 'The pivotal role of glucose metabolism in determining oocyte developmental competence', *Reproduction*, 139(4), pp. 685–695. doi: 10.1530/rep-09-0345.

Tajima, K. *et al.* (2007) 'Ovarian theca cells in follicular function', *Reproductive BioMedicine Online*, 15(5), pp. 591–609. doi: 10.1016/S1472-6483(10)60392-6.

Tanghe, S. *et al.* (2002) 'Minireview: Functions of the cumulus oophorus during oocyte maturation, ovulation, and fertilization', *Molecular Reproduction and Development*, 61(3), pp. 414–424. doi: 10.1002/mrd.10102.

Tessaro, F. H. G., Ayala, T. S. and Martins, J. O. (2015) 'Lipid Mediators Are Critical in Resolving Inflammation: A Review of the Emerging Roles of Eicosanoids in Diabetes Mellitus', *BioMed Research International*, 2015, pp. 1–8. doi: 10.1155/2015/568408.

Thelie, A. *et al.* (2009) 'Regulation of bovine oocyte-specific transcripts during in vitro oocyte maturation and after maternal-embryonic transition analyzed using a transcriptomic approach', *Molecular Reproduction and Development*, 76(8), pp. 773–782. doi: 10.1002/mrd.21031.

Tomek, W., Torner, H. and Kanitz, W. (2002) 'Comparative analysis of protein synthesis, transcription and cytoplasmic polyadenylation of mRNA during maturation of bovine oocytes in vitro', *Reproduction in Domestic Animals*, 37(2), pp. 86–91. doi: 10.1046/j.1439-0531.2002.00336.x.

Trigatti, B. *et al.* (1999) 'Influence of the high density lipoprotein receptor SR-BI on reproductive and cardiovascular pathophysiology.', *Proceedings of the National Academy of Sciences of the United States of America*, 96(August), pp. 9322–9327. doi: 10.1073/pnas.96.16.9322.

Trigatti, B., Rigotti, A. and Krieger, M. (2000) 'The role of the high-density lipoprotein receptor SR-BI in cholesterol metabolism', *Current Opinion in Lipidology*, 11(2), pp. 123–131. doi: 10.1097/00041433-200004000-00004.

Urlep, Z. and Rozman, D. (2013) 'The interplay between circadian system, cholesterol synthesis, and steroidogenesis affects various aspects of female reproduction', *Frontiers in Endocrinology*, 4(SEP), pp. 1–10. doi: 10.3389/fendo.2013.00111.

Uyar, A., Torrealday, S. and Seli, E. (2013) 'Cumulus and granulosa cell markers of oocyte and embryo quality', *Fertility and Sterility*. American Society for Reproductive Medicine, 99(4), pp. 979–997. doi: 10.1016/j.fertnstert.2013.01.129.

Uzbekova, S. *et al.* (2015) 'MALDI Mass Spectrometry Imaging of Lipids and Gene Expression Reveals Differences in Fatty Acid Metabolism between Follicular Compartments in Porcine Ovaries', *Biology*, 4(1), pp. 216–236. doi: 10.3390/biology4010216.

Valckx, S. D. *et al.* (2014) 'Fatty acid composition of the follicular fluid of normal weight, overweight and obese women undergoing assisted reproductive treatment: a descriptive cross-sectional study', *Reproductive Biology and Endocrinology*, 12(1), p. 13. doi: 10.1186/1477-7827-12-13.

Valckx, S. D. M. *et al.* (2012) 'BMI-related metabolic composition of the follicular fluid of women undergoing assisted reproductive treatment and the consequences for oocyte and embryo quality', *Human Reproduction*, 0(0), pp. 1–9. doi: 10.1093/humrep/des350.

Vance, J. E. (2014) 'Phospholipid Synthesis and Transport in Mammalian Cells', (1). doi: 10.1111/tra.12230.

Vance, J. E. and Steenbergen, R. (2005) 'Progress in Lipid Research Metabolism and functions of phosphatidylserine', 44, pp. 207–234. doi: 10.1016/j.plipres.2005.05.001.

Vanholder, T. *et al.* (2005) 'Effect of non-esterified fatty acids on bovine granulosa cell steroidogenesis and proliferation in vitro', *Animal Reproduction Science*, 87(1), pp. 33–44. doi: 10.1016/j.anireprosci.2004.09.006.

Velasco, M. *et al.* (2006) 'Association of lower plasma estradiol levels and low expression of scavenger receptor class B, type I in infertile women', *Fertility and Sterility*, 85(5), pp. 1391–1397. doi: 10.1016/j.fertnstert.2005.10.046.

Vireque, A. A. *et al.* (2017) 'Dataset on lipid profile of bovine oocytes exposed to Lα-phosphatidylcholine during in vitro maturation investigated by MALDI mass spectrometry and gas chromatography-flame ionization detection', *Data in Brief*. Elsevier Inc., 13, pp. 480–486. doi: 10.1016/j.dib.2017.06.026.

Vireque, A. A. *et al.* (2017) 'MALDI mass spectrometry reveals that cumulus cells modulate the lipid profile of in vitro- matured bovine oocytes', *Systems Biology in Reproductive Medice*.

Vitti, M. *et al.* (2016) 'Peroxisome Proliferator-Activated Receptors in Female Reproduction and Fertility', *PPAR Research*. Hindawi Publishing Corporation, 2016, pp. 1–12. doi:

10.1155/2016/4612306.

Wahli, W. and Michalik, L. (2012) 'PPARs at the crossroads of lipid signaling and inflammation', *Trends in Endocrinology and Metabolism*. Elsevier Ltd, 23(7), pp. 351–363. doi: 10.1016/j.tem.2012.05.001.

Wald, T. Von *et al.* (2010) 'Age-related variations in follicular apolipoproteins may influence human oocyte maturation and fertility potential', *Fertility and Sterility*. Elsevier Ltd, 93(7), pp. 2354–2361. doi: 10.1016/j.fertnstert.2008.12.129.

Wallace, M. *et al.* (2012) 'An investigation into the relationship between the metabolic profile of follicular fluid, oocyte developmental potential, and implantation outcome', *Fertility and Sterility*, 97(5). doi: 10.1016/j.fertnstert.2012.01.122.

Wang, Q. J. (2006) 'PKD at the crossroads of DAG and PKC signaling', *Trends in Pharmacological Sciences*, 27(6), pp. 317–323. doi: 10.1016/j.tips.2006.04.003.

Warzych, E. *et al.* (2017) 'Interactions of bovine oocytes with follicular elements with respect to lipid metabolism', *Animal Science Journal*, 88(10), pp. 1491–1497. doi: 10.1111/asj.12799.

Wathes, D. C., Abayasekara, D. R. E. and Aitken, R. J. (2007) 'Polyunsaturated Fatty Acids in Male and Female Reproduction 1', *Biology of reproduction*, 77(April), pp. 190–201. doi: 10.1095/biolreprod.107.060558.

Wen, X. *et al.* (2018) 'Lipidomic Components Alterations of Human Follicular Fluid Reveal the Relevance of Improving Clinical Outcomes in Women Using Progestin-Primed Ovarian Stimulation Compared to Short-Term Protocol.', *Medical science monitor : international medical journal of experimental and clinical research*, 24, pp. 3357–3365. doi: 10.12659/MSM.906602.

Wenk, M. R. (2005) 'THE EMERGING FIELD OF LIPIDOMICS', *Nature*, 4(July), pp. 594–610. doi: 10.1038/nrd1776.

Wigglesworth, K. *et al.* (2015) 'Transcriptomic Diversification of Developing Cumulus and Mural Granulosa Cells in Mouse Ovarian Follicles1', *Biology of Reproduction*, 92(1), pp. 1–14. doi: 10.1095/biolreprod.114.121756.

Yamashita, A. *et al.* (2014) 'Acyltransferases and transacylases that determine the fatty acid composition of glycerolipids and the metabolism of bioactive lipid mediators in mammalian cells and model organisms', *Progress in Lipid Research*. doi: 10.1016/j.plipres.2013.10.001.

Yang, Kui; Han, X. (2017) 'Lipidomics: Techniques, applications, and outcomes related to biomedical sciences', *Trends Biochem Sci*, 41(11), pp. 954–969. doi: 10.1016/j.tibs.2016.08.010.

Yang, X. *et al.* (2010) 'Identification of Perilipin-2 as a lipid droplet protein regulated in oocytes during maturation', *Reproduction, Fertility and Development*, 22(8), pp. 1262–1271. doi: 10.1071/RD10091.

Yang, X. *et al.* (2012) 'Exposure to lipid-rich follicular fluid is associated with endoplasmic reticulum stress and impaired oocyte maturation in cumulus-oocyte complexes', *Fertility and Sterility*. Elsevier Inc., 97(6), pp. 1438–1443. doi: 10.1016/j.fertnstert.2012.02.034.

Yang, Y., Lee, M. and Fairn, G. D. (2018) 'Phospholipid subcellular localization and dynamics', *Journal of Biological Chemistry*, 293(17), pp. 6230–6240. doi: 10.1074/jbc.R117.000582.

Yates, M. *et al.* (2011) 'Clinical impact of scavenger receptor class B type i gene polymorphisms on human female fertility', *Human Reproduction*, 26(7), pp. 1910–1916. doi: 10.1093/humrep/der124.

Yesilaltay, A. *et al.* (2006) 'Effects of Hepatic Expression of the High-Density Lipoprotein Receptor SR-BI on Lipoprotein Metabolism', *Endocrine Reviews*, 147(4), pp. 1577–1588. doi: 10.1210/en.2005-1286.

Young, J. M. and McNeilly, A. S. (2010) 'Theca: The forgotten cell of the ovarian follicle', *Reproduction*, 140(4), pp. 489–504. doi: 10.1530/REP-10-0094.

Zachut, M. *et al.* (2010) 'Effects of dietary fats differing in n-6:n-3 ratio fed to high-yielding dairy cows on fatty acid composition of ovarian compartments, follicular status, and oocyte quality', *Journal of Dairy Science*, 93(2), pp. 529–545. doi: 10.3168/jds.2009-2167.

Zemski Berry, K. A. *et al.* (2011) 'MALDI Imaging of Lipid Biochemistry in Tissues by Mass Spectrometry', *Chemical Reviews*, 111(10), pp. 6491–6512. doi: 10.1021/cr200280p.

Zemski Berry, K. A. *et al.* (2017) 'Lipidomic characterization and localization of phospholipids in the human lung', *Journal of Lipid Research*, 58(5), pp. 926–933. doi: 10.1194/jlr.m074955.

Zeron, Y. *et al.* (2002) 'Effect of Polyunsaturated Fatty Acid Supplementation on Biophysical Parameters and Chilling Sensitivity of Ewe Oocytes Separation of Plasma and', 278(June 2001). doi: 10.1002/mrd.1156.

Zhang, L. *et al.* (1995) 'Cumulus Cell Function During Bovine Oocyte Maturation , Fertilization , andEmbryo Development In Vitro', *Molecular Reproduction and Development*, 40, pp. 338–344.

Zhang, W. *et al.* (2012) 'Advances on in vitro production and cryopreservation of porcine embryos', *Animal Reproduction Science*. Elsevier B.V., 132(3–4), pp. 115–122. doi: 10.1016/j.anireprosci.2012.05.008.

Zheng, P. and Dean, J. (2007) 'Oocyte-Specific Genes Affect Folliculogenesis, Fertilization, and Early Development', *Seminars in Reproductive Medicine*, 25(4), pp. 243–251. doi: 10.1055/s-2007-980218.

Zheng, W. *et al.* (2006) 'Ceramides and other bioactive sphingolipid backbones in health and disease: Lipidomic analysis, metabolism and roles in membrane structure, dynamics, signaling and autophagy', *Biochimica et Biophysica Acta - Biomembranes*, 1758(12), pp. 1864–1884. doi: 10.1016/j.bbamem.2006.08.009.

Zhou, C.-J. *et al.* (2016) 'The beneficial effects of cumulus cells and oocyte-cumulus cell gap junctions depends on oocyte maturation and fertilization methods in mice', *PeerJ*, 4, p. e1761. doi: 10.7717/peerj.1761.

Zschörnig, O. *et al.* (2005) 'Cholesterol esterase action on human high density lipoproteins and inhibition studies: Detection by MALDI-TOF MS', *Journal of Lipid Research*, 46(4), pp. 803–811. doi: 10.1194/jlr.M400265-JLR200.

PUBLICATION LIST

PUBLICATION LIST

Publications in peer-reviewed journals

- first author

Bertevello PS, Teixeira-Gomes AP, Seyer A, Vitorino Carvalho A, Labas V, Blache MC, Banliat C, Cordeiro LAV, Duranthon V, Papillier P, Maillard V, Elis S and Uzbekova S (2018) *Lipid Identification and Transcriptional Analysis of Controlling Enzymes in Bovine Ovarian Follicle.* Int J Mol Sci 19. doi: 10.3390/ijms19103261

Submission: **Bertevello PS**, Teixeira-Gomes AP, Labas V, Cordeiro LAV, Blache MC, Duranthon V, Papillier P, and Uzbekova S. *Drastic changes of lipid composition occurs in follicular fluid but not in the enclosed oocyte during final growth of bovine follicle* (prepared for submission in *Molecular Reproduction and Development*)

- co-author

Elis S, Oseikria M, Vitorino Carvalho A, **Bertevello PS**, Corbin E, Teixeira-Gomes AP, Lecardonnel J, Archilla C, Duranthon V, Labas V, Uzbekova S. *Docosahexaenoic acid mechanisms of action on the bovine oocyte-cumulus complex.* J Ovarian Res. 2017 Nov 9; 10(1):74. doi: 10.1186/s13048-017-0370-z.

Freret S, Oseikria M, Le Bourhis D, Desmarchais A , Briant E, Desnoes O, Dupont M, Le Berre L, Ghazouani O, **Bertevello PS**, Teixeira-Gomes AP, Labas V, Uzbekova S, Salvetti P, Maillard V, Elis S. *Effects of a n-3 PUFA enriched diet on embryo production in dairy cows.* Reproduction 2019 Apr 1; doi.org/10.1530/REP-18-0644.

Poster presentations at conferences

Bertevello PS, Ghazouani O, Banliat C, Elis S, Teixeira-Gomes AP, Maillard V, Labas V, Uzbekova S. *MALDI-TOF mass spectrometry analysis of lipids in single bovine oocytes during IVM.* 32nd Annual Meeting A.E.T.E., 9th - 10th September 2016, Barcelona, Spain. – Best poster award

Bertevello PS, Labas V, Banliat C, Teixeira-Gomes AP, Elis S, Maillard V, Uzbekova S. *Lipid profiling of ovarian follicular cells.* 21 ème Journée Thésard et 5ème Journée Post-Doctorants, 17 Mai 2016, Nouzilly, France.

Bertevello P.S., Labas V., Dalbies-Tran R., Touze J-L. , Dupont M., Briant E., Papillier P., Corbin E. Uzbekova S. *Analysis of lipid profiling by MALDI-TOF mass spectrometry in granulosa cells of postpartum Holstein dairy cows*. 18th International Congress on Animal Reproduction, 27 - 30 June 2016, Tours, France.

Bertevello PS, Banliat C, Teixeira-Gomes AP, Labas V, Uzbekova S. *Analysis of lipid profiling by MALDI-TOF Mass Spectrometry in bovine ovarian follicle.* 30th Colloque Biotechnocentre. 12 - 13 Août 2017, Domaine de Seillac, France.

Bertevello PS, Banliat C, Teixeira-Gomes AP, Elis S, Maillard V, Carvalho AV, Duranthon V, Labas V, Uzbekova S. *Comparison of lipid profiles and gene expression in granulosa and cumulus cells in bovine.* 33rd Annual Meeting A.E.T.E., 8th - 9th September 2017, Bath, UK.

Bertevello PS, Labas V, Teixeira AP, Maillard V, Elis S, Carvalho A, Duranthon V, Banliat C, Uzbekova S, *Bovine ovary lipidomics***.** 2st Whorkshop on Imaging Mass Spectrometry, 03 - 05 April 2018, Saint Malo, France.

Bertevello P.S., Teixeira-Gomes A.P., Maillard V, Blanche MC, Elis S, Labas V., Uzbekova S. *Lipids metabolism in small and large antral ovarian follicles.* 31th Colloque Biotechnocentre. 11 - 12 Août 2018, Domaine de Seillac, France.

Uzbekova S, **Bertevello PS**, Ghazouani O, Teixeira-Gomes AP, Seyer A, Maillard V, Oseikria M, Banliat C, Labas V, Elis S. *Enriched n-3 polyunsaturated fatty acid diet modified oocyte lipid composition and may influence oocyte quality in Prim Holstein dairy cows.* 34th Annual Meeting A.E.T.E., 7th -8th September 2018, Nantes, France.

Oral presentations at conferences

Bertevello PS, Banliat C, Teixeira-Gomes AP, Labas V and Uzbekova S. *Lipidomics of bovine ovarian follicle using MALDI-TOF Mass Spectrometry***.** 2th Journée Reprosciences, 10-12 Avril 2017, Tours, France.

Bertevello PS, Banliat C, Teixeira-Gomes AP, Labas V and Uzbekova S. *Analysis of lipid profiling by MALDI-TOF mass spectrometry in bovine ovarian follicle.* 22 ème Journée Thésard et 6ème Journée Post-Doctorants, 1 Juin 2017, Nouzilly, France.

Bertevello PS, Labas V, Teixeira-Gomes AP, Maillard V, Elis S, Carvalho A, Duranthon V, Banliat C, Uzbekova S. *Lipids metabolism in ovarian follicular cells.* 23ème Journée Thésards et 7ème Journée Post-doctorants - 18 Juin 2018, Nouzilly, France.

Other publication

Bertevello PS. *Imaging mass spectrometry: From laboratory curiosity to state of the art molecular technology.* Le Mag n°74 Automne 2018, Société Française d'Electrophorèse & d'Analyse Protéomique (SFEAP/SFSM) http://www.sfeap.fr/index.php?rub=la_lettre_a_le_mag

Participation in Workshops and Meetings

- 1st Workshop on Imaging Mass Spectrometry, 29 - 31 March 2016, Saint Malo, France.
- Meeting "Lipidomystes" - Journée Technique du Réseau Français de Lipidomystes, 27 - 28 Octobre 2016, Toulouse, France.
- Séminaire RUMinantes et LIPides (RUMLIP) – Lipides et fonctions de reproduction: exemples des ruminants et des monogastriques, 24 novembre 2016, Nouzilly, France.
- 2nd Whorkshop on Imaging Mass Spectrometry, 03 - 05 April 2018, Saint Malo, France.

Priscila Silvana BERTEVELLO

Lipids in Bovine Ovarian Follicle: Mass Spectrometry Analysis and Regulation

Résumé

Le follicule ovarien constitue un environnement favorable aux ovocytes, qui acquière sa compétence à soutenir le développement embryonnaire au cours de la folliculogenese, en communication permanente avec les cellules et le liquide folliculaire (LF). Parmi d'éclairer la régulation du métabolisme lipidique au sein des follicules ovariens, les objectifs de cette étude étaient d'analyser la composition lipidique et la régulation des gènes dans les compartiments folliculaires et les ovocytes. En utilisant la chromatographie liquide et MALDI-TOF spectrométrie de masse (SM), le profil lipidique et la localisation moléculaires par imagerie (IMS) ont été identifiés plus de 400 espèces lipidiques dans les follicules bovins. Par analyse de l'expression génique à l'aide de données transcriptomiques globales, les gènes liés au métabolisme des lipides exprimaient des fonctions spécifiques, notamment l'absorption des lipides, la dégradation lipolytique, le transport et l'oxydation des AG, la synthèse de novo AG, l'allongement des AG, la production de lipoprotéines, la construction de membranes, le stockage de lipides, etc. Le follicule ovarien est capable de transformer l'AG de l'apport nutritif et de l'utiliser pour fournir aux cellules folliculaires et l'ovocyte des lipides membranaires, de l'énergie et des médiateurs de signalisation. Le métabolisme des lipides est donc probablement impliqué dans le maintien de l'homéostasie folliculaire et la régulation de l'atrésie ou de la dominance folliculaire, assurant ainsi le développement l'ovocyte compétent pour le développement embryonnaire ultérieur.

Mots-clés: follicule ovarien; lipides; imagerie par spectrométrie de masse (IMS); profilage MALDI MS; expression du gène; ovocyte; cellules da granulosa; cellules da thèque; fluide folliculaire; bovine; taille du follicule.

Résumé en anglais

Ovarian follicle provides a favorable environment for enclosed oocytes, which acquire their competence to support embryo development in tight communications with somatic follicular cells and follicular fluid. In order to enlighten lipid metabolism regulation within the ovarian follicles, the objectives of this study were analyze lipid composition and gene regulation in follicular compartments and oocyte in development stages. Using liquid chromatography and MALDI-TOF mass spectrometry (MS) the lipid profiling and imaging localization identified more than 400 lipid species in bovine follicles. Gene expression analysis, using global transcriptomic data, showed lipid metabolism-related genes with specific functions including lipid uptake, lipolytic degradation, FA transport and oxidation, de novo FA synthesis and elongation, lipoprotein production, membrane building, lipid storage, and others. The ovarian follicle is capable to transform FA from nutrition uptake and use them to supplement follicular cells and enclosed oocyte with membrane lipids, energy, and signaling mediators. Lipid metabolism is therefore likely involved in the maintenance of follicular homeostasis and regulation of follicular atresia or dominance thus assuring the development of oocyte competence for subsequent embryonic development.

Keywords: ovarian follicle; lipids; mass spectrometry imaging; MALDI MS profiling; gene expression; oocyte; granulosa; theca; follicular fluid; bovine; follicle size.